12-7-2018 3:00 PM

Experimental testing and modeling of partial nitrification at different temperatures

Xiaoguang Liu
The University of Western Ontario

Supervisor
Nakhla, George.
The University of Western Ontario

Graduate Program in Civil and Environmental Engineering
A thesis submitted in partial fulfillment of the requirements for the degree in Doctor of Philosophy

Abstract

Nitrogen in wastewater treatment plant effluents has adverse environmental effects on aquatic systems. Excessive concentrations of nitrogen in water bodies can result in the depletion of dissolved oxygen, deterioration of water quality, and shifts of biotic community. Conventional biological nitrogen removal (BNR) processes consume high energy for nitrification and require external carbon for denitrification. Alternatively, partial nitrification is of interest as an emerging technology for its lower need of organic carbon addition and cost savings in aeration.

In this study, the main objectives are: 1- developing a mathematical model involving operational parameters for the determination of successful partial nitrification conditions; 2- analyzing the factors affecting the performance of partial nitrification in a sequencing batch reactor (SBR) using kinetic models at 35^{o}C; 3- investigating the effect of dissolved oxygen (DO) on nitrification in a sequencing batch reactor (SBR) treating low ammonia wastewater (40 mg N/L) at low temperature (14^{o}C); 4- investigating the effect of nickel on nitrification in a sequencing batch reactor (SBR) treating low ammonia wastewater (40 mg N/L) at low temperature (10^{o}C).

First, a mathematical model based on the minimum DO concentration (DO_{min}), minimum/maximum substrate concentration (S_{min} and S_{max}), was developed. The model evaluated the influence of pH (7-9), temperature (10^{o}C-35^{o}C), and solids retention time (SRT) (5days-infinity) on the minimum/maximum substrate concentration (MSC) values. In addition, specific application for shortcut nitrification-anammox process at 10^{o}C was analyzed. Furthermore, experimental data from different literature studies was used for model simulation

and the model prediction fitted experimental data well. The model provides a method to identify feasible combinations of pH, DO, total ammonium nitrogen (TAN), total nitrite nitrogen (TNN), and solids retention time (SRT) for successful shortcut nitrification.

Second, to meet objective 2, a sequencing batch reactor (SBR) was operated at 35^{o}C for over 4 months with dissolved oxygen (DO) and influent ammonia concentration as operating variables to evaluate nitrite accumulation. Stable partial nitrification was observed at two conditions, influent ammonia concentration of 190 mg N/L and a DO of 0.6-3.0 mg/L as well as influent ammonia concentration of 100 mg N/L and a DO of 0.15-2.0 mg/L with intermittent aeration. Kinetic parameters were determined or estimated with batch tests and model simulation. The kinetic model predicted the SBR performance well.

Third, a sequencing batch reactor (SBR) treating low ammonia wastewater (40 mg N/L) at a low temperature (14 °C) was operated for 130 days. Three dissolved oxygen levels (5–6 mg O_2/L, 2–3 mg O_2/L, and 0.8–1.0 O_2/L) were tested. Dissolved oxygen reduction resulted in lower ammonia oxidizing bacteria (AOB) and nitrite oxidizing bacteria (NOB) activity, with decreasing ammonia conversion ratio (ACR) and increasing nitrite accumulation ratio (NAR). The maximum growth rates of AOB and NOB determined in this study (0.28 and 0.38 d^{-1}) were below the median literature values (0.47 and 0.62 d^{-1}), whereas the oxygen half-saturation coefficients of AOB and NOB (1.36 and 2.79 mg/L) were higher than those found in the literature. The kinetic model explained the SBR performance well. Low dissolved oxygen, together with long solids retention time, was recommended for partial nitrification at a low temperature.

Lastly, acute and chronic toxicity of nickel to nitrifiers was inverstigated. Chronic toxicity of nickel to nitrification of low ammonia synthetic wastewater was investigated at 10^{o}C in two

SBRs with 1 mg/L nickel dosing either from the beginning or after biomass concentration decreased to 300 mg/L. Significant nickel inhibition occurred at Ni/MLSS ratio of 2.7 mg Ni/ g MLSS. At a Ni/MLSS ratio of 4-7 mg Ni/g MLSS, ammonia oxidizing bacteria (AOB) activity was inhibited by 47%-58% after acclimatization. After long-term acclimatization to nickel at 10ºC, high DO(~7mg/L) and SRT of 63-70 days, the μ_{max}, b and Ko of AOB and NOB were determined as 0.16 d^{-1}, 0.098 d^{-1} and 2.08 mg O_2/L, and 0.16 d^{-1}, 0.098 d^{-1} and 2.12 mg O_2/L, respectively. Acute toxicity of nickel to nitrification at 10ºC, 23ºC, and 35ºC was evaluated by short-term batch tests. The nickel inhibition constants based on a modified non-competitive model for nitrification at 10ºC, 23ºC, and 35ºC were determined. Long-term SBRs operation and short-term batch tests results were consistent. Short-term nickel inhibition of nitrifying bacteria was completely reversible.

Keywords

Partial nitrification, biological nitrogen removal, model, dissolved oxygen, temperature, kinetics, nickel

Co-Authorship Statement

This PhD thesis contains material that is published or “under review” for publication in peer reviewed journals as listed below.

Chapter 3

Title of the Paper: A model for determination of operational conditions for successful shortcut nitrification

Authors: Xiaoguang Liu,Mingu Kim, George Nakhla

Status: Published

Journal: Environmental Science and Pollution Research

Reference: Liu, X., Kim, M., & Nakhla, G. (2017). A model for determination of operational conditions for successful shortcut nitrification. *Environmental Science and Pollution Research*, 24(4), 3539-3549.

Chapter 4

Title of the Paper: Operational conditions for successful partial nitrification in a sequencing batch reactor (SBR) based on process kinetics

Authors: Xiaoguang Liu,Mingu Kim, George Nakhla

Status: Published

Journal: Environmental technology

Reference: Liu, X., Kim, M., & Nakhla, G. (2017). Operational conditions for successful partial nitrification in a sequencing batch reactor (SBR) based on process kinetics. *Environmental technology*, *38*(6), 694-704.

Chapter 5

Title of the Paper: Performance and kinetics of nitrification of low ammonia wastewater at low temperature

Authors: Xiaoguang Liu,Mingu Kim, George Nakhla

Status: Published

Journal: Water Environment Research

Reference: Liu, X., Kim, M., & Nakhla, G. (2018). Performance and Kinetics of Nitrification of Low Ammonia Wastewater at Low Temperature. *Water Environment Research*, *90*(6), 498-509.

Chapter 6

Title of the Paper: Acute and chronic toxicity of nickel to nitrifiers at low temperature

Authors: Xiaoguang Liu, Mohammad M.I. Chowdhury, Masuduz Zaman, Mingu Kim, George Nakhla

Status: Submitted

Journal: Biochemical engineering Journal

Acknowledgments

First, I would like to express my deepest gratitude to my supervisor, Dr.George Nakhla (Professor and Salamander Chair in Environmental Engineering, Chemical and Biochemical Engineering, University of Western Ontario) for his support and guidance throughout my PhD study in Western. I feel very lucky to work under his supervision as he is knowledgeable, experienced, and passionate.

Second, I would like to extend my appreciation to Mohammad Chowdhury for his friendship and support. I would like to thank current and former colleagues: August Wang, Basem Haroun, Chinaza Akobi, Kai Li, Joseph Donohue, Kyriakos Manoli, Medhavi Gupta, Maritza Gomez-Flores, Masuduz Zaman, Nan Yang and Dr. Mingu Kim. They all contributed to creating a very friendly working environment and a highly efficient team. Thanks for being such great colleagues.

I acknowledge the Clean Technologies for Water Refining and Nutrients and Energy Recovery (TWNER) - Natural Science and Engineering Research Council (NSERC) – Collaborative Research and Training Experience (CREATE) Training Program, Canada, for the financial support.

Finally, I also want to appreciate the tremendous love, support, and encouragement from my parents, Yizhang Liu and Huiping Yang, as well as my wife, Chuyun Zhang. Without you, I would not have achieved what I have today.

Table of Contents

List of Tables

List of Figures

List of Appendices

List of Acronyms

ALR ammonia loading rate

AMO ammonia monooxygenase

AOB Ammonia-oxidizing bacteria

AVN ammonia versus nitrate-plus-nitrite

BF blower frequency

BNR Biological nitrogen removal

CASP conventional activated sludge process

CSTR Continuous stirred-tank reactor

HAO hydroxylamine oxidoreductase

HH Hydrazine hydrolase

HZO Hydrazine-oxidizing enzyme

HZS Hydrazine synthase

IBS Immobilised biomass system

MABR Membrane aerated biofilm reactor

MBR membrane biofilm reactor

MBBR Moving bed biofilm reactor

MSC Minimum/maximum substrate concentration

NBP nitrogen break point

NOB Nitrite-oxidizing bacteria

NR Nitrite-reducing enzyme

NXR nitrite oxidoreductase

RSP set-point ratio

SBNR Shortcut biological nitrogen removal reactor

SBR Sequencing batch reactor

SBS Suspended biomass system

SND simultaneous nitrification and denitrification

S_{max} Maximum substrate concentration

S_{min} Minimum substrate concentration

TKN Total Kjeldahl Nitrogen

Nomenclature

Symbol	Description	Units
ACR	Ammonia converstion ratio	%
AOR	Maximum ammonia oxidation rate	mg N/(L·min)
b	Decay coefficient	d^{-1}
b_{AOB}	Decay coefficient for AOB	d^{-1}
b_{NOB}	Decay coefficient for NOB	d^{-1}
DO	Dissolved oxygen	mg O_2/L
FA	Free ammonia	mg N/L
FNA	Free nitrous acid	mg N/L
HRT	Hydraulic retention time	h
K_{FA}	Monod half-saturation concentrations for FA	mg N/L
K_{IFA}	inhibition concentration for FA	mg N/L
K_{IFNA}	inhibition concentration for FNA	mg N/L
$K_{I,Ni}$	Half-velocity inhibition nickel concentration	mg Ni/L
$K_{I, Ni/MLSS}$	Half-velocity inhibition constant based on Ni/MLSS ratio	mg Ni/g MLSS
Ko	Monod half-saturation concentrations for DO	mg O_2/L
K_{TNN}	Monod half-saturation concentrations for TNN	mg N/L
NAR	Nitrite accumulation ratio	%
NOR	Maximum nitrite oxidation rate	mg N/(L·min)
OUR	Oxygen utilization rate	mg O2/L/hr
ORP	Oxidation Reduction Potential	mV
pH_{opt}	Optimal pH	
Q	Q is inflow rate	L/d
q_{AOB}	Maximum specific substrate utilization rates for AOB	mg N/(mg VSS·d)

q_{NOB}	Maximum specific substrate utilization rates for NOB	mg N/(mg VSS·d)
SRT	Solids retention time	d
SAOR	Spercific ammonia oxidation rate	mg N/g MLSS-hr
SNOR	Specific nitrite oxidation rate	mg N/g MLSS-hr
S_{NH}	Effluent ammonia concentrations	mg N/L
S_{NO2}	Effluent nitrite concentrations	mg N/L
S_{NO3}	Effluent nitrate concentrations	mg N/L
T	Temperature	^{o}C
TAN	Total ammonium nitrogen	mg N/L
TNN	Total nitrite nitrogen	mg N/L
V	Volume	L
w	pH range	
X_{AOB}	AOB biomass concentration	mg VSS/L
X_{NOB}	NOB biomass concentration	mg VSS/L
Y_{AOB}	Yield coefficient for AOB	mg VSS/mg N
Y_{NOB}	Yield coefficient for NOB	mg VSS/mg N
μ_{max}	Maximum growth rate	d^{-1}
θ_{Ks}	Temperature coefficient for Ks	
θ_{μ}	Temperature coefficient for μ_{max}	
θ_{b}	Temperature coefficient for b	

Chapter 1

1 Introduction

1.1 Rationale

Eutrophication can be stimulated by nitrogen as well as phosphorus. Thus, the discharge of nitrogen from wastewater treatment plants has been strictly regulated in the last two decades. Conventional biological nitrogen removal processes, which consist of nitrification–denitrification, have been applied worldwide. However, there are three concerns about the conventional BNR process. First, it consumes high amount of energy for nitrification; second, it requires external organic carbon sources for denitrification; third, it can release considerable amounts of nitrous oxide (N_2O), the carbon footprint of which is over 300 times greater than CO_2 over a 100-year period on climate [1].

Alternatively, new processes including partial nitrification-denitrification and partial nitrification-anammox have been put forward. Compared with conventional BNR process, these new processes consume lower energy, require less organic carbon, and produce less sludge [2,3]. However, the N_2O emissions of partial nitrification has been reported as 4 to 14 times higher than full nitrification [4].

One hot topic that recently emerged centers on the feasibility and performance of nitritation at low temperature and low nitrogen concentration due to the motivation to further apply nitritation-anammox process for mainstream wastewater, which is characterized by low nitrogen concentrations (20 to 60 mg NH_4-N l^{-1}) and low temperatures (5-25°C) [5–7].

This topic is more applicable to northern countries like Canada. In southern Ontario, the wastewater temperature can be as low as 14^{o}C [8].

Several strategies have been adopted to realize partial nitrification. The strategies are: high temperature, pH, low dissolved oxygen (DO), short sludge retention time (SRT), high free ammonia (FA), and chemical inhibitors [9–11]. The operational conditions are correlated to each other. Also, despite the chemical inhibitors, the optimal operational conditions to realize partial nitrification are determined by microbial kinetics.

1.2 Thesis objectives

The specific objectives of this thesis are as follows:

1) development of a mathematical model involving operational parameters for determination of successful partial nitrification conditions;

2) analyzing the factors affecting the performance of partial nitrification in a sequencing batch reactor (SBR) using kinetic models at 35^{o}C;

3) investigating the effect of DO on nitrification in a sequencing batch reactor (SBR) treating low ammonia wastewater (40 mg N/L) at low temperature (14^{o}C);

4) investigating the chronic and acute effect of nickel on nitrification in a sequencing batch reactor (SBR) treating low ammonia wastewater (40 mg N/L) at low temperature (10^{o}C).

1.3 Thesis Organization

This PhD thesis is written in the article-integrated format specified by the school of Graduate and Postdoctoral Studies at The University of Western Ontario. The contents of the seven chapters included in this thesis are presented below:

Chapter 1 presents a general introduction related to the background and motivation for studying the effect of operational conditions on nitrification at different temperatures. The research objectives of the thesis are also included in Chapter 1.

A literature review including background on biological nitrogen removal (BNR) is presented in chapter 2. The research progress related to three generations of BNR processes (conventional BNR process, partial nitrification-denitrification and partial nitrification-anammox) is presented.

Chapter 3 is a research article entitled "A model for determination of operational conditions for successful shortcut nitrification". In this study, a model based on minimum dissolved oxygen concentration (DO_{min}), minimum/maximum substrate concentration (S_{min} and S_{max}), was developed. In addition, the effect of temperature (10-35^{o}C), pH (7-9), and SRT (5d-infinity) was analyzed. Specific application for partial nitrification-anammox process at 10^{o}C was analyzed. Comparison of the model predicted DO_{min} with experimental data suggested that this model can be a useful and practical tool for shortcut nitrification systems design and operation.

Chapter 4 is a research article entitled "Operational conditions for successful partial nitrification in a sequencing batch reactor (SBR) based on process kinetics". In this study,

an SBR was operated for 4 months treating synthetic wastewater with ammonia in the range of 35–200 mg N/L at varying DO concentrations as well as continuous and intermittent aeration. Stable nitrite accumulation was observed at two conditions. Kinetic parameters were determined or estimated with batch tests and model simulation. The kinetic model predicted the SBR performance well.

Chapter 5 is a research article entitled "Performance and kinetics of nitrification of low ammonia wastewater at low temperature". In this study, an SBR was operated for over 4 months treating low-ammonia (40 mg N/L) synthetic wastewater at low temperature (14^{o}C) and an SRT of 10 days. The DO effect was invstestigated at DO levels of 5-6 mg/L, 2-3 mg/L and 0.8-1.0 mg/L. This is the first attempt to directly measure the kinetics of the nitrifiers which are cultivated at low temperature.

Chapter 6 is a research article entitled "Acute and chronic toxicity of nickel to nitrifiers at low temperature". In this study, chronic toxicity of nickel to nitrification of low ammonia synthetic wastewater was investigated at 10^{o}C in two SBRs with 1 mg/L nickel dosing either from the beginning or after biomass concentration decreased to 300 mg/L. Acute toxicity of nickel to nitrification at 10^{o}C, 23^{o}C, and 35^{o}C was evaluated by short-term batch tests. This is the first study to compare the acute toxicity of nickel to nitrification at different temperatures and the first study on the chronic toxicity of nickel to nitrification at 10^{o}C.

Chapter 7 includes the main conclusions of the thesis along with scientific contributions, study limitations and recommendations for future work.

1.4 References

[1] D.J. Griggs, M. Noguer, Climate change 2001: the scientific basis. Contribution of working group I to the third assessment report of the intergovernmental panel on climate change, Weather. 57 (2002) 267–269.

[2] M. Beccari, R. Passino, R. Ramadori, V. Tandoi, Kinetics of dissimilatory nitrate and nitrite reduction in suspended growth culture, J. Water Pollut. Control Fed. (1983) 58–64.

[3] R. Van Kempen, J.W. Mulder, C.A. Uijterlinde, M.C.M. Loosdrecht, Overview: full scale experience of the SHARON® process for treatment of rejection water of digested sludge dewatering, Water Sci. Technol. 44 (2001) 145–152.

[4] J.H. Ahn, T. Kwan, K. Chandran, Comparison of partial and full nitrification processes applied for treating high-strength nitrogen wastewaters: microbial ecology through nitrous oxide production, Environ. Sci. Technol. 45 (2011) 2734–2740.

[5] Z. Hu, T. Lotti, M. de Kreuk, R. Kleerebezem, M. van Loosdrecht, J. Kruit, M.S.M. Jetten, B. Kartal, Nitrogen removal by a nitritation-anammox bioreactor at low temperature, Appl. Environ. Microbiol. 79 (2013) 2807–2812.

[6] E.M. Gilbert, S. Agrawal, S.M. Karst, H. Horn, P.H. Nielsen, S. Lackner, Low temperature partial nitritation/anammox in a moving bed biofilm reactor treating low strength wastewater, Environ. Sci. Technol. 48 (2014) 8784–8792.

[7] H. De Clippeleir, S.E. Vlaeminck, F. De Wilde, K. Daeninck, M. Mosquera, P. Boeckx, W. Verstraete, N. Boon, One-stage partial nitritation/anammox at 15 C on pretreated sewage: feasibility demonstration at lab-scale, Appl. Microbiol. Biotechnol. 97 (2013) 10199–10210.

[8] X. Liu, M. Kim, G. Nakhla, Performance and kinetics of nitrification of low ammonia wastewater at low temperature, Water Environ. Res. 90 (2018) 498–509.

[9] J. Surmacz-Górska, A. Cichon, K. Miksch, Nitrogen removal from wastewater with high ammonia nitrogen concentration via shorter nitrification and denitrification, Water Sci. Technol. 36 (1997) 73–78.

[10] U. van Dongen, M.S.M. Jetten, M.C.M. Van Loosdrecht, The SHARON®-Anammox® process for treatment of ammonium rich wastewater, Water Sci. Technol. 44 (2001) 153–160.

[11] J. López-Fiuza, B. Buys, A. Mosquera-Corral, F. Omil, R. Méndez, Toxic effects exerted on methanogenic, nitrifying and denitrifying bacteria by chemicals used in a milk analysis laboratory, Enzyme Microb. Technol. 31 (2002) 976–985.

Chapter 2

2 Literature review

2.1 Introduction

Nitrogen in wastewater treatment plant effluents has adverse environmental effects on aquatic systems. Excessive concentrations of nitrogen in water bodies can result in eutrophication which would translate to accelerated growth of algae and plankton over other plants, leading to the depletion of dissolved oxygen, deterioration of water quality, and shifts of biotic community [1,2]. Therefore, most countries apply stringent discharge standards on organic and ammonium nitrogen.

Most nitrogen in raw municipal wastewaters is in the form of organic nitrogen, and ammonia with limited nitrate and nitrite concentrations. Ammonia and organic nitrogen are often combined together, and measured as Total Kjeldahl Nitrogen (TKN). Both physico-chemical and biological methods have been put forward to eliminate nitrogen from wastewater [3]. Among all these strategies, BNR, is still the most economically feasible and effective treatment for municipal and industrial wastewaters [4].

Till now, three generations of biological processes have been put forward: conventional BNR process, partial nitrification-denitrification process, and partial nitrification-anammox process.

2.2 Biological nitrogen removal processes

2.2.1 Conventional BNR process

Conventional biological wastewater treatment process consists of two steps: nitrification followed by denitrification, as shown in Figure 2-1.

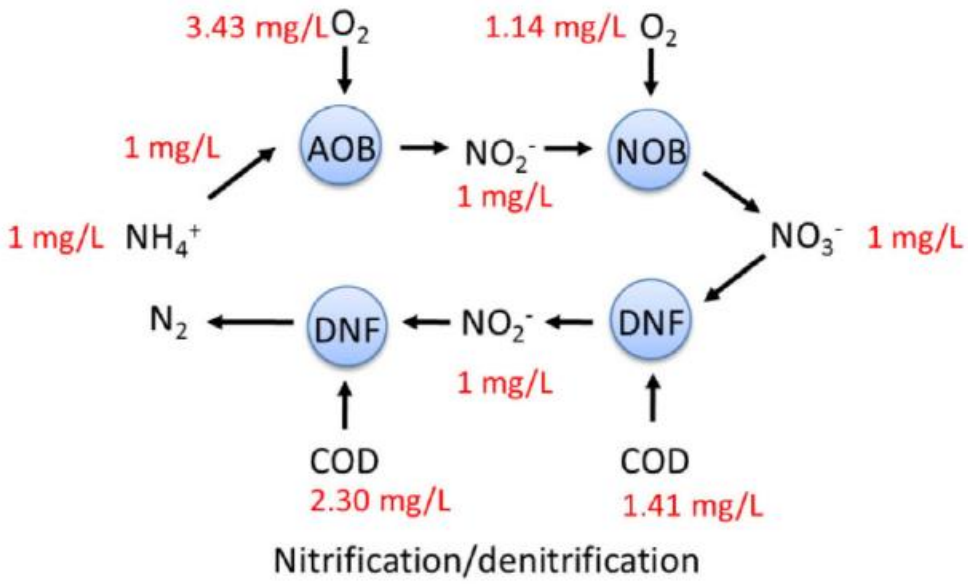

Figure 2-1. Conventional BNR process (adapted from [5])

Nitrification implies an autotrophic oxidation of ammonia to nitrate under aerobic conditions. Nitrification is conducted in two steps: first, ammonia is oxidized to nitrite by ammonia oxidizing bacteria (AOB); second, nitrite is further oxidized to nitrate by nitrite oxidizing bacteria (NOB). Both AOB and NOB are autotrophic bacteria. They use carbon dioxide as the carbon source and molecular oxygen as an electron acceptor. Ammonia or nitrite are the electron donor for AOB and NOB, respectively [6,7].

The stoichiometry of biological nitrification is as follows:

AOBs: $2NH_4^+ + 3O_2 \rightarrow 2NO_2^- + 2H_2O$ (Eq.2.1)

NOBs: $2NO_2^- + O_2 \rightarrow 2NO_3^-$ (Eq.2.2)

Total oxidation reaction: $NH_4^+ + 2O_2 \rightarrow NO_3^- + 2H^+ + H_2O$ (Eq.2.3)

Based on the above stoichiometry, complete oxidation of 1g ammonia nitrogen requires 4.57 g O_2, with 3.43 g O_2 and 1.14 g O_2 in each stage, respectively. As acid is generated alkalinity is needed to neutralize the solution.

The full nitrification reaction can be approximated by Equation 2.4.

$NH_4^+ + 2HCO_3^- + 2O_2 \rightarrow NO_3^- + 2CO_2 + 3H_2O$ (Eq.2.4)

In this equation, for each gram of ammonia nitrogen (as N), 7.14g of alkalinity as $CaCO_3$ will be required.

Along with obtaining energy, a portion of the ammonium ion is assimilated into cell tissue. Equations for the biochemical conversion of ammonia to nitrate with cell synthesis using a representative measurement of yield and oxygen consumption for AOBs and NOBs are as follows [3]:

AOBs: $55NH_4^+ + 76O_2 + 109HCO_3^- \rightarrow C_5H_7O_2N + 54NO_2^- + 57H_2O + 104H_2CO_3$ (Eq.2.5)

NOBs: $400NO_2^{-+}NH_4^+ + 4H_2CO_{3+}195O_2 + HCO_3^- \rightarrow C_5H_7O_2N + 400NO_3^- + 3H_2O$ (Eq.2.6)

Overall reaction:

$$NH_4^+ + 1.83O_2 + 1.98HCO_3^- \rightarrow 0.021C_5H_7O_2N + 0.98NO_3^- + 1.041H_2O + 1.88H_2CO_3 \quad \text{(Eq.2.7)}$$

In the above equations, yields of AOBs and NOBs are 0.15 mg cells/mg NH_4-N oxidized and 0.02 mg cells/mg NO_2-N oxidized, respectively. Oxygen consumption ratios in the equations are 3.16 mg O_2/mg NH_4-N oxidized and 1.11 mg O_2/mg NO_2-N oxidized, respectively. Also, 7.07 mg alkalinity as $CaCO_3$ is required per mg ammonia nitrogen oxidized to nitrate nitrogen.

Denitrification is an anoxic process, during which nitrite or nitrate is converted to nitrogen gas (N_2) by heterotrophic denitrifying bacteria. Denitrification utilizes organic matter as electron donor and nitrite or nitrate as electron acceptor instead of oxygen. Commonly used carbon source includes acetate, glucose, sugar, methanol and a variety of food and beverage wastes with the general chemical formula of $C_{10}H_{19}O_3N$ [3]. The general reaction of denitrification is shown below:

$$C_{10}H_{19}O_3N + 10NO_3^- \rightarrow 5N_2 + 10CO_2 + 3H_2O + NH_3 + 10OH^- \quad \text{(Eq.2.8)}$$

However, for different organic carbons, the specific denitrification reaction are different. For example, the stoichiometry for acetate is shown in equation 2.9.

$$5CH_3COOH + 8NO_3^- \rightarrow 4N_2 + 10CO_2 + 6H_2O + NH_3 + 8OH^- \quad \text{(Eq.2.9)}$$

Based on the above equations, contrary to nitrification, alkalinity is produced rather than consumed in denitrification. For each gram of nitrate reduced, 3.57 gram of alkalinity is produced, which is half that consumed in nitrification.

Optimum operational conditions for denitrification are depicted below in Table 2-1.

Table 2-1. Optimums operational conditions for denitrification process

Parameters	Value
Temperature (^{o}C)	20-40
Dissolved oxygen (mg/L)	<0.2
Free nitrous acid (FNA) (mg N/L)	<0.01
pH	7.0-7.5
SRT (d)	3-6

2.2.2 Simultaneous Nitrification and Denitrification (SND)

As nitrification and denitrification are carried out by different microorganisms under different conditions (aerobic and anoxic), they should be designed and operated in separate time sequences or spaces, which is common in conventional BNR processes [8]. As a result, a long retention time or a large volume is required to accomplish complete nitrogen removal. Conversely, in simultaneous nitrification and denitrification (SND), nitrification and denitrification occur concurrently in the same reactor [9,10]. Thus, both time and space are saved greatly. There are two mechanisms involved in SND: physical and biological [11–13].

Physically, SND occurs as a result of DO concentration gradients within activated sludge flocs or biofilms due to diffusional limitations (Figure 2.2), which has been confirmed by microelectrode measurements [14–17]and ^{15}N tracer techniques [18]. The nitrifiers and the denitrifiers exist in aerobic regions with DO higher than 1-2 mg/L, and in anoxic zones with DO less than 0.5 mg/L, respectively.

The biological mechanism for SND is very complex. From a microbiological point of view, SND results from oxidization of ammonia by heterotrophic nitrifiers and the reduction of nitrate or nitrite by aerobic denitrifiers [18–20]. For example, *T. pantotropha* was identified as not only a heterotrophic nitrifier but also an aerobic denitrifier, which can carry out the following reactions sequentially and simultaneously in the presence of a suitable electron donor (e.g. acetate)[19].

$$NH_4^+ \longrightarrow NH_2OH \longrightarrow NO_2^- \longrightarrow N_2O \longrightarrow N_2$$

SND has significant advantages over conventional processes [21,22]. Not only is the cost for anoxic tanks saved, but also the overall process design is simplified.

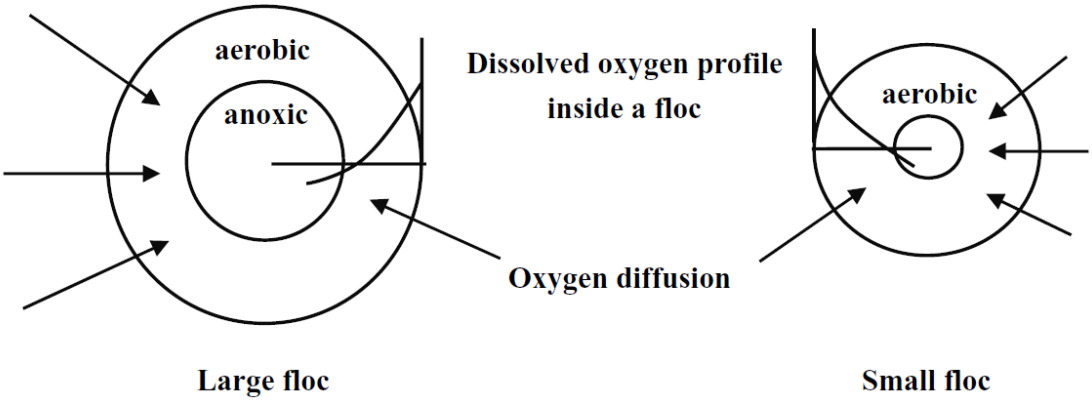

Figure 2-2. Schematic of oxygen concentration profile within a microbial floc. (adapted from [23])

2.2.3 Partial nitrification-denitrification

Partial nitrification-denitritation process is a partial nitrification to nitrite followed by nitrite denitrification [24,25].

The reactions involved in this process are shown below [26]:

Partial nitrification:

$NH_4^+ + 1.5O_2 + 2HCO_3^- \rightarrow NO_2^- + 2CO_2 + 3H_2O$ (Eq.2.10)

Denitrification:

$NO_2^- + 4H^+ + 3e^- \rightarrow 0.5N_2 + 2H_2O$ (Eq.2.11)

Global equation of partial nitrification-denitritation:

$NH_4^+ + 1.5O_2 + 2H^+ + 3e^- \rightarrow 0.5N_2 + 3H_2O$ (Eq.2.12)

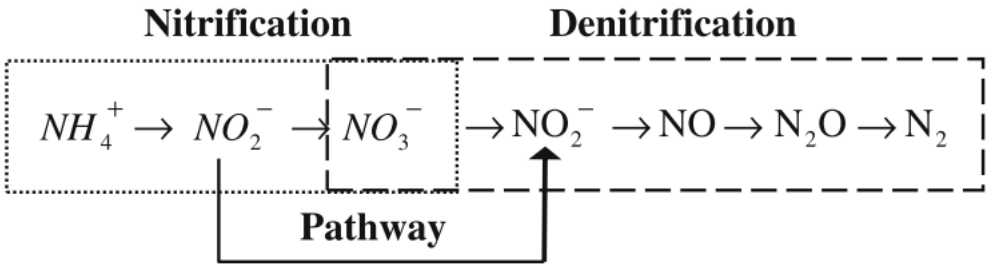

Figure 2-3. Partial nitrification-denitrification process (adapted from [26])

Compared with conventional BNR processes, the main reported advantages of partial nitrification and denitrification via nitrite are as followed [27–29]:

1) 25% lower oxygen consumption in the aerobic stage.

2) In the anoxic stage, the electron donor requirement is lower (up to 40%).

3) Nitrite denitrification rates are 1.5 to 2 times higher than with nitrates.

4) 33%-35% lower sludge production in nitrification and 55% lower sludge production in denitrification, respectively.

2.2.4 Partial nitrification-anammox

An alternative route for biological nitrogen removal is provided by anammox-based processes. Anammox is the shortcut of ammonia removal cycles, which directly converts ammonium to nitrogen gas and a small amount of nitrate using nitrite as an electron acceptor under strict anoxic conditions [30]. Anammox bacteria account for about 50% of all N_2 released into the atmosphere [31]. Anammox bacteria are strict anaerobes and autotrophs. They are characterized by slow growth rates and have a long doubling time of 10 to 12 days at 35ºC [32, 33]. Anammox bacteria utilize CO_2 as the sole carbon source and NO_2 as the electron acceptor for ammonium oxidation [34]. The stoichiometry of the overall anammox metabolic reaction is described below:

$$NH_4^+ + 1.32NO_2^- + 0.066HCO_3^- + 0.13H^+ \rightarrow 1.02N_2 + 0.256NO_3^- + 0.066CH_2O_{0.5}N_{0.15} + 2.03H_2O \quad \text{(Eq.2.13)}$$

As can be seen in Eq.2.13, anammox bacteria need nitrite as an electron acceptor. Thus, combination of nitritation and anammox process is a good choice for biological nitrogen removal. Approximately 55% of the ammonia is converted to nitrite during nitritation and then the effluent enters the anammox process.

The possible mechanism for anaerobic ammonium oxidation is shown in Fig 2-4 [35]. Part a in Fig 2-4 depicts the organellelike structure of the anammox microbe in which the energy-generating process involving the combination of ammonia with nitrite uptakes

occurs. Part b in Fig 2.4 shows the anammoxosome membrane and the anammox reaction pathway. The nitrite-reducing enzyme (NR) is on the cytoplasm side of the cell membrane. It catalyzes the reduction of NO_2^- to hydroxylamine. Hydrazine hydrolase (HH) across the cell membrane condenses hydroxylamine and ammonia to hydrazine. Hydrazine-oxidizing enzyme (HZO) is on the anammoxosome side of the cell membrane and catalyzes hydrazine to nitrogen. The electrons generated from these reactions are transferred back to NR.

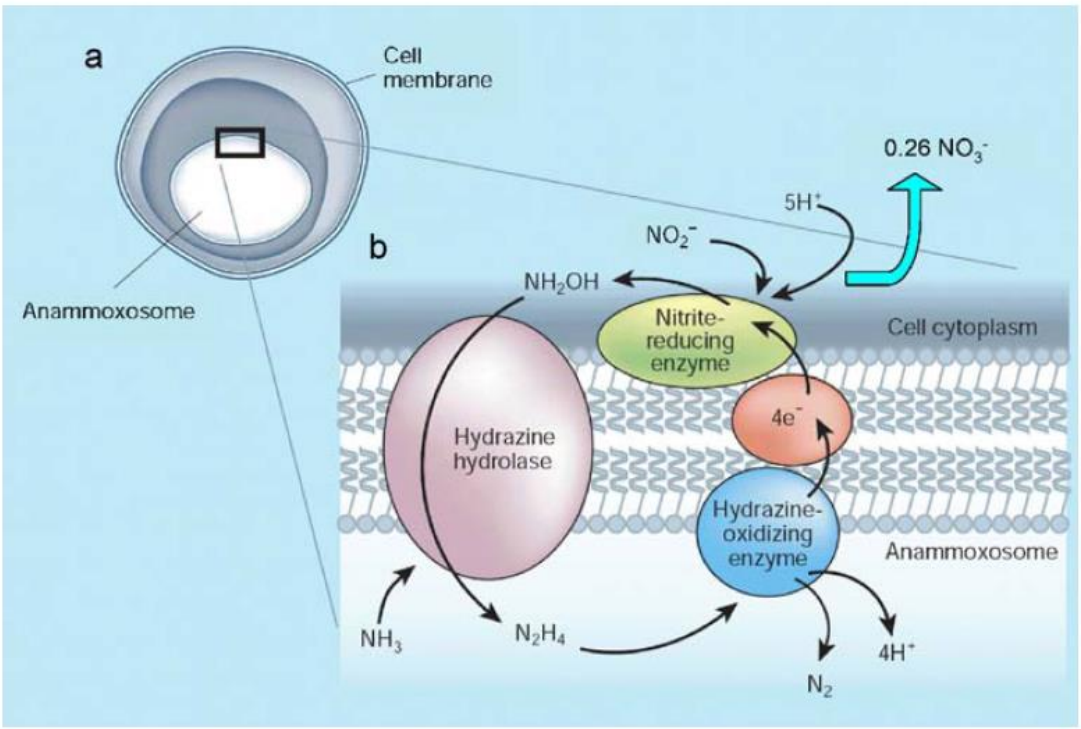

Figure 2-4. Mechanism of anaerobic ammonium oxidation.(adapted from [35]).

In addition to this, it has been proposed that anammox is a three-reaction process (Eqs. 2.14-2.16) [36,37]. NO_2^- is reduced by nitrite reductase (NirS) to NO, which subsequently reacts with NH_4^+ to form N_2H_4, catalyzed by the unique hydrazine synthase (HZS), and

finally N_2H_4 is oxidized to N_2 by hydrazine dehydrogenase/oxidoreductase (HDH/HZO). It should be noted that the reactions only consider chemical mechanisms and neglect biomass synthesis.

$$NH_2OH+NH_3 \rightarrow N_2H_4+H_2O \quad \text{(Eq.2.14)}$$

$$N_2H_4 \rightarrow N_2+4[H] \quad \text{(Eq.2.15)}$$

$$HNO_2+4[H] \rightarrow NH_2OH+H_2O \quad \text{(Eq.2.16)}$$

$$NH_3+HNO_2 \rightarrow N_2+2H_2O \quad \text{(Eq.2.17)}$$

$$HNO_2+H_2O+NAD \rightarrow HNO_3+NADH_2 \quad \text{(Eq.2.18)}$$

Partial nitrification-anammox process is also called the nitritation-anammox process. First, around 57% of the ammonia is oxidized to nitrite by AOBs. Second, the remaining ammonia and the nitrite are converted to nitrogen gas by anammox bacteria. The scheme of partial nitrification-anammox process is shown below in Figure 2-5.

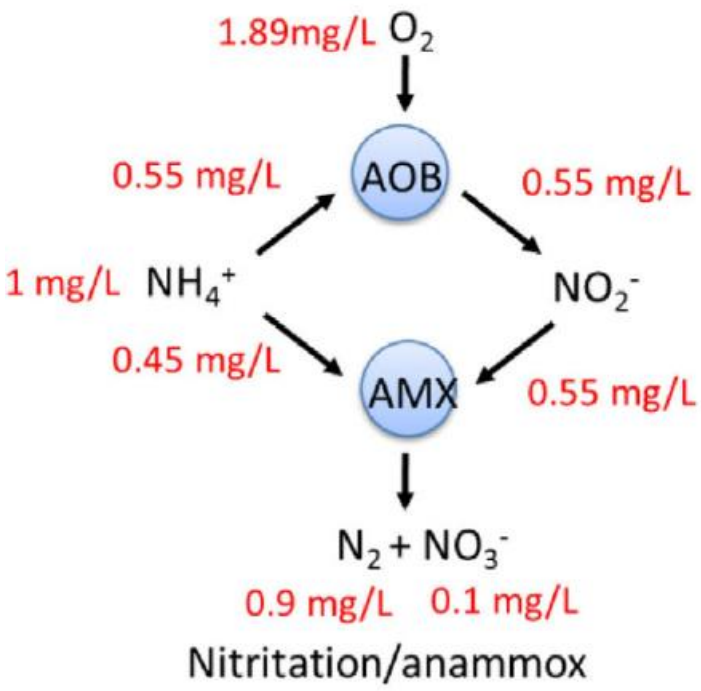

Figure 2-5. Partial nitrification-anammox process (adapted from [4])

2.2.5 Comparison of N removal processes

The comparison of the three biological nitrogen removal processes is depicted below in Table 2.2 with respect to bacteria involved, oxygen demand, COD needed, and alkalinity consumption and operational cost. The operational cost includes the aeration tank cost, i.e. aeration cost, as well as the cost of sludge treatment and disposal.

Table 2-2. Comparison of N removal processes

Processes	Conventional BNR	Partial nitrification-denitrification	Partial nitrification-anammox
Bacteria involved	AOBs/NOBs/denitrifiers	AOBs/denitrifiers	AOBs/Anammox
Oxygen demand (g O_2/g N) [a]	4.18	3.16	1.94
COD needed (g COD/g N)[b]	4.0	2.4	0
Operational cost [c]	2-4 Euro/kg N removed	1 Euro/kg N removed	1 Euro/kg N removed; Sludge treatment and disposal cost decrease
Alkalinity consumption (g $CaCO_3$/g N) [a]	7.07/-3.57	7.07/-3.57	4.02

[a] source:[4]

[b] source:[38]

[c] source:[39,40]

2.3 Microbiology

2.3.1 AOBs and NOBs

The most commonly recognized genus of bacteria that carries out ammonia oxidation is *Nitrosomonas* while *Nitrosococcus, Nitrosopira, Nitrosovibrio, and Nitrosolobus* are also able to oxidize ammonia to nitrite. These five recognized genera of AOB can be divided into two different phylogenetically distinct groups, β- and γ-subclass of *Proteobacteria* based on comparative 16S rRNA sequence analyses [41,42]. *Nitrosomonas, Nitrosopira,*

Nitrosovibrio, and Nitrosolobus are grouped in the β- subclass while *Nitrosococcus* is the only one within the γ-subclass [43,44].

In the nitrite oxidation stage, several genera such as *Nitrospira*, *Nitrospina* and *Nitrococcus* are known to be involved while the most famous nitrite oxidizer genus is *Nitrobacter* [4]. *Nitrococcus* and *Nitrobacter* are assigned to the α- and γ-subclass of *Proteobacteria*, respectively [45]. The genus of *Nitrospira* is grouped closely to the δ-subclass [42].

The characteristics and environmental conditions of different autotrophic AOB and NOB species are presented in Tables 2.3 and 2.4 [46,47].

Table 2-3. Characteristics and environmental conditions of different AOB species

Parameters	*Nitrosomonas*	*Nitrosococcus*	*Nitrosopira*	*Nitrosolobus*	*Nitrosovibrio*
Shape	Straight rods	Spherical to ellipsoidal	Tightly coiled spirals	Pleomorphic lobate	Slender curved rods
Size (μm)	(0.7-1.5)× (1.0-2.4)	(1.5-1.8)× (1.7-2.5)	(0.3-0.8)× (1.0-8.0)	(1.0-1.5)× (1.0-2.5)	(0.3-0.4)× (1.1-3.0)
pH	7.0-8.5	6.0-8.0	6.5-8.5	6.0-8.2	7.5-7.8
Temperature (ºC)	5-40	2-40	20-35	15-30	25-40

Table 2-4. Characteristics and environmental conditions of different NOB species

Parameters	Nitrobacter	Nitrospina	Nitrococcus	Nitrospira
Shape	Pear-shaped/ pleomorphic rods	Slender straight rods	Spherical	Loosely coiled spirals
Size (μm)	(0.5-0.8)× (1.0-2.0)	(0.3-0.4)× (1.7-6.6)	1.5-1.8	(0.3-0.4)× (0.8–1.0)
pH	6.0-7.5	6.5-7.0	6.8-8.0	6.5-7.0
Temperature (ºC)	5-30	25-30	15-30	25-30

2.3.2 Key enzymes of AOB

Two key enzymes, the ammonia monooxygenase (AMO) and the hydroxylamine

oxidoreductase (HAO), catalyze the conversion of ammonia to nitrite via NH_2OH. AMO is a membrane-bound hetero-trimeric copper enzyme, and has broad substrate ranges [48]. It is coded by three gene subunits amoC (31.4 kDa), amoA (31.4 kDa) and amoB (38 kDa) while only a small portion of amoA acts as a function gene of AOBs [43,49,50].

Compared with AMO, HAO was isolated and studied more extensively. HAO is coded by the gene clusters of hao (hydroxylamine oxidoreductase, 1710 bp) (Figure 2.6) [43,51]. Three copies of hao gene, that constitute 40% of the c-type heme, are contained in the genus of *Nitrosomonas europaea* [52].

NirK is another enzyme found in multiple AOBs. The function of NirK was assumed to be related to nitrite reduction, which, however, has not been confirmed [53].

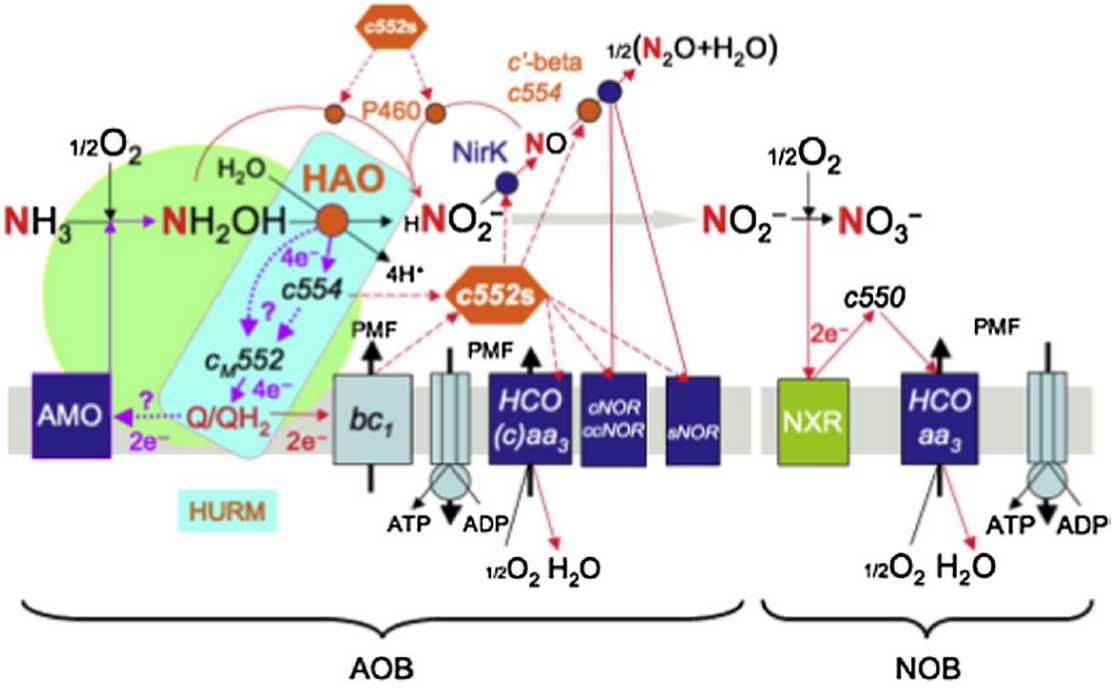

Figure 2-6. Flow of energy and reductants in nitrification through pertinent catabolic modules in AOB and NOB (adapted from [54])

2.3.3 Key enzymes of NOB

The key enzyme involved in the nitrite oxidation to nitrate is nitrite oxidoreductase (NXR) in *Nitrobacter*, and nitrite oxidizing system in the genera of *Nitro*coccus, *Nitrospina*, and *Nitrospira* (Figure 2-6). NXR composition is quite complex. It consistes of subunits such as α-subunit, NorA (115-130 kDa), β-subunit, and NorB (65 kDa) [55]. The function of NorA might be the acceletration of the nitrite oxidation, while NorB might work effectively as an electron-channeling protein between NorA and the membrane-integrated electron-transport chain [55].

2.3.4 Kinetics of AOB and NOB

AOB and NOB kinetics, including maximum growth rate (μ_{max}), decay rate (b), substrate half saturation constant (Ks), oxygen half saturation constant (Ko), yield coefficient (Y), free ammonia half-velocity constant (K_{iFA}), and free nitrous acid half-velocity constant (K_{iFNA}) have been thoroughly studied due to their crucial importance in controlling and optimizing nitrogen removal processes. However, the reported kinetic values varied in a very wide range, as summarized in Table 2-5 and 2-6 for AOB and NOB, respectively. The big differences result from various wastewater characteristics, reactor configurations, as well as operational conditions.

Influent ammonia concentration affects the K_{iFA} of AOB. In some studies, ammonia oxidation was observed at relatively low FA concentrations (~10 mg N/L). In the study of Abeling and Seyfried [56], nitritation inhibition was observed at 7 mg FA/L. Anthonisen [57] found nitritation inhibition at a FA range from 10-150 mg N/L (pH 7-9, temperature

of 20ºC, TAN of 60-3000 mg N/L). Neufeld et al. [58] and Groeneweg et al. [59] also reported the beginning of nitritation at a FA concentration of 10 mg N/L (pH of 7-9 and 8, temperature of 23ºC and 30ºC, TAN of 20-1500 mg N/L and 100 mgN/L). Jubany et al.[60] reported a K_{iFA} of around 7 mg N/L (pH 7.5, temperature of 25ºC, TAN of 450 mg N/L). On the contrary, there are some other studies reporting a much higher FA concentration for nitritation inhibition. For example, nitritation was only observed at concentrations above 300 mg FA/L (pH 8, temperature of 35ºC, TAN of 2500 mg N/L)[61]. Hellinga et al. [62] found no nitritation inhibition up to 93 mg FA/L (pH 7, temperature 40ºC, TAN of 5000 mg N/L). Baquerizo et al. [63] determined an FA inhibition coefficient of 116±24 mg FA/L. The substrate inhibition constant in the study of Pambrun et al. [64] was 241 mg FA/L (pH 8.25, temperature of 35ºC, TAN of 1200 mg N/L). Acclimatization of the AOB to high ammonia concentrations (500-1000 mg N/L) after 400 days exposure was presumed to be the reason for the high FA inhibition constant [64]. The highest inhibition coefficient of 605±87 mg N/L reported by Ganigue´ et al. [65] was attributed to acclimatization of the biomass to the inhibitory effects of FA due to a long term exposure (160 days) to high influent ammonia concentrations(518-1440 mg N/L) as well. The tolerance of NOB to FA may be enhanced by long-term acclimatization to high FA environment. Wong-Chong and Loehr [66] observed that the *Nitrobacter* could tolerate FA concentrations as high as 40 mg N/L after acclimatization to high FA for 2-3 weeks, while the unacclimated cultures were inhibited at a FA concentrations of 3.5 mg N/L.

The effect of reactor configuration on biomass kinetics has not been confirmed yet. In the study of Carrera et al. [67], with the same influent ammonia concentration of 1000 mg N/L, the same operational conditions (pH of 7.5 ± 0.1 and temperature of 23 ± 0.5), biomass

from a suspended biomass system (SBS) and an immobilised biomass system (IBS) have different μ_{max} (0.97 vs 0.34 d^{-1}), K_s (11 vs 28 mg N/L) and K_{iFA} (13.9 vs 58.8 mg N/L). On the contrary, Munz et al. [68] reported the same μ_{max} of 0.45±0.04 d^{-1} and quite similar b of 0.08±0.04 d^{-1} and 0.10±0.06 d^{-1} for biomass from a membrane biofilm reactor (MBR) and a conventional activated sludge process (CASP) with the same influent ammonia concentration of 35±7.7 mg N/L and the same operational conditions (SRT of 20 days, temperature of 18-20ºC and pH of 7.7±0.1 or 7.6±0.1).

Temperature traditionally was regarded as having a clear effect on the ammonia oxidation in partial nitrification systems. Both AOB and NOB acitivity are enhanced as temperature increases [69]. Typical temperature coefficients for $\mu_{max,AOB}$ and $\mu_{max,NOB}$ are 1.072 and 1.063, respectively [70]. The typical temperature coefficient for b of both AOB and NOB is 1.04[70]. In addition, Weon et al. [71] reported that $K_{o,AOB}$ and $K_{o,NOB}$ decreased from 1.61 mg O_2/L and 1.10 mg O_2/L at 5ºC to 0.27 mg O_2/L and 0.87 mg O_2/L at 30ºC, which suggested that both $K_{o,AOB}$ and $K_{o,NOB}$ may decrease as temperature increase. pH affects the activity of nitrifiers directly or indirectly through FA and FNA. The model equations of direct pH effects on AOB and NOB by Park et al. [72] are depicted below.

$$\mu = \frac{\mu_{max}}{2} \cdot \{1 + \cos[\frac{\pi}{w} \cdot (pH - pH_{opt}) \quad (|pH - pH_{opt}|<w)) \qquad \text{(Eq.2.19)}$$

μ and μ_{max} are, respectively, the maximum specific growth rate at a given pH and at the optimal pH, d^{-1}. w is the pH range within which the q is larger than one-half of $q_{max.}$

Besides, it has been reported that Ks of AOB is also a function of pH and the relationship between pH and $K_{s,AOB}$/ $K_{s,NOB}$ are shown in Eq.22.20 and 2.21, respectively [73].

$$K_{s,AOB} = 0.56 \cdot \left[\frac{1}{1+\frac{[H^+]}{10^{-6.96}}}\right] \cdot [1 + \frac{[H^+]}{10^{-9.093}}] \quad \text{(Eq.2.20)}$$

$$K_{s,NOB} = 4.018 \cdot [1 + \frac{8.04\times10^{-9}}{[H^+]}] \quad \text{(Eq.2.21)}$$

Where Ks is expressed in mg N/L.

Table 2-5. Summary of AOB kinetic parameters from literature

Ref	SRT (d)	T (°C)	Reactor type	DO (mg O_2/L)	pH	Influent NH_4^+-N (mg N/L)	μ_{max} (d^{-1})	b (d^{-1})	Ks (mg N/L)	Ko (mg O_2/L)	Y (mg COD/ mg N)	K_{iFA} (mg N/L)	K_{iFNA} (mg N/L)	Biomass type
[74]	3.0	Room	CSTR	1.54±0.87	7.5±0.1	500	1.1±1.0	0.32±0.34			0.15±0.06			S
[75]	2.4	21±2	CSTR	0.40±0.05	7.3±0.1	1100	0.54±0.09				0.20±0.03			S
[76]		30	CSTR		7.5				28	1.45	0.14			S
[67]		23 ± 0.5	SBS		7.5 ± 0.1	1000	0.97		11			13.9		S
			IBS				0.34		28			58.8		A
[77]	15	20	ASR						12	0.99				S
[60]	15-25	23±2	CSTR	3.0	7.5	3000	1.21	0.20	0.24	0.74	0.18	7.0	0.55	S
[78]	10-20	20	CSTR	2	7.0-7.5	48 ± 2					0.24			S
[79]	5-40	20	CSTR	>4	7.0-7.5	24-96	0.24±0.01	0.066±0.003	0.023±0.003					S
[80]		20	SBR	>2		20-200	2.16		9.3		0.21			S
[68]	20	18-20	MBR	2	7.7±0.1	35±7.7	0.45±0.04	0.08±0.04						A
	8	18-20	Conventional activated sludge system	2	7.6±0.1	35±7.7	0.72±0.2	0.10±0.06						S
	20						0.45±0.04							
[81]	5	30±0.5	SBR	3	6.5–8	800 ±50	1.00		5.1±0.4	0.34±0.07				S
	1	35±0.5	CSTR	3	6.5–6.7	700 ±50	2.00		5.7±0.4	0.49±0.06				S

[62]	1	30	CSTR			1000	2.1		0.47	1.45	0.15		0.21	S
[82]	1.47	35	CSTR	3	7.1-7.3	730	0.9	0.17	0.7	0.25	0.15		0.07	S
[83]		30	CSTR		7±0.2		0.74		2.1		0.24			S
[84]	15	21	SBR	3		50	1.40	0.12	0.80		0.18			S
[85]	2	35	CSTR	1.5-5.0	7.8-8.9	1000	1.75	0.23	0.44	0.34		24.9	0.44	S
[61]	1.54	35	CSTR	6.1	6.83	500-2000	1.0±0.2		0.75±0.05	0.94±0.091			2.04±0.017	S
[86]		26±0.5	SBR	0.5 or 3.5		50-65	0.46		1.4	0.307	0.37			S
[87]	9.2±2	20	SBR	3.5	7.0	3000	0.5	0.071	1	0.5				S
[88]		22-23	SBR		7.5-8.2	150			0.11-0.28	0.33±0.04				S
[89]	10-40	35±2	SBR	0.15-3.0	6.7-8	90-190	0.94-0.99	0.245		0.36				S
[90]	10	14	SBR	1.0-5.5	6.6-7.3	40	0.28	0.10		1.36				S
[91]	30 or 100	30	SBR		7.5±0.05	250			5	1 for 30 d and 3 for 100 d SRT				S
[64]	16-18	30	SBR		7.5-8.2	500-1000	1.96	0.44	0.5	0.5	0.21	241	0.053	S
[92,93]	1.68	30±1	SBR	2.8-3.3	>6.4	1000	1.02±0.17	0.26±0.07	0.36±0.02				0.40	S
[94]	20	20	MBR	2.5-3.0	7.5				0.13±0.05	0.18±0.04				A

			CAS						0.14±0.10	0.79± 0.08				S
[95]		30±1	SBR		8.0 ± 0.2	3790	0.12		66	1.07	0.37			S
[96]		32.1-33.6	MBR-MBBR	0.2-0.5 or >1.5	7.8-8.2	1200-1600	0.445-0.639							A
[97]		30±1	MABR		7.2 ± 0.2	200	1.2			0.16-1.17				A
[98]		30	Biofilm	0.4-2.0	7.5	320	0.71-2.09		0.11-16	0.10-0.47	0.11-0.18			A
[99]		30	Upflow reactor	>3.8	7.3-8.0	1000			0.72					A
[100]	20	20	MBR	2.5-3	7.2±0.1					0.42±0.11				A
			CAS							0.65±0.015				S
[101]		20	Biofilm	8.8	7.5-8		1.08		18	0.176	0.119	0.271		A
[102]		23±1	Airlift		7.5± 0.1	180			11±5			63.5 ± 26.9		A
[103]		20					1.023	0.15	1.5	0.50	0.47			
[104]		20					0.20-0.90	0.05-0.15	0.5-1.0	0.40-0.60				
[105]		20					1.0	0.15	1	0.5				
[106]	20	20	SBR			18	0.63	0.061	0.5		0.1			S
[107]	10-15	20	AAO	2.5		34	0.48	0.175						S
[108]	122	28-32	SBR	>2.0	7.9-8.7	500 and 1000			53 ± 6	1.35 ± 0.24				S
[109]		10	Airlift reactor	0.5-2.5	8.0 ± 0.1	70	0.63 ± 0.05		2.1 ± 0.7					A
	20	29 ± 2	SBR	0.4–2.5	7.8	300–900	0.92	0.01	29	0.17				S

[110]			CSTR	3.0–3.3			0.42	0.01	3.5	0.10				
[111]	12	35±0.5	SBR	0.5- 3.0	>7.2	300	2.04					4	0.15	S
[112,113]	31 ± 7	30	SBNR	>2.0 or <1.0	8.0	1000			25-33			15.1-22.3	0.168	S
			WWTP						37-51			5.0 - 5.2		
			SBR		6.3-8.0	100			24-37			22.0-27.3		
[114]		30	MBBR	7.55 ± 0.61	7-8	50			8.8					A
				7.64 ± 0.47		1			1.2					
[59]		20 and 30	CSTR	8.00±0.02		392			0.52		0.09			S
[71]		5-30	SBR	2-3		31-335				0.27-1.63				S
[115]		35	Continuous fermenter		7.5	100-300			0.61-2.5					S
[116]	4, 7 and 10	25	Activated sludge reactor						0.2-1.7					S
[117]			Activated sludge reactor						4			36		S
[65]	5	36±1	SBR	2	6.8-7.1	518-1440						605.48 ±87.18	0.49±0.09	S
[118]	10-40	20	SBR	>2.0	6.0-8.0	226-1176	0.32±0.05							S

Table 2-6.Summary of NOB kinetic parameters from literature

References	SRT (d)	Temperature (°C)	Reactor type	DO (mg O_2/L)	pH	Influent nitrogen concentration (mg N/L)	μ_{max} (d^{-1})	b (d^{-1})	Ks (mg N/L)	Ko (mg O_2/L)	Y (mg COD/mg N)	K_{iFA} (mg N/L)	K_{iFNA} (mg N/L)	Biomass type
[119]		30			7.6				1.6				0.189	S
[74]	3.0	Room	CSTR	1.54±0.87	7.5±0.1	500	2.6±2.05	1.7±1.9			0.04±0.02			S
[75]		21±2	SBR	3.0±0.25	7.3±0.1	1000	0.67±0.03				0.10±0.01			S
[67]		23 ± 0.5	SBS		7.5 ± 0.1	1000	0.24		1.6				0.06	S
			IBS						4.1				0.35	A
[77]	15	20	Activated sludge reactor						3.53	1.40				S
[120]		20	"Fed batch" fermentor	>6		200	0.33	0.14			0.015			S
[78]	10-20	20	CSTR	2	7.0-7.5	48 ± 2					0.08			S
[79]	5-40	20	CSTR	>4	7.0-7.5	24-96	0.18±0.01	0.045±0.006	0.023±0.001					S
[80]		20	SBR	>2		20-200	2.64		4.85		0.05			S
[68]	20	18-20	MBR	2	7.7±0.1	35±7.7	0.41±0.06	0.11±0.05						A
	8	18-20	CASP	2	7.6±0.1	35±7.7	0.42±0.03	0.11±0.02						S
	20													
[62]	1	30	CSTR			1000	1.05		0.0014	1.1	0.041		0.27	S

[82]	1.47	35	CSTR	3	7.1-7.3	730	0.7	0.17	0.05	0.5	0.09		1.05	S
[83]		30	CSTR		8		0.86		1.89		0.20			S
[84]	15	21	SBR	3		50	0.65	0.12	0.50		0.06			S
[85]	2	35	CSTR	1.5-5.0	7.8-8.9	1000	0.56	0.04	0.02	0.73		14.8	2.31	S
[87]	9.2±2	20	SBR	3.5	7.0	3000	0.56	0.08	3	1				S
[88]	3-5	22-23	SBR		7.5-8.2	150			9.59 ± 1.42	0.36±0.02				S
[89]	10-40	35±2	SBR	0.15-3.0	6.7-8	90-190	2.25-2.51	0.245		0.54				S
[90]	10	14	SBR	1.0-5.5	6.6-7.3	40	0.38	0.10		2.79				S
[91]	30 or 100	30	SBR		7.5±0.05	250			2	1				S
[64]	16-18	30	SBR		7.5-8.2	500-1000	0.67	0.38	1.62	1	0.03	11.1		S
[121,122]		22±1	SBR	2.8-3.3	7.3	1000	0.48±0.07	0.069±0.004	1.49±0.08				0.018	S
[94]	20	20	CAS	2.5-3.0	7.5				0.17±0.06	0.13±0.06				S
			MBR						0.28±0.20	0.47±0.04				A
[96]		32.1-33.6	MBR-MBBR	0.2-0.5 or >1.5	7.8-8.2	1200-1600	0.312-0.575							A
[97]		30±1	MABR		7.2 ± 0.2	200	1			1.15-4.65				A
[98]		30	Biofilm	0.4-2.0	7.5	320	0.43-1.92		0.11-38.28	0.10-0.37	0.11-0.21			A
[100]	20	20	MBR	2.5-3.0	7.5					0.28±0.05				A
			CAS							0.23±0.				S

										07				
[101]		20	Biofilm	8.8	7.5-8		1.53		5.04	0.544		0.0208		A
[102]		23±1	Airlift		7.5± 0.1	180			4.1 ± 0.9				0.35 ± 0.04	A
[123]		22	MABR	2.2-5.5			0.28-0.31		0.27-0.39	0.4-0.51				A
[103]		20					1.079	0.15	2.70	0.68	0.12			
[104]							0.20-0.90	0.05-0.15	0.5-1.0	0.40-0.60				
[105]							1.0	0.15	1	0.5				
[106]	20	20	SBR			18	1.05	0.061	0.5		0.14			S
[112,113]	31 ± 7	30	SBNR	>2.0 or <1.0	8.0	1000			11.6-11.9				0.19-0.97	S
			WWTP						7.8-10.2				0.09-0.11	
			SBR		6.3-8.0	100			23.3-28.3				0.10-0.32	
[114]		30	MBBR	7.55 ± 0.61	7-8	50			2.57					S
				7.64 ± 0.47		1			1.34					
[71]		5-30	SBR	2-3		31-335				0.87-1.10				S
[118]	10-40	20	SBR	>2.0	6.0-8.0	226-1176	0.67±0.17					3.78±0.56	0.14±0.098	S

2.3.5 Anammox bacteria

Five anammox bacteria, tentatively named *Candidatus Brocadia, Candidatus Kuenenia, Candidatus Jettenia, CandidatusScalindua* and *Candidatus Anammoxoglobus*, were found to carry out anaerobic ammonium oxidation [124]. The first three exist commonly in freshwater ecosystems [125] and bioreactors [126], while the fourth genera is the only marine anammox [33].

2.4 Strategies for achieving partial nitrification

In the partial nitrification process, nitrite accumulation is required, and the second step must be restrained to accumulate AOB and washout NOB [127]. To date, researchers have developed many control methods and strategies to achieve and maintain partial nitrification. These methods mainly include appropriate regulation of temperature, pH, dissolved oxygen (DO) concentration, sludge retention time (SRT), operational and aeration pattern, inhibitors, etc [40,128,129]. These various parameters will be elaborated on below.

2.4.1 DO concentration

In addition to other substrates, like ammonia nitrogen for AOB and nitrite nitrogen for NOB, DO is also an substrate for both AOB and NOB. With low DO concentration, both AOB and NOB growth rates are reduced [5]. It is generally accepted the oxygen Monod half saturation constant for AOB ($K_{O,AOB}$) is lower than for NOB ($K_{O,NOB}$) [130,131], which means that AOB have a higher affinity for oxygen than NOB. The dissolved oxygen half-saturation coefficients

of AOB and NOB are 0.2-0.5 mg/l and 0.7-2.0 mg/l, respectively [99,104,132]. Thus, when competing for DO, NOB are often at a disadvantage. For example, one study reported that the AOB growth rate was 2.6 times faster than NOB at a low DO level (<1.0 mg/L) [133]. It was suggested that DO concentration should be maintained about 1.0–1.5 mg/L, considering both ammonia oxidation rate and nitrite accumulation [26].

However, the suitable DO concentration for achieving partial nitrification varied in a wide range (0.16-5.0 mg/L) in different studies due to different operational conditions [134]. Yamamoto et al. [135] achieved 93% nitrite accumulation at a high DO of 5 mg/L at 25^{o}C in an upflow column reactor with carrier media while Chuang et al., [136] reported that over 90% nitrite accumulation was achieved at a low DO of 0.16-0.2 mg/L at 30 ^{o}C in a closed down-flow hanging sponge reactor . Below 0.5 mg/l of DO, ammonia accumulated and over 1.7 mg/L complete nitrification to nitrate was achieved [137].

2.4.2 Temperature

With temperature increase, both AOB and NOB growth rates increase. Nitrification usually proceeds better in warmer seasons. The ammonia removal efficiency was more than 80% at 25 °C decreasing to below 30% at 15 °C and lower [138]. It has been reported that AOB could outcompete NOB at higher temperature while NOB are able to oxidize nitrite much faster at lower temperature [139]. The typical growth rate curves of AOB and NOB with temperature were developed by Zhu et al. [69], as depicted in Figure 2-7. Nitrite accumulation in an activated sludge plant especially over the summer period has been reported [140]. In addition,

raising temperature to a range between 20 °C and 25 °C enhanced the ammonia oxidation activity while decreasing the nitrite oxidation activity [141]. Besides, a decrease in nitrate concentration was observed with a simultaneous increase in the nitrite concentration in an inverse turbulent bed reactor upon increasing the temperature from 30 °C to 35 °C [142]. It should be noted that partial nitrification could still be achieved at low temperatures if the operational conditions for AOB to outcompete NOB, i.e. DO, pH, FNA, FA, were prevalent [47].

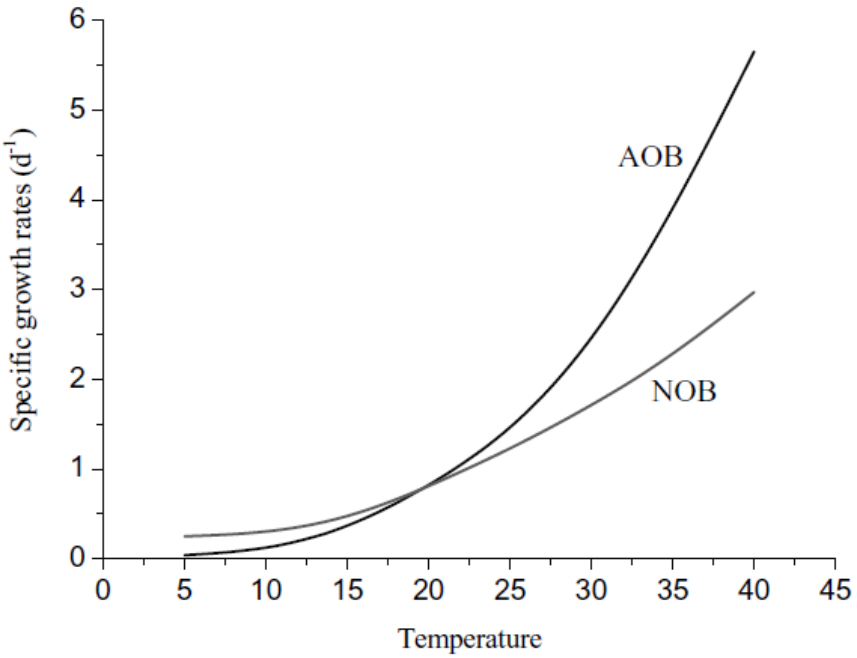

Figure 2-7. Effect of temperature on growth rate of AOB and NOB (adapted from [69])

2.4.3 pH and free ammonia and nitrous acid concentrations

pH affects the activities of AOBs and NOBs directly by changing the enzymatic reaction mechanism [72] or indirectly through free ammonia (FA) and free nitrous acid (FNA) [62,112]. The optimum pH for both AOBs and NOBs lies between 7 and 8. The growth rate of NOBs decreased from 0.17 d^{-1} at pH 7 to 0.02 d^{-1} pH 8 while the variation in the growth rate of AOBs at these pH values was negligible [143]. Thus, pH control is commonly used as a strategy to achieve partial nitrification.

The direct pH effect on the maximum specific substrate utilization rate of AOB or NOB had been considered in different models from literature. The equations suggested by US EPA [3], Siegrist and Gujer [144], and Park et al. [72] are listed as Eq.2.22-2.23, and Eq.2.17, respectively.

$$\mu = \mu_{7.2} \cdot [1 - 0.833(7.2 - \mathrm{pH})] \quad \text{(Eq.2.22)}$$

in which μ and $\mu_{7.2}$ are the maximum specific cell-growth rate at any pH and pH 7.2, respectively, d^{-1}.

$$\mu = \mu_{\max} \cdot \left[1 + 10^{(6.5-\mathrm{pH})}\right]^{-1} \quad \text{(Eq.2.23)}$$

FA and FNA are determined by pH, temperature, ammonia, or nitrite levels (Eqs. 2.24-2.25, respectively) [57].

$$\mathrm{FA} = \frac{17}{14} \cdot \frac{TAN \cdot}{\exp\left(\frac{6344}{273+T}\right)+10^{pH}} \quad \text{(Eq.2.24)}$$

$$\text{FNA} = \frac{47}{14} \cdot \frac{TNN}{\exp[\left(\frac{-2300}{273+T}\right) \cdot 10^{pH}]+1} \quad \text{(Eq.2.25)}$$

where TAN is total ammonium nitrogen, mg N/L; TNN is total nitrite nitrogen, mg N/L; T is temperature (^{o}C).

FA inhibits both AOBs and NOBs. It has been confirmed that nitrite accumulation could be achieved by regulating pH to control free ammonia concentration. However, the reported threshold inhibition concentrations of FA fare different. It was first reported that NOBs are inhibited by free ammonia in the range of 0.1-1.0 mg/L, while AOBs can tolerate free ammonia as high as 10–150 mg/L, as depicted in Figure 2-8 [26,57]. Zone 1 represents the condition when the FA concentration is high enough to inhibit both *Nitrosomonas* and *Nitrobacter*. No nitrification will occur, and ammonia will accumulate in the system. At lower concentrations of FA, only *Nitrobacter* may be inhibited and nitrite accumulation will occur. This condition is represented by Zone 2. At still lower FA concentrations, neither *Nitrobacter* nor *Nitrosomonas* will be inhibited and complete nitrification will occur (Zone 3). In Zone 4, due to the presence of high FNA (>2.8 mg N/L), *Nitrobacter* will be inhibited and nitrite accumulation will occur. Bae et al. [145] reported thatinfluent FA concentrations at 0.1-4.0 mg/L are inhibitory to NOBs. Abeling and Seyfried [56] reported that NOBs were inhibited at a range of 1-5 mg FA/L while AOB activity stopped at 20 mg FA/L.

Additionally, FNA plays an important role at low pH as NOBs are more sensitive to FNA than AOB [146]. The threshold FNA inhibition levels affecting a 50% reduction in AOB activity were in the range of 0.42-1.72 mg N/L, while lower concentrations of 0.011-0.07 mg N/L

would start to inhibit NOB and 0.026-0.22 mg N/L could completely inhibit NOB [47,147]. FA and FNA inhibitions of nitrifiers were reversible [148,149].

The suggested pH to inhibit NOB in the literature is 7.5-8.5. Abeling and Seyfried [56] reported that pH should be maintained above 7.5 to realize partial nitrification. Likewise, a pH between 7.5 and 7.8 was suggested favorable for partial nitrification [150]. The optimal pH for *Nitrosomonas* species and *Nitrobacter* species range between 7.9 and 8.2, and 7.2 and 7.6, respectively [151]. Similarly, Park et al. [72] reported that the optimum pH (pH_{opt}) lied in the range of 8.2 ± 0.3 for AOB and 7.9 ± 0.4 for NOB.

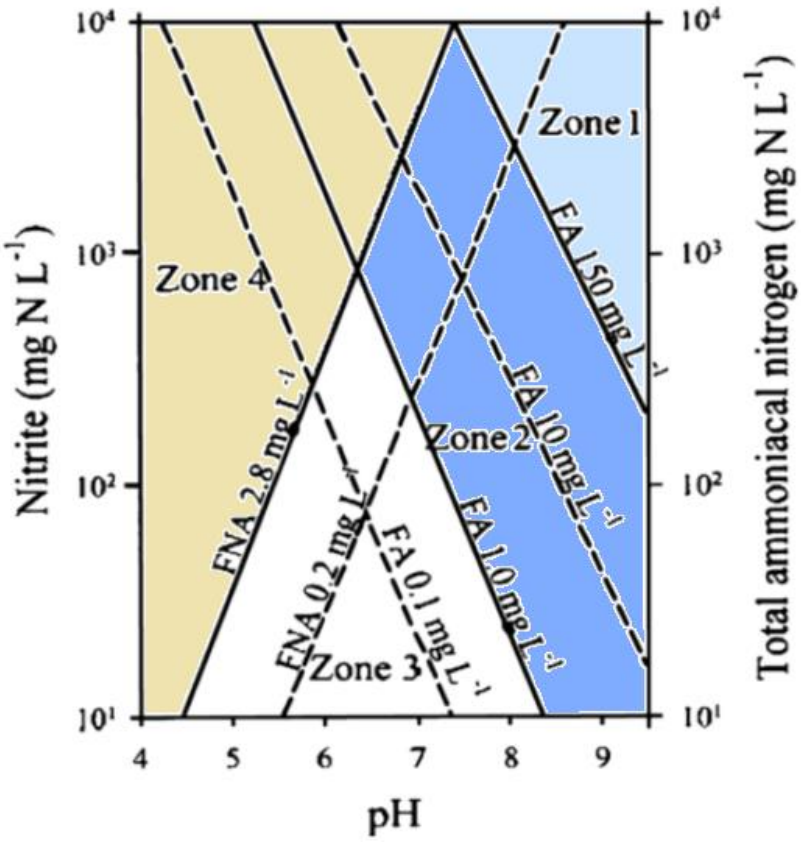

Figure 2-8. Relationship between concentrations of free ammonia (FA) and free nitrous acid (FNA) and inhibition to nitrifiers. (adapted from [57])

2.4.4 Sludge retention time (SRT)

The SRT also has a crucial influence on bacterial communities in partial nitrification reactors. Long SRTs are required for microorganisms with low maximum specific growth rates. The minimum doubling time for AOBs is 7-8 h and for NOBs 10-13 h at 35^{o}C [26,152]. Thus, it is feasible to washout NOBs by controlling SRT for nitrite accumulation. The full-scale experience shows that SRT between 1 and 2.5 days at temperatures of 30-35°C resulted in good nitritation in a Sharon reactor [29]. Ahn et al. [74] successfully washed out NOB in an CSTR at a SRT of 3 days. However, longer SRTs were reported in other studies to realize partial nitrification. For example, SRTs of 10–13 days were reported to be more appropriate for AOB accumulation with a nitrite accumulation ratio of 95% in an activated sludge system [153], which maybe due to the room temperature rather than 35°C. Furthermore, in the study of Mohammed et al. [154], stable partial nitrification deteriorated at short SRT of 7 days, whereas increasing the SRT to 16 days resulted as well in a decrease in nitrite accumulation rate from 93% to 37%. Pollice et al. [155] successfully realized partial nitrifcation under oxygen limitation at SRTs of 10, 14, and 40 days and temperature of 32^{o}C. Thus, it can be concluded that SRT is not the only factor to wash out NOB, successful partial nitrifcation can be achieved at long SRT by adopting other strategies like low DO, intermittent aeration, and aerobic HRT control.

Since NOBs grow faster than AOB at cold temperature (<20^{o}C) as shown in Fig. 2-7, it is difficult to wash out NOB simply with SRT control.

2.4.5 Real-time control

Real-time control strategy has been proposed as an effective way to achieve partial nitrification. The aeration duration and intensity is determined through direct and indirect online parameters, i.e. pH, OUR, DO, NH_4^+-N, et al [129,146–148,150]. The direct online control strategy is based on nitrogen concentration measurements with NH_4^+-N, NO_2^--N and/or NO_3^--N sensors, to get indicative information for aeration supply. For example, a full nitritation (complete ammonia conversion to nitrite) was achieved with an automatic feed-forward control system, in which NH_4^+-N and DO probes were applied to keep an optimal DO level of 5 mg/L[156]. The control stragety is presented as a conventional block diagram in Figure 2-9. The ratio is applied to the set points; therefore, once a TAN concentration set point ($[TAN]_{SP}$) of 20-30 mg N/L and a set-point ratio (RSP) of 0.17-0.25 are selected, the resulting DO concentration set point is imposed by the ratio control strategy as $[DO]_{SP}=R_{SP}[TAN]_{SP}$.

Taking stoichiometry and diffusivity coefficients from the literature [3,104,132], the oxygen-limiting conditions for nitrification will appear when

$$\frac{[DO]}{[TAN]} < \frac{\gamma_{O_2/NH_4^+} D_{NH_4^+}}{D_{O_2}} = \frac{4.57 \cdot 1.9 \cdot 10^{-9}}{2.2 \cdot 10^{-9}} = 3.9 \ \frac{g\ of\ O_2}{g\ of\ N} \qquad \text{(Eq.2.26)}$$

where [DO] and [TAN] represent the concentrations of DO and TAN in the bulk liquid, respectively. D_{NH4+} and D_{O2} are the diffusivity coefficients for ammonium and oxygen respectively, and $\gamma_{O2/NH4+}$ is the ratio of the stoichiometric coefficients of ammonium and

oxygen, i.e. 4.57 g O_2/g NH_4-N. From the literature, D_{NH4+} and D_{O2} are 1.9×10^{-9} m^2/s and 2.2×10^{-9} m^2/s at 20°C, respectively[132].

If strong oxygen-limiting conditions were applied in a biofilm reactor (i.e., DO/TAN concentration ratios much lower than 1, AOB would outcompete NOB, and nitrite build up would appear in the effluent, even without any nitrate formation.

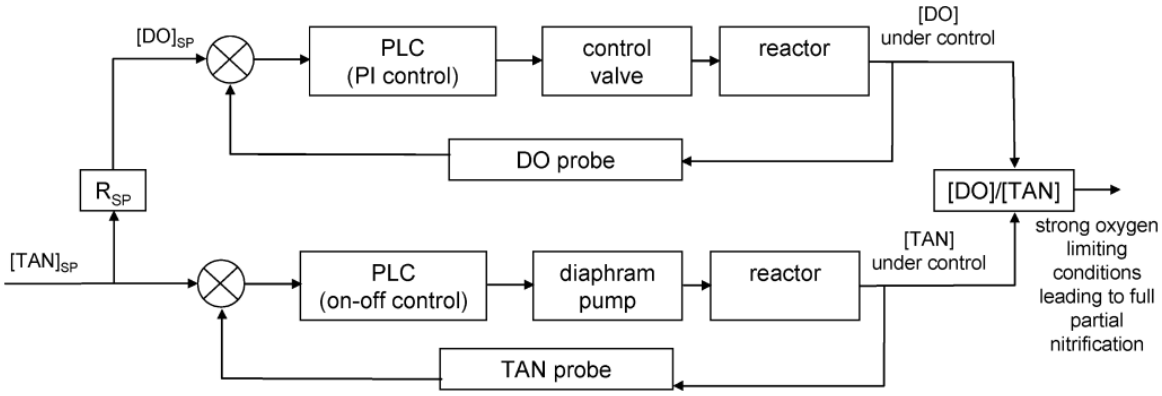

Figure 2-9. Block diagram of the automatic control for partial nitrification to nitrite in biofilm reactors used to ensure the required oxygen-limiting conditions in the biofilm to obtain and maintain continuous full nitritation under stable operating conditions [156].

Figure 2-10 shows the chemical profiles of COD, ammonia, nitrite, nitrate and TN, and online signals of DO, pH, and ORP, from which the end point of nitrification could be obtained. When ammonium was almost depleted after aeration for nearly 555 min, DO reached breakpoint B, followed by the ORP knee point A. When the valley point appeared in the pH profile at point C (585min), chemical analyses showed complete removal of ammonia and therefore indicated the end of nitrification [157].

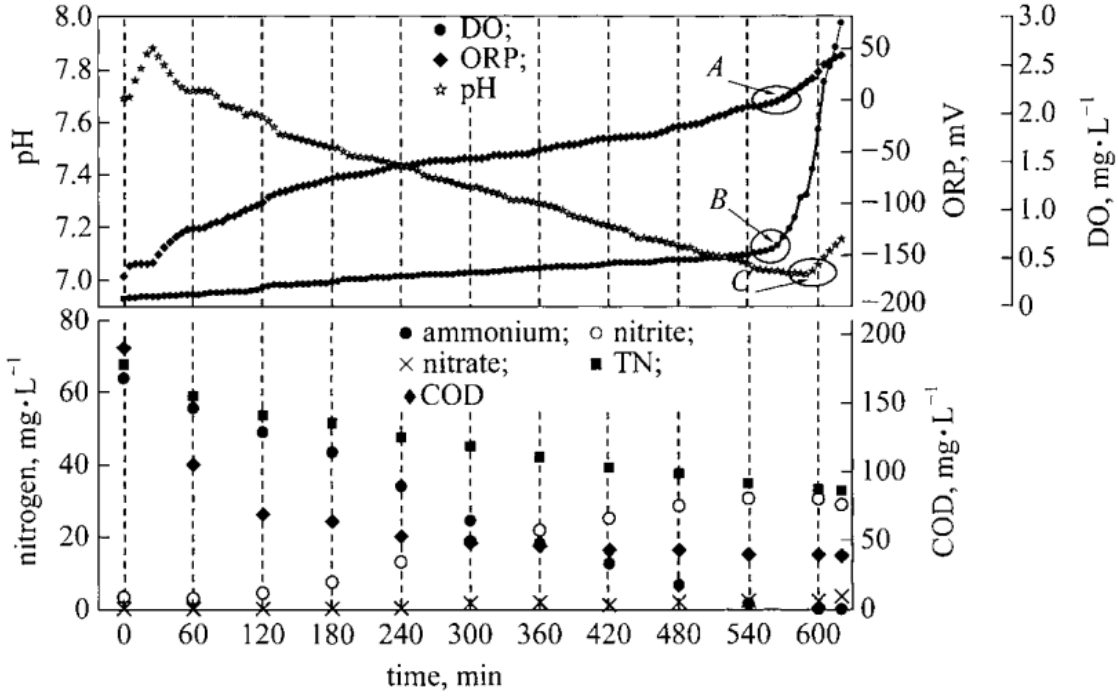

Figure 2-10. Typical pH, ORP and pH profiles with nitrogen and COD in a typical cycle of an SBR (Adapted from [157])

On the contrary, the indirect real-time control strategy includes general water quality probes (i.e. pH, DO, redox potential (ORP), oxygen utilization rate (OUR), and blower frequency (BF)), which are more cost-efficient and dependable than direct online control strategy [158–160].The overview of real-time control strategies for partial nitrification is depicted in Fig.2-11.

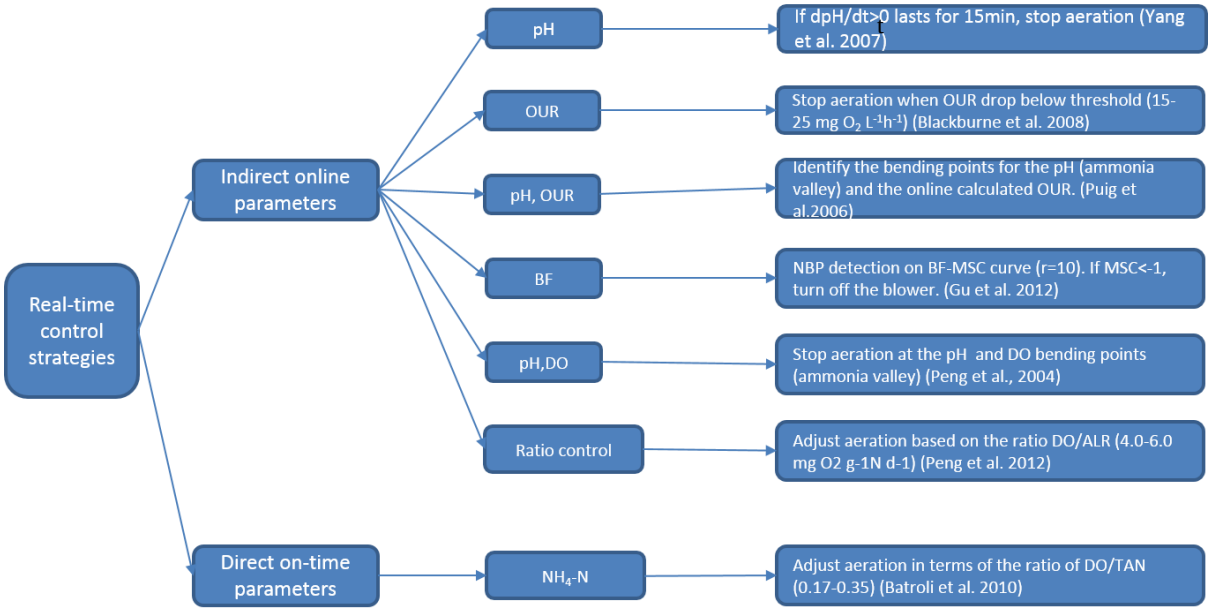

BF: blower frequency; NBP: nitrogen break point; MSC: moving slope change; ALR: ammonia loading rate; TAN: total ammonia nitrogen

Figure 2-11. Overview of real-time control strategies for partial nitrification(adapted from [47]).

In addition, Regmi et al. [161] proposed the AOB versus NOB or ammonia versus nitrate- plus-nitrite (AVN) reactor based on online in-situ DO, NH_4^+-N, NO_2^--N and NO_3^--N sensors. The AVN control system consists of the aerobic duration controller and the DO controller. In the AVN reactor, the cycle duration is fixed while the aerobic duration alters between the minimum and maximum aeration times based on NH_4^+-N/ NO_x^--N ratio. The DO was maintained at a desired set-point of 1.5 mg/L during the aerated period by the DO controller. The goal of the AVN reactor is to maintain equal effluent NH_4^+-N and NO_x^--N at all times.

The real-time aeration duration control led to full nitritation with all ammonia converted to nitrite while AVN control led to partial nitritation with half of the ammonia converted to NO_x-N. The effluent of the AVN reactor is ideal for anammox processes.

2.4.6 Intermittent aeration

Intermmitent aeration was proposed as a strategy to control ammonium oxidation to nitrite [162]. Duration of aeration time was found to be inversely related to the degree of nitrite build-up [28]. Using intermittent aeration favored nitrite accumulation [155]. Nitrate formation can be effectively prevented by frequent switching between aerobic and anoxic phases. Recently, 81.5±9.2% of nitrite accumulation was achieved in a continuous plug-flow step-feed process treating municipal wastewater by appropriately alternating anoxic/aerobic conditions following a pattern of anoxic mixing (10 min), aeration (20 min), anoxic mixing (10 min) and aeration (20 min) [163]. A model has been proposed to explain the mechanism, in which NOB were inhibited under periodic aerobic/anoxic operation, since the enzyme of NOB was deactivated under anoxic conditions and reactivated under aerobic conditions [164].

2.5 Partial nitrification in a sequencing batch reactor (SBR)

Sequencing batch reactors (SBR) is a simple technology for wastewater treatment that has been successfully used to treat both municipal and industrial wastewater. Basically, SBR is considered as fill-and-draw version of the activated sludge. Both biological treatment and sedimentation are performed within the same reactor.

Typical SBR operation consists of fill, react, settle, draw and idle, as shown in Figure 2-12. The summary of the SBRs cycles used in partial nitrification systems is illustrated in Table 2-7. The cycle times ranged from 180 min (3 hrs) to 1440 min (24 hrs). Long cycle time is required for treatment of high-strength wastewater. For example, the longest cycle time of 1440 min was reported in an SBR treating landfill leachate with extremely high nitrogen concentration (6000 mg N/L) at both 25^{o}C and 35 ^{o}C. On the contrary, Guo et al. [165] achieved stable partial nitrification in an SBR treating domestic wastewater with a cyle time of 240-360 min. In addition, the cycle time is also affected by temperature. At low temperature, long cycle time is required. For example, Yang et al. [158] adopted a cycle time of 700-800 min in an SBR treating municipal wastewater with influent ammonia concentration of 60 mg N/L at 11.9-25^{o}C.

Successful nitrite accumulation has been achieved in SBRs. Table 2-8 summarizes the operational condition and strategies of partial nitrification in SBRs. Commonly used strategies include FA and/or FNA inhbition, intermittent aeration, real-time aeration control, low DO, among others. Wei et al. [166] observed 96.1% nitrite accumulation in an SBR by increasing the influent ammonia to 400-720 mg N/L at 24^{o}C -26^{o}C, which was attributed to the high FA (40.4-86.3 mg N/L) and FNA (0.03-0.36 mg N/L) concentrations. Yang et al. [158] achieve stable nitrite accumulation (95%) in an SBR treating municipal wastewater with influent ammonia concentration of 60 mg N/L using real-time control with temperature ranging from 11.9^{o}C-26.5°C under normal dissolved oxygen condition (>2.5mg/L) . Li et al. [167] reported

over 90% nitrite accumulation in an SBR treating ammonium-rich wastewater (300 mg N/L) at 20ºC and pH of 7.1-7.4 by adopting intermittent aeration and low DO (<0.2 mg/L). In addition, some chemicals could inhibit NOB activity. For example, nitrite builtup occurred at the hydroxylamine dosing of 10 mg/L in aerobic granules cultures [168], and 2.5–5 mg/L in a submerged filter system[169].

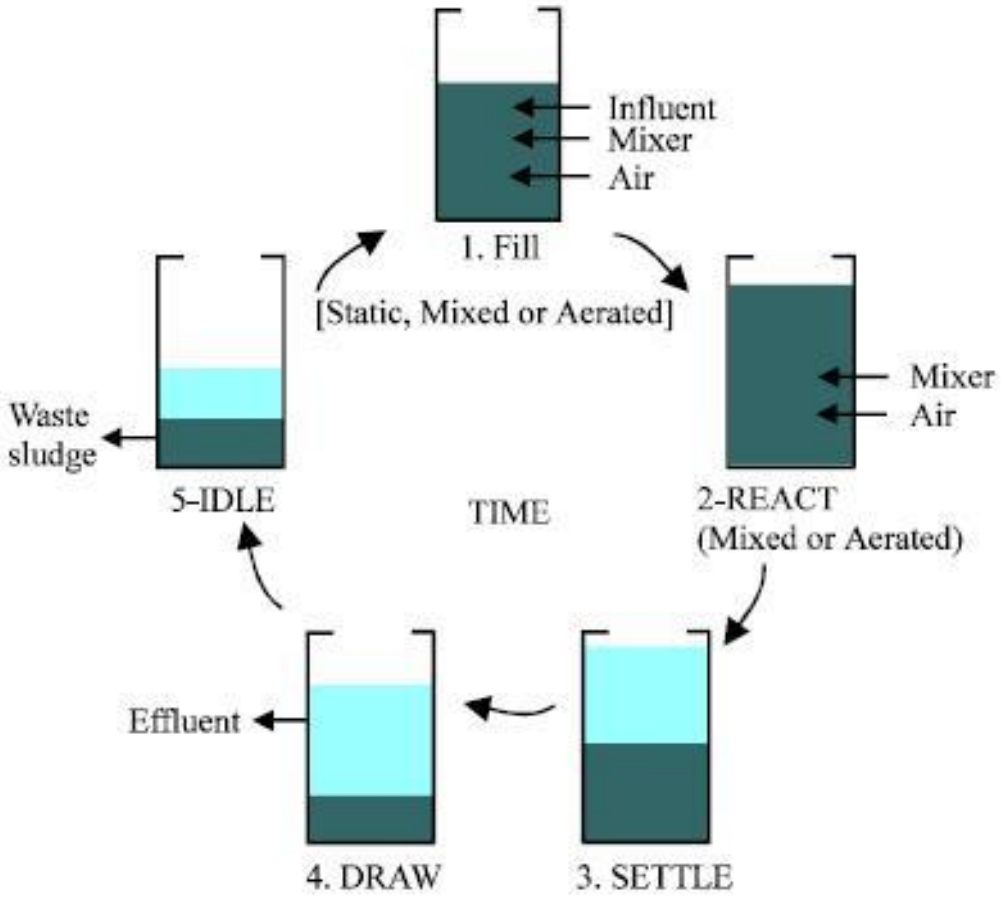

Figure 2-12. SBR operation for each tank for one cycle for the five discrete time periods of Fill, React, Settle, Draw, and Idle (adapted From [170])

Table 2-7. SBR cycle duration for different partial nitrification studies

Reference	Cycle time (min)	Fill (min)	Reaction (min)	Settle (min)	Decant and idle (min)
[171]	1440	140	1260	20	20
[158]	700-800	60	500-600	60	80
[165]	240-360	3	192-312	30	15
[172]	1440	30	1320	60	30
[168]	180-240	2	175–235	2	1
[173]	240	5	200	30	5
[174]	720	10	300	45	5
[175]	767	2	720	30	15
[176]	480	5	445	20	10
[166,177]	480	5	385	20	70
[65]	480	360	80	15	25
[178]	720	25	660	30	5
[81]	240	5	210	20	5
[179]	303-423	3	240-360	30	30
[159]	705	15	540	120	30
[89]	360	20	300	20	20
[90]	240	20	180	20	20

Table 2-8. Operational conditions and control strategies of SBRs for partial nitrifcation

Reference	Temperature (°C)	HRT (h)	SRT (d)	Influent ammonia concentration (mg N/L)	DO (mg/L)	pH	Control stategy
[171]	25 or 35	108 or 288		6000	2.0	8	FA, FNA
[176]	25–27	16	20	200	4.0	8.99-9.52	FA
[166]	24-28	16	30	200-720		7.8-8.5	FA, FNA
[180]	32±1 or 21±1	8-12	14	domestic			Real-time control
[181]	18-22	42	15	141-157 or 223-229	1.5-2.0	7.1-7.9	Real-time control
[158]	11.9-25		13	60.05	>2.5		Real-time control
[175]	10-30.6			131-180	0.5-2.0	7.5-8.8	Real-time control
[165]	12-25	8-12	30	58.1±12.8	2-6	7.3-7.6	Real-time control
[167]	20	48	>100	300	<0.2	7.1–7.4	Low DO, intermittent aeration
[182]	12.6-24		16	domestic	<0.2	7.2-7.6	Low DO, intermittent aeration
[183]	25±0.2		Very high	50	2-6.5	7.2-7.3	Intermittent aeration
[172]	23-28	24 or 48		700	<0.5	7.5± 0.2	Sulfide dose
[168]	33±1	6-8		100	5.5	7.8-8.2	hydroxylamine
[184]	Room temperature	6		100	>9	7.8–8.2	Chlorate dose
[173]	31	12-20		149.5-990	0.5-1.2	7.9–8.2	Low DO, FA, FNA
[174]	28±1	36	10	1253-1307	1.0–2.0	7.2-7.8	Low DO, FA, FNA

[177]	23-27			300	0.5-1	7.5-8.5	Low DO, FA
[65]	36±1	36	5	518-1440	2	6.8-7.1	FA, FNA
[178]	30±0.1			360	0.5	7.5	Low DO, FA
[81]	30±0.5	8.4	5	800±50	3	6.5–8	FA, FNA
[179]	Room temperature			46.8–75.6	>3 or 0.4-0.8	7.1-7.6	Real-time control
[159]	11-16 and 17-26	16-20	15–18	41.2–78.3	2.0	7.1-7.7	Real-time control
[89]	35 ± 2	12	10-40	90-190	0.6-3.0 and 0.15-2.0	6.7-8.0	FA, intermittent aeration
[185]	20±1		70–92	96.6-254.9	1.0±0.5	>8	FA, low DO
[186]	29 ± 1		28-42	688-1748	<2.0	8.18–8.39	Intermittent aeration, FA
[187]	30±1			1600−3100	0.8-2.3	8.6	FA

2.6 References

[1] V.H. Smith, G.D. Tilman, J.C. Nekola, Eutrophication: impacts of excess nutrient inputs on freshwater, marine, and terrestrial ecosystems, Environ. Pollut. 100 (1999) 179–196.

[2] A.H. Wolfe, J.A. Patz, Reactive nitrogen and human health: acute and long-term implications, AMBIO J. Hum. Environ. 31 (2002) 120–125.

[3] U.S. Epa, Process design manual of nitrogen control, EP ALinks. (1993).

[4] Y.-H. Ahn, Sustainable nitrogen elimination biotechnologies: a review, Process Biochem. 41 (2006) 1709–1721.

[5] B. Ma, S. Wang, S. Cao, Y. Miao, F. Jia, R. Du, Y. Peng, Biological nitrogen removal from sewage via anammox: recent advances, Bioresour. Technol. 200 (2016) 981–990.

[6] Metcalf and Eddy, Wastewater Engineering: Treatment, Disposal, Reuse, Metcalf & Eddy, Inc McGraw-Hill N. Y. (2003).

[7] B.E. Rittmann, P.L. McCarty, Environmental biotechnology: principles and applications, Tata McGraw-Hill Education, 2012.

[8] H.-J. Lee, J.-H. Bae, K.-M. Cho, Simultaneous nitrification and denitrification in a mixed methanotrophic culture, Biotechnol. Lett. 23 (2001) 935–941.

[9] J. Keller, K. Subramaniam, J. Gösswein, P. Greenfield, Nutrient removal from industrial wastewater using single tank sequencing batch reactors, Water Sci. Technol. 35 (1997) 137–144.

[10] C. Helmer, S. Kunst, Simultaneous nitrification/denitrification in an aerobic biofilm system, Water Sci. Technol. 37 (1998) 183–187.

[11] L.A. Robertson, J.G. Kuenen, Aerobic denitrification: a controversy revived, Arch. Microbiol. 139 (1984) 351–354.

[12] B. Baumann, M. Snozzi, A. Zehnder, J.R. Van Der Meer, Dynamics of denitrification activity of Paracoccus denitrificans in continuous culture during aerobic-anaerobic changes., J. Bacteriol. 178 (1996) 4367–4374.

[13] K. Hibiya, A. Terada, S. Tsuneda, A. Hirata, Simultaneous nitrification and denitrification by controlling vertical and horizontal microenvironment in a membrane-aerated biofilm reactor, J. Biotechnol. 100 (2003) 23–32.

[14] D. Snidaro, F. Zartarian, F. Jorand, J.-Y. Bottero, J.-C. Block, J. Manem, Characterization of activated sludge flocs structure, Water Sci. Technol. 36 (1997) 313–320.

[15] J. Holman, D. Wareham, COD, ammonia and dissolved oxygen time profiles in the simultaneous nitrification/denitrification process, Biochem. Eng. J. 22 (2005) 125–133.

[16] D. de Beer, A. Schramm, C.M. Santegoeds, H.K. Nielsen, Anaerobic processes in activated sludge, Water Sci. Technol. 37 (1998) 605–608.

[17] B. Li, P.L. Bishop, Micro-profiles of activated sludge floc determined using microelectrodes, Water Res. 38 (2004) 1248–1258.

[18] S. Wyffels, K. Pynaert, P. Boeckx, W. Verstraete, O. Van Cleemput, Identification and quantification of nitrogen removal in a rotating biological contactor by 15N tracer techniques, Water Res. 37 (2003) 1252–1259.

[19] L.A. Robertson, E.W. Van Niel, R.A. Torremans, J.G. Kuenen, Simultaneous nitrification and denitrification in aerobic chemostat cultures of Thiosphaera pantotropha, Appl. Environ. Microbiol. 54 (1988) 2812–2818.

[20] L.A. Robertson, T. Dalsgaard, N.-P. Revsbech, J.G. Kuenen, Confirmation of ‘aerobic denitrification’in batch cultures, using gas chromatography and 15N mass spectrometry, FEMS Microbiol. Ecol. 18 (1995) 113–119.

[21] K. Pochana, J. Keller, P. Lant, Model development for simultaneous nitrification and denitrification, Water Sci. Technol. 39 (1999) 235–243.

[22] D. Zhang, P. Lu, T. Long, W. Verstraete, The integration of methanogensis with simultaneous nitrification and denitrification in a membrane bioreactor, Process Biochem. 40 (2005) 541–547.

[23] K. Pochana, J. Keller, Study of factors affecting simultaneous nitrification and denitrification (SND), Water Sci. Technol. 39 (1999) 61–68.

[24] F. Fdz-Polanco, S. Villaverde, P.A. Garcia, Nitrite accumulation in submerged biofilters—combined effects, Water Sci. Technol. 34 (1996) 371–378.

[25] F. Çeçen, Investigation of partial and full nitrification characteristics of fertilizer wastewaters in a submerged biofilm reactor, Water Sci. Technol. 34 (1996) 77–85.

[26] Y. Peng, G. Zhu, Biological nitrogen removal with nitrification and denitrification via nitrite pathway, Appl. Microbiol. Biotechnol. 73 (2006) 15–26.

[27] M. Beccari, R. Passino, R. Ramadori, V. Tandoi, Kinetics of dissimilatory nitrate and nitrite reduction in suspended growth culture, J. Water Pollut. Control Fed. (1983) 58–64.

[28] O. Turk, D.S. Mavinic, Benefits of using selective inhibition to remove nitrogen from highly nitrogenous wastes, Environ. Technol. 8 (1987) 419–426.

[29] R. Van Kempen, J.W. Mulder, C.A. Uijterlinde, M.C.M. Loosdrecht, Overview: full scale experience of the SHARON® process for treatment of rejection water of digested sludge dewatering, Water Sci. Technol. 44 (2001) 145–152.

[30] A.A. Van de Graaf, P. de Bruijn, L.A. Robertson, M.S. Jetten, J.G. Kuenen, Autotrophic growth of anaerobic ammonium-oxidizing micro-organisms in a fluidized bed reactor, Microbiology. 142 (1996) 2187–2196.

[31] B. Kartal, L. van Niftrik, J.T. Keltjens, H.J.M. Op den Camp, M.S.M. Jetten, Anammox—Growth Physiology, Cell Biology, and Metabolism, Adv. Microb. Physiol. 60 (2012) 212.

[32] M. Strous, J.J. Heijnen, J.G. Kuenen, M.S.M. Jetten, The sequencing batch reactor as a powerful tool for the study of slowly growing anaerobic ammonium-oxidizing microorganisms, Appl. Microbiol. Biotechnol. 50 (1998) 589–596.

[33] B. Kartal, J.G. Kuenen, M.C.M. Van Loosdrecht, Sewage treatment with anammox, Science. 328 (2010) 702–703.

[34] A. Mulder, A.A. Graaf, L.A. Robertson, J.G. Kuenen, Anaerobic ammonium oxidation discovered in a denitrifying fluidized bed reactor, FEMS Microbiol. Ecol. 16 (1995) 177–184.

[35] M.S.M. Jetten, M. Wagner, J. Fuerst, M. van Loosdrecht, G. Kuenen, M. Strous, Microbiology and application of the anaerobic ammonium oxidation (‘anammox’) process, Curr. Opin. Biotechnol. 12 (2001) 283–288.

[36] B. Kartal, W.J. Maalcke, N.M. de Almeida, I. Cirpus, J. Gloerich, W. Geerts, H.J.M.O. den Camp, H.R. Harhangi, E.M. Janssen-Megens, K.-J. Francoijs, Molecular mechanism of anaerobic ammonium oxidation, Nature. 479 (2011) 127–130.

[37] M. Strous, E. Pelletier, S. Mangenot, T. Rattei, A. Lehner, M.W. Taylor, M. Horn, H. Daims, D. Bartol-Mavel, P. Wincker, Deciphering the evolution and metabolism of an anammox bacterium from a community genome, Nature. 440 (2006) 790–794.

[38] S.W.H. Van Hulle, H.J.P. Vandeweyer, B.D. Meesschaert, P.A. Vanrolleghem, P. Dejans, A. Dumoulin, Engineering aspects and practical application of autotrophic nitrogen removal from nitrogen rich streams, Chem. Eng. J. 162 (2010) 1–20.

[39] S.E. Vlaeminck, A. Terada, B.F. Smets, D.V. der Linden, N. Boon, W. Verstraete, M. Carballa, Nitrogen removal from digested black water by one-stage partial nitritation and anammox, Environ. Sci. Technol. 43 (2009) 5035–5041.

[40] U. van Dongen, M.S.M. Jetten, M.C.M. Van Loosdrecht, The SHARON®-Anammox® process for treatment of ammonium rich wastewater, Water Sci. Technol. 44 (2001) 153–160.

[41] U. Purkhold, A. Pommerening-Röser, S. Juretschko, M.C. Schmid, H.-P. Koops, M. Wagner, Phylogeny of all recognized species of ammonia oxidizers based on comparative

16S rRNA and amoA sequence analysis: implications for molecular diversity surveys, Appl. Environ. Microbiol. 66 (2000) 5368–5382.

[42] H. Koops, A. Pommerening-Röser, Distribution and ecophysiology of the nitrifying bacteria emphasizing cultured species, FEMS Microbiol. Ecol. 37 (2001) 1–9.

[43] P. Junier, V. Molina, C. Dorador, O. Hadas, O.-S. Kim, T. Junier, K.-P. Witzel, J.F. Imhoff, Phylogenetic and functional marker genes to study ammonia-oxidizing microorganisms (AOM) in the environment, Appl. Microbiol. Biotechnol. 85 (2010) 425–440. doi:10.1007/s00253-009-2228-9.

[44] C. Woese, W. Weisburg, B. Paster, C. Hahn, R. Tanner, N. Krieg, H.-P. Koops, H. Harms, E. Stackebrandt, The phylogeny of purple bacteria: the beta subdivision, Syst. Appl. Microbiol. 5 (1984) 327–336.

[45] D. Werner, W.E. Newton, Nitrogen fixation in agriculture, forestry, ecology, and the environment, Springer Science & Business Media, 2005.

[46] Kai Li, A study of Low C/N Ratio Waste Water Treatment Using Fluidized Bed Bioreactor, The University of Western Ontario, n.d. https://ir.lib.uwo.ca/etd/3523.

[47] S. Ge, S. Wang, X. Yang, S. Qiu, B. Li, Y. Peng, Detection of nitrifiers and evaluation of partial nitrification for wastewater treatment: a review, Chemosphere. 140 (2015) 85–98.

[48] J. Semrau, A. Chistoserdov, J. Lebron, A. Costello, J. Davagnino, E. Kenna, A. Holmes, R. Finch, J. Murrell, M. Lidstrom, Particulate methane monooxygenase genes in methanotrophs., J. Bacteriol. 177 (1995) 3071–3079.

[49] D.H.-W. Kuo, K.G. Robinson, A.C. Layton, A.J. Meyers, G.S. Sayler, Transcription levels (amoA mRNA-based) and population dominance (amoA gene-based) of ammonia-

oxidizing bacteria, J. Ind. Microbiol. Biotechnol. 37 (2010) 751–757. doi:10.1007/s10295-010-0728-3.

[50] T. Fukushima, Y.-J. Wu, L.-M. Whang, The influence of salinity and ammonium levels on amoA mRNA expression of ammonia-oxidizing prokaryotes, Water Sci. Technol. 65 (2012) 2228–2235.

[51] D.J. Bergmann, A.B. Hooper, M.G. Klotz, Structure and sequence conservation of hao cluster genes of autotrophic ammonia-oxidizing bacteria: evidence for their evolutionary history, Appl. Environ. Microbiol. 71 (2005) 5371–5382.

[52] N.G. Hommes, L.A. Sayavedra-Soto, D.J. Arp, Transcript Analysis of Multiple Copies ofamo (Encoding Ammonia Monooxygenase) and hao (Encoding Hydroxylamine Oxidoreductase) in Nitrosomonas europaea, J. Bacteriol. 183 (2001) 1096–1100.

[53] P. Chain, J. Lamerdin, F. Larimer, W. Regala, V. Lao, M. Land, L. Hauser, A. Hooper, M. Klotz, J. Norton, Complete genome sequence of the ammonia-oxidizing bacterium and obligate chemolithoautotroph Nitrosomonas europaea, J. Bacteriol. 185 (2003) 2759–2773.

[54] M.G. Klotz, L.Y. Stein, Nitrifier genomics and evolution of the nitrogen cycle, FEMS Microbiol. Lett. 278 (2007) 146–156.

[55] H. Sundermeyer-Klinger, W. Meyer, B. Warninghoff, E. Bock, Membrane-bound nitrite oxidoreductase of Nitrobacter: evidence for a nitrate reductase system, Arch. Microbiol. 140 (1984) 153–158.

[56] U. Abeling, C. Seyfried, Anaerobic-aerobic treatment of high-strength ammonium wastewater-nitrogen removal via nitrite, Water Sci. Technol. 26 (1992) 1007–1015.

[57] A.C. Anthonisen, R.C. Loehr, T.B.S. Prakasam, E.G. Srinath, Inhibition of nitrification by ammonia and nitrous acid, J. Water Pollut. Control Fed. (1976) 835–852.

[58] R. Neufeld, J. Greenfield, B. Rieder, Temperature, cyanide and phenolic nitrification inhibition, Water Res. 20 (1986) 633–642.

[59] J. Groeneweg, B. Sellner, W. Tappe, Ammonia oxidation in Nitrosomonas at NH3 concentrations near Km: effects of pH and temperature, Water Res. 28 (1994) 2561–2566.

[60] I. Jubany, J. Carrera, J. Lafuente, J.A. Baeza, Start-up of a nitrification system with automatic control to treat highly concentrated ammonium wastewater: experimental results and modeling, Chem. Eng. J. 144 (2008) 407–419.

[61] S.W. Van Hulle, E.I. Volcke, J.L. Teruel, B. Donckels, M. van Loosdrecht, P.A. Vanrolleghem, Influence of temperature and pH on the kinetics of the Sharon nitritation process, J. Chem. Technol. Biotechnol. 82 (2007) 471–480.

[62] C. Hellinga, M.C.M. Van Loosdrecht, J.J. Heijnen, Model based design of a novel process for nitrogen removal from concentrated flows, Math. Comput. Model. Dyn. Syst. 5 (1999) 351–371.

[63] G. Baquerizo, J.P. Maestre, T. Sakuma, M.A. Deshusses, X. Gamisans, D. Gabriel, J. Lafuente, A detailed model of a biofilter for ammonia removal: model parameters analysis and model validation, Chem. Eng. J. 113 (2005) 205–214.

[64] V. Pambrun, E. Paul, M. Spérandio, Modeling the partial nitrification in sequencing batch reactor for biomass adapted to high ammonia concentrations, Biotechnol. Bioeng. 95 (2006) 120–131.

[65] R. Ganigué, H. Lopez, M. Balaguer, J. Colprim, Partial ammonium oxidation to nitrite of high ammonium content urban landfill leachates, Water Res. 41 (2007) 3317–3326.

[66] G. Wong-Chong, R. Loehr, Kinetics of microbial nitrification: nitrite-nitrogen oxidation, Water Res. 12 (1978) 605–609.

[67] J. Carrera, I. Jubany, L. Carvallo, R. Chamy, J. Lafuente, Kinetic models for nitrification inhibition by ammonium and nitrite in a suspended and an immobilised biomass systems, Process Biochem. 39 (2004) 1159–1165.

[68] G. Munz, G. Mori, C. Vannini, C. Lubello, Kinetic parameters and inhibition response of ammonia-and nitrite-oxidizing bacteria in membrane bioreactors and conventional activated sludge processes, Environ. Technol. 31 (2010) 1557–1564.

[69] G. Zhu, Y. Peng, B. Li, J. Guo, Q. Yang, S. Wang, Biological removal of nitrogen from wastewater, in: Rev. Environ. Contam. Toxicol., Springer, 2008: pp. 159–195.

[70] E. Metcalf, M. Eddy, Wastewater engineering: treatment and Resource recovery, Mic Graw-Hill USA. (2014).

[71] S.Y. Weon, S.I. Lee, B. Koopman, Effect of temperature and dissolved oxygen on biological nitrification at high ammonia concentrations, Environ. Technol. 25 (2004) 1211–1219.

[72] S. Park, W. Bae, J. Chung, S.-C. Baek, Empirical model of the pH dependence of the maximum specific nitrification rate, Process Biochem. 42 (2007) 1671–1676.

[73] J.H. Hunik, H.J.G. Meijer, J. Tramper, Kinetics of Nitrosomonas europaea at extreme substrate, product and salt concentrations, Appl. Microbiol. Biotechnol. 37 (1992) 802–807.

[74] J.H. Ahn, R. Yu, K. Chandran, Distinctive microbial ecology and biokinetics of autotrophic ammonia and nitrite oxidation in a partial nitrification bioreactor, Biotechnol. Bioeng. 100 (2008) 1078–1087.

[75] R. Blackburne, V.M. Vadivelu, Z. Yuan, J. Keller, Determination of growth rate and yield of nitrifying bacteria by measuring carbon dioxide uptake rate, Water Environ. Res. 79 (2007) 2437–2445.

[76] M. Brouwer, Biologische stikstofverwijdering op Sluisjesdijk met het SHARON-proces, BODL Rep. Delft UT. (1995).

[77] G. Ciudad, A. Werner, C. Bornhardt, C. Munoz, C. Antileo, Differential kinetics of ammonia-and nitrite-oxidizing bacteria: A simple kinetic study based on oxygen affinity and proton release during nitrification, Process Biochem. 41 (2006) 1764–1772.

[78] G. Liu, J. Wang, Probing the stoichiometry of the nitrification process using the respirometric approach, Water Res. 46 (2012) 5954–5962.

[79] G. Liu, J. Wang, Role of solids retention time on complete nitrification: mechanistic understanding and modeling, J. Environ. Eng. 140 (2013) 48–56.

[80] F. Fang, B.-J. Ni, X.-Y. Li, G.-P. Sheng, H.-Q. Yu, Kinetic analysis on the two-step processes of AOB and NOB in aerobic nitrifying granules, Appl. Microbiol. Biotechnol. 83 (2009) 1159–1169.

[81] A. Galí, J. Dosta, M.C.M. Van Loosdrecht, J. Mata-Alvarez, Two ways to achieve an anammox influent from real reject water treatment at lab-scale: Partial SBR nitrification and SHARON process, Process Biochem. 42 (2007) 715–720.

[82] R. Jones, P. Dold, I. Takács, K. Chapman, B. Wett, S. Murthy, M. Shaughnessy, Simulation for operation and control of reject water treatment processes, Proc. Water Environ. Fed. 2007 (2007) 4357–4372.

[83] G.A. Keen, J.I. Prosser, Steady state and transient growth of autotrophic nitrifying bacteria, Arch. Microbiol. 147 (1987) 73–79. doi:10.1007/BF00492908.

[84] T. Katipoglu-Yazan, C. Merlin, M.-N. Pons, E. Ubay-Cokgor, D. Orhon, Chronic impact of tetracycline on nitrification kinetics and the activity of enriched nitrifying microbial culture, Water Res. 72 (2015) 227–238.

[85] A. Magrí, L. Corominas, H. López, E. Campos, M. Balaguer, J. Colprim, X. Flotats, A model for the simulation of the SHARON process: pH as a key factor, Environ. Technol. 28 (2007) 255–265.

[86] D. Gao, Y. Peng, W.-M. Wu, Kinetic model for biological nitrogen removal using shortcut nitrification-denitrification process in sequencing batch reactor, Environ. Sci. Technol. 44 (2010) 5015–5021.

[87] M.J. Kampschreur, C. Picioreanu, N. Tan, R. Kleerebezem, M.S.M. Jetten, M. van Loosdrecht, Unraveling the source of nitric oxide emission during nitrification, Proc. Water Environ. Fed. 2007 (2007) 843–860.

[88] C. Rongsayamanont, T. Limpiyakorn, B. Law, E. Khan, Relationship between respirometric activity and community of entrapped nitrifying bacteria: implications for partial nitrification, Enzyme Microb. Technol. 46 (2010) 229–236.

[89] X. Liu, M. Kim, G. Nakhla, Operational conditions for successful partial nitrification in a sequencing batch reactor SBR based on process kinetics, Environ. Technol. 38 (2017) 694–704.

[90] X. Liu, M. Kim, G. Nakhla, Performance and kinetics of nitrification of low ammonia wastewater at low temperature, Water Environ. Res. 90 (2018) 498–509.

[91] M.S. Moussa, C.M. Hooijmans, H.J. Lubberding, H.J. Gijzen, M.C.M. Van Loosdrecht, Modelling nitrification, heterotrophic growth and predation in activated sludge, Water Res. 39 (2005) 5080–5098.

[92] V.M. Vadivelu, J. Keller, Z. Yuan, Stoichiometric and kinetic characterisation of Nitrosomonas sp. in mixed culture by decoupling the growth and energy generation processes, J. Biotechnol. 126 (2006) 342–356.

[93] V.M. Vadivelu, J. Keller, Z. Yuan, Effect of free ammonia and free nitrous acid concentration on the anabolic and catabolic processes of an enriched Nitrosomonas culture, Biotechnol. Bioeng. 95 (2006) 830–839.

[94] R. Manser, W. Gujer, H. Siegrist, Consequences of mass transfer effects on the kinetics of nitrifiers, Water Res. 39 (2005) 4633–4642.

[95] P. Dan, DETERMINATION OF AMMONIA OXIDATION BACTERIA KINETICS IN PARTIAL NITRITATION PROCESS USING RESPIROMETRIC METHOD, J. Sci. Technol. 52 (2014) 3A.

[96] R. Canziani, V. Emondi, M. Garavaglia, F. Malpei, E. Pasinetti, G. Buttiglieri, Effect of oxygen concentration on biological nitrification and microbial kinetics in a cross-flow membrane bioreactor (MBR) and moving-bed biofilm reactor (MBBR) treating old landfill leachate, J. Membr. Sci. 286 (2006) 202–212.

[97] S. Lackner, A. Terada, H. Horn, M. Henze, B.F. Smets, Nitritation performance in membrane-aerated biofilm reactors differs from conventional biofilm systems, Water Res. 44 (2010) 6073–6084.

[98] T. Vannecke, E. Volcke, Modelling microbial competition in nitrifying biofilm reactors, Biotechnol. Bioeng. 112 (2015) 2550–2561.

[99] A. Schramm, D. de Beer, J.C. van den Heuvel, S. Ottengraf, R. Amann, Microscale Distribution of Populations and Activities ofNitrosospira and Nitrospira spp. along a Macroscale Gradient in a Nitrifying Bioreactor: Quantification by In Situ Hybridization and the Use of Microsensors, Appl. Environ. Microbiol. 65 (1999) 3690–3696.

[100] H. Daebel, R. Manser, W. Gujer, Exploring temporal variations of oxygen saturation constants of nitrifying bacteria, Water Res. 41 (2007) 1094–1102.

[101] J. Pérez, E. Costa, J.-U. Kreft, Conditions for partial nitrification in biofilm reactors and a kinetic explanation, Biotechnol. Bioeng. 103 (2009) 282–295.

[102] L. Carvallo, J. Carrera, R. Chamy, Nitrifying activity monitoring and kinetic parameters determination in a biofilm airlift reactor by respirometry, Biotechnol. Lett. 24 (2002) 2063–2066.

[103] B.E. Rittmann, P.L. McCarty, Environmental biotechnology: principles and applications, Tata McGraw-Hill Education, 2012.

[104] Metcalf and Eddy, Wastewater Engineering: Treatment, Disposal, Reuse, Metcalf & Eddy, Inc McGraw-Hill N. Y. (2003).

[105] M. Henze, W. Gujer, T. Mino, M. Van Loosedrecht, Activated sludge models ASM1, ASM2, ASM2d and ASM3, (2006).

[106] P. Ratini, A. Spagni, G. Bortone, Implementation, study and calibration of a modified ASM2d for the simulation of SBR processes, Water Sci. Technol. 43 (2001) 69–76.

[107] Z. Zhou, D. Hu, L. Jiang, C. Xing, Y. Zhu, M. Jiang, W. Qiao, Z. Li, Nitrification kinetics of a full-scale anaerobic/anoxic/aerobic wastewater treatment plant, Desalination Water Treat. 56 (2015) 2046–2054.

[108] H.N. Biec, T.T.T. Van, D. Van Tuan, N.L.H. Trung, V.T.K. Nghi, N.P. Dan, Stability of partial nitritation in a sequencing batch reactor fed with high ammonium strength old urban landfill leachate, Int. Biodeterior. Biodegrad. 124 (2017) 56–61.

[109] C. Reino, M.E. Suárez-Ojeda, J. Pérez, J. Carrera, Kinetic and microbiological characterization of aerobic granules performing partial nitritation of a low-strength wastewater at 10 °C, Water Res. 101 (2016) 147–156. doi:10.1016/j.watres.2016.05.059.

[110] A. Terada, S. Sugawara, T. Yamamoto, S. Zhou, K. Koba, M. Hosomi, Physiological characteristics of predominant ammonia-oxidizing bacteria enriched from bioreactors with different influent supply regimes, Biochem. Eng. J. 79 (2013) 153–161.

[111] G. Munz, C. Lubello, J.A. Oleszkiewicz, Factors affecting the growth rates of ammonium and nitrite oxidizing bacteria, Chemosphere. 83 (2011) 720–725.

[112] S. Park, W. Bae, Modeling kinetics of ammonium oxidation and nitrite oxidation under simultaneous inhibition by free ammonia and free nitrous acid, Process Biochem. 44 (2009) 631–640.

[113] J. Chung, W. Bae, Y.-W. Lee, B.E. Rittmann, Shortcut biological nitrogen removal in hybrid biofilm/suspended growth reactors, Process Biochem. 42 (2007) 320–328.

[114] T. Charoanwoodtipong, T. Limpiyakorn, B.B. Suwannasilp, Kinetics of Ammonia-Oxidizing Microorganisms and Nitrite-Oxidizing Bacteria Enriched at High and Low Ammonia Concentrations, in: 2015: pp. 1–5.

[115] R. Charley, D. Hooper, A. McLee, Nitrification kinetics in activated sludge at various temperatures and dissolved oxygen concentrations, Water Res. 14 (1980) 1387–1396.

[116] P.M. Sutton, K.L. Murphy, B.E. Jank, B.A. Monaghan, Efficacy of biological nitrification, J. Water Pollut. Control Fed. (1975) 2665–2673.

[117] J.D. Keenan, R. Steiner, A. Fungaroli, Substrate inhibition of nitrification, J. Environ. Sci. Health Part A. 14 (1979) 377–397.

[118] M. Zheng, S. Wu, Z. Zuo, Z. Wang, Y. Qiu, Y. Liu, X. Huang, Z. Yuan, Predictions of the influent and operational conditions for partial nitritation with a model incorporating pH dynamics, Environ. Sci. Technol. (2018).

[119] B. Boon, H. Laudelout, Kinetics of nitrite oxidation by Nitrobacter winogradskyi, Biochem. J. 85 (1962) 440.

[120] J.B. Copp, K.L. Murphy, Estimation of the active nitrifying biomass in activated sludge, Water Res. 29 (1995) 1855–1862.

[121] V.M. Vadivelu, Z. Yuan, C. Fux, J. Keller, Stoichiometric and kinetic characterisation of Nitrobacter in mixed culture by decoupling the growth and energy generation processes, Biotechnol. Bioeng. 94 (2006) 1176–1188.

[122] V.M. Vadivelu, Z. Yuan, C. Fux, J. Keller, The inhibitory effects of free nitrous acid on the energy generation and growth processes of an enriched Nitrobacter culture, Environ. Sci. Technol. 40 (2006) 4442–4448.

[123] L.S. Downing, R. Nerenberg, Effect of oxygen gradients on the activity and microbial community structure of a nitrifying, membrane-aerated biofilm, Biotechnol. Bioeng. 101 (2008) 1193–1204.

[124] J.G. Kuenen, Anammox bacteria: from discovery to application, Nat. Rev. Microbiol. 6 (2008) 320–326.

[125] G. Zhu, S. Wang, W. Wang, Y. Wang, L. Zhou, B. Jiang, H.J.O. Den Camp, N. Risgaard-Petersen, L. Schwark, Y. Peng, Hotspots of anaerobic ammonium oxidation at land–freshwater interfaces, Nat. Geosci. 6 (2013) 103.

[126] S. Wang, Y. Peng, B. Ma, S. Wang, G. Zhu, Anaerobic ammonium oxidation in traditional municipal wastewater treatment plants with low-strength ammonium loading: widespread but overlooked, Water Res. 84 (2015) 66–75.

[127] H.J. Laanbroek, S. Gerards, Competition for limiting amounts of oxygen between Nitrosomonas europaea and Nitrobacter winogradskyi grown in mixed continuous cultures, Arch. Microbiol. 159 (1993) 453–459.

[128] J. Surmacz-Górska, A. Cichon, K. Miksch, Nitrogen removal from wastewater with high ammonia nitrogen concentration via shorter nitrification and denitrification, Water Sci. Technol. 36 (1997) 73–78.

[129] J. López-Fiuza, B. Buys, A. Mosquera-Corral, F. Omil, R. Méndez, Toxic effects exerted on methanogenic, nitrifying and denitrifying bacteria by chemicals used in a milk analysis laboratory, Enzyme Microb. Technol. 31 (2002) 976–985.

[130] R. Blackburne, Z. Yuan, J. Keller, Demonstration of nitrogen removal via nitrite in a sequencing batch reactor treating domestic wastewater, Water Res. 42 (2008) 2166–2176.

[131] A. Guisasola, I. Jubany, J.A. Baeza, J. Carrera, J. Lafuente, Respirometric estimation of the oxygen affinity constants for biological ammonium and nitrite oxidation, J. Chem. Technol. Biotechnol. 80 (2005) 388–396.

[132] C. Picioreanu, M.C.M. Van Loosdrecht, J.J. Heijnen, Modelling the effect of oxygen concentration on nitrite accumulation in a biofilm airlift suspension reactor, Water Sci. Technol. 36 (1997) 147–156.

[133] T. Tokutomi, Operation of a nitrite-type airlift reactor at low DO concentration, Water Sci. Technol. 49 (2004) 81–88.

[134] X. Liu, M. Kim, G. Nakhla, A model for determination of operational conditions for successful shortcut nitrification, Environ. Sci. Pollut. Res. 24 (n.d.) 3539–3549. doi:10.1007/s11356-016-8017-y.

[135] T. Yamamoto, K. Takaki, T. Koyama, K. Furukawa, Long-term stability of partial nitritation of swine wastewater digester liquor and its subsequent treatment by Anammox, Bioresour. Technol. 99 (2008) 6419–6425.

[136] H.-P. Chuang, A. Ohashi, H. Imachi, M. Tandukar, H. Harada, Effective partial nitrification to nitrite by down-flow hanging sponge reactor under limited oxygen condition, Water Res. 41 (2007) 295–302.

[137] G. Ruiz, D. Jeison, R. Chamy, Nitrification with high nitrite accumulation for the treatment of wastewater with high ammonia concentration, Water Res. 37 (2003) 1371–1377.

[138] J. Kim, B. Lee, Effect of temperature on nitrogen removal and microbial community composition in nitrifying biofilm reactors, in: IEEE, 2011: pp. 476–479.

[139] U. Wiesmann, Biological nitrogen removal from wastewater, in: Biotechnics/Wastewater, Springer, 1994: pp. 113–154.

[140] Z. Tonkovic, Nitrite accumulation at the Mornington sewage treatment plant–causes and significance, in: 1998: pp. 165–172.

[141] B. Balmelle, K. Nguyen, B. Capdeville, J. Cornier, A. Deguin, Study of factors controlling nitrite build-up in biological processes for water nitrification, Water Sci. Technol. 26 (1992) 1017–1025.

[142] D. Bougard, N. Bernet, D. Cheneby, J.-P. Delgenès, Nitrification of a high-strength wastewater in an inverse turbulent bed reactor: effect of temperature on nitrite accumulation, Process Biochem. 41 (2006) 106–113.

[143] C. Hellinga, A. Schellen, J.W. Mulder, M.C.M. Van Loosdrecht, J.J. Heijnen, The SHARON process: an innovative method for nitrogen removal from ammonium-rich waste water, Water Sci. Technol. 37 (1998) 135–142.

[144] H. Siegrist, W. Gujer, Demonstration of mass transfer and pH effects in a nitrifying biofilm, Water Res. 21 (1987) 1481–1487.

[145] W. Bae, S. Baek, J. Chung, Y. Lee, Optimal operational factors for nitrite accumulation in batch reactors, Biodegradation. 12 (2001) 359–366.

[146] B. Sinha, A.P. Annachhatre, Partial nitrification—operational parameters and microorganisms involved, Rev. Environ. Sci. Biotechnol. 6 (2007) 285–313.

[147] Y. Zhou, A. Oehmen, M. Lim, V. Vadivelu, W.J. Ng, The role of nitrite and free nitrous acid (FNA) in wastewater treatment plants, Water Res. 45 (2011) 4672–4682.

[148] D. Han, J. Chang, D. Kim, Nitrifying microbial community analysis of nitrite accumulating biofilm reactor by fluorescence in situ hybridization, Water Sci. Technol. 47 (2003) 97–104.

[149] D.L. Ford, R.L. Churchwell, J.W. Kachtick, Comprehensive analysis of nitrification of chemical processing wastewaters, J. Water Pollut. Control Fed. (1980) 2726–2746.

[150] Y. He, W. Tao, Z. Wang, W. Shayya, Effects of pH and seasonal temperature variation on simultaneous partial nitrification and anammox in free-water surface wetlands, J. Environ. Manage. 110 (2012) 103–109.

[151] J. Alleman, Elevated nitrite occurrence in biological wastewater treatment systems, Water Sci. Technol. 17 (1985) 409–419.

[152] E. Bock, H.-P. Koops, H. Harms, Cell biology of nitrifying bacteria, (1986).

[153] M. Soliman, A. Eldyasti, Ammonia-Oxidizing Bacteria (AOB): opportunities and applications—a review, Rev. Environ. Sci. Biotechnol. (n.d.) 1–37.

[154] R. Mohammed, S. Abu-Alhail, L. Xi-Wu, Long-term operation of a novel pilot-scale six tanks alternately operating activated sludge process in treating domestic wastewater, Environ. Technol. 35 (2014) 1874–1885.

[155] A. Pollice, V. Tandoi, C. Lestingi, Influence of aeration and sludge retention time on ammonium oxidation to nitrite and nitrate, Water Res. 36 (2002) 2541–2546.

[156] A. Bartrolí, J. Pérez, J. Carrera, Applying ratio control in a continuous granular reactor to achieve full nitritation under stable operating conditions, Environ. Sci. Technol. 44 (2010) 8930–8935.

[157] Peng Yongzhen, Gao Shouyou, Wang Shuying, Bai Lu, Partial Nitrification from Domestic Wastewater by Aeration Control at Ambient Temperature, Chin. J. Chem. Eng. 15 (2007) 115–121.

[158] Q. Yang, Y. Peng, X. Liu, W. Zeng, T. Mino, H. Satoh, Nitrogen removal via nitrite from municipal wastewater at low temperatures using real-time control to optimize nitrifying communities, Environ. Sci. Technol. 41 (2007) 8159–8164.

[159] S. Gu, S. Wang, Q. Yang, P. Yang, Y. Peng, Start up partial nitrification at low temperature with a real-time control strategy based on blower frequency and pH, Bioresour. Technol. 112 (2012) 34–41.

[160] P.-H. Lee, S.F. Cotter, S.C.R. Prieri, D. Attalage, S. Sung, pH-gradient real-time aeration control for nitritation community selection in a non-porous hollow fiber membrane biofilm reactor (MBfR) with dilute wastewater, Chemosphere. 90 (2013) 2320–2325.

[161] P. Regmi, M.W. Miller, B. Holgate, R. Bunce, H. Park, K. Chandran, B. Wett, S. Murthy, C.B. Bott, Control of aeration, aerobic SRT and COD input for mainstream nitritation/denitritation, Water Res. 57 (2014) 162–171.

[162] T. Hidaka, H. Yamada, M. Kawamura, H. Tsuno, Effect of dissolved oxygen conditions on nitrogen removal in continuously fed intermittent-aeration process with two tanks, Water Sci. Technol. 45 (2002) 181–188.

[163] S. Ge, Y. Peng, S. Qiu, A. Zhu, N. Ren, Complete nitrogen removal from municipal wastewater via partial nitrification by appropriately alternating anoxic/aerobic conditions in a continuous plug-flow step feed process, Water Res. 55 (2014) 95–105.

[164] M.C. Bournazou, K. Hooshiar, H. Arellano-Garcia, G. Wozny, G. Lyberatos, Model based optimization of the intermittent aeration profile for SBRs under partial nitrification, Water Res. 47 (2013) 3399–3410.

[165] J.H. Guo, Y.Z. Peng, S.Y. Wang, Y.N. Zheng, H.J. Huang, S.J. Ge, Effective and robust partial nitrification to nitrite by real-time aeration duration control in an SBR treating domestic wastewater, Process Biochem. 44 (2009) 979–985.

[166] D. Wei, X. Xue, L. Yan, M. Sun, G. Zhang, L. Shi, B. Du, Effect of influent ammonium concentration on the shift of full nitritation to partial nitrification in a sequencing batch reactor at ambient temperature, Chem. Eng. J. 235 (2014) 19–26.

[167] J. Li, D. Elliott, M. Nielsen, M.G. Healy, X. Zhan, Long-term partial nitrification in an intermittently aerated sequencing batch reactor (SBR) treating ammonium-rich wastewater under controlled oxygen-limited conditions, Biochem. Eng. J. 55 (2011) 215–222.

[168] G. Xu, X. Xu, F. Yang, S. Liu, Y. Gao, Partial nitrification adjusted by hydroxylamine in aerobic granules under high DO and ambient temperature and subsequent Anammox for low C/N wastewater treatment, Chem. Eng. J. 213 (2012) 338–345.

[169] O.J. Hao, J.M. Chen, Factors affecting nitrite buildup in submerged filter system, J. Environ. Eng. 120 (1994) 1298–1307.

[170] R.L. Irvine, L. Ketchum, The sequencing batch reactor and batch operation for the optimal treatment of wastewater, SBR Technol. Inc. (2004).

[171] J. Gabarró, R. Ganigué, F. Gich, M. Ruscalleda, M. Balaguer, J. Colprim, Effect of temperature on AOB activity of a partial nitritation SBR treating landfill leachate with extremely high nitrogen concentration, Bioresour. Technol. 126 (2012) 283–289.

[172] T.H. Erguder, N. Boon, S.E. Vlaeminck, W. Verstraete, Partial nitrification achieved by pulse sulfide doses in a sequential batch reactor, Environ. Sci. Technol. 42 (2008) 8715–8720.

[173] M. Soliman, A. Eldyasti, Development of partial nitrification as a first step of nitrite shunt process in a Sequential Batch Reactor (SBR) using Ammonium Oxidizing Bacteria (AOB) controlled by mixing regime, Bioresour. Technol. 221 (2016) 85–95.

[174] L. Wang, G. Zeng, Z. Yang, L. Luo, H. Xu, J. Huang, Operation of partial nitrification to nitrite of landfill leachate and its performance with respect to different oxygen conditions, Biochem. Eng. J. 87 (2014) 62–68.

[175] H. Sun, Y. Peng, S. Wang, J. Ma, Achieving nitritation at low temperatures using free ammonia inhibition on Nitrobacter and real-time control in an SBR treating landfill leachate, J. Environ. Sci. 30 (2015) 157–163.

[176] D. Wei, K. Zhang, H.H. Ngo, W. Guo, S. Wang, J. Li, F. Han, B. Du, Q. Wei, Nitrogen removal via nitrite in a partial nitrification sequencing batch biofilm reactor treating high strength ammonia wastewater and its greenhouse gas emission, Bioresour. Technol. 230 (2017) 49–55.

[177] D. Wei, B. Du, X. Xue, P. Dai, J. Zhang, Analysis of factors affecting the performance of partial nitrification in a sequencing batch reactor, Appl. Microbiol. Biotechnol. 98 (2014) 1863–1870. doi:10.1007/s00253-013-5135-z.

[178] J. Yan, Y. Hu, Partial nitrification to nitrite for treating ammonium-rich organic wastewater by immobilized biomass system, Bioresour. Technol. 100 (2009) 2341–2347.

[179] J. Guo, Y. Peng, S. Wang, Y. Zheng, H. Huang, Z. Wang, Long-term effect of dissolved oxygen on partial nitrification performance and microbial community structure, Bioresour. Technol. 100 (2009) 2796–2802.

[180] Y. Peng, Y. Chen, C. Peng, M. Liu, S. Wang, X. Song, Y. Cui, Nitrite accumulation by aeration controlled in sequencing batch reactors treating domestic wastewater, Water Sci. Technol. 50 (2004) 35–43.

[181] R. Lemaire, M. Marcelino, Z. Yuan, Achieving the nitrite pathway using aeration phase length control and step-feed in an SBR removing nutrients from abattoir wastewater, Biotechnol. Bioeng. 100 (2008) 1228–1236.

[182] M. Kornaros, C. Marazioti, G. Lyberatos, A pilot scale study of a sequencing batch reactor treating municipal wastewater operated via the UP-PND process, Water Sci. Technol. 58 (2008) 435–438.

[183] A.N. Katsogiannis, M. Kornaros, G. Lyberatos, Enhanced nitrogen removal in SBRs bypassing nitrate generation accomplished by multiple aerobic/anoxic phase pairs, Water Sci. Technol. 47 (2003) 53–59.

[184] G. Xu, X. Xu, F. Yang, S. Liu, Selective inhibition of nitrite oxidation by chlorate dosing in aerobic granules, J. Hazard. Mater. 185 (2011) 249–254.

[185] S. Fudala-Ksiazek, A. Luczkiewicz, K. Fitobor, K. Olanczuk-Neyman, Nitrogen removal via the nitrite pathway during wastewater co-treatment with ammonia-rich landfill leachates in a sequencing batch reactor, Environ. Sci. Pollut. Res. 21 (2014) 7307–7318.

[186] H. Li, S. Zhou, G. Huang, B. Xu, Partial nitritation of landfill leachate with varying influent composition under intermittent aeration conditions, Process Saf. Environ. Prot. 91 (2013) 285–294.

[187] Z. LIANG, J. LIU, Control factors of partial nitritation for landfill leachate treatment, J. Environ. Sci. 19 (2007) 523–529.

Chapter 3 *

3 A model for determination of operational conditions for successful shortcut nitrification

Accumulation of nitrite in shortcut nitrification is influenced by several factors including dissolved oxygen concentration (DO), pH, temperature, free ammonia (FA) and free nitrous acid (FNA). In this study, a model based on minimum dissolved oxygen concentration (DO_{min}), minimum/maximum substrate concentration (S_{min} and S_{max}), was developed. The model evaluated the influence of pH (7-9), temperature (10^oC-35^oC) and solids retention time (SRT) (5days-infinity) on Minimum/maximum substrate concentration (MSC) values. The evaluation was conducted either by controlling total ammonium nitrogen (TAN) or total nitrite nitrogen (TNN), concentration at 50 mg N/L while allowing the other to vary from 0 to 1000 mg N/L. In addition, specific application for shortcut nitrification-anammox process at 10^oC was analyzed. At any given operational condition, the model was able to predict if shortcut nitrification can be achieved and provide the operational DO range which is higher than the DO_{min} of AOB and lower than that of NOB. Furthermore, experimental data from different literature studies were taken for model simulation and the model prediction fit well the experimental data. For the Sharon process, model prediction with default kinetics did not work but the model could make good prediction after adjusting the kinetic values based on the

* This chapter has been published in a manuscript entitled "Liu, X., Kim, M., & Nakhla, G. (2017). A model for determination of operational conditions for successful shortcut nitrification. *Environmental Science and Pollution Research*, *24*(4), 3539-3549."

Sharon-specific kinetics reported in the literature. This is the first model that provides a method to identify feasible combinations of pH, DO, TAN, TNN, and SRT for successful shortcut nitrification. This model can be a useful and practical tool for shortcut nitrification systems design and operation.

3.1 Introduction

Conventional biological nitrogen removal (BNR) consists of two successive steps: autotrophic nitrification and heterotrophic denitrification. Nitrification consists of two steps: ammonia is first oxidized to nitrite by ammonia-oxidizing bacteria (AOB), and then nitrite is oxidized to nitrate by nitrite-oxidizing bacteria (NOB). From a biochemical perspective, AOB utilize ammonium (NH_4^+-N) as their electron donor and NOB utilize nitrite (NO_2^-) as electron donor. Both AOB and NOB utilize dissolved oxygen (DO) as their electron acceptor, suggesting that a competition for DO between AOB and NOB exists in nitrification systems. Shortcut nitrification/denitrification and shortcut nitrification/anammox are two promising technologies to replace conventional biological nitrogen removal (BNR) [1,2]. The benefits of shortcut nitrification processes include lower oxygen and carbon requirements [3–5]. Enrichment of AOB and washout or inhibition of NOB are important for realizing the partial-nitrification process.

When competing for DO, NOB are often at a disadvantage due to their higher dissolved oxygen half-saturation coefficients. Thus, DO control has been adopted by many researchers to achieve shortcut nitrification. However, DO concentrations for achieving stable shortcut nitrification

varied in different studies, as shown in Appendix A Table A3-1. As apparent from SI-Table 3-1, DO values range from 0.16 to 5 mg DO/L. The wide differences in operational DO concentrations resulted directly from the changes in pH, free ammonia (FA), free nitrous acid (FNA), and temperature, as well as the type of system (attached growth or suspended growth). Thus, optimization of DO concentration at any given operational conditions such as pH, FA, FNA, temperature is critical for the design and operation of a successful shortcut nitrification system.

In this study, we developed a mathematical model proposing the concept of the minimum/maximum substrate (MSC) concentrations to include oxygen limitations and the effect of pH, FA and FNA, temperature and SRT at a given ambient TNN and TAN concentration. The choice of free ammonia as the AOB substrate is rationalized by [6,7], who demonstrated from batch tests that NH_3 rather than NH_4^+ is the actual substrate, which is also supported by the fact that biomass can only transport the uncharged NH_3 over its membrane [8]. The model was also validated with data from the literature.

3.2 Methodology

3.2.1 General MSC equation.

S_{min} is the minimum substrate concentration to support steady-state biomass [9,10]. S_{min} and DO_{min} can be derived from the Monod equation as eq.3.1 and eq.3.2, respectively [10].

$$S_{min} = K_s \cdot \frac{b}{\frac{\mu_{max} \cdot DO}{DO + K_O} - b} \quad \text{(Eq.3.1)}$$

$$DO_{min} = K_O \cdot \frac{b}{\frac{\mu_{max} \cdot S}{S+K_S} - b} \quad \text{(Eq.3.2)}$$

S_{min} refers to the minimum electron donor. K_s and K_o are the Monod half-saturation concentrations for the electron donor (S) and electron acceptor (DO), respectively, μ_{max} is the maximum growth rate and b is the endogenous decay rate.

3.2.2 MSC equation for AOB.

In this study, by adopting free ammonia as substrate, Eq.3.1 and Eq.3.2 are converted to Eq. 3.3 and Eq.3.4.

$$FA_{min} = K_{FA} \cdot \frac{b}{\frac{\mu_{max} \cdot DO}{DO+K_O} - b} \quad \text{(Eq.3.3)}$$

$$DO_{min} = K_O \cdot \frac{b}{\frac{\mu_{max} \cdot FA}{FA+K_{FA}} - b} \quad \text{(Eq.3.4)}$$

In which, FA is free ammonia, mg N/L; DO is dissolved oxygen, mg O_2/L; Ko is the Monod half-saturation rate concentration for dissolved oxygen, mg O_2/L; K_{FA} is the Monod half-saturation rate concentration for FA, mg N/L; μ_{max} is the maximum growth rate and b is the endogenous decay rate, d^{-1};

3.2.3 MSC equation for NOB.

In this study, TNN is chosen as the substrate for NOB [11,12]. Eq.3.1 and Eq.3.2 are converted to Eq.3.5 and Eq.3.6:

$$\text{TNN} = K_{TNN} \cdot \frac{b}{\frac{\mu_{max} \cdot DO}{DO+K_O} - b} \quad \text{(Eq.3.5)}$$

$$DO_{min} = K_O \cdot \frac{b}{\frac{\mu_{max} \cdot TNN}{TNN + K_{TNN}} - b} \quad \text{(Eq.3.6)}$$

In which TNN is total nitrite nitrogen, mg N/L; K_{TNN} is the Monod half-saturation concentration for TNN, mg N/L.

3.2.4 Effect of pH.

The pH can influence nitrification directly by changing the enzymatic reaction mechanism [7,13] and indirectly by changing the concentrations of FA and FNA, which inhibit AOB and NOB [6,7,12].

The direct pH effect on the maximum specific substrate utilization rate of AOB or NOB can be captured by the empirical bell-shaped Eq.3.7 [13]:

$$q = \frac{q_{max}}{2} \cdot \{1 + \cos[\frac{\pi}{w} \cdot (pH - pH_{opt})]\} \quad \text{(Eq.3.7)}$$

($|pH - pH_{opt}|$<w))

q and q_{max} are, respectively, the maximum specific substrate utilization rate at a given pH and at the optimal pH, mg N/(mg VSS d). w is the pH range within which the q is larger than one-half of $q_{max.}$

Since the biomass yield is a constant, μ is also affected by pH similar to q:

$$\mu = \frac{\mu_{max}}{2} \cdot \{1 + \cos[\frac{\pi}{w} \cdot (pH - pH_{opt})]\} \quad \text{(Eq.3.8)}$$

In which, μ is the maximum specific substrate utilization rate at a given pH, d^{-1}.

FA and FNA, both of which inhibit AOB and NOB, are influenced by pH. FA and FNA concentrations can be calculated based on pH and TAN or TNN concentration [8,13].

$$\mathrm{FA} = \frac{17}{14} \cdot \frac{TAN \cdot 10^{pH}}{\exp\left(\frac{6344}{273+T}\right)+10^{pH}} \quad \text{(Eq.3.9)}$$

$$\mathrm{FNA} = \frac{47}{14} \cdot \frac{TNN}{\exp[\left(\frac{-2300}{273+T}\right) \cdot 10^{pH}]+1} \quad \text{(Eq.3.10)}$$

where T is temperature (^{o}C), TAN is total ammonium nitrogen, mg N/L.

Given that FA is the substrate for AOB and FNA is not a substrate for AOB, the inhibition of FA and FNA may potentially be modeled by the following substrate inhibition model [14,15] and non-substrate inhibition model [6], as shown below in eq.3.11 and eq.3.12, respectively.

$$\mu = \mu_{max} \cdot \frac{DO}{DO+K_O} \cdot \frac{FA}{K_{FA}+FA+\frac{FA^2}{K_{IFA}}} \quad \text{(Eq.3.11)}$$

$$\mu = \mu_{max} \cdot \frac{DO}{DO+K_O} \cdot \frac{FA}{FA+K_{FA}} \cdot \frac{K_{IFNA}}{K_{IFNA}+FNA} \quad \text{(Eq.3.12)}$$

Thus, integrating the direct and indirect effects of pH on AOB yields:

$$\mu_{obs} = \frac{\mu_{max}}{2} \cdot \{1 + \cos[\frac{\pi}{w} \cdot (pH - pH_{opt})]\} \cdot \frac{DO}{DO+K_O} \cdot \frac{FA}{K_{FA}+FA+\frac{FA^2}{K_{IFA}}} \cdot \frac{K_{IFNA}}{K_{IFNA}+FNA}$$

(Eq.3.13)

K_{IFA} and K_{IFNA} are the inhibition concentrations for FA and FNA on AOB, mg N/L. μ_{obs} is the observed specific biomass growth rate, d^{-1}.

A non-substrate inhibition model was adopted for FA inhibition of NOB as FA is not a substrate for NOB. The model by Boon and Laudelout (1962) was chosen to describe the FNA inhibition

of NOB [11]. Thus, integrating the direct and indirect effects of pH on NOB yields the following:

$$\mu_{obs} = \frac{\mu_{max}}{2} \cdot \{1 + \cos[\frac{\pi}{w} \cdot (pH - pH_{opt})]\} \cdot \frac{DO}{DO+K_O} \cdot \frac{TNN}{(K_{TNN}+TNN)(1+\frac{FNA}{K'_{IFNA}})} \cdot \frac{K'_{IFA}}{K'_{IFA}+FA}$$

(Eq.3.14)

K'_{IFA} and K'_{IFNA} are the inhibition concentration for FA and FNA on NOB, mg N/L.

3.2.5 Effect of Temperature.

The Monod maximum growth rate (μ_{max}), the half-saturation concentration (K_S) and the endogenous decay rate (b)were adjusted for temperature:

$$\mu_{max} = \mu_{max20} \cdot \theta_{\mu}^{T-20} \quad \text{(Eq.3.15)}$$

$$K_S = K_{S20} \cdot \theta_{K_S}^{T-20} \quad \text{(Eq.3.16)}$$

$$b = b_{20} \cdot \theta_{b}^{T-20} \quad \text{(Eq.3.17)}$$

where T is temperature (^oC), θ is the temperature coefficient.

3.2.6 SRT effect.

The effect of SRT on the MSC equations is shown in eq.3.18:

$$\mu_{max} \cdot \frac{DO}{K_O+DO} \cdot \frac{S}{S+K_S} - b - \frac{1}{SRT} = 0 \quad \text{(Eq.3.18)}$$

3.2.7 Integration of Effects.

DO_{min} equations for AOB and NOB are shown in eq.3.19 and eq.3.20, respectively.

$$DO_{min} = \frac{(b_{20}\cdot\theta_b^{T-20}+\frac{1}{SRT})\cdot K_o}{\frac{\mu_{max20}\cdot\theta_\mu^{T-20}}{2}\cdot\{1+\cos[\frac{\pi}{w}\cdot(pH-pH_{opt})]\}}{\left(1+\frac{FNA}{K_{IFNA}}\right)\cdot\left(1+\frac{K_{FA20}\cdot\theta_{K_{FA}}^{T-20}}{FA}+\frac{FA}{K_{IFA}}\right)}-b_{20}\cdot\theta_b^{T-20}-\frac{1}{SRT}} \text{ for AOB} \quad \text{(Eq.3.19)}$$

$$DO_{min} = \frac{(b_{20}\cdot\theta_b^{T-20}+\frac{1}{SRT})\cdot K_o}{\frac{\mu_{max20}\cdot\theta_\mu^{T-20}}{2}\cdot\{1+\cos[\frac{\pi}{w}\cdot(pH-pH_{opt})]\}}{\left(1+\frac{FNA}{K'_{IFNA}}\right)\cdot\left(1+\frac{FA}{K'_{IFA}}\right)\cdot\left(1+\frac{K_{TNN20}\cdot\theta_{K_{TNN}}^{T-20}}{TNN}\right)}-b_{20}\cdot\theta_b^{T-20}-\frac{1}{SRT}} \text{ for NOB} \quad \text{(Eq.3.20)}$$

FA_{min} and FA_{max} for AOB and TNN_{min} and TNN_{max} for NOB can be calculated from Eq.3.21- Eq.3.24, respectively, since FA for AOB and TNN for NOB have two limiting values with FA and FNA inhibition. The lower limiting value (FA_{min} or TNN_{min}) has the same meaning as the traditional S_{min} i.e. the minimum substrate concentration to support steady-state biomass while the higher value (FA_{max} or TNN_{max}) represents the maximum substrate concentration able to sustain steady-state biomass, above which inhibition by FA or FNA will lead to wash out of AOB or NOB.

For AOB,

$$\mathrm{FA}_{min}=\frac{\frac{\frac{\mu\, max20\cdot\theta_{\mu}^{T-20}}{2}\times\{1+\cos[\frac{\pi}{w}(pH-pH_{opt})]\}\times DO}{(1+\frac{FNA}{K_{IFNA}})\cdot(K_O+DO)}-\mathrm{b}_{20}\cdot\theta_{\mathrm{b}}^{T-20}-\frac{1}{SRT}-\sqrt{(\frac{\frac{\mu\, max20\cdot\theta_{\mu}^{T-20}}{2}\cdot\{1+\cos[\frac{\pi}{w}(pH-pH_{opt})]\}\cdot DO}{(1+\frac{FNA}{K_{IFNA}})\cdot(K_O+DO)}-\mathrm{b}_{20}\cdot\theta_{\mathrm{b}}^{T-20}-\frac{1}{SRT})^2-4\cdot\frac{(\mathrm{b}_{20}\cdot\theta_{\mathrm{b}}^{T-20}+\frac{1}{SRT})^2\cdot\mathrm{K}_{FA20}\cdot\theta_{\mathrm{K}_{FA}}^{T-20}}{K_{IFA}}}}{2\cdot(\mathrm{b}_{20}\cdot\theta_{\mathrm{b}}^{T-20}+\frac{1}{SRT})\cdot\frac{1}{K_{IFA}}} \quad \text{(Eq.3.21)}$$

$$\mathrm{FA}_{max}=\frac{\frac{\frac{\mu\, max20\cdot\theta_{\mu}^{T-20}}{2}\times\{1+\cos[\frac{\pi}{w}(pH-pH_{opt})]\}\cdot DO}{(1+\frac{FNA}{K_{IFNA}})\cdot(K_O+DO)}-\mathrm{b}_{20}\cdot\theta_{\mathrm{b}}^{T-20}-\frac{1}{SRT}+\sqrt{(\frac{\frac{\mu\, max20\cdot\theta_{\mu}^{T-20}}{2}\cdot\{1+\cos[\frac{\pi}{w}(pH-pH_{opt})]\}\cdot DO}{(1+\frac{FNA}{K_{IFNA}})\cdot(K_O+DO)}-\mathrm{b}_{20}\cdot\theta_{\mathrm{b}}^{T-20}-\frac{1}{SRT})^2-4\cdot\frac{(\mathrm{b}_{20}\cdot\theta_{\mathrm{b}}^{T-20}+\frac{1}{SRT})^2\times\mathrm{K}_{FA20}\times\theta_{\mathrm{K}_{FA}}^{T-20}}{K_{IFA}}}}{2\times(\mathrm{b}_{20}\times\theta_{\mathrm{b}}^{T-20}+\frac{1}{SRT})\times\frac{1}{K_{IFA}}} \quad \text{(Eq.3.22)}$$

For NOB,

$$\mathrm{TNN}_{min}=\frac{\frac{\mu\, max20\times\theta_{\mu}^{T-20}\times DO}{(1+\frac{FA}{\mathrm{K}_{IFA}})\times(K_O+DO)}-(\mathrm{b}_{20}\times\theta_{\mathrm{b}}^{T-20}+\frac{1}{SRT})\left(1+\mathrm{K}_{TNN20}\times\theta_{\mathrm{K}_{TNN}}^{T-20}\times\frac{f_{FNA}}{\mathrm{K}_{IFNA}}\right)-\sqrt{\left(\frac{\mu\, max20\times\theta_{\mu}^{T-20}\times DO}{(1+\frac{FA}{\mathrm{K}_{IFA}})\times(K_O+DO)}-(\mathrm{b}_{20}\times\theta_{\mathrm{b}}^{T-20}+\frac{1}{SRT})\left(1+\mathrm{K}_{TNN20}\times\theta_{\mathrm{K}_{TNN}}^{T-20}\times\frac{f_{FNA}}{\mathrm{K}_{IFNA}}\right)\right)^2-4\times(\mathrm{b}_{20}\times\theta_{\mathrm{b}}^{T-20}+\frac{1}{SRT})^2\cdot\mathrm{K}_{TNN20}\cdot\theta_{\mathrm{K}_{TNN}}^{T-20}\cdot\frac{f_{FNA}}{\mathrm{K}_{IFNA}}}}{2\cdot(\mathrm{b}_{20}\cdot\theta_{\mathrm{b}}^{T-20}+\frac{1}{SRT})\cdot\frac{f_{FNA}}{\mathrm{K}_{IFNA}}} \quad \text{(Eq.3.23)}$$

$$\mathrm{TNN}_{min}=\frac{\frac{\mu\, max20\cdot\theta_{\mu}^{T-20}\cdot DO}{(1+\frac{FA}{\mathrm{K}_{IFA}})\cdot(K_O+DO)}-\left(\mathrm{b}_{20}\cdot\theta_{\mathrm{b}}^{T-20}+\frac{1}{SRT}\right)\left(1+\mathrm{K}_{TNN20}\cdot\theta_{\mathrm{K}_{TNN}}^{T-20}\cdot\frac{f_{FNA}}{\mathrm{K}_{IFNA}}\right)+\sqrt{\left(\frac{\mu\, max20\cdot\theta_{\mu}^{T-20}\times DO}{(1+\frac{FA}{\mathrm{K}_{IFA}})\cdot(K_O+DO)}-(\mathrm{b}_{20}\cdot\theta_{\mathrm{b}}^{T-20}+\frac{1}{SRT})\left(1+\mathrm{K}_{TNN20}\cdot\theta_{\mathrm{K}_{TNN}}^{T-20}\cdot\frac{f_{FNA}}{\mathrm{K}_{IFNA}}\right)\right)^2-4\cdot(\mathrm{b}_{20}\cdot\theta_{\mathrm{b}}^{T-20}+\frac{1}{SRT})^2\cdot\mathrm{K}_{TNN20}\cdot\theta_{\mathrm{K}_{TNN}}^{T-20}\cdot\frac{f_{FNA}}{\mathrm{K}_{IFNA}}}}{2\cdot(\mathrm{b}_{20}\cdot\theta_{\mathrm{b}}^{T-20}+\frac{1}{SRT})\cdot\frac{f_{FNA}}{\mathrm{K}_{IFNA}}} \quad \text{(Eq.3.24)}$$

For AOB, using the relationship between TAN and FA of Eq.3.9, TAN_{min} and TAN_{max} can be derived as Eq.3.25 and Eq.3.26, respectively.

$$\mathrm{TAN}_{min} = \mathrm{FA}_{min} \cdot \frac{14}{17} \cdot \frac{[\exp\left(\frac{6344}{273+℃}\right)+10^{pH}]}{10^{pH}} \quad \text{(Eq.3.25)}$$

$$\mathrm{TAN}_{max} = \mathrm{FA}_{max} \cdot \frac{14}{17} \cdot \frac{[\exp\left(\frac{6344}{273+℃}\right)+10^{pH}]}{10^{pH}} \quad \text{(Eq.3.26)}$$

3.2.8 Modeling Simulations

Simulations were conducted based on Eq.3.19- Eq.3.24 using six cases to evaluate the effect of pH, temperature, and SRT on a CSTR without biomass recycle. The kinetic parameter values used for modelling are summarized in Table 3-1 while the simulation conditions are presented in Table 3-2. Taking case 1 as an example, the TNN and temperature were kept constant at 50 mg N/L and 35^{o}C, respectively, SRT was set as infinity, at each pH, the input ws TAN as mg N/L and the output was DO_{min} for AOB and NOB as mg O_2/L.

Table 3-1. Various Kinetic Parameters Selected for the Model Simulation (at 20°C)

	Kinetic parameters	AOB	NOB	Reference
K_S	half-max-rate concentration (mg N/L)	0.75(NH_3-N)	2.7(TNN)	[7,16];
K_O	half-max-rate concentration (mg DO/L)	0.51	1.98	[7,17]
μ_{max}	maximum growth rate(d^{-1})	0.9	1.0	[18]
b	decay coefficient (d^{-1})	0.17	0.17	
W	pH range	3.2	2.4	[12]
pH_{opt}	optimal pH	8.4	7.7	
θ_{Ks}	Temperature coefficient for Ks	1.029	1.029	
θ_{μ}	Temperature coefficient for μ_{max}	1.072	1.063	[14]
θ_b	Temperature coefficient for b	1.04	1.04	
K_{IFA}	inhibition concentration (mgFA/L)	10	0.75	[16]
K_{IFNA}	inhibition concentration (mgFNA/L)	0.5	0.1	

Table 3-2. Operational Conditions for Six Simulation Cases

Case	TAN (mg N/L)	TNN (mg N/L)	pH	Temperature (°C)	SRT (d)
1	0-1000	50	7, 7.5, 8, 8.5, 9	35	infinity
2	50	0-1000	7, 7.5, 8, 8.5, 9	35	infinity
3	0-1000	50	8	10, 15, 20, 25, 30, 35	infinity
4	50	0-1000	8	10, 15, 20, 25, 30, 35	infinity
5	0-1000	50	8	35	5,10,20,30, infinity
6	50	0-1000	8	35	5,10,20,30, infinity

3.3 Results and Discussion

3.3.1 Impact of pH: Cases 1 and 2.

Figures 3-1A and 3-1B show the DO_{min}curves for AOB and NOB at different pHs. For each pH in case 1, the curves are generated by fixing TNN at 50 mg N/L, temperature of 35^{o}C, pH of 8 as an example, and predicting the DO_{min} for AOB and NOB at TAN from 0 to 1000 mg N/L. Generally, if the operating DO is above the DOmin curves for AOB and/or NOB, the conditions support the growth of AOBs, NOBs, or both. FA inhibition increases with pH increase while FNA inhibition increases with pH decrease. For case 1, the TAN_{min} and TAN_{max} represent the maximum and minimum TAN concentration for AOB to grow. When the TAN is lower than TAN_{min}, AOB can not be sustained due to substrate limitation. When the TAN is higher than TAN_{max}, AOB can not grow due to FA inhibition. For AOB, when the TAN concentration is below TAN_{min} or over TAN_{max}, DO_{min} approaches infinity, which identifies the washout range (WR) for AOBs. Similar boundaries of TNN_{min} or over TNN_{max} also exist for NOB.

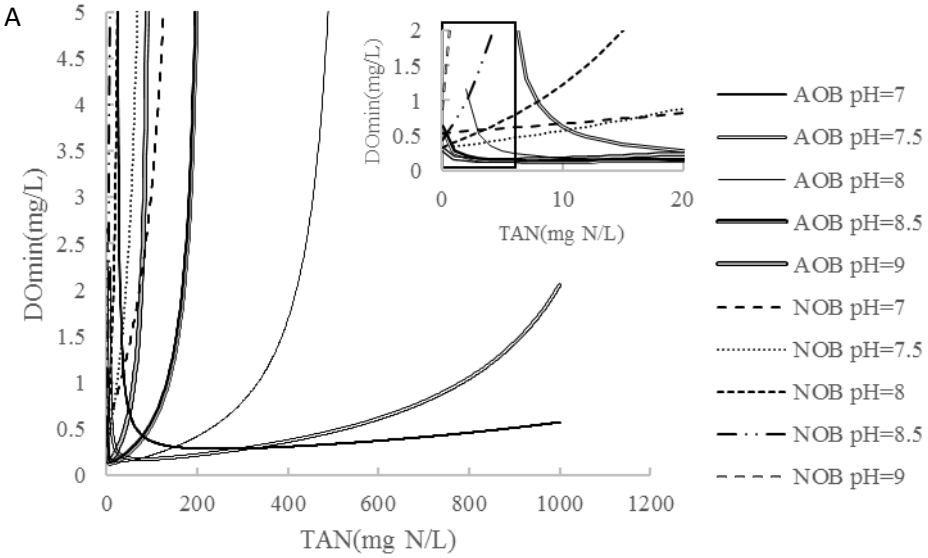

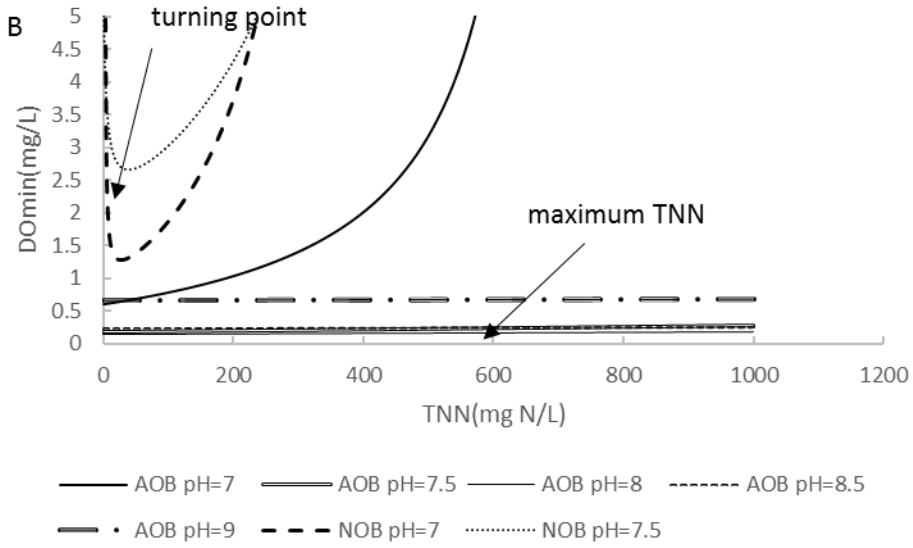
B
turning point
maximum TNN
DOmin(mg/L)
TNN(mg N/L)
AOB pH=7
AOB pH=7.5
AOB pH=8
AOB pH=8.5
AOB pH=9
NOB pH=7
NOB pH=7.5

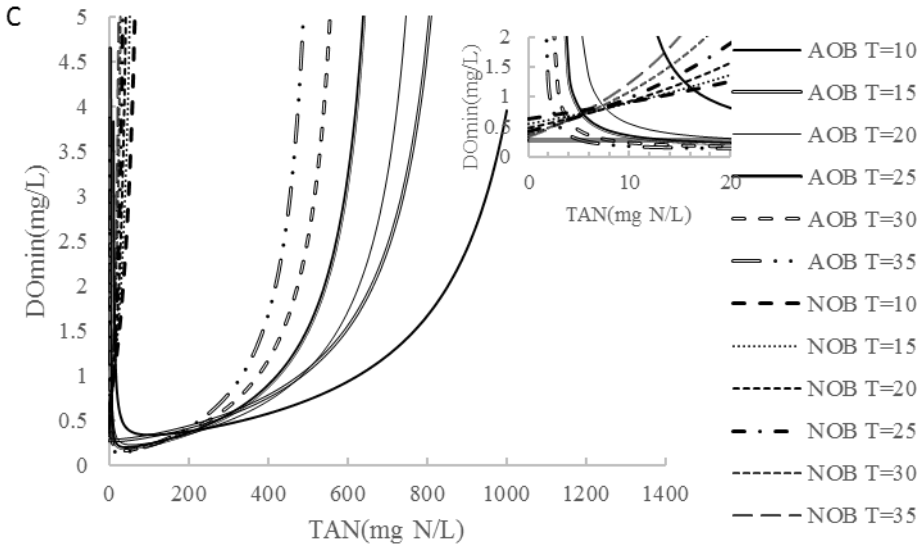
C
DOmin(mg/L)
TAN(mg N/L)
AOB T=10
AOB T=15
AOB T=20
AOB T=25
AOB T=30
AOB T=35
NOB T=10
NOB T=15
NOB T=20
NOB T=25
NOB T=30
NOB T=35

D

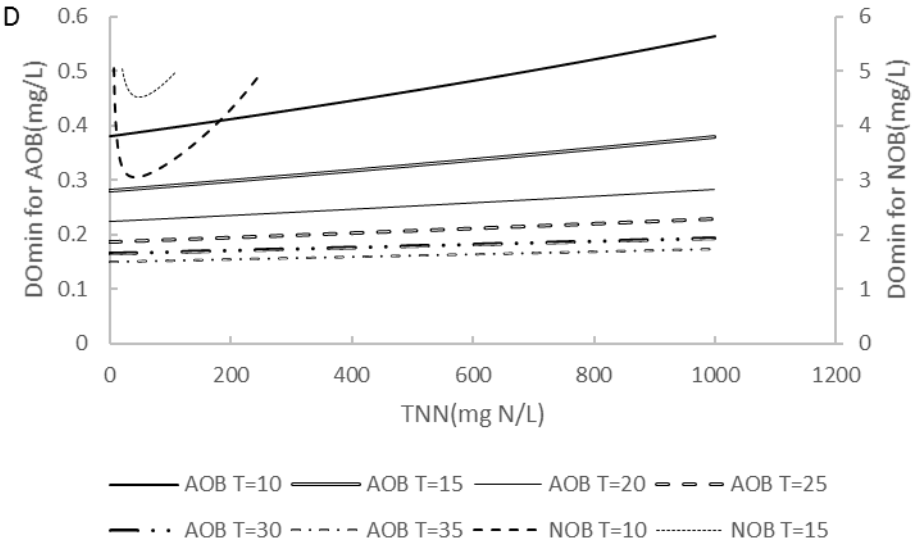
DOmin for AOB(mg/L)
DOmin for NOB(mg/L)
TNN(mg N/L)
AOB T=10
AOB T=15
AOB T=20
AOB T=25
AOB T=30
AOB T=35
NOB T=10
NOB T=15

E

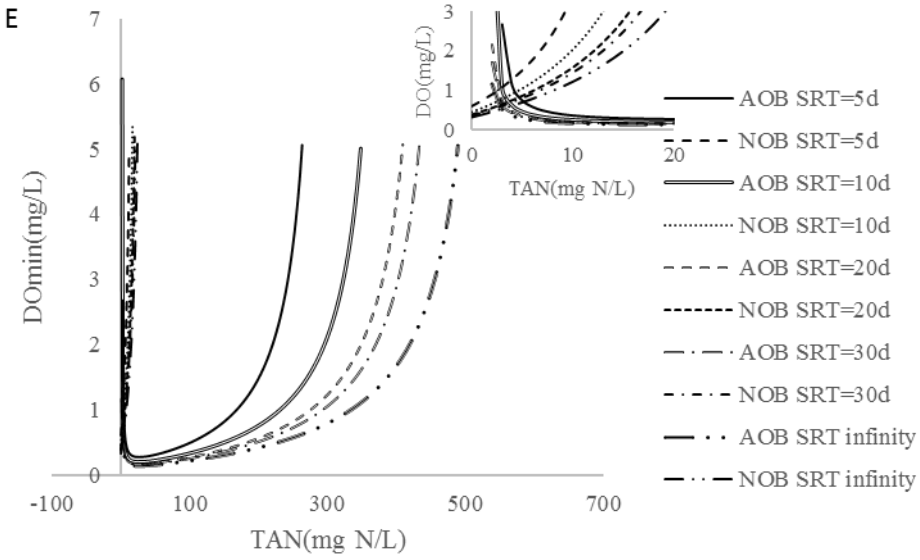
DOmin(mg/L)
TAN(mg N/L)
DO(mg/L)
TAN(mg N/L)
AOB SRT=5d
NOB SRT=5d
AOB SRT=10d
NOB SRT=10d
AOB SRT=20d
NOB SRT=20d
AOB SRT=30d
NOB SRT=30d
AOB SRT infinity
NOB SRT infinity

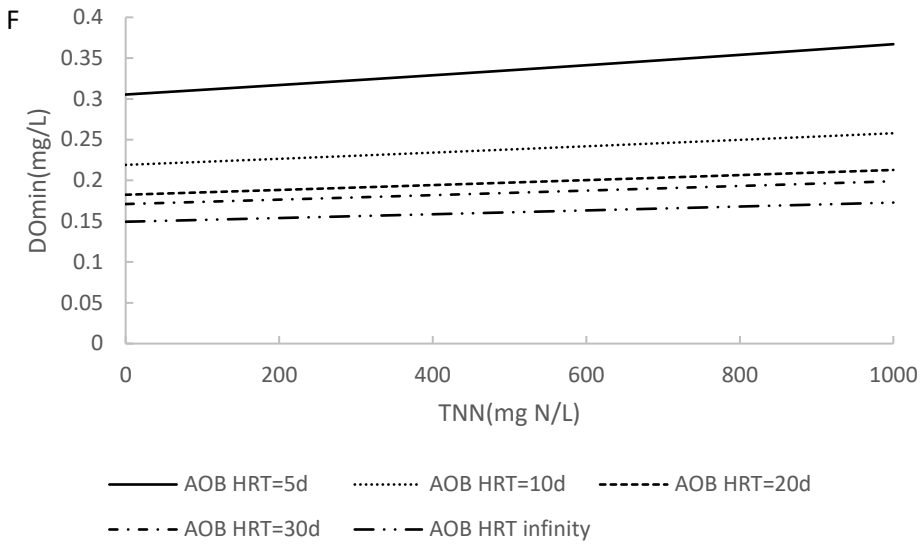

Figure 3-1. Comparison with MSC curves. (A-F represent case 1-6, respectively)

Case 1 simulates the effect of pH on AOB and NOB at a constant TNN concentration of 50 mg N/L and TAN concentration of 0-1000 mg N/L. At pH 7, AOB and NOB curves intersect at 38 mg N/L, implying that below 38 mg N/L it is impossible to wash out NOB and maintain AOB by DO control as DO_{min} for NOB is lower than DO_{min} for AOB. The intersection TAN concentrations at pH 7.5, 8, 8.5 and 9 are 10 mg N/L, 3 mg N/L, 0 mg N/L and 0 mg N/L, implying that the minimum operational TAN concentration decreases as pH increases. Both TAN_{min} and TAN_{max} concentrations for AOB decrease as pH increases. For example, for pH in the 7 to 9 range, the TAN_{min} concentration for AOB decreases from 24 mg N/L to 0.3 mg N/L. Similarly, the TAN_{max} values for AOB at pH 7 and 7.5 are over 1000 mg N/L and at 8, 8.5 and 9 are approximately 489 mg N/L, 200 mg N/L and 90 mg N/L. Due to FA inhibition, the TAN_{max} for NOB also decreases from 126 mg N/L at pH 7 to 0.3 mg N/L at pH 9. In this analysis, both TAN_{min} and TAN_{max} represent the TAN concentration at which DO_{min} reaches 5 mg /L. When the DO is 2 mg/L and TNN concentration is constant at 50 mg N/L, the TAN concentration range for shortcut

nitrification at pH 7, 7.5, 8, 8.5 and 9 are 74-1000 mg N/L, 43-1000 mg N/L, 16-489 mg N/L, 5-200 mg N/L, and 1-90 mg N/L, respectively. Yan and Hu (2009) operated a CSTR, at SRTs of 1 to 2 day, DO of 2 mg/L, temperature of 35 ºC, pH 8 and achieved nitrite accumulation at a TAN of 150 and TNN of 180 mg N/L for CSTR [19]. The computed DO_{min} for AOB growth and complete NOB washout based on this model for the conditions of Yan and Hu (2009) are 0.29-0.78 mg/L which are less than 2 mg/L and consistent with the experimental results.

Case 2 simulates the effect of pH on AOB and NOB at a constant TAN concentration of 50 mg N/L and TNN concentration of 0-1000 mg N/L (Figure 1B). The DO_{min} for NOB are always higher than those for AOB, implying that shortcut nitrification is achievable at any pH, especially at pH over 8, when DO_{min} for NOB goes to infinity meaning that NOB are always washed out. The optimal pH is around 8 as the DO_{min} range for AOB with TNN ranging from 0 mg/L to 1000 mg/L are 0.15-0.17 mg/L at pH 8, 0.24-0.26 mg/L at pH 8.5 and 0.66-0.68 mg/L at pH 9. TNN concentrations exert minimal impact on the DO_{min} for AOB. As apparent from cases 1 and 2, the TAN has a much greater effect on the DO_{min} of AOB and NOB than the TNN. There is a turning point which corresponds to the minima of the DO_{min} curves (Fig 1B as an example) on the TAN-DO curve for AOB and on the TNN-DO curve for NOB, when TNN or TAN is fixed. For example, in Fig 1A, when TAN is lower than the turning point value, DO_{min} for AOB will increase significantly with TAN decrease. As discussed above, pH 8 seems to be optimal for AOB at constant TAN values at 50 mg N/L. However, the optimal pH may not be applicable to specific circumstances. For example, if an effluent TAN of 800 mg N/L and TNN of 50 mg N/L is required, only pH 7 or 7.5 can be utilized.

3.3.2 Impact of Temperature: Cases 3 and 4.

The effect of temperature in the 10^{o}C to 35^{o}C range on the DO MSC curves for AOB and NOB is shown in Figures 3-1C and 3-1D. Case 3 is similar to case 1 at a constant TNN concentration of 50 mg N/L and TAN concentration of 0-1000 mg N/L while case 4 is similar to case 2 at a constant TAN concentration of 50 mg N/L and TNN concentration of 0-1000 mg N/L.

In case 3, both TAN_{min} and TAN_{max} values for AOB decreased as temperature increased. The TAN_{min} and TAN_{max} values for AOB decreased from 11 mg N/L and over 1000 mg N/L at 10^{o}C to 1.5 mg N/L and 489 mg N/L at 35^{o}C. The TAN_{max} for NOB also decreased from 65 mg N/L at 10^{o}C to 24 mg N/L at 35^{o}C. The intersection TAN concentration of AOB and NOB curves decreased from 16 mg N/L at 10^{o}C to 3 mg N/L at 35^{o}C. From the aforementioned point of intersection to TAN_{max} for AOB, it is possible to maintain AOB and wash out NOB by adopting specific DO control. For example, from TAN_{max} for NOB to TAN_{max} for AOB, nitrite accumulation can always be achieved with DO higher than DO_{min} for AOB. In case 4, when TAN is fixed at 50 mg N/L, the DO_{min} for NOB are always higher than that for AOB, meaning that shortcut nitrification is achievable at any temperature in the 10 ^{o}C to 35 ^{o}C range.

3.3.3 Impact of SRT: Cases 5 and 6.

The effect of SRT on DO MSC curves for AOB and NOB is shown in Figure 3-1E and 3-1F by changing SRT from 5 days to infinity while maintaining pH and temperature constant at 8 and 35^{o}C, respectively.

Case 5 simulates the effect of SRT on AOB and NOB at a constant TNN concentration of 50 mg N/L and TAN concentration of 0-1000 mg N/L. The TAN_{min} concentrations for AOB at any SRT

are lower than 3 mg N/L. BothTAN_{max} values for AOB and NOB increased with SRT. The TAN_{max} concentration for AOB increases from 263 mg N/L at an SRT of 5d to 489 mg N/L at an infinite SRT. The TAN_{max} for NOB increased from 13 mg N/L at an SRT of 5d to 24 mg N/L at an infinite SRT. The intersection point of the DO curves for AOB and NOB corresponds to the TAN concentration at which both species survive. The common TAN concentration for both AOB and NOB decreased as SRT increased from 5d to infinity but always fell within the range of 3 to 4 mg N/L.

Case 6 simulates the effect of SRT on AOB at a constant TAN concentration of 50 mg N/L and TNN concentration of 0-1000 mg N/L. At all SRTs, NOB will be washed out, ending up with nitrite accumulation when DO is higher than DO_{min} for AOB. From figure 1F, DO_{min} for AOB decreased as SRT increased at a given TNN concentration.

3.3.4 Special Applications of the DO_{MSC} Curves.

Recently, the feasibility and performance of nitritation-anammox system at low nitrogen concentrations (20 to 60 mg NH_4-N/L) and low temperatures (5-25°C) has elicited the attention of both researchers and practitioners [20–23]. The MSC curves for various pHs for the special case of shortcut nitrification-anammox process at 10^{o}C are shown in Figure 3-2. In this simulation, SRT were set at 10, 20, and 30 days, temperature was set as 10, 15 and 20 ^{o}C, the pH was set at 8. Stoichiometrically, anammox needs an influent that has almost the same concentrations of ammonium- and nitrite-nitrogen [24]. Thus, the TAN/TNN was set at 1:1.32 with total nitrogen (TN) as the sum of TAN and TNN i.e. completely ignoring nitrates. As presented in Figure 3-2, the DO_{min} for both AOB and NOB decreased when SRT or temperature increased. The minimum

SRT decreased with temperature increase. At a given condition, for example, a TN of 60 mg N/L, pH 8, the minimum SRT was 13 d at 10ºC, decreasing to 7d at 15ºC, and further to 3.6 d at 35ºC.

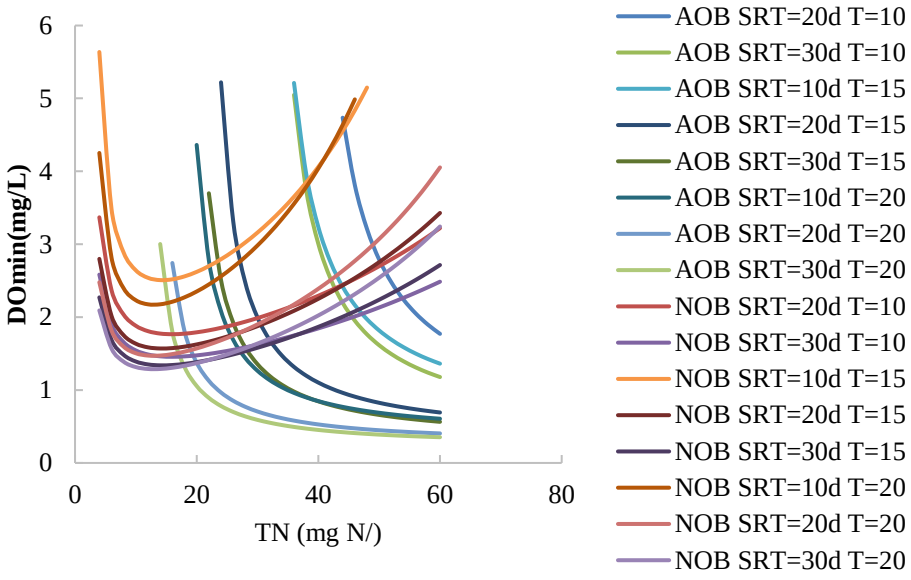

Figure 3-2. DO_{min} curves by SRT (10-30d) and temperature(10-20ºC) for shortcut nitritation to provide an input to the ANAMMOX process.

Specifically, the DO_{min} curves of AOB and NOB as a function of TN (based on NO_2-N/NH_4-N of 1.32) at SRT of 30 d, temperature of 20ºC and pH of 8, are shown in Figure 3-3. Three areas were marked as area A, B and C, respectively in the figure. Based on AOB curve, areas B and C represent the conditions for AOB to grow. Based on NOB curve, areas A and B represent the conditions for NOB to grow. Thus, full nitrification can be achieved inarea B, in which the operational DO is higher than DO_{min} of both AOB and NOB, i.e. DO of 2 mg/L, SRT of 30 days, temperature of 20ºC, and TN of 40 mg N/L. Partial nitrification could be achieved under conditions of area C, in which the operational DO is higher than DO_{min} of AOB but lower than that of NOB. For example, at a TN of 40 mg N/L, the DO should be in the range from 0.45 mg O_2/L to 0.9 mg O_2/L for partial nitrification.

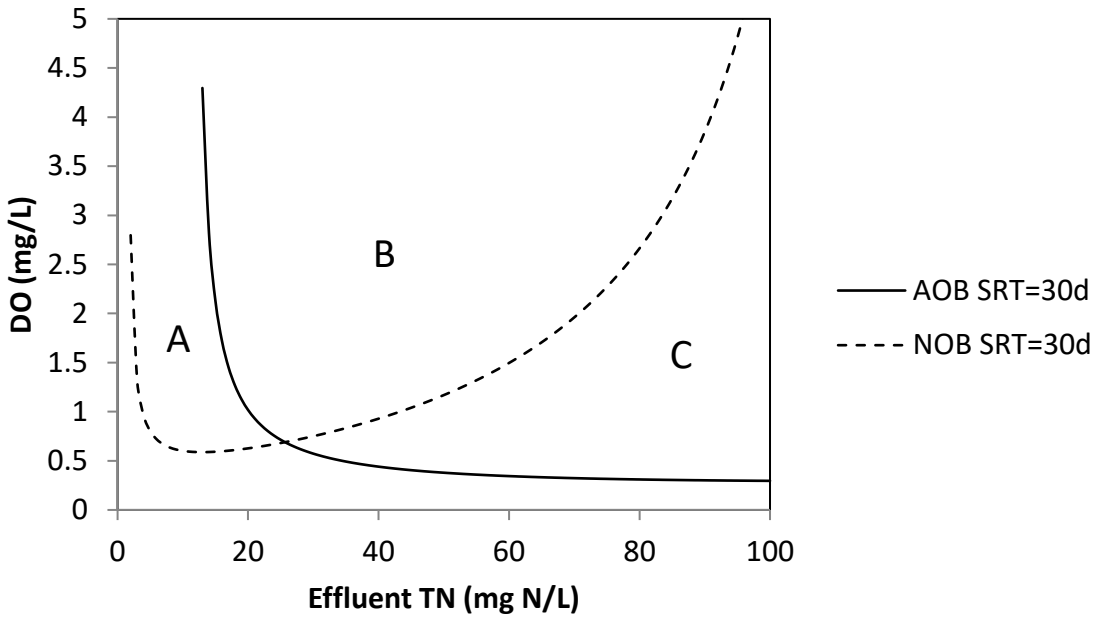

Figure 3-3. DOmin curves of AOB and NOB at SRT of 30d, temperature of 20°C, and pH of 8-Effluent NO_2-N/NH_4-N=1.32

3.3.5 Analysis of literature results with the MSC model.

Table 3-3 summarizes the comparison of literature operational conditions and performance data with the computed DO_{min} values based on this model. Columns 1 to 8 are from the experimental data, columns 10 to 11 are AOB and NOB DO_{min} values calculated using the experimental values in this model. Almost all experimental DO values are higher than DO_{min} for AOB and lower than DO_{min} for NOB, suggesting that this model may become a predictive tool for successful shortcut nitrification system.

Table 3-3. Determination of the Minimum DO Concentration in Short-cut Nitrification Systems

reference	TAN (mg N/L)	TNN (mg N/L)	pH	T(°C)	NO_2/NO_x	SRT(d)	DO (mg/L)	Duration(d)	System	DO_{min} AOB	DO_{min} NOB
[25]	250	170	8	30	93%	31	<2	800	activated sludge with biofilm carriers and a clarifier	0.66	WR
[26]	350	350	6.5-6.7	35	>90%	1	3	180	SHARON	WR	WR
[27]	550	600	6.4-7	30-40	100%	1	NA	250	SHARON	WR	WR
[28]	400	400	6.2-7	30	94%	infinity	2-4	90	moving bed biofilm reactor	0.73-WR	WR
[29]	137.3	353.9	8	30	95.7%	8-12	>1.5	70	continuous stirred-tank reactor	2.55-4.25	WR
	73.2	391.4	7-7.5	30	85.3%	14-18	>1	55	continuous stirred-tank reactor	0.48-WR	WR
[30]	127.5	154.2	8	35	81%	12-14	0.3-0.5	120	continuous stirred-tank reactor with a settler	0.37-0.39	WR
[31]	50	45	7.6	30	>90%	infinity	0.2	150	closed down-flow hanging sponge reactor	0.20	2.67
[32]	12	390	7.8-7.9	30	67%	infinity	0.7	50	activated sludge reactor with a settler	0.27-0.34	1.24-1.38
[33]	30	400	7.8	25	80%	infinity	1.4	300	activated sludge reactor with a settler	0.27	3.29
[34]	80	163	8.2	30	98%	20-25	1.3±0.3	96	suspended-growth shortcut biological nitrogen removal with a clarifier	0.30-0.31	WR

When analyzing the effect of SRT in this work, SRT ranged from 5 to 30 days. However, the SHARON process usually has an SRT less than 2 days [26,27,35,36]. As apparent from Table 3-3, this model was unable to predict the SHARON process as the DO_{min} for AOB by the model suggested that the AOB would be washed out under the Sharon conditions. The reason for the aforementioned discrepancy is different kinetics. The maximum observed growth rates of AOB in the SBR and SHARON were 1.0 d^{-1} and 2.0 d^{-1} , 1.3 d^{-1} and 2.4 d^{-1} in the study of Galí et al. (2007a) and Galí et al. (2007b), respectively [26,35]. One set of SHARON kinetic parameters for AOB determined by Van Hulle et al.[7] at pH 7, and a temperature of 35ºC are: b= 0.045d^{-1}, K_{NH3}=0.75 mgNH_3-N L^{-1}, K_{INH3} was very high and K_{IHNO2}=2.04 mgHNO_2-N L^{-1} and Ko=0.94 mg/L. By using the aforementioned kinetic parameters and μ_{max} of 2.4 d^{-1}, the predicted DO_{min} for AOB was 1.09 to 1.36 mg/L in the case of van Dongen et al. [27]. The model predictions for several typical Sharon processes are shown in Table 3-4. Although in some studies the actual DO was not mentioned, the model suggested that the AOB could survive with DO higher than DO_{min} while NOB would be washed at any operational DO. This indicates that the model could predict the SHARON process based on its specific kinetic parameters. In this study, b of 0.17 d^{-1} at 20ºC and θ_b of 1.04 were used, resulting in b value of 0.31 d^{-1} at 35ºC, which is actually higher than the b value of 0.23 d^{-1} at 35ºC reported by Magrí et al. [37]. In fact, the reported b values at 35ºC range from 0.045 d^{-1} to 0.31 d^{-1} [7,14,38,39]. In addition, the FA and FNA inhibition threshold concentrations range from 5.0 to 27.3 mg FA/L, and 0.09 to 0.97 mg FNA/L [12].

Table 3-4. Model prediction of Sharon reactors based on specific kinetic values

reference	TAN (mg N/L)	TNN (mg N/L)	pH	T(ºC)	NO_2/NO_x	SRT(d)	DO (mg/L)	DOmin AOB	DOmin NOB
[26]	350	350	6.5-6.7	35	>90%	1	3	2-2.86	WR
[27]	550	600	6.4-7	30-40	100%	1	NA	1.09-1.36	WR
[35]	350	400	7	35	88%	1.4	3	0.65	WR
[36]	130	345	7.4	35	100%	1.5	NA	1.05	WR

3.3.6 Model use for bioreactor design.

This model not only suggests a DO range in which nitrite accumulation can be successfully achieved, but also provides bioreactor design information such as SRT.

For example, if a CSTR is to be designed to treat wastewater, with Q_{in}, influent TAN of 220 mg N/L to achieve an effluent concentration of TAN 20 mg N/L and TNN 200 mg N/L at a pH of 7.5 and a temperature of 35ºC, the SRT ranges from 2.4 d to infinity, i.e. any SRT>2.4 days is feasible. Furthermore, the operational DO ranges from 0.31 to 1.19 mg/L atlong SRT (>40 days) to over 4.5 mg/L at an SRT of 2.4 d. Obviously, from a practical perspective, the minimum SRT is recommended despite the high energy costs.

3.4 Conclusions

A model for successful shortcut nitrification conditions determination was derived based on MSC values. In addition, the effect of temperature, pH and SRT was analyzed. Specific application of this model for shortcut nitrification coupled with anaerobic ammonium oxidation (ANAMMOX)

in which the effluent concentrations of nitrite and ammonium from shortcut nitrification were equal, was discussed. Comparison of the model predicted DO_{min} with experimental data suggested that this model can be a useful and practical tool for shortcut nitrification systems design and operation.

3.5 Acknowledgments

This work was supported by National Science and Engineering Research council of Canada.

3.6 References

[1] J.H. Guo, Y.Z. Peng, S.Y. Wang, Y.N. Zheng, H.J. Huang, S.J. Ge, Effective and robust partial nitrification to nitrite by real-time aeration duration control in an SBR treating domestic wastewater, Process Biochem. 44 (2009) 979–985.

[2] M. Van Loosdrecht, M. Jetten, Microbiological conversions in nitrogen removal, Water Sci. Technol. 38 (1998) 1–7.

[3] M. Beccari, R. Passino, R. Ramadori, V. Tandoi, Kinetics of dissimilatory nitrate and nitrite reduction in suspended growth culture, J. Water Pollut. Control Fed. (1983) 58–64.

[4] O. Turk, D.S. Mavinic, Benefits of using selective inhibition to remove nitrogen from highly nitrogenous wastes, Environ. Technol. 8 (1987) 419–426.

[5] R. Van Kempen, J.W. Mulder, C.A. Uijterlinde, M.C.M. Loosdrecht, Overview: full scale experience of the SHARON® process for treatment of rejection water of digested sludge dewatering, Water Sci. Technol. 44 (2001) 145–152.

[6] C. Hellinga, M.C.M. Van Loosdrecht, J.J. Heijnen, Model based design of a novel process for nitrogen removal from concentrated flows, Math. Comput. Model. Dyn. Syst. 5 (1999) 351–371.

[7] S.W. Van Hulle, E.I. Volcke, J.L. Teruel, B. Donckels, M. van Loosdrecht, P.A. Vanrolleghem, Influence of temperature and pH on the kinetics of the Sharon nitritation process, J. Chem. Technol. Biotechnol. 82 (2007) 471–480.

[8] A.C. Anthonisen, R.C. Loehr, T.B.S. Prakasam, E.G. Srinath, Inhibition of nitrification by ammonia and nitrous acid, J. Water Pollut. Control Fed. (1976) 835–852.

[9] B.E. Rittmann, P.L. McCarty, Model of steady-state-biofilm kinetics, Biotechnol. Bioeng. 22 (1980) 2343–2357.

[10] B.E. Rittmann, P.L. McCarty, Environmental biotechnology: principles and applications, Tata McGraw-Hill Education, 2012.

[11] B. Boon, H. Laudelout, Kinetics of nitrite oxidation by Nitrobacter winogradskyi, Biochem. J. 85 (1962) 440.

[12] S. Park, W. Bae, Modeling kinetics of ammonium oxidation and nitrite oxidation under simultaneous inhibition by free ammonia and free nitrous acid, Process Biochem. 44 (2009) 631–640.

[13] S. Park, W. Bae, J. Chung, S.-C. Baek, Empirical model of the pH dependence of the maximum specific nitrification rate, Process Biochem. 42 (2007) 1671–1676.

[14] Metcalf and Eddy, Wastewater Engineering: Treatment, Disposal, Reuse, Metcalf & Eddy, Inc McGraw-Hill N. Y. (2003).

[15] V.M. Vadivelu, J. Keller, Z. Yuan, Effect of free ammonia and free nitrous acid concentration on the anabolic and catabolic processes of an enriched Nitrosomonas culture, Biotechnol. Bioeng. 95 (2006) 830–839.

[16] S. Park, W. Bae, B.E. Rittmann, Operational boundaries for nitrite accumulation in nitrification based on minimum/maximum substrate concentrations that include effects of oxygen limitation, pH, and free ammonia and free nitrous acid inhibition, Environ. Sci. Technol. 44 (2009) 335–342.

[17] A. Schramm, D. de Beer, J.C. van den Heuvel, S. Ottengraf, R. Amann, Microscale Distribution of Populations and Activities ofNitrosospira and Nitrospira spp. along a Macroscale Gradient in a Nitrifying Bioreactor: Quantification by In Situ Hybridization and the Use of Microsensors, Appl. Environ. Microbiol. 65 (1999) 3690–3696.

[18] E. Metcalf, M. Eddy, Wastewater engineering: treatment and Resource recovery, Mic Graw-Hill USA. (2014).

[19] J. Yan, Y. Hu, Comparison of partial nitrification to nitrite for ammonium-rich organic wastewater in sequencing batch reactors and continuous stirred-tank reactor at laboratory-scale, Water Sci. Technol. 60 (2009) 2861–2868.

[20] H. De Clippeleir, S.E. Vlaeminck, F. De Wilde, K. Daeninck, M. Mosquera, P. Boeckx, W. Verstraete, N. Boon, One-stage partial nitritation/anammox at 15 C on pretreated sewage:

feasibility demonstration at lab-scale, Appl. Microbiol. Biotechnol. 97 (2013) 10199–10210.

[21] B. Dong, X. Liu, L. Dai, X. Dai, Changes of heavy metal speciation during high-solid anaerobic digestion of sewage sludge, Bioresour. Technol. 131 (2013) 152–158.

[22] T. Lotti, R. Kleerebezem, Z. Hu, B. Kartal, M.S.M. Jetten, M.C.M. Van Loosdrecht, Simultaneous partial nitritation and anammox at low temperature with granular sludge, Water Res. 66 (2014) 111–121.

[23] F. Persson, R. Sultana, M. Suarez, M. Hermansson, E. Plaza, B.-M. Wilén, Structure and composition of biofilm communities in a moving bed biofilm reactor for nitritation–anammox at low temperatures, Bioresour. Technol. 154 (2014) 267–273.

[24] M. Strous, E. Van Gerven, J.G. Kuenen, M. Jetten, Effects of aerobic and microaerobic conditions on anaerobic ammonium-oxidizing (anammox) sludge, Appl. Environ. Microbiol. 63 (1997) 2446–2448.

[25] J. Chung, W. Bae, Y.-W. Lee, B.E. Rittmann, Shortcut biological nitrogen removal in hybrid biofilm/suspended growth reactors, Process Biochem. 42 (2007) 320–328.

[26] A. Galí, J. Dosta, M.C.M. Van Loosdrecht, J. Mata-Alvarez, Two ways to achieve an anammox influent from real reject water treatment at lab-scale: Partial SBR nitrification and SHARON process, Process Biochem. 42 (2007) 715–720.

[27] U. van Dongen, M.S.M. Jetten, M.C.M. Van Loosdrecht, The SHARON®-Anammox® process for treatment of ammonium rich wastewater, Water Sci. Technol. 44 (2001) 153–160.

[28] C. Fux, S. Velten, V. Carozzi, D. Solley, J. Keller, Efficient and stable nitritation and denitritation of ammonium-rich sludge dewatering liquor using an SBR with continuous loading, Water Res. 40 (2006) 2765–2775.

[29] J. Chen, P. Zheng, Y. Yu, Q. Mahmood, C. Tang, Enrichment of high activity nitrifers to enhance partial nitrification process, Bioresour. Technol. 101 (2010) 7293–7298.

[30] B. Sinha, A.P. Annachhatre, Partial nitrification—operational parameters and microorganisms involved, Rev. Environ. Sci. Biotechnol. 6 (2007) 285–313.

[31] H.-P. Chuang, A. Ohashi, H. Imachi, M. Tandukar, H. Harada, Effective partial nitrification to nitrite by down-flow hanging sponge reactor under limited oxygen condition, Water Res. 41 (2007) 295–302.

[32] G. Ruiz, D. Jeison, R. Chamy, Nitrification with high nitrite accumulation for the treatment of wastewater with high ammonia concentration, Water Res. 37 (2003) 1371–1377.

[33] G. Ciudad, A. Werner, C. Bornhardt, C. Munoz, C. Antileo, Differential kinetics of ammonia-and nitrite-oxidizing bacteria: A simple kinetic study based on oxygen affinity and proton release during nitrification, Process Biochem. 41 (2006) 1764–1772.

[34] S. Park, W. Bae, B.E. Rittmann, S. Kim, J. Chung, Operation of suspended-growth shortcut biological nitrogen removal (SSBNR) based on the minimum/maximum substrate concentration, Water Res. 44 (2010) 1419–1428.

[35] A. Galí, J. Dosta, S. Mace, J. Mata-Alvarez, Comparison of reject water treatment with nitrification/denitrification via nitrite in SBR and SHARON chemostat process, Environ. Technol. 28 (2007) 173–176.

[36] C. Hellinga, A. Schellen, J.W. Mulder, M.C.M. Van Loosdrecht, J.J. Heijnen, The SHARON process: an innovative method for nitrogen removal from ammonium-rich waste water, Water Sci. Technol. 37 (1998) 135–142.

[37] A. Magrí, L. Corominas, H. López, E. Campos, M. Balaguer, J. Colprim, X. Flotats, A model for the simulation of the SHARON process: pH as a key factor, Environ. Technol. 28 (2007) 255–265.

[38] M. Henze, W. Gujer, T. Mino, M. Van Loosedrecht, Activated sludge models ASM1, ASM2, ASM2d and ASM3, (2006).

[39] X. Liu, M. Kim, G. Nakhla, Operational conditions for successful partial nitrification in a sequencing batch reactor SBR based on process kinetics, Environ. Technol. 38 (2017) 694–704.

Chapter 4 *

4 Operational conditions for successful partial nitrification in an SBR based on process kinetics

The objective of this study is to analyze the factors affecting the performance of partial nitrification in a sequencing batch reactor (SBR) using kinetic models. During the 4-month operation, dissolved oxygen (DO) and influent ammonia concentration were selected as operating variables to evaluate nitrite accumulation. Stable partial nitrification was observed with two conditions, influent ammonia concentration of 190 mg N/L and a DO of 0.6-3.0 mg/L as well as influent ammonia concentration of 100 mg N/L and a DO of 0.15-2.0 mg/L with intermittent aeration. At a DO of 0.6-3.0 mg O_2/L and influent ammonia concentration of 90 mg N/L, NOB growth was not suppressed. Kinetic parameters were determined or estimated with batch tests and model simulation. The kinetic model predicted the SBR performance well.

4.1 Introduction

Partial nitrification is a prerequisite for emerging novel biological nitrogen removal processes such as shortcut nitrification/denitrification and shortcut nitrification/anammox as nitrite is required as a substrate or intermediary product [1]. Compared to conventional biological nitrogen removal (CBNR), the advantages of shortcut nitrification were reported as follows [1]: 1- 25% lower

* This chapter has been published in a manuscript entitled "Liu, X., Kim, M., & Nakhla, G. (2017). Operational conditions for successful partial nitrification in a sequencing batch reactor (SBR) based on process kinetics. *Environmental technology*, *38*(6), 694-704."

oxygen consumption; 2- lower electron donor requirements for denitrification (up to 40%); 3- higher denitrification rate; 4- CO_2 reduction emission by 20%; 5- lower sludge production.

Strategies for successful partial nitrification include low dissolved oxygen (DO) [2], intermittent aeration [3], solids retention time (SRT) control [4], high temperature [5], substrate inhibition, i.e. free ammonia (FA) and free nitous acid (FNA) [6], and chemical (NH_2OH) inhibition [7] among others. In addition, the combination of free nitrous acid-based sludge treatment and oxygen limitation has been recently reported as an effective way to achieve stable nitritation (> 80%) for mainstream deammonification [8].

At high temperature, SRT control is often used to wash out nitrite oxidizing bacteria (NOB) as ammonia oxidizing bacteria (AOB) grow faster than NOB. Dissolved oxygen is another important selective factor because AOBs have lower oxygen half saturation coefficients than NOB, which means that NOB lose more activity as DO decreases [2]. Alternation of aeration pattern from continuous aeration to intermittent aeration is favorable for AOB but unfavorable for NOB as the delay time in nitrate production after an anoxic period is longer than in ammonium conversion [9]. High concentrations of free nitrous acid (FNA) and free ammonia (FA) have adverse impacts on nitrification. NOB are inhibited by free ammonia in the range of 0.1-1.0 mg/L [10,11], while AOB can tolerate free ammonia as high as 10–150 mg/L. Chang et al. [11] and Hellinga et al. [5] reported that FNA inhibited nitrite oxidation at concentrations of 0.2-0.22 mg/L.

Previously, it was believed that low DO is favorable for NOB suppression [12]. However, recently, it has been discovered that NOBs can be divided into two kinds of species, that is, r-strategists and K-strategists [13]. *Nitrospira sp.* and *Nitrobacter sp.* are widely regarded as the two major types of NOB present in WWTPs. *Nitrobacter sp.* are considered to be r-strategists which

catalyze the reactions with high rates, high Ks values, and low affinity for oxygen, while *Nitrospira sp.* are K-strategists with lower rates, low Ks values, and high affinity for oxygen. There is a wide variation of reported operational conditions for partial nitrification. DO is a very important factor for partial nitrification. Practically the DO adopted in different studies varied from 0.16 to 5 mg/L [12]. It was suggested that all these factors are not isolated but correlated with each other [12]. Thus, kinetic models are very useful and quantitative tools for analyzing biochemical processes.

To our knowledge, using partial nitrification SBR treating relatively low ammonium wastewater (100-200 mg N/L) at 35^{o}C has not been studied extensively. To date, the major strategies for partial nitrification in low strength wastewater are real time aeration duration control and intermittent aeration with low DO [14–17]. All the aforementioned studies were conducted at low temperature or ambient temperatures and treated very low ammonia wastewater (40-80 mgN/L). The study of Li et al. [18] was conducted at 20^{o}C treating wastewater with 300 mg NH_4-N/L using intermittent aeration with limited DO (<0.2 mg O_2/L). With temperature increasing from ambient to 35^{o}C, the growth rates of both AOB and NOB increase, while the inhibition of FA and FNA also become more significant. Additionally, the numerous partial nitrification studies have rarely been supported by kinetic analysis.

The objectives of this paper are: a- determination of the optimum DO, aeration pattern and influent concentration conditions for successful partial nitrification; b- delineation of the kinetic parameters and c- using kinetic model analysis to rationalize the conditions for successful partial nitrification.

4.2 Materials and methods

4.2.1 Partial nitrification reactor

A sequencing batch reactor (SBR) with a working volume of 10 L was used in this study. The reactor height and the diameter are 24cm and 30 cm, respectively. The schematic diagram of the SBR is depicted in Figure 4-1. Two pumps (Masterflex L/S, Cole-Parmer, Montreal, Canada) were used, one feeding the wastewater to the SBR and the other withdrawing the treated wastewater. Aeration was provided with an air pump (Rena air 400, Rena Aquatic Supply, Charlotte, US) through an air diffuser. The operating sequence of the SBR consisted of four 6 h cycles with feed (20 min), aeration (300 min), settle (20 min), and decant (20 min) phases in each cycle. In each cycle, 5 L of supernatant were withdrawn from the reactor after the settling phase, and replaced with fresh wastewater, resulting in a hydraulic retention time (HRT) of 12 h. Temperature in the reactor was maintained at $35 \pm 2^{o}C$ with a water bath (VWR® Heated Circulating Bath, VWR International, Mississauga, Canada).

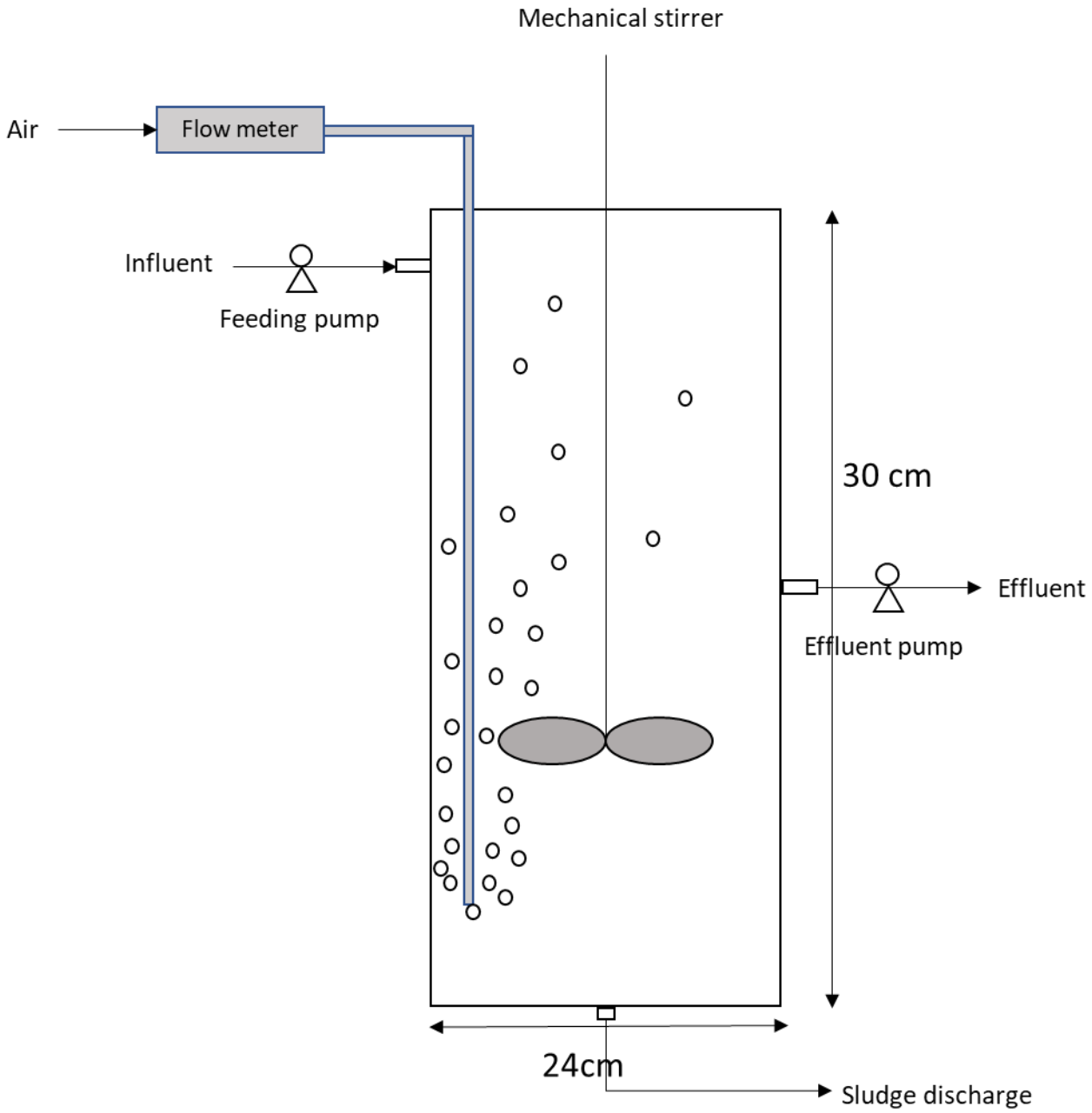

Figure 4-1. SBR schematic diagram

4.2.2 Synthetic Wastewater and Activated Sludge Characteristics.

The synthetic wastewater was composed of NH_4Cl (35-200 mg N/L), $NaHCO_3$ (420-2400 mg/L) (as carbon source for nitrification), KH_2PO_4, $MgSO_4 \cdot 7H_2O$(100 mg/L), $CaCl_2$(100 mg/L), 1 ml/L water of trace elements solution I (composition in g/L as follows: EDTA 15, $ZnSO_4$ 0.43, $CoCl_2$ 0.24, $MnCl_2$ 0.63, $CuSO_4$ 0.25, Na_2MoO_4 0.22, $NiCl_2$ 0.19, Na_2SeO_4 0.21, H_3BO_3 0.01 and $NaWO_4$ 0.05) and 1 ml/L water of trace elements solution II containing $FeSO_4$ and EDTA at 5 g/L each. For full nitrification, the $NaHCO_3$:NH_4-N:P mass ratio was 60:5:1, corresponding to an alkalinity to ammonia nitrogen ratio of 7.14:1 while for partial nitritation, the $NaHCO_3$:NH_4-N:P mass ratio was 34.2:5:1, corresponding to an alkalinity to ammonia nitrogen ratio of 4.1:1 The seed sludge was return activated sludge (RAS) taken from the Adelaide wastewater treatment plant in London, Ontario. The initial concentration of the sludge in the SBR after seeding was approximately 1.5 g/L (MLSS).

4.2.3 Analytical methods

MLSS/MLVSS were determined using Whatman GF/A filters (VWR International, Mississauga, Canada) in accordance with Standard Methods [19]. DO and pH were measured using a DO meter (HACH HQ 40d, HACH Co, London, Canada) and a pH meter (VWR B10P, VWR International, Mississauga, Canada), respectively. Nitrogen species were determined using HACH methods i.e. ammonium (method 10031), nitrite (8153) and nitrate (10020).

FA and FNA concentrations were calculated by Eq.4.1 and Eq.4.2 [10]:

$$FA = \frac{17}{14} \cdot \frac{TAN \cdot 10^{pH}}{\exp\left(\frac{6344}{273+T}\right)+10^{pH}} \qquad \text{(Eq.4.1)}$$

$$FNA = \frac{47}{14} \cdot \frac{TNN}{\exp\left(\frac{-2300}{273+T}\right) \cdot 10^{pH}+1} \quad \text{(Eq.4.2)}$$

In which, FA is the free ammonia and FNA is the free nitrous acid, mg N/L.

4.2.4 Batch test

Conventional batch kinetics tests were conducted in the reactor at each operational condition by temporarily stopping feed flow and maintaining a constant DO of 4.0 mg/L to determine the biomass ammonia oxidation rate (AOR) and nitrite oxidization rate (NOR), as suggested by Liu and Wang [20].

Without alkalinity and substrate limitation,

$$X = \frac{Y \cdot (S_0 - S) \cdot Q}{V \cdot (b + \frac{1}{SRT})} \quad \text{(Eq.4.3)}$$

$$AOR = X_{AOB} \cdot q_{AOB} = q_{AOB} \cdot \frac{Y_{AOB} \cdot (S_{0,NH} - S_{NH})}{HRT \cdot (b_{AOB} + \frac{1}{SRT})} \quad \text{(Eq.4.4)}$$

$$NOR = X_{NOB} \cdot q_{NOB} = q_{NOB} \cdot \frac{Y_{NOB} \cdot (S_{NO2} - S_{0,NO2})}{HRT \cdot (b_{NOB} + \frac{1}{SRT})} \quad \text{(Eq.4.5)}$$

where b_{AOB} and b_{NOB} are endogenous decay coefficients for AOB and NOB, respectively, d^{-1}; Y_{AOB} and Y_{NOB} are biomass yield coefficients for AOB and NOB, respectively, mg VSS/mg N; q_{AOB} and q_{NOB} are maximum specific substrate utilization rates for AOB and NOB, respectively, mg N/(mg VSS·d); X_{AOB} and X_{NOB} are active AOB and NOB biomass concentrations, respectively, mg VSS/L; AOR and NOR are sample maximum ammonia oxidation rate and maximum nitrite oxidation rate, respectively, mg N/(L·min); $S_{NH}$and S_{NO2} are effluent ammonia and nitrite concentrations, respectively, mg N/L;$(S_{0,NH} - S_{NH})$ and $(S_{NO2} - S_{0,NO2})$ are ammonia

and nitrite oxidized, respectively; Q is inflow rate, L/d; and V is effective volume of the SBR, L. At the end of the study, the reactor was fed with deionized water mixed and aerated for several days to determine the decay coefficient (b).

4.2.5 Model analysis

The inhibition model by Park & Bae [21] was used in this study for the calculation of AOR_{max}, as shown below:

$$\mathrm{AOR} = \mathrm{AORmax} \cdot \frac{DO}{DO+K_{O,AOB}} \cdot \frac{TAN}{TAN\cdot(1+\frac{FNA}{K_{IFNA,AOB}}+\frac{FA}{K_{IFA,AOB}})+K_{S,AOB}\cdot(1+\frac{FNA}{K_{IFNA,AOB}})} \quad \text{(Eq.4.6)}$$

$$\mathrm{NOR} = \mathrm{NORmax} \cdot \frac{DO}{DO+K_{O,NOB}} \cdot \frac{TNN}{TNN\cdot(1+\frac{FNA}{K_{IFNA,NOB}}+\frac{FA}{K_{IFA,NOB}})+K_{S,NOB}\cdot(1+\frac{FNA}{K_{IFNA,NOB}})} \quad \text{(Eq.4.7)}$$

The inhibition kinetic parameters used for calculation were as follows: K_{IFA} 10 and 0.75 mg N/L, K_{IFNA} 0.5 and 0.1 mg N/L for AOB and NOB, respectively [12]. Other kinetic parameters were determined in this study. The free ammonia (FA) and free nitrous acid (FNA) concentration used for calculation were the average values during the batch test.

4.3 Results

4.3.1 Start-up performance

In the 26 days of start-up, air flowrate was constant at 1.5 L/min, resulting in 0.6 to 2.0 mg DO/L in the SBR. The SBR was fed with increasing influent ammonia concentrations from 35 mg N/L to 100 mg N/L at an HRT of 12 hours, corresponding to volumetric nitrogen loading rates (VNLRs) of 0.07 kg N m^{-3} d^{-1} to 0.20 kg N m^{-3} d^{-1}. The NH_4^+-N, NO_2^--N and NO_3^--N concentrations shown

in Fig.4-2 indicate that under the above conditions, NOBs were not inhibited as nitrate accumulation was observed. To limit the activity of NOBs, SRT was set at 3d from day 23 to day 28. As apparent from Fig.4-1, NOBs were washed out while the activity of AOBs was not significantly affected. At the end of the start-up stage, volumetric ammonia conversion rate (VACR) and volumetric nitrite conversion rate (VNCR) were 0.29 kg N m^{-3} d^{-1} and 0.03 kg N m^{-3} d^{-1}, resulting in an ammonia removal efficiency (ARE) of 96% and a nitrite accumulation ratio (NAR) of 87%, confirming the successful start-up of the system.

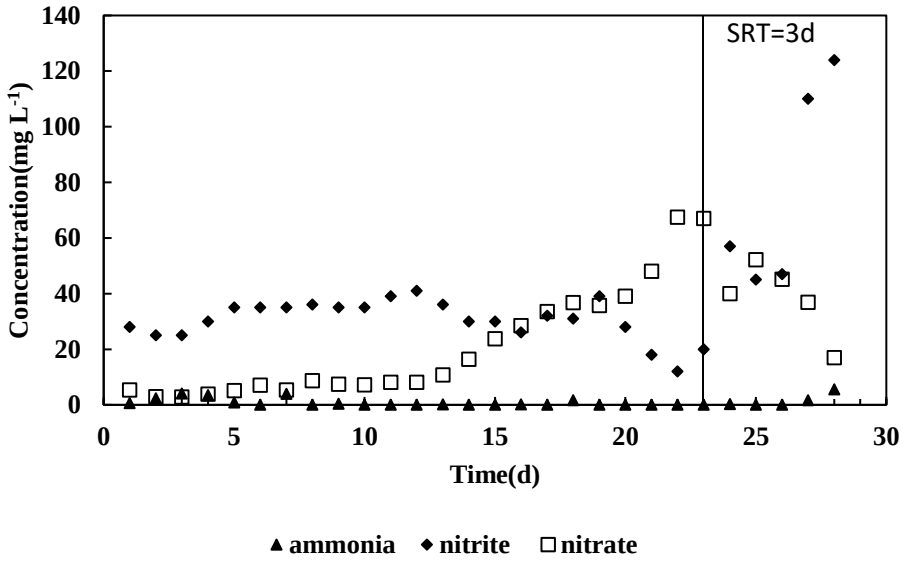

Figure 4-2. Start-up of the SBR

4.3.2 Performance of the SBR

Following the successful start-up, the SBR was operated for about 98 days. Different operational conditions were tried by changing influent ammonia concentration, SRT, aeration pattern and DO level. The performance of the SBR is shown in Fig.4-3. Two operational periods with stable effluent ammonia, nitrite and nitrate concentrations were achieved. Besides, from day 22 to day

35, although the performance is not stable, the operational conditions were maintained constant. The detailed conditions and performance of the SBR during all these periods are summarized in Table 4-1. At the end of period 1, the influent ammonia concentration was further increased to 250 mg N/L. However, the SBR started to exihibit inhibition as the ARE decreased from 94% on day 21 to 36% in two days on day 23. To recover the system, the influent ammonia concentration was decreased to 90 mg N/L. As the inhibition diminished, the NOB started to grow and the system became unstable during period 2 with NAR decreasing from 74% to 17% in 10 days. From day 36 to 43, SRT control was exercised with the SRT set at 7 days. At the same time, the influent ammonia concentration was increased back to 180 mg N/L. On day 43, the ARE and NAR were 60% and 85%, respectively, suggesting that SRT control washed out both AOB and NOB. On day 44, sludge wastage was stopped. However, both AOB and NOB activity recovered in 6 days, with ARE and NAR of 94% and 73% on day 49, respectively. Then from day 55 to 57, the SRT was set at 3d, after which the ARE and NAR were 89% and 78%, respectively. From day 60, the condition was changed and the SBR was operated with intermittent aeration. Intermittent aeration was applied with air off for 15 minutes and on for 15 minutes. No sludge wastage was carried out during these three periods and the SRTs were estimated based on reactor and effluent biomass. For example, in period 2, the biomass concentration in the SBR was 100 mg MLVSS/L and the effluent biomass concentration was 5 mg MLVSS/L, resulting in the SRT of 10 d.

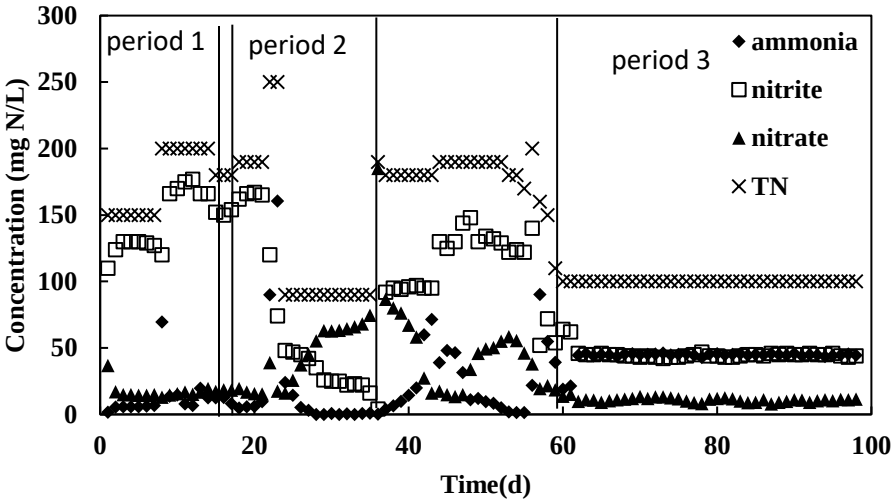

Figure 4-3. Temporal variation of performance parameters of partial nitrification SBR.

Table 4-1. Stable operational conditions and performance of the SBR

Period	1	2	3
DO level (mg/L)	0.6-3.0	0.6-3.0	0.15-2.0
Airflowrate (L/min)	0.6	0.6	0.2
Aeration pattern	continuous	continuous	intermittent
Influent concentration (mg N/L)	190*	90	100
Biomass concentration (MLVSS/L)	400	400	100
SRT	40	40	10
Alkalinity/N	7.14	7.14	4.10
Effluent ammonia (mg N/L)	10.4±4.2	0.3±0.3	44.8±1.0
Effluent nitrite (mg N/L)	164.3±7.8	22.83±2.3	44.4±1.7
Effluent nitrate (mg N/L)	18.5±1.6	64.6±2.0	10.9±1.7
Average FA (mg N/L)	4.4	1.0	2.2
Average FNA (mg N/L)	0.04	0.01	0.01
Duration (d)	0-21	22-35	60-98

* The influent concentration increased in two steps to 150 mgN/L and then to 190 mgN/L.

4.3.3 Kinetic study

4.3.3.1 Decay coefficient (b)

The sludge was starved for 5 days with aeration and biomass concentration was measured every day. The result is shown in Fig. 4-4. Based on the data, the decay coefficient b was calculated as 0.245 d^{-1} at 35^{o}C.

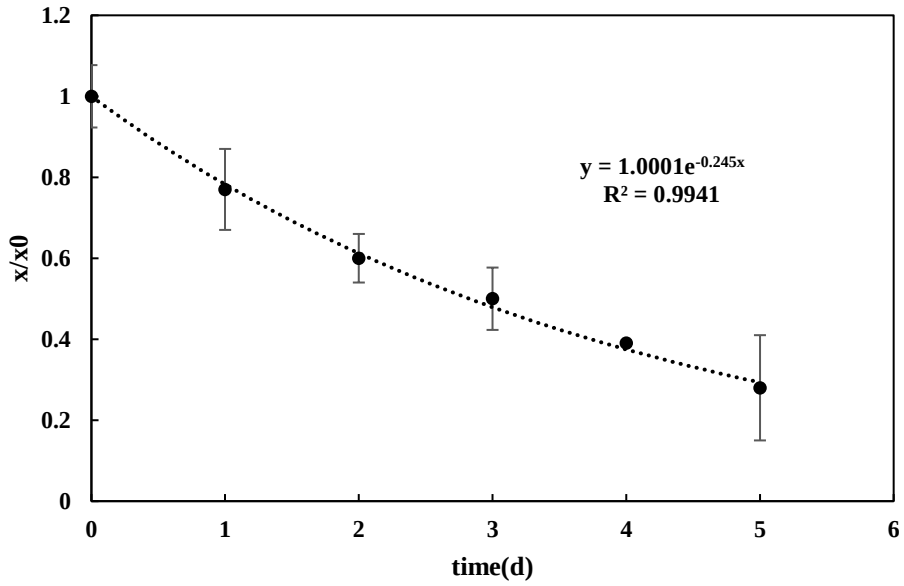

Figure 4-4. Evolution of biomass concentration during starvation test

4.3.3.2 Batch tests

Typical batch test results during period 1 are shown in Fig.4-5 with the results summarized in Table 4-2. At each DO condition a single batch test was conducted. The ammonia range in this study was 10 to 70 mg N/L while the nitrite was above 90 mg N/L. Reported half-velocity constant for substrate for AOB(K_{AOB}) and NOB(K_{NOB}) range from 0.07-1.62 mg N/L and 0.11-2.7 mg N/L [22–24]. As the ammonia and nitrite ranges in this study were much higher than K_{AOB} and K_{NOB}, both ammonia oxidation and nitrite oxidation followed zero order kinetics. The maximum AOR with FA and FNA inhibition, and oxygen half saturation coefficient (Ko) of AOB was 0.6 mg N/(L min) and 0.36 mg O_2/L. The maximum NOR with FA and FNA inhibition, and oxygen half saturation coefficient (Ko) of NOB was 0.037 mg N/(L min) and 0.54 mg/L. Free ammonia (FA) and free nitrous acid (FNA) changes during the AOR tests are shown in Fig 4D and 4E. The average FA and FNA concentrations were 4 mg N/ L and 0.012 mg N/L, respectively. Based on

the AOR test results and the inhibition coefficients of Park et al. [12], the actual maximum AOR and NOR without inhibition during were 0.87 and 0.22 mg N/(L min), respectively. As a result, the maximum growth rate of AOB and NOB were 0.94 and 2.51 d^{-1}, respectively. The maximum specific substrate utilization rates using the yield coefficient of 0.24 and 0.1 mg COD/mg N for AOB and NOB were 5.6 and 35.7 mg N/(mg VSS d), respectively [25].

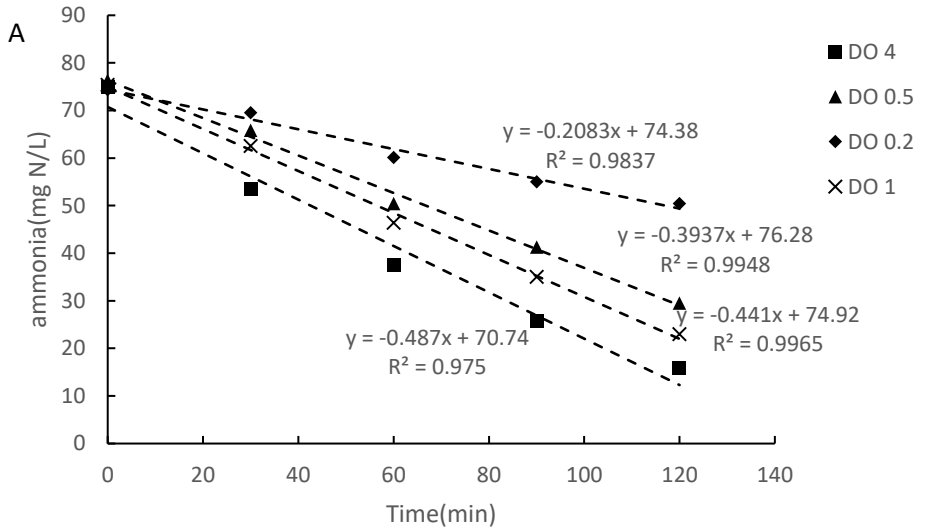

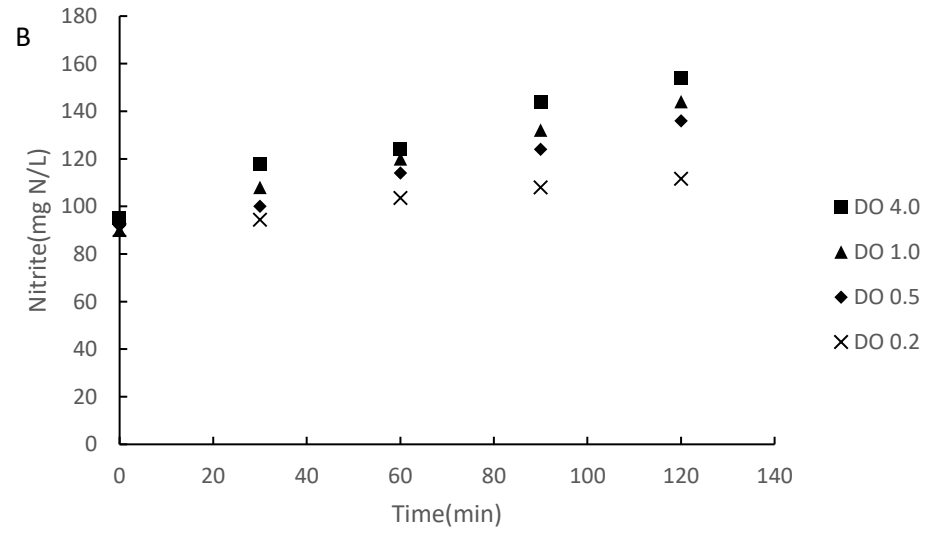

C

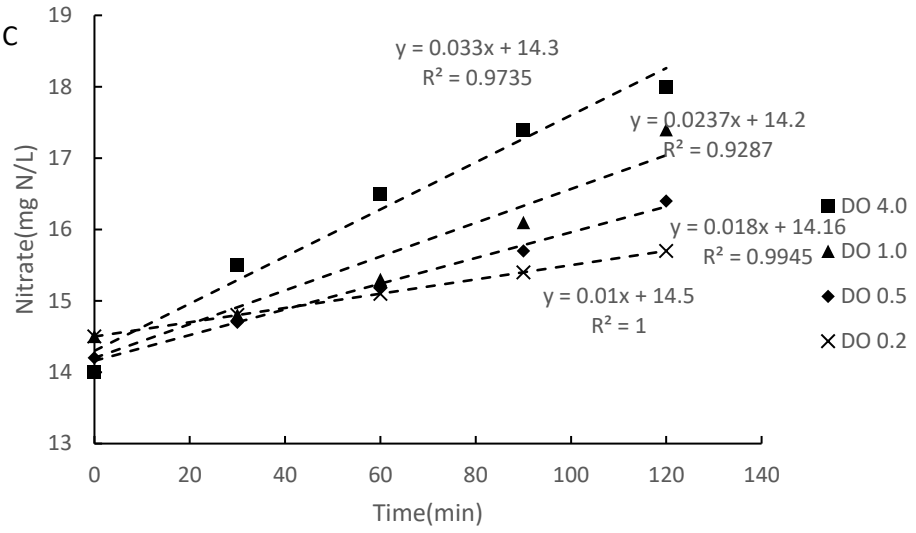
y = 0.033x + 14.3
R² = 0.9735
y = 0.0237x + 14.2
R² = 0.9287
y = 0.018x + 14.16
R² = 0.9945
y = 0.01x + 14.5
R² = 1
DO 4.0
DO 1.0
DO 0.5
DO 0.2
Nitrate(mg N/L)
Time(min)

D

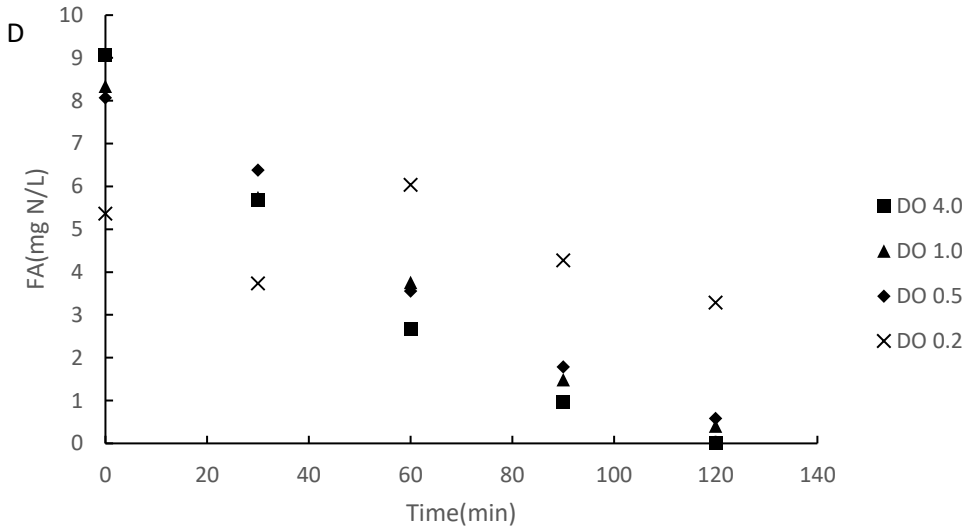
DO 4.0
DO 1.0
DO 0.5
DO 0.2
FA(mg N/L)
Time(min)

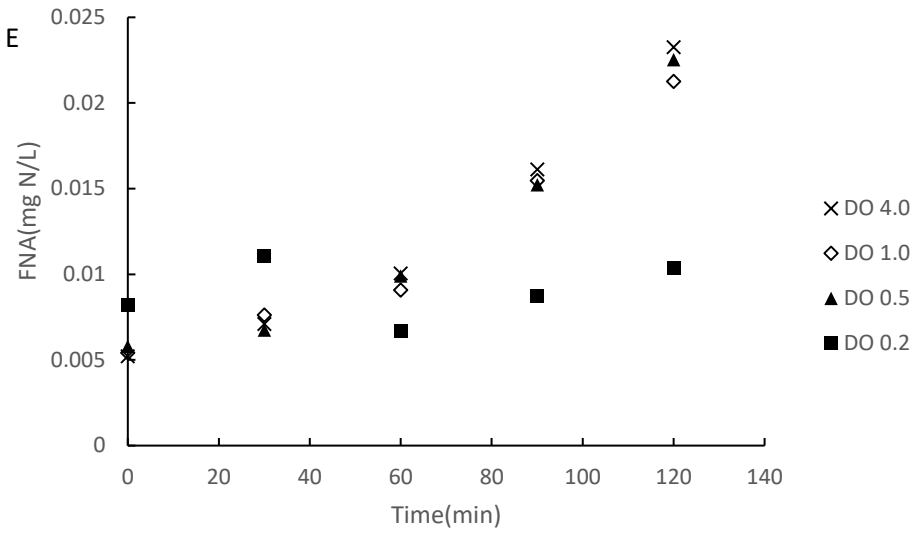

Figure 4-5. Batch test results during period 1 in the reactor

Table 4-2. Summary of Batch Test Conditions and Results (at 35ºC)

Condition	1				3
DO (mg O_2/L)	4.0	1.0	0.5	0.2	4.0
AOR (mg N/(L min))	0.49	0.44	0.39	0.21	0.159±0.001
NOR (mg N/(L min))	0.033	0.024	0.018	0.01	0.021±0.003
Average FA (mg N/L)	4				2.4
Average FNA (mg N/L)	0.012				0.01
AOR_{max} with inhibition	0.6				0.18
NOR_{max} with inhibition	0.037				0.023
AOR_{max}	0.87				0.22
NOR_{max}	0.22				0.1

Additionally, batch tests at a DO of 4.0 mg/L were also conducted three times during period 3. Typical batch test results during period 3 are shown in Fig.4-6. The AOR and NOR with substrate inhibition were 0.159±0.001 and 0.021±0.003 mg N/(L min). Assuming that the respective oxygen half saturation coefficients of 0.36 and 0.54 mg/L do not change, the maximum AOR and NOR with inhibition were 0.18 and 0.023 mg N/(L min). The average FA and FNA concentrations were respectively 2.4 mg N/ L and 0.01 mg N/L, respectively. The actual maximum AOR and NOR without inhibition were 0.22 and 0.1 mg N/(L min), respectively. As a result, the maximum growth rates of AOB and NOB were 0.99 and 2.25 d^{-1}, respectively. It is evident that the growth rate of both AOB and NOB did not change significantly, with DO in the range of 0.2 to 4.0 mg/L, increasing marginally from 0.94 in period 1 to 0.99 d^{-1} in period 3 for AOB and decreasing from

2.51 in period 1to 2.25 d^{-1} in period 3 for NOB. The maximum specific substrate utilization rate for AOB and NOB in period 3 were 5.9 and 32.1 mg N/(mg VSS d) , respectively.

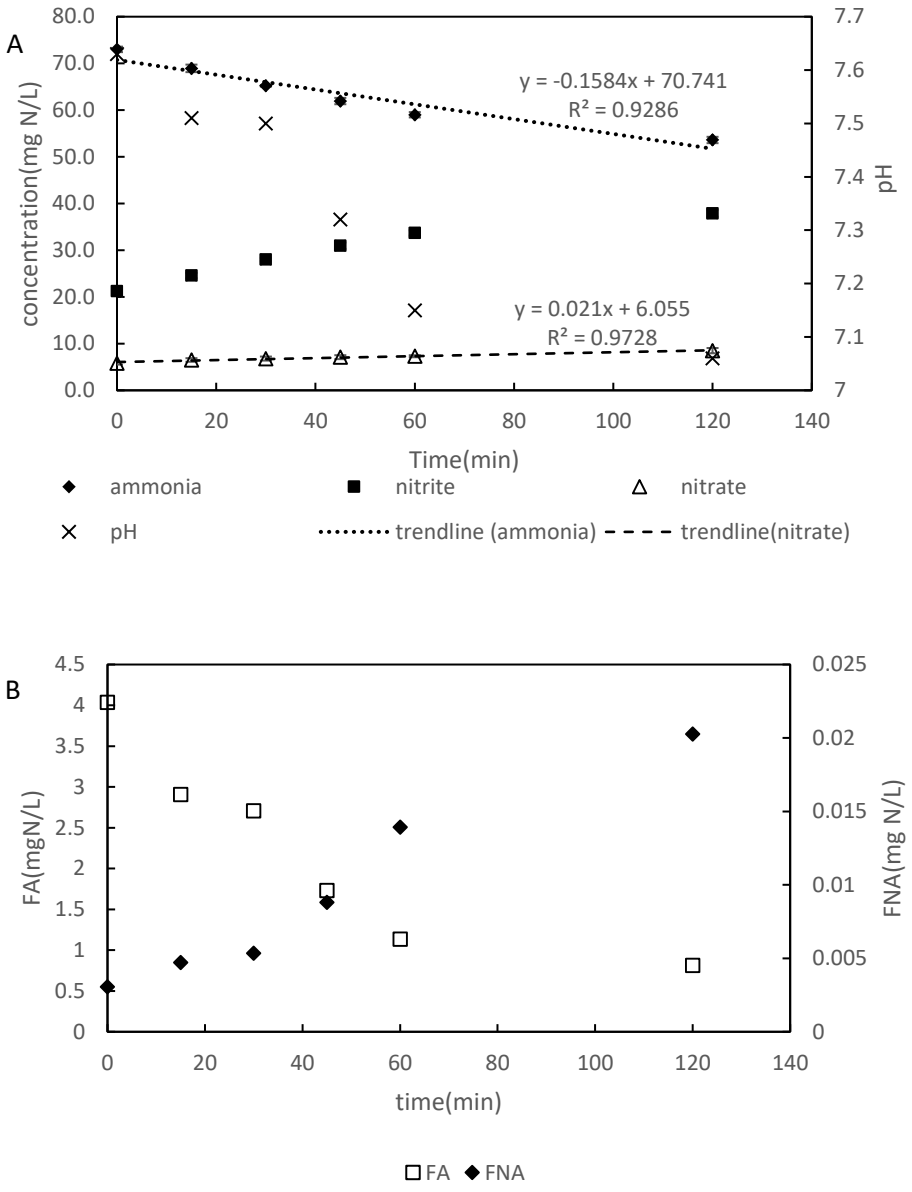

Figure 4-6. Batch test results during period 3 in the reactor

4.3.3.3 Comparison of Kinetic Parameters

The kinetic parameters from this study are compared with the literature, as shown below in Table 4-3. For each kinetic parameter, literature values vary widely. The kinetic values from this study fall within the reported range from the literature.

Table 4-3. Kinetics Parameters for AOB, T=35°C

Parameter	This study	literature
Max specific growth rate of AOB, μ_{max} (d^{-1})	0.94-0.99	0.56-2.55[a], 1.0[b], 1.4[c], 2.1[d], 0.68[e]
Max specific growth rate of NOB, μ_{max} (d^{-1})	2.25-2.51	1.05[d], 1.55-2.33[f], 3.21[g], 0.51[e]
Max specific substrate utilization rate of AOB, q (mg N/(mg VSS d))	5.6-5.87	5.4[e], 13[h]
Max specific substrate utilization rate of NOB, q (mg N/(mg VSS d))	32.1-32.8	32.5-54.0(based on temperature coefficient 1.06-1.1)[a], 36.36[d]
Oxygen half saturation coefficient (Ko) for AOB	0.36	0.5 [a,i], 0.51[j], 0.74[k], 0.40[l]
Oxygen half saturation coefficient for NOB	0.54	0.68[i],0.9[a], 1.75[k], 1.98 [j], 0.43[m]
Aerobic decay coefficient, b (d^{-1})	0.245	0.09-0.27 [a]

[a] Metcalf and Eddy (2003)[24]; [b] Van Hulle et al. (2007)[26]; [c] Galí et al. (2007)[27]; [d] Hellinga et al. (1999)[28]; [e] Liu and Wang (2013)[20]; [f] Kampschreur et al. (2007)[29]; [g] Wett and Rauch (2003)[30]; [h] Rittmann and McCarty (2001)[22]; [i] Park et al. (2010)[12]; [j] Schramm et al. (1999)[13]; [k] Grady Jr et al. (2011)[25]; [l] Wett et al. (2013)[31]; [m] Blackburne et al. (2008)[2].

4.4 Discussion

As evident from Table 4.1, successful nitrite accumulation was achieved under operational periods 1 and 3, which may be explained by kinetic analysis.

The effects of DO limitation on μ_{max} are shown in Eq.4.8-4.9.

$$\mu_{max,AOB}^{DO-limitation} = \mu_{max} \cdot \frac{DO}{DO+K_{O,AOB}} \quad \text{(Eq.4.8)}$$

$$\mu_{max,NOB}^{DO-limitation} = \mu_{max} \cdot \frac{DO}{DO+K_{O,NOB}} \quad \text{(Eq.4.9)}$$

Taking inhibition into consideration, Eq.4.10 and Eq.4.11 can be derived:

$$\mu_{max,AOB}^{DO-limitation} = \mu_{max} \cdot \frac{DO}{DO+K_{O,AOB}} \cdot \frac{TAN}{TAN\cdot(1+\frac{FNA}{K_{IFNA}}+\frac{FA}{K_{IFA}})+K_{S,AOB}\cdot(1+\frac{FNA}{K_{IFNA}})} \quad \text{(Eq.4.10)}$$

$$\mu_{max,NOB}^{DO-limitation} = \mu_{max} \cdot \frac{DO}{DO+K_{O,NOB}} \cdot \frac{TNN}{TNN\cdot(1+\frac{FNA}{K_{IFNA}}+\frac{FA}{K_{IFA}})+K_{S,NOB}\cdot(1+\frac{FNA}{K_{IFNA}})} \quad \text{(Eq.4.11)}$$

In this study, K_s for both AOB and NOB were quite small as evident from the zero-order kinetics depicted in Figures 4.4 and 4.5. In this case, Eq.4.10 and Eq.4.11 can be simplified as:

$$\mu_{max,AOB}^{DO-limitation} = \mu_{max} \cdot \frac{DO}{DO+K_{O,AOB}} \cdot \frac{1}{1+\frac{FNA}{K_{IFNA}}+\frac{FA}{K_{IFA}}} \quad \text{(Eq.4.12)}$$

$$\mu_{max,NOB}^{DO-limitation} = \mu_{max} \cdot \frac{DO}{DO+K_{O,NOB}} \cdot \frac{1}{1+\frac{FNA}{K_{IFNA}}+\frac{FA}{K_{IFA}}} \quad \text{(Eq.4.13)}$$

The calculated $\mu_{max,AOB}^{DO-limitation}$ and $\mu_{max,NOB}^{DO-limitation}$ during the three periods are shown in Table 4-4. Besides, actual growth rate (μ) as $(\mu_{max} - b - \frac{1}{SRT})$ were also calculated. The calculation was based on the average FA and FNA shown above in Table 4-1. Average DO values of 1.9, 1.9 and 1.1 mg/L during 3 periods were used for calculations. In period 3, intermittent aeration was applied. As a result, the DO decreased from 2.0 to 0.15 mg DO/L during the anoxic period and then increased from 0.15 to 2.0 mg/L during the aerobic period. Thus, the average DO of 1.1 mg/L was used for the above calculations.

Table 4-4. Calculated growth conditions for AOB and NOB during different periods

period	1	2	3
$\mu_{max}^{DO-limitation}$ for AOB	0.79	0.79	0.76
$\mu_{max}^{DO-limitation}$ for NOB	1.94	1.94	1.5
$\mu_{max}^{DO-limitation}$ for AOB with inhibition	0.52	0.70	0.61
$\mu_{max}^{DO-limitation}$ for NOB with inhibition	0.26	0.80	0.37
μ for AOB	0.25	0.44	0.27
μ for NOB	0	0.53	0.02

For period 1, the actual growth rate of NOB is 0 d^{-1}, suggesting that the growth of NOB can be neglected. For period 2, the growth rate of NOB is even higher than AOB. The estimated doubling time for NOB is 1.9 d, which explains the high effluent nitrates. As the operational period 2 was favorable for NOB growth, it is anticipated that with longer operation, the NOB would have completely dominated the SBR with no nitrite accumulation observed. Period 3 is stable based on kinetic modelling as the growth rate of NOB is 0.02 d^{-1}, which means that the NOB need up to 50 d to double, hence the lowest effluent nitrate concentrations were observed.

However, based on the data in Table 4-4, for the different periods, the major factors contributing to nitrite accumulation in the different periods are different. In period 1, an average DO of 1.9 mg/L resulted in the growth rate of NOB decreasing from 2.51 to 1.94 d^{-1} while the FA inhibition further decreased it to 0.26 d^{-1}. DO contributed about 23% decrease of the maximum NOB growth rate while FA inhibition caused a 67% decrease. In period 3, the average DO of 1.1 mg O_2/L decreased the maximum growth rate of NOB by about 33% from 2.25 to 1.5 d^{-1} while the FA inhibition decreased it by 50% from 1.5 to 0.37 d^{-1}. In addition, intermittent aeration is another important factor as NOB have a longer lag phase when alternating from anoxic to aerobic

conditions. Thus, it can be concluded that in both periods 1 and 3, FA inhibition was more important than DO in nitrite accumulation and intermittent aeration also contributed to NOB suppressionFor period 2, the DO effect was the same as period 1. However, as the average FA was only 1.0 mg N/L compared with 4.4 mg N/L during period 1, the growth rate of NOB only decreased from 1.94 to 0.8 d^{-1}. Taking decay and SRT effects into consideration, the actual growth rate of NOB was still 0.53 d^{-1}, higher than that of AOB as evidenced by conversion of 72% of the ammonia to nitrates.

A major finding of this study is that the growth rate of AOB at 35^{o}C is 0.94-0.99d^{-1} while that of NOB is 2.25-2.51 d^{-1}. Galí et al. [27] also observed an AOB growth rate of 1.0 d^{-1} in a SBR, corresponding to 1.4 d^{-1}.at 35^{o}C with temperature coefficient of 1.072, compared to 2.0 d^{-1} in a Sharon reactor at a temperature of 30^{o}C. Liu and Wang [20] suggested an AOB growth rate of 0.24 d^{-1} in a SBR at 20^{o}C, corresponding to 0.68 d^{-1}.at 35^{o}C. While the values fall within the reported ranges in the literature, the NOB grow faster than AOB, which is contradictory to the literature that AOB grow faster than NOB at temperatures above 15^{o}C [5]. However, the growth rate of AOB and NOB vary in a very wide range. For example, Ahn et al. [32] reported the growth rate of AOB and NOB to be 1.08 and 2.6 d^{-1} at 20^{o}C, corresponding to 3.06 and 6.3 d^{-1} at 35^{o}C with temperature coefficients of 1.07 and 1.06 for AOB and NOB, respectively. In this study, the growth rates of AOB and NOB were not directly determined but estimated based on the model. Calculation of the growth rates was affected by the kinetic parameters. In this study, a relatively low free ammonia inhibition coefficient (K_{iFA}) for NOB (0.75 mg N/L) was adopted. Despite the fact that AOB are less likely to be inhibited by FA as the free ammonia inhibition coefficient (K_{iFA}) for AOB is high (10-3000 mgN/L) [12, 30, 33], different free ammonia inhibition coefficient (K_{iFA}) ranging from 0.1 to 20 mg N/L for NOB have been reported [33-36]. However, the relatively high

values of K_{iFA} for NOB of 6-11mg N/L and 19.9 mg N/L were both determined with biomass adapted to high ammonia concentrations (500-1000 mg N/L) [33, 36]. In this study, utilization of K_{iFA} for NOB of 0.75 mg N/L is consistent with the reported values for biomass treating low ammonia wastewater, i.e, 0.1-1.0 mg N/L by Chang et al. [11], 0.33 mg N/L by Wu et al. [34] and 0.95 mg N/L by Jubany et al. [35].

As discussed above, despite the impact of the variability, the kinetic analysis in general confirmed that the operational conditions during periods 1 and 3 imposed a kinetic selection for AOB.

In addition, the model developed in Chapter 3 was adopted for analysis using the average data during phases 1-3, with kinetic parameters, and input and output depicted in Table 3-1 and Tables 4-5, respectively. The model prediction fitted the SBR performance well. For example, during period 1, the operational DO of 0.6-3.0 mg/L was higher than the DOmin for AOB of 0.2 mg/L but lower than the DOmin for AOB of 3.0-3.8 mg/L. Thus, model predicted that partial nitrification should be achieved in the SBR, which was confirmed by the performance as shown in Table 4-1.

Table 4-5. Comparison between performance and model DO predictions

	Parameters	Period 1	Period 2	Period 3
Input of the model	NH_4-N_{avg}	55	23	60
	NO_2-N_{avg}	125	17	35
	pH_{avg}	7.4-7.5	7.2-7.3	7.2-7.3
	Operational DO (mgO_2/L)	0.6-3.0	0.6-3.0	0.15-2.0
	Average DO (mgO_2/L)	1.9	1.9	1.1
Output of the model	DO_{min} for AOB (mgO_2/L)	0.2	0.5-0.7	0.2-0.3
	DO_{min} for NOB (mgO_2/L)	3.0-3.8	0.8-0.9	1.8-2.2

4.5 Conclusions

An SBR was operated for 4 months treating synthetic wastewater with ammonia in the range of 35 to 200 mg N/L at varying DO concentrations as well as continuous and intermittent aeration. Stable nitrite accumulation was observed at two conditions: a-influent ammonia concentration of 190 mg N/L and continuous aeration and a DO of 0.6-3.0 mg/L, and b-influent ammonia concentration of 100 mg N/L, intermittent aeration and a DO of 0.15-2.0 mg/L. Various kinetic parameters were determined or estimated. Kinetic analysis indicated that free ammonia inhibition was the major cause of nitrite accumulation. Period 2 with 90 mg N/L influent and DO 0.6 to 3.0 mg/L turned out favorable for NOB growth as the FA inhibition was not pronounced and the DO was not low enough.

4.6 Acknowledgments

This work was supported by National Science and Engineering Research council of Canada.

4.7 References

[1] Y. Peng, G. Zhu, Biological nitrogen removal with nitrification and denitrification via nitrite pathway, Appl. Microbiol. Biotechnol. 73 (2006) 15–26.

[2] R. Blackburne, Z. Yuan, J. Keller, Partial nitrification to nitrite using low dissolved oxygen concentration as the main selection factor, Biodegradation. 19 (2008) 303–312.

[3] A. Pollice, V. Tandoi, C. Lestingi, Influence of aeration and sludge retention time on ammonium oxidation to nitrite and nitrate, Water Res. 36 (2002) 2541–2546.

[4] R. Van Kempen, J.W. Mulder, C.A. Uijterlinde, M.C.M. Loosdrecht, Overview: full scale experience of the SHARON® process for treatment of rejection water of digested sludge dewatering, Water Sci. Technol. 44 (2001) 145–152.

[5] C. Hellinga, A. Schellen, J.W. Mulder, M.C.M. Van Loosdrecht, J.J. Heijnen, The SHARON process: an innovative method for nitrogen removal from ammonium-rich waste water, Water Sci. Technol. 37 (1998) 135–142.

[6] Y. Peng, Y. Chen, C. Peng, M. Liu, S. Wang, X. Song, Y. Cui, Nitrite accumulation by aeration controlled in sequencing batch reactors treating domestic wastewater, Water Sci. Technol. 50 (2004) 35–43.

[7] T. Kindaichi, S. Okabe, H. Satoh, Y. Watanabe, Effects of hydroxylamine on microbial community structure and function of autotrophic nitrifying biofilms determined by in situ hybridization and the use of microelectrodes, Water Sci. Technol. 49 (2004) 61–68.

[8] D. Wang, Q. Wang, A. Laloo, Y. Xu, P.L. Bond, Z. Yuan, Achieving stable nitritation for mainstream deammonification by combining free nitrous acid-based sludge treatment and oxygen limitation, Sci. Rep. 6 (2016) 25547.

[9] E.M. Gilbert, S. Agrawal, F. Brunner, T. Schwartz, H. Horn, S. Lackner, Response of different Nitrospira species to anoxic periods depends on operational DO, Environ. Sci. Technol. 48 (2014) 2934–2941.

[10] A.C. Anthonisen, R.C. Loehr, T.B.S. Prakasam, E.G. Srinath, Inhibition of nitrification by ammonia and nitrous acid, J. Water Pollut. Control Fed. (1976) 835–852.

[11] J.-S. Chang, G.-C. Cha, D.-J. Kim, Nitrite accumulation characteristics in the nitrification of high strength ammonia wastewater with biofilm airlift suspension reactor, J.-KOREAN Inst. Chem. Eng. 40 (2002) 114–120.

[12] S. Park, W. Bae, B.E. Rittmann, Operational boundaries for nitrite accumulation in nitrification based on minimum/maximum substrate concentrations that include effects of oxygen limitation, pH, and free ammonia and free nitrous acid inhibition, Environ. Sci. Technol. 44 (2009) 335–342.

[13] A. Schramm, D. de Beer, J.C. van den Heuvel, S. Ottengraf, R. Amann, Microscale Distribution of Populations and Activities ofNitrosospira and Nitrospira spp. along a Macroscale Gradient in a Nitrifying Bioreactor: Quantification by In Situ Hybridization and the Use of Microsensors, Appl. Environ. Microbiol. 65 (1999) 3690–3696.

[14] Q. Yang, Y. Peng, X. Liu, W. Zeng, T. Mino, H. Satoh, Nitrogen removal via nitrite from municipal wastewater at low temperatures using real-time control to optimize nitrifying communities, Environ. Sci. Technol. 41 (2007) 8159–8164.

[15] B. Ma, P. Bao, Y. Wei, G. Zhu, Z. Yuan, Y. Peng, Suppressing nitrite-oxidizing bacteria growth to achieve nitrogen removal from domestic wastewater via anammox using intermittent aeration with low dissolved oxygen, Sci. Rep. 5 (2015) 13048.

[16] J. Guo, Y. Peng, H. Huang, S. Wang, S. Ge, J. Zhang, Z. Wang, Short-and long-term effects of temperature on partial nitrification in a sequencing batch reactor treating domestic wastewater, J. Hazard. Mater. 179 (2010) 471–479.

[17] J.H. Guo, Y.Z. Peng, S.Y. Wang, Y.N. Zheng, H.J. Huang, S.J. Ge, Effective and robust partial nitrification to nitrite by real-time aeration duration control in an SBR treating domestic wastewater, Process Biochem. 44 (2009) 979–985.

[18] J. Li, D. Elliott, M. Nielsen, M.G. Healy, X. Zhan, Long-term partial nitrification in an intermittently aerated sequencing batch reactor (SBR) treating ammonium-rich wastewater under controlled oxygen-limited conditions, Biochem. Eng. J. 55 (2011) 215–222.

[19] A. Apha, Wef, Stand. Methods Exam. Water Wastewater 20th Ed Wash. DC Am. Public Health Assoc. Am. Water Work Assoc. Water Environ. Fed. 252 (1998).

[20] G. Liu, J. Wang, Role of solids retention time on complete nitrification: mechanistic understanding and modeling, J. Environ. Eng. 140 (2013) 48–56.

[21] S. Park, W. Bae, Modeling kinetics of ammonium oxidation and nitrite oxidation under simultaneous inhibition by free ammonia and free nitrous acid, Process Biochem. 44 (2009) 631–640.

[22] B.E. Rittmann, P.L. McCarty, Environmental biotechnology: principles and applications, Tata McGraw-Hill Education, 2012.

[23] G. Munz, C. Lubello, J.A. Oleszkiewicz, Factors affecting the growth rates of ammonium and nitrite oxidizing bacteria, Chemosphere. 83 (2011) 720–725.

[24] Metcalf and Eddy, Wastewater Engineering: Treatment, Disposal, Reuse, Metcalf & Eddy, Inc McGraw-Hill N. Y. (2003).

[25] C.L. Grady Jr, G.T. Daigger, N.G. Love, C.D. Filipe, Biological wastewater treatment, CRC press, 2011.

[26] S.W. Van Hulle, E.I. Volcke, J.L. Teruel, B. Donckels, M. van Loosdrecht, P.A. Vanrolleghem, Influence of temperature and pH on the kinetics of the Sharon nitritation process, J. Chem. Technol. Biotechnol. 82 (2007) 471–480.

[27] A. Galí, J. Dosta, M.C.M. Van Loosdrecht, J. Mata-Alvarez, Two ways to achieve an anammox influent from real reject water treatment at lab-scale: Partial SBR nitrification and SHARON process, Process Biochem. 42 (2007) 715–720.

[28] C. Hellinga, M.C.M. Van Loosdrecht, J.J. Heijnen, Model based design of a novel process for nitrogen removal from concentrated flows, Math. Comput. Model. Dyn. Syst. 5 (1999) 351–371.

[29] M.J. Kampschreur, C. Picioreanu, N. Tan, R. Kleerebezem, M.S.M. Jetten, M. van Loosdrecht, Unraveling the source of nitric oxide emission during nitrification, Proc. Water Environ. Fed. 2007 (2007) 843–860.

[30] B. Wett, W. Rauch, The role of inorganic carbon limitation in biological nitrogen removal of extremely ammonia concentrated wastewater, Water Res. 37 (2003) 1100–1110.

[31] B. Wett, A. Omari, S.M. Podmirseg, M. Han, O. Akintayo, M.G. Brandón, S. Murthy, C. Bott, M. Hell, I. Takács, Going for mainstream deammonification from bench to full scale for maximized resource efficiency, Water Sci. Technol. 68 (2013) 283–289.

[32] J.H. Ahn, R. Yu, K. Chandran, Distinctive microbial ecology and biokinetics of autotrophic ammonia and nitrite oxidation in a partial nitrification bioreactor, Biotechnol. Bioeng. 100 (2008) 1078–1087.

[33] A. Magrí, L. Corominas, H. López, E. Campos, M. Balaguer, J. Colprim, X. Flotats, A model for the simulation of the SHARON process: pH as a key factor, Environ. Technol. 28 (2007) 255–265.

[34] J. Wu, G. Yan, G. Zhou, T. Xu, New insights in partial nitrification start-up revealed by a model based approach, RSC Adv. 5 (2015) 100299–100308.

[35] I. Jubany, J. Carrera, J. Lafuente, J.A. Baeza, Start-up of a nitrification system with automatic control to treat highly concentrated ammonium wastewater: experimental results and modeling, Chem. Eng. J. 144 (2008) 407–419.

[36] V. Pambrun, E. Paul, M. Spérandio, Modeling the partial nitrification in sequencing batch reactor for biomass adapted to high ammonia concentrations, Biotechnol. Bioeng. 95 (2006) 120–131.

Chapter 5 *

5 Performance and Kinetics of Nitrification of Low Ammonia Wastewater at Low Temperature

The objective of this study was to investigate the effect of dissolved oxygen on nitrification in a sequencing batch reactor (SBR) treating low ammonia wastewater (40 mg N/L) at a low temperature (14 °C). During the 130 days of operation, three dissolved oxygen levels (5–6 mg dissolved oxygen/L, 2–3 mg dissolved oxygen/L, and 0.8–1.0 mg dissolved oxygen/L) were tested. Dissolved oxygen reduction resulted in lower ammonia oxidizing bacteria (AOB) and nitrite oxidizing bacteria (NOB) activity, with decreasing ammonia conversion ratio and increasing nitrite accumulation ratio. The maximum growth rates of AOB and NOB determined in this study (0.28 and 0.38 d^{-1}) were below the median values from the literature (0.47 and 0.62 d^{-1}), whereas the oxygen half-saturation coefficients of AOB and NOB (1.36 and 2.79 mg/L) were higher than those found in the literature. The kinetic model explained the SBR performance well. Low dissolved oxygen, together with long solids retention time, was recommended for partial nitrification at a low temperature.

5.1 Introduction

Conventionally, ammonia in wastewater is removed biologically by nitrification-denitrification. Nitrification is a two-step process involving nitritation (ammonia oxidized to nitrite) by ammonia

* This chapter has been published in a manuscript entitled "Liu, X., Kim, M., & Nakhla, G. (2018). Performance and Kinetics of Nitrification of Low Ammonia Wastewater at Low Temperature. Water Environment Research, 90(6), 498-509."

oxidizing bacteria (AOB), and nitratation (nitrite oxidized to nitrate) by nitrite oxidizing bacteria (NOB) [1]. Nitritation is a prerequisite for some emerging novel biological nitrogen processes, such as partial nitritation-anammox and nitritation-denitrification, as nitrite is the substrate, or intermediary product, of both anammox and denitrification [2]. Compared to full nitrification, nitritation consumes less oxygen, which translates to significant energy savings, given that the energy used for aeration accounts for approximately 50% of the total energy consumption of a typical wastewater resource recovery facility [3].

The operational dissolved oxygen may influence nitrification. It has been reported that low dissolved oxygen below 2.0 mg O_2/L led to inhibition of nitrifier growth, resulting in incomplete nitrification [1,4]. Generally, it is believed that NOB are more sensitive to dissolved oxygen than AOB as they have a higher dissolved oxygen half-saturation coefficient (*K*o) [5–8]. As a result, low dissolved oxygen is used as a strategy to wash-out NOB to realize nitritation [9]. However, some studies still reported a higher *K*o for AOB than NOB [10–12]. In fact, very wide *K*o ranges of 0.03 to 1.5 mg O_2/L and 0.13 to 3.00 mg O_2/L were reported for AOB and NOB, respectively [13,14].

Recently, the application of partial nitrification-anammox process for mainstream wastewater treatment, which is characterized by low nitrogen concentrations and low temperatures, has received wide attention. Single-stage partial nitrification-anammox processes have been conducted in various reactors, that is, sequencing batch reactor (SBR) [15], moving bed biofilm reactor [16,17], and rotating biological contactor [18]. However, the single-stage partial nitrification-anammox process suffers from nitrite accumulation, leading to complete process collapse at low temperatures, as the activity of AOB is greater than that of the anammox bacteria [15], suggesting that two-stage systems may be a good alternative at low temperatures because of ease of control.

In addition, most of the studies adopted the strategy of starting partial nitrification at relatively high temperatures, and then gradually decreasing the temperature [19,20].

Previous studies on nitrification kinetics have predominantly used biomass cultivated at 20 °C or 35 °C (as shown in Table 5-1), although temperature may affect the microbial consortia composition and kinetics of the cultivated biomass. Shammas [21] studied the effect of temperature on nitrification process using short term batch tests conducted with biomass cultivated at 20 to 25 °C. In the study of Salvetti et al. [22], the effect of temperature on the rate of nitrification was studied in two pure-oxygen moving-bed biofilm reactors at an average temperature of 17.9 °C and 19.2 °C, respectively. However, only the temperature coefficient (θ) was determined, whereas AOB and NOB maximum specific growth rates (μ_{max}) and the dissolved oxygen half-saturation coefficient (Ko) were not measured. To date, and to the best of the authors' knowledge, there is no direct measurement of the nitrifiers' maximum growth rate (μ_{max}) and *K*o at temperatures lower than 20 °C. The μ_{max} at low temperatures are usually calculated based on μ at 35 °C or 20 °C and temperature coefficient, which, however, may not be accurate because of the different temperature coefficients reported in the literature. More importantly, K_o cannot be calculated in the same way because of a lack of temperature dependency. Thus, K_o at 20 °C is assumed to be pertinent at low temperature, although temperature may impact it.

Table 5-1. Summary of kinetic parameters during phase II

Kinetic parameters	Phase II	Literature*	Median value
Oxygen half-saturation coefficient (*K*o) for AOB (mg DO/L)	1.36	0.50[a], 0.03[b], 0.42[c], 0.79[d], 0.18[d], 0.74[e], 1.16[f], 0.18[g], 1.00[h], 0.36[i], 0.51[j], 0.40[k], 0.2–1.5[l]	0.46
Oxygen half-saturation coefficient (*K*o) for NOB (mg DO/L)	2.79	0.68[a], 0.43[b], 0.28[c], 0.47[d],0.13[d],1.75[e], 0.16[f], 0.54[g], 3.00[h], 0.54[i], 1.98[j]	0.54
Max. specific growth rate of AOB, μ_{max} (d^{-1})	0.28	0.13–0.59[l], 0.23[m], 0.33[n],0.49[o], 0.16[p],0.22[i], 0.99[q], 0.47–0.54[r], 0.57-0.78[s], 0.35[t]	0.47
Max. specific growth rate of NOB, μ_{max} (d^{-1})	0.38	0.29[o], 0.43–0.65[t], 0.89[u], 0.14[p], 0.62–0.7[i]	0.62
Aerobic decay coefficient, b (d^{-1})	0.10	0.04–0.12[l], 0.11[i,j], 0.13[q] 0.035–0.065[r], 0.06[t]	0.065

a. Rittmann and McCarty, at 20 °C[23]; b. Blackburne et al., 20 °C[5]; c. Daebel et al., 20 °C[10]; d. Manser et al. (2005), 20 °C[11]; e. Guisasola et al. (2005), 25 °C[24]; f. Regmi et al. (2014), 25 °C[12]; g. Pérez et al. (2009), 20 °C[25]; h. Moussa et al. (2005), 20 °C[26]; i. Liu et al. (2016), 35 °C[2]; j. Schramm et al. (1999), 30 °C[27]; k. Wett et al. (2013), 20 °C[28]; l. Ge et al. (2015), 20 °C[14]; m. Metcalf and Eddy, 20 °C[1]; n. Van Hulle et al., 35 °C[29]; o. Galí et al., 30-35 °C[30]; p. Hellinga et al., 20 °C[31]; q. Liu and Wang, 20 °C[32]; r. Hunik et al., 20 °C[33]; s. Park and Noguera, 30 °C[34]; t. Kaelin et al., 20 °C[35]; u. Kampschreur et al., 20 °C[36]; v. Wett and Rauch, 20 °C[37].

* μ_{AOB}, μ_{NOB} and b values have been converted to 14 °C using temperature coefficients of 1.072, 1.063, and 1.04; for μ_{AOB}, μ_{NOB}, and b, respectively [1]. *K*o values have not been converted. DO = dissolved oxygen.

Furthermore, the short-term effect of dissolved oxygen on biological nitrogen removal has been discussed in many studies, using batch tests [9,38]. Until now, limited reports have been available on comparisons of partial nitrification performance, at different dissolved oxygen concentrations, based on long-term operation, especially at low temperature. The objectives of this study are: (1) to investigate the effect of dissolved oxygen on the nitrification performance; (2) to test if partial nitrification of low ammonia wastewater could be achieved under low dissolved oxygen and low

temperature conditions; and (3) to determine the kinetics of the cultivated biomass at low temperature. Since, in southern Ontario, the wastewater temperature in winter is as low as 14 °C, 14 °C was chosen for this work.

5.2 Methodology

5.2.1 Partial Nitrification Reactor.

An SBR with a working volume of 10 L was used in this study. The reactor height and the diameter are 30 cm and 24 cm, respectively. Two pumps (Masterflex L/S, Cole-Parmer, Montreal, Canada) were used, one feeding the wastewater to the SBR and the other withdrawing the treated wastewater. Aeration was provided with an air pump (Rena Air 400, Rena Aquatic Supply, Charlotte, U.S.) through an air diffuser. The operating sequence of the SBR consisted of six 4 h cycles with feed (20 min), aeration (180 min), settle (20 min), and decant (20 min) phases in each cycle. In each cycle, 5 L of supernatant were withdrawn from the reactor after the settling phase, and replaced with fresh wastewater, resulting in a hydraulic retention time (HRT) of 8 h. Temperature in the reactor was maintained at 14 °C with a water bath (PolySciences Heated Circulating Bath, 1 SD07R-20-A11B, Polysciences, Inc., Warrington, PA 18976). pH was not controlled, and during each cycle pH decreased with time. Solids retention time (SRT) was maintained at around 10 d, and the nitrification performance was tested at three different dissolved oxygen levels (averaging 5.5 mg /L, 2.5 mg /L, and 0.8 mg /L) denoted as phases I, II, and III, respectively.

5.2.2 Synthetic Wastewater and Activated Sludge Characteristics.

The synthetic wastewater was composed of NH_4Cl (40 mg N/L), $NaHCO_3$ (480 mg/L) (as carbon source for nitrification), KH_2PO_4 (8 mg P/L), $MgSO_4 \cdot 7H_2O$ (100 mg/L), $CaCl_2$ (100 mg/L), 1 ml/L water of trace elements solution I (composition in g/L as follows: EDTA 15, $ZnSO_4$ 0.43, $CoCl_2$ 0.24, $MnCl_2$ 0.63, $CuSO_4$ 0.25, Na_2MoO_4 0.22, $NiCl_2$ 0.19, Na_2SeO_4 0.21, H_3BO_3 0.01, and $NaWO_4$ 0.05), and 1 ml/L water of trace elements solution II containing $FeSO_4$ and EDTA at 5 g/L each[2]. Although, theoretically, the required $NaHCO_3$:NH_4-N:P mass ratio was around 34.2:5:1, corresponding to an alkalinity to ammonia nitrogen ratio of 4.1:1 mg $CaCO_3$/mg N; to maintain residual alkalinity and effluent pH, an additional 30 mg $CaCO_3$/L of alkalinity was added. The alkalinity was controlled to allow conversion of around 60% of the feed ammonia to nitrite, in order to provide the right influent conditions for anammox [2]. The seed sludge was return activated sludge taken from the Greenway water pollution control plant in London, Ontario.

5.2.3 Analytical Methods.

Effluent samples were analyzed for ammonia, nitrite, and nitrate daily. The mixed liquid suspended solids to mixed liquid volatile suspended solids ratio (MLSS/MLVSS) were determined in triplicates using Whatman GF/A filters (VWR International, Mississauga, Canada), in accordance with Standard Methods [39]. Specifically, biomass was filtered, and the aluminum dishes with the filter paper were put into an oven and heated at 105 °C for 1h and 550 °C for 20 min, respectively. Dissolved oxygen and pH were measured using a dissolved oxygen meter (HACH HQ 40d, HACH Co., London, Canada) and a pH meter (VWR B10P, VWR International, Mississauga, Canada), respectively. Nitrogen species were determined using HACH methods, that is, ammonium (method 10031), nitrite (8153), and nitrate (10020) every day.

5.2.4 Batch Tests.

Kinetic batch tests were also conducted to determine the ammonia oxidation rate (AOR) and nitrite oxidation rate (NOR) when the system stabilized at each operating condition after at least three SRT turnovers. The batch tests were conducted following Liu et al. [2] at three different dissolved oxygen levels. Specifically, the online batch tests were conducted in the SBR as follows: for the AOR test, the same influent with an ammonia concentration of 40 mg N/L, and alkalinity to ammonia nitrogen mass ratio of 4.1:1, was used. The dissolved oxygen was adjusted by changing the air flowrate. Two sets of batch tests were conducted during phase II, at dissolved oxygen levels of 5.2, 2.4, and 1.0 mg/L, and 5.0, 2.0, and 1.0 mg/L, respectively. The AOR and NOR tests were conducted by measuring ammonia and nitrite concentrations in the SBR every 30 min until the end of the cycle. For the NOR test, the influent nitrite concentration was 40 mg N/L. Alkalinity was added to adjust the influent pH to approximately 7.3.

5.2.5 Kinetic Modelling.

Kinetic modelling was carried out based on the important pertinent equations summarized below:

$$Y \cdot Q \cdot (S_0 - S) - b \cdot V \cdot X - \frac{V \cdot X}{SRT} = 0 \qquad \text{(Eq.5.1)}$$

$$X = \frac{Y \cdot Q \cdot (S_0 - S)}{V \cdot (b + \frac{1}{SRT})} = \frac{SRT}{HRT} \cdot \frac{Y \cdot (S_0 - S)}{b \cdot SRT + 1} \qquad \text{(Eq.5.2)}$$

$$AOR = X_{AOB} \cdot q_{AOB} = q_{AOB} \cdot \frac{Y_{AOB} \cdot (S_{0,NH} - S_{NH})}{HRT \cdot (b_{AOB} + \frac{1}{SRT})} \qquad \text{(Eq.5.3)}$$

$$NOR = X_{NOB} \cdot q_{NOB} = q_{NOB} \cdot \frac{Y_{NOB} \cdot (S_{NO3} - S_{0,NO3})}{HRT \cdot (b_{NOB} + \frac{1}{SRT})} \qquad \text{(Eq.5.4)}$$

$$\mu_{AOB} = \frac{\text{AOR} \cdot \text{HRT} \cdot (b_{AOB} + \frac{1}{SRT})}{S_{0,NH} - S_{NH}} \quad \text{(Eq.5.5)}$$

$$\mu_{NOB} = \frac{\text{NOR} \cdot \text{HRT} \cdot (b_{NOB} + \frac{1}{SRT})}{S_{NO3} - S_{0,NO3}} \quad \text{(Eq.5.6)}$$

$$q = \frac{\mu}{Y} \quad \text{(Eq.5.7)}$$

where b_{AOB} and b_{NOB} are endogenous decay coefficients for AOB and NOB, respectively, d^{-1}; Y_{AOB} and Y_{NOB} are biomass yield coefficients for AOB and NOB, respectively, mg VSS/mg N; q_{AOB} and q_{NOB} are the maximum specific substrate utilization rates for AOB and NOB, respectively, mg N/(mg VSS·d); $\mu_{m,AOB}$ and $\mu_{m,NOB}$ are the maximum growth rates for AOB and NOB, respectively, d^{-1}; X_{AOB} and X_{NOB} are the active AOB and NOB biomass concentrations, respectively, mg VSS/L; AOR and NOR are the maximum ammonia oxidation rate and maximum nitrite oxidation rate, respectively, mg N/(L·min); $S_{NH}$and S_{NO2} are effluent ammonia and nitrite concentrations, respectively, mg N/L;$(S_{0,NH} - S_{NH})$ and $(S_{NO3} - S_{0,NO3})$ are ammonia and nitrite oxidized, respectively; and HRT is the hydraulic retention time, h.

In addition, the Monod model was used in this study to calculate AOR_{max} and NOR_{max} as well as *K*o, as shown below:

$$\text{AOR} = AOR_{max} \cdot \frac{DO}{DO + K_{O,AOB}} \quad \text{(Eq.5.8)}$$

$$\text{NOR} = \text{NOR}_{max} \cdot \frac{DO}{DO + K_{O,NOB}} \quad \text{(Eq.5.9)}$$

The ammonia conversion ratio (ACR) and nitrite accumulation ratio (NAR) were calculated based on influent and effluent quality as shown below in Eq.5.10 and Eq.5.11.

$$\text{ACR} = \frac{S_{0,NH} - S_{NH}}{S_{0,NH}} \quad \text{(Eq.5.10)}$$

$$\text{NAR} = \frac{S_{NO2}}{S_{NO2} + S_{NO3}} \quad \text{(Eq.5.11)}$$

in which, $S_{0,NH}$ is influent ammonia, and S_{NH}, S_{NO2} and S_{NO3} are effluent ammonia, nitrite, and nitrate, respectively, mg N/L.

The theoretical nitrite accumulation ratio (NAR) was calculated based on eq Eq.5.12.

$$\text{NAR} = 1 - \frac{NOR}{AOR} \quad \text{(Eq.5.12)}$$

5.3 Results

5.3.1 Effluent Quality.

Figure 5-1A shows the nitrification performance for the 10d SRT reactor. The detailed performance data are shown in Table 5-2. The data for phases I and II were collected from day 21 to day 28, and day 60 to day 100, respectively, as shown in Figure 1A. In phase I, the MLVSS between day 21 and day 28 averaged 107 ± 4 mg/L, whereas, in phase II, from day 60 to 100, it averaged 59 ± 4 mg/L, indicating relative biomass stability. Thus, the data reported in Table 2 reflects the steady-state operation of the SBR in phases I and II. During phase I, as influent alkalinity was controlled, only around 57% to 60% of the ammonia could theoretically be converted by AOB. The reactor was operated at this condition for 28 d, which is almost 3 SRT turnovers, until stable performance was achieved. The results suggest that at the high dissolved oxygen level of 5 to 6 mg/L, NOB had a very high activity, resulting in average effluent ammonia, nitrite, and nitrate concentrations of 17.6 ± 1.5 mg N/L, 1.4 ± 0.8 mg N/L, and 20.2 ± 1.6 mg N/L,

respectively. Accordingly, as apparent from Figure 5-1B, the average ammonia conversion ratio (ACR) and nitrite accumulation ratio (NAR) were 55.1 ± 3.7% and 6.3 ± 3.7%, respectively. The average values were determined based on data from day 21 to day 28, after two SRT turnovers. With such a low NAR, obviously, NOB dominated the system and full nitrification was achieved.

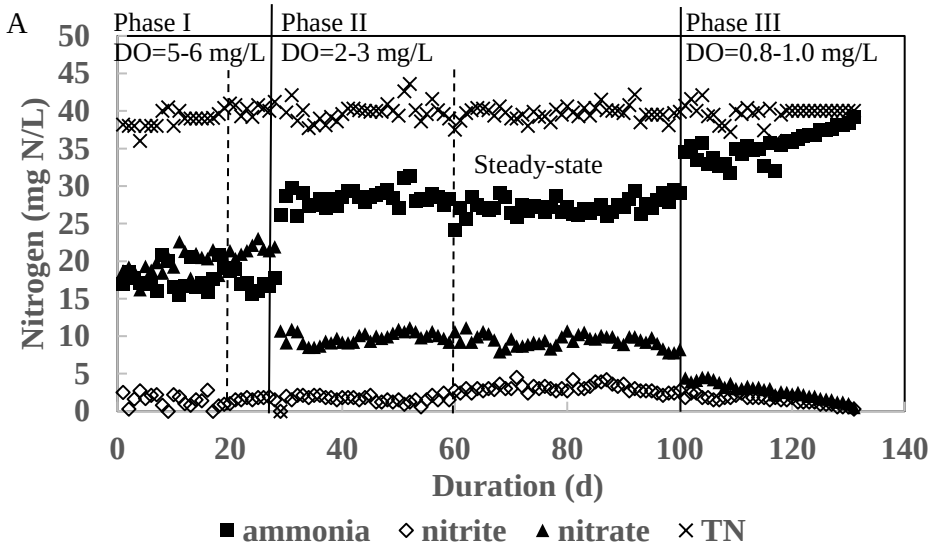

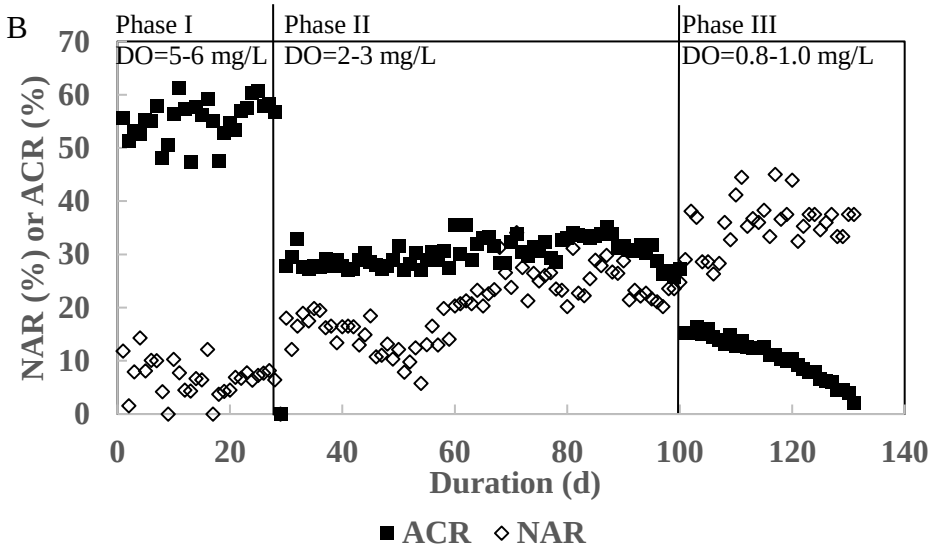

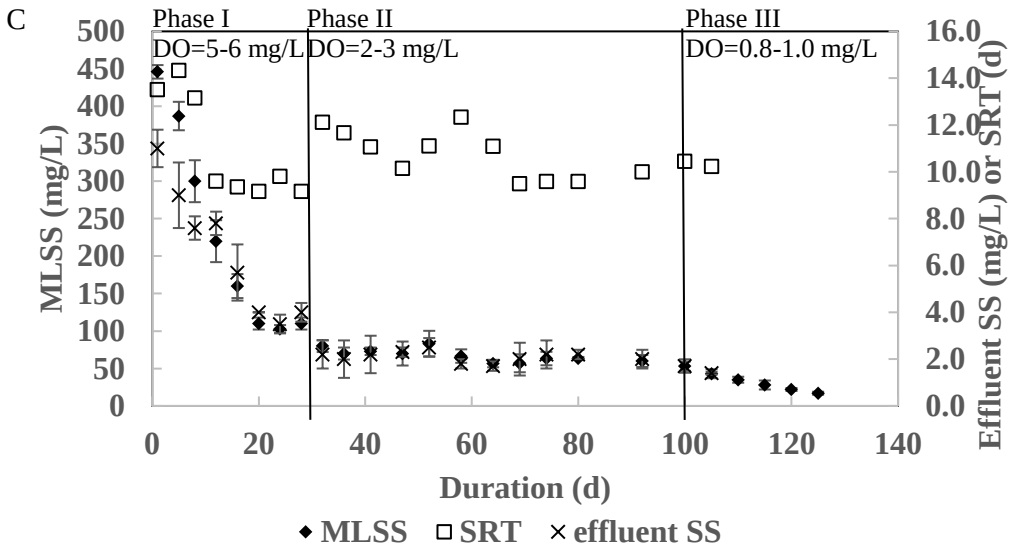

Figure 5-1. (A) Effluent ammonia, nitrite, and nitrate concentrations, (B) ammonia conversion ratio (ACR) and nitrite accumulation ratio (NAR), and (C) MLSS and SRT change at different dissolved oxygen concentrations (SRT = 10 d; temperature = 14 °C; TN, total nitrogen; SS, suspended solids.). (Phases I to III with dissolved oxygen range of 5–6 mg/L, 2–3 mg/L and 0.8–1.0 mg/L, respectively.)

As apparent from Figure.5-1A, the decrease of dissolved oxygen from 5 to 6 mg/L to 2 to 3 mg/L resulted in ammonia accumulation, that is, poor conversion to NO*x*. The effluent ammonia increased from 17.8 mg N/L on day 28, to 26.2 mg N/L on day 29, whereas the effluent nitrate decreased from 21.9 mg N/L to 10.7 mg N/L. Thus, incomplete nitrification was observed. The SBR was then operated at the same conditions for 70 days, almost 6 SRTs. The performance of the SBR was relatively stable with average effluent ammonia, nitrite, and nitrate concentrations of 27.7 ± 1.3 mg N/L, 2.4 ± 0.9 mg N/L, and 9.7 ± 0.8 mg N/L, respectively. Accordingly, from Figure 5-1B, the average ACR and NAR were 30.4 ± 2.5% and 19.5 ± 6.3%, respectively.

As shown in Figure 5-1A, on day 100, the dissolved oxygen concentration decreased to 0.8 to1.0 mg/L. The effluent ammonia, nitrite, and nitrate concentrations changed from 29, 2.7, and 8.2 mg N/L on day 100, to 34.5, 1.8, and 4.4 mg N/L on day 101, after which the ammonia almost continued to increase. After operating for over 30 days at dissolved oxygen 0.8 to 1.0 mg/L, the effluent ammonia concentration increased to over 39 mg N/L, with only less than 2.5% ammonia removal, suggesting that AOB were washed out at dissolved oxygen 0.8 to 1.0 mg/L, SRT 10d, and a temperature of 14 °C. In the study of Liu and Wang [32], AOB wash-out was observed at a dissolved oxygen of 0.19 mg/L. The washout dissolved oxygen for AOB of 0.8 to 1.0 mg/L in this study was much higher than that of Liu and Wang [32], which may be the result of the lower μ_{max} at 14 °C compared to 20 °C. Although unstable performance in phase III was observed, as shown in Figure 5-1B, the NAR was relatively stable at 35.7 ± 4.5%. Obviously, the NAR increased from 6.3% to 19.5%, and, again, to 35.7%, with the dissolved oxygen decreasing from 5 to 6 mg/L towards 2 to 3 mg/L, and, again, towards 0.8 to 1.0 mg/L, perhaps because of the difference in oxygen affinity for AOB and NOB, which will be further discussed.

Table 5-2. Performance of the SBR at different dissolved oxygen levels (the average data for phases I and II were collected from day 20 to day 28, and day 60 to day 100, respectively).

	Phase I		Phase II		Phase III	
Parameter	average	STD	average	STD	average	STD
Ammonia (mg N/L)	17.6	1.5	27.3	1.1	NA	NA
Nitrite (mg N/L)	1.4	0.8	3.0	0.5	NA	NA
Nitrate (mg N/L)	20.2	1.6	9.4	0.8	NA	NA
NAR (%)	6.3	3.7	24.4	3.4	35.7	4.5
ACR (%)	55.1	3.7	31.3	2.5	NA	NA
Calculated NAR (%)	9.2		23.7		34.2	
Biomass concentration (mg MLSS/L)	107	4	59	4		

To conclude, decreases in operational dissolved oxygen led to ACR decrease and NAR increase. In this study, the SRT was maintained at around 10 d, with biomass concentrations of 100 to 120 and 55 to 65 mg MLSS/L, at dissolved oxygen of 5 to 6 mg/L and 2 to 3 mg/L, respectively, as can be seen from Figure 5-1C. With dissolved oxygen decreasing further towards 0.8 to 1.0 mg/L, the biomass concentration continued to decrease. The effluent suspended solids concentration after 105 d was not determined as it was too low (<1 mg/L) and could not be measured accurately.

5.3.2 Online Batch Tests.

Two rounds of batch tests were completed during phase II, and the duplicate results are shown in Figures 5-2 and 5-3, with the results summarized in Table 5-1. The results demonstrate that not only both the specific ammonia oxidation and the nitrite oxidation were very reproducible, but they also increased with dissolved oxygen, as dissolved oxygen was the cosubstrate for both AOB and NOB [40]. During the entire batch test, the free nitrous acid (FNA) and free ammonia concentrations were below 0.0025 and 0.17 mg N/L, respectively. Thus, free ammonia and FNA inhibition did not occur since free ammonia and FNA concentrations of 1.0 and 0.1 mg N/L did not inhibit AOB and NOB [2]. Alkalinity and pH are two important factors affecting nitrification. In this study, during phase I, the pH gradually decreased from 7.3 to 6.6 in one cycle, as evident from Figure 4. The activity of AOB and NOB dropped by approximately 40% as a result of pH changes. Thus, kinetics were not determined based on phase I data. Influent alkalinity was around 190 mg $CaCO_3$/L, and effluent alkalinity was around 30 mg $CaCO_3$/L, with over 160 mg $CaCO_3$/L consumed. The effluent NO_x of 22.6 mg N/L, corresponding to an alkalinity consumption of 161 mg $CaCO_3$/L based on an alkalinity-to-nitrite ratio of 7.14:1 and the minimal alkalinity consumption during nitratation [41], confirms a good alkalinity balance. It is suggested that limited alkalinity provision, that is, an alkalinity to nitrogen ratio of less than 5 mg $CaCO_3$/mg N, may be favorable for partial nitrification, as it is the carbon source for nitrifiers [1,42]. However, in this study, during phase I, a NAR of only 6.3% was observed, suggesting that alkalinity limitation may be a supportive factor for partial nitrification, but not the sole one because in phases II and III ammonia accumulated, despite the high effluent alkalinity of over 95 mg $CaCO_3$/L.

A

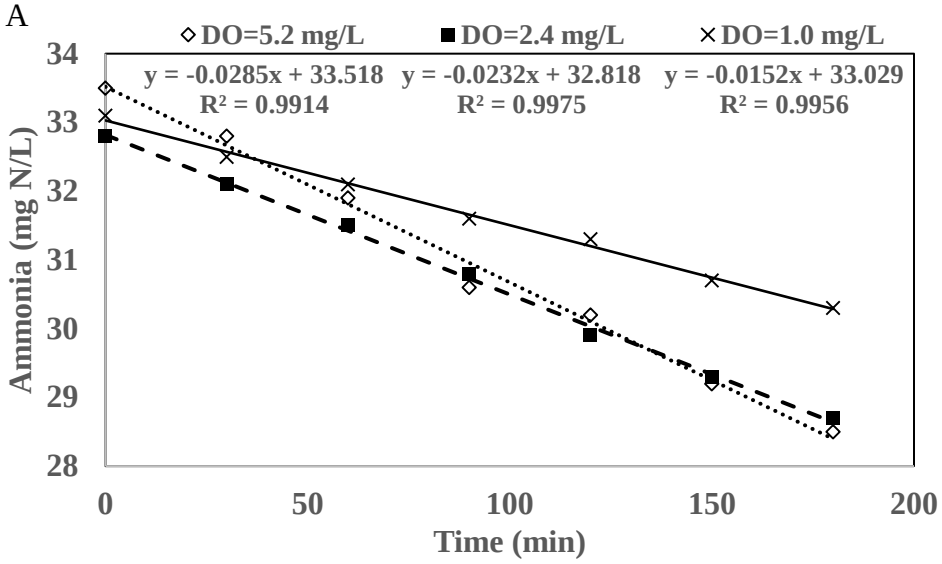
DO=5.2 mg/L
DO=2.4 mg/L
DO=1.0 mg/L
y = -0.0285x + 33.518
R² = 0.9914
y = -0.0232x + 32.818
R² = 0.9975
y = -0.0152x + 33.029
R² = 0.9956
Ammonia (mg N/L)
34
33
32
31
30
29
28
0
50
100
150
200
Time (min)

B

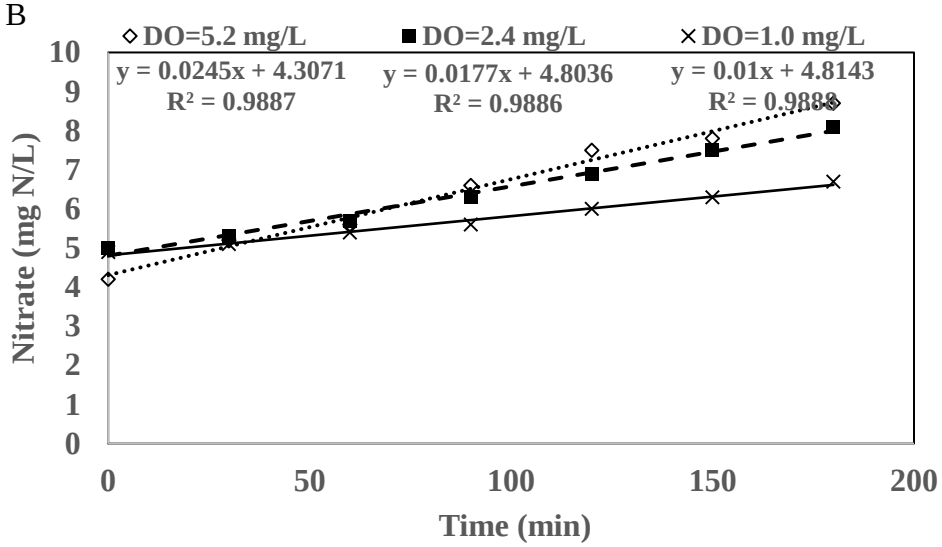
DO=5.2 mg/L
DO=2.4 mg/L
DO=1.0 mg/L
y = 0.0245x + 4.3071
R² = 0.9887
y = 0.0177x + 4.8036
R² = 0.9886
y = 0.01x + 4.8143
R² = 0.9888
Nitrate (mg N/L)
10
9
8
7
6
5
4
3
2
1
0
0
50
100
150
200
Time (min)

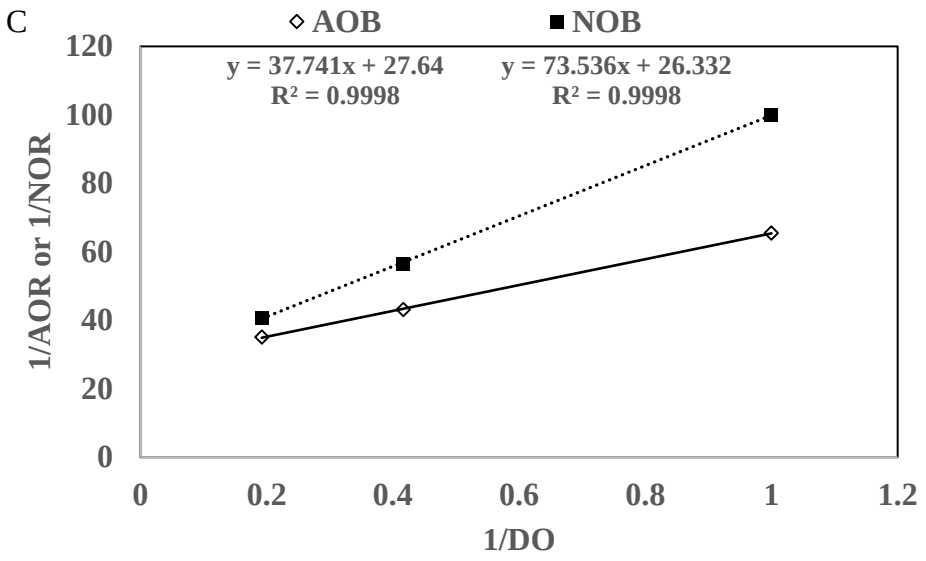

Figure 5-2. First set of batch test results during phase II: (A) ammonia concentration, (B) nitrate concentration, and (C) relationship between 1/AOR (or 1/NOR) and 1/dissolved oxygen.

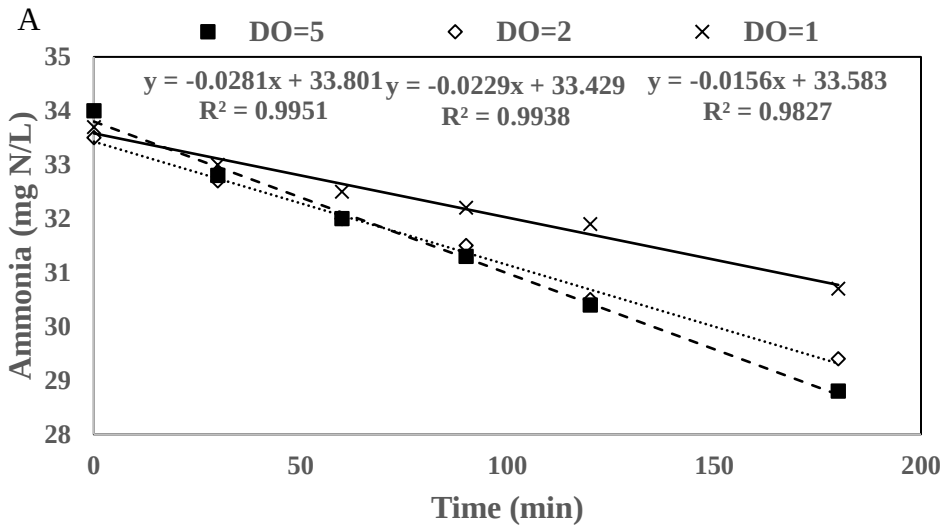

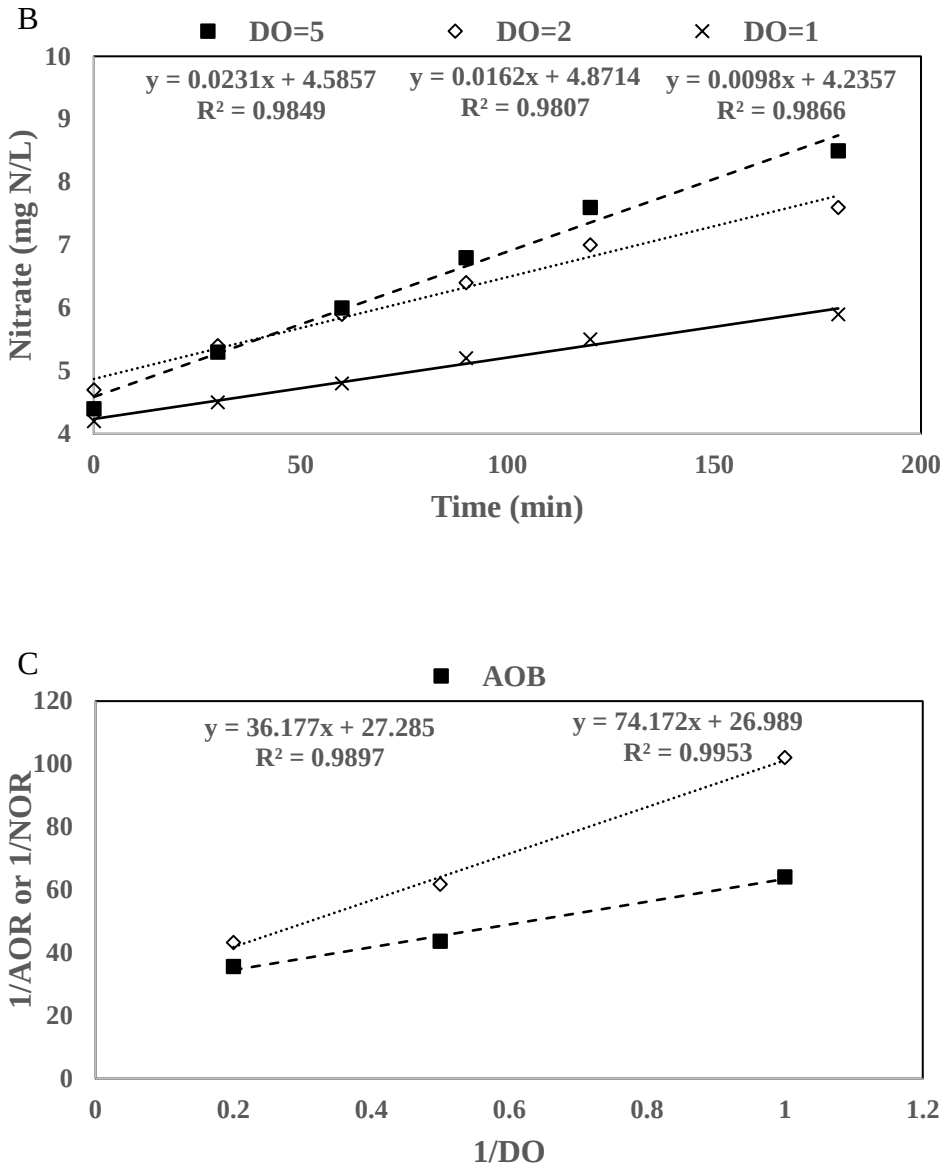

Figure 5-3. Second set of batch test results during phase II: (A) ammonia concentration, (B) nitrate concentration, and (C) relationship between 1/AOR (or 1/NOR) and 1/dissolved oxygen.

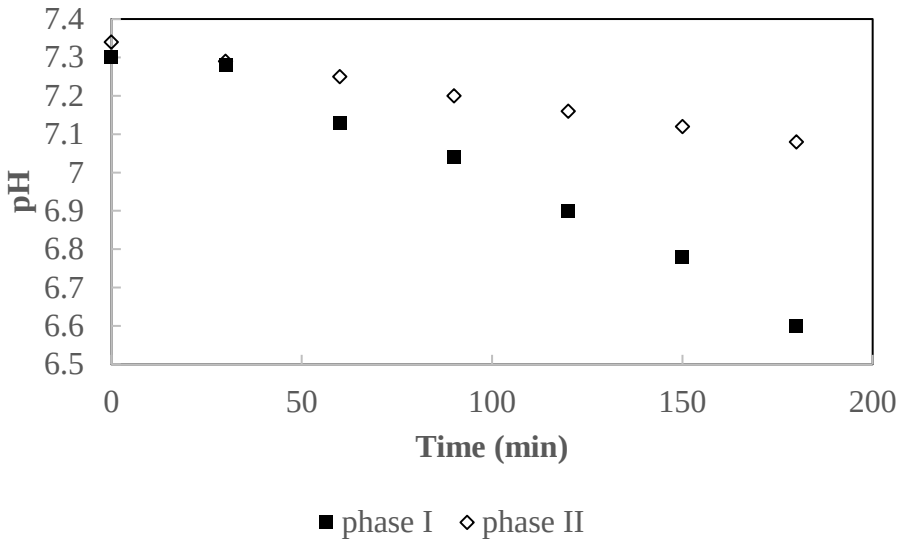

Figure 5-4. Typical pH cycle change during phase I and II.

During phases II and III, as ammonia accumulation was observed, less alkalinity was consumed. During phase II, the pH gradually decreased from 7.3 to 7.1 in one cycle. Influent alkalinity was about 190 mg $CaCO_3$/L, and effluent alkalinity was around 90 to 100 mg$CaCO_3$/L, with around 90 to 100 mg $CaCO_3$/L consumed. The effluent NO*x* of 12.4 mg N/L was consistent with approximately 90 mg $CaCO_3$/L alkalinity consumption. In this study, the kinetics were derived based on batch tests carried out during phase II, during which the pH range was 7.1 to 7.3. Thus, there was almost no change in the activity of AOB and NOB because of pH ranging between 7.1 and 7.3 [43]. In activated sludge model (ASM)2, the default alkalinity half-saturation coefficient (K_{alk}) for autotrophs was 0.5 mmol HCO_3^-/L, which corresponds to 25 mg $CaCO_3$/L [42]. During phase II, the initial alkalinity in the SBR, after mixing, was about 140 mg $CaCO_3$/L, and the effluent alkalinity was about 95 mg $CaCO_3$/L. Based on the Monod equation, the difference between AOB or NOB growth rates at the initial alkalinity concentration of 140 mg $CaCO_3$/L, and the final alkalinity concentration of 95 mg $CaCO_3$/L, is less than 6%, which is negligible. In fact,

as apparent from Figure 5-2, both ammonia consumption and nitrate production were almost linear, suggesting that pH and alkalinity had very limited effects on AOB and NOB activity.

Both ammonia oxidation and nitrite oxidation followed zero-order kinetics [2]. The AOR and NOR at dissolved oxygen 5.2, 2.4, and 1.0 mg/L were 0.0285, 0.0232, and 0.015 mg N/L·min, and 0.0245, 0.0177, and 0.01 mg N/ L·min, respectively. Based on Figure 5-2C and eqs 8 and 9, the AOR_{max} and NOR_{max} were 0.036 and 0.038 mg N/L·min, whereas the *K*o for AOB and NOB were 1.36 and 2.79 mg dissolved oxygen/L, respectively. Thus, based on eqs 5 and 6, using the data in Table 5-2, and yield coefficients of 0.24 and 0.1 mg COD/mg N for AOB and NOB, the maximum growth rates of AOB and NOB were 0.28 and 0.38 d^{-1}, respectively [44]. Based on eq 7, the maximum specific substrate utilization rates (q) for AOB and NOB were 1.66 and 5.40 mg N/mg VSS·d, respectively.

The kinetic parameters from this study were compared with the literature, as shown in Table 5-1. It must be emphasized that the *K*o values in Table 5-1 have not been corrected for temperature, with most of the literature values at 20 to 30 °C, whereas the data of this study are at 14 °C. On the other hand, μ_{max} for both AOB and NOB, as well as decay coefficient (b) from the literature, have all been converted to 14 °C using temperature coefficients (θ) of 1.072, 1.063, and 1.04, respectively [1]. However, different temperature coefficients have been reported in the literature. Table 5-3 summarizes the range of temperature coefficients reported in the literature. As apparent from Table 5-3, the temperature coefficients for AOB ranged from 1.023 to 1.172 while those for NOB ranged from 1.06 to 1.123. Figure 5A,B show the AOB and NOB growth rates of selected literature studies plus this study. There are bars for data from past studies as they were converted to 14 °C, based on the aforementioned temperature coefficient ranges, that is, 1.023 to 1.172 for AOB and 1.06 to 1.123 for NOB. There are no bars for this study as the AOB and NOB growth

rates were determined at 14 °C, and thus no temperature coefficients were applied. Previously, the kinetic parameters for AOB and NOB at low temperatures were not directly determined, but calculated using temperature coefficients, which may not be accurate enough, as low temperatures may lead to nitrifier community change. As seen in Table 5-1, even with the same growth rates of AOB and NOB measured at 20 °C, the calculated growth rates at 14 °C may vary widely because of the different temperature coefficients. This study is the first attempt to directly determine the kinetic parameters of nitrifiers with sludge cultivated at 14 °C. For each kinetic parameter, literature values vary widely. While the maximum growth rates from this study fall within the reported literature range, the *K*o for AOB and NOB of 1.36 and 2.79 mg dissolved oxygen/L were much higher than the median values reported in the literature. In fact, the *K*o values for AOB of 1.36 mg dissolved oxygen/L was the second highest of 15 literature studies, and, similarly, the *K*o for NOB of 2.79 mg dissolved oxygen/L was the second highest of 12 literature studies. The significantly greater *K*o values in this study are attributed to temperature effects.

Table 5-3. Summary of temperature coefficients (θ) for AOB and NOB, from the literature.

	Literature
AOB	1.023–1.081[a], 1.172 (5 °C–20 °C) and 1.062 (5 °C–20 °C)[b], 1.098–1.118[c], 1.098[d], 1.045[e], 1.120[f],1.095–1.113[g]
NOB	1.068–1.112[c], 1.06[h], 1.094–1.102[g]
Nitrifiers (AOB and NOB)	1.06–1.123[i]

a. Salvetti et al. [22]; b. Guo et al. [45]; c. Grady Jr. et al. [44]; d. Sözen et al. [46]; e. Görgün et al. [47]; f. Henze et al. [42]; g. Zhang et al. [48]; h. Munz et al. [49]; i. Metcalf and Eddy [1].

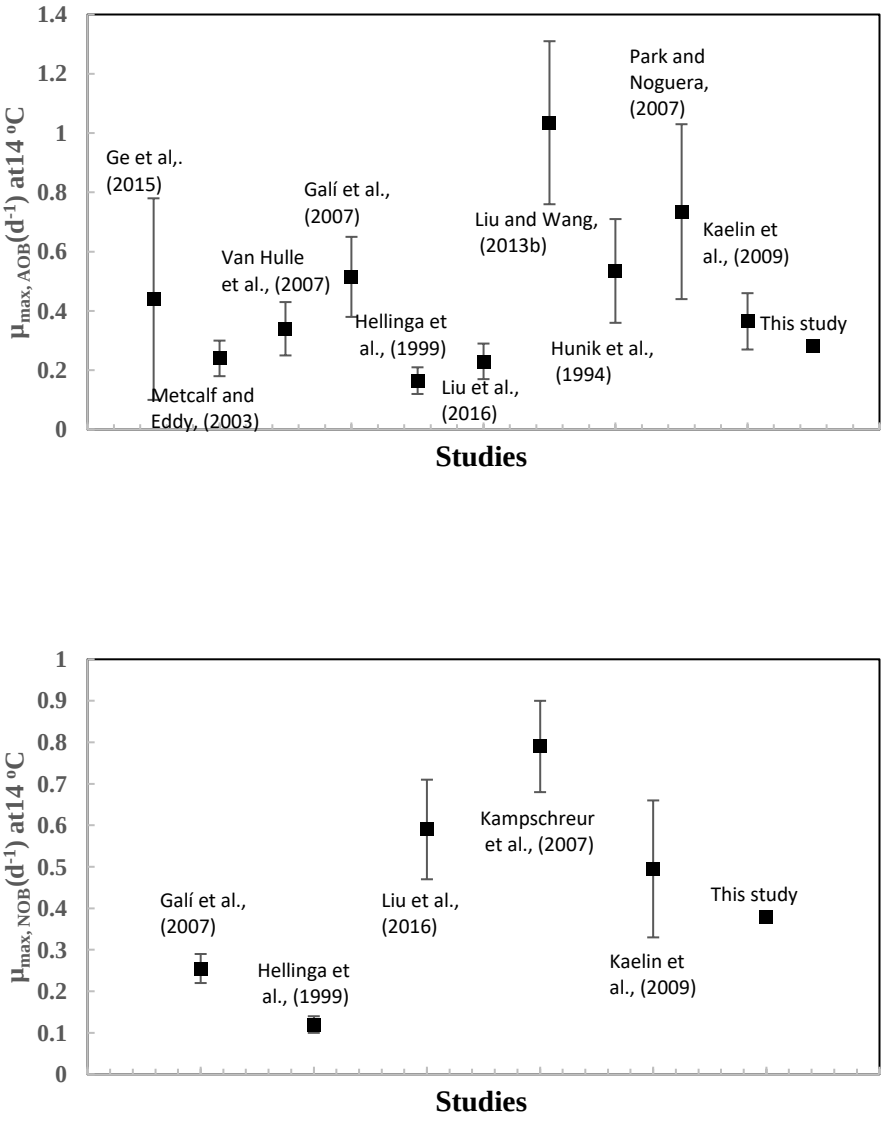

Figure 5-5. Comparison of (A) $\mu_{max,AOB}$ and (B) $\mu_{max, NOB}$ between this study and literature studies (all literature values have been converted to 14 °C using a θ range of 1.023–1.12 for AOB and 1.06–1.112 for NOB).

The calculated NAR for phases I to III are shown in Table 5-2. For phase III, the values of μ_{max} (0.28 d^{-1} for AOB and 0.38 d^{-1} for NOB), and *K*o (1.36 mg dissolved oxygen/L for AOB and 2.79 mg dissolved oxygen/L for NOB) in phase II, were used to calculate the NAR. The calculated NAR fall within the range of measured NAR for each phase. In this study, b was not directly measured but calculated as 0.1 d^{-1} using the Metcalf and Eddy [1] value of 0.15 d^{-1} at 20 °C and a temperature coefficient of 1.04, whereas the median literature value is 0.065 d^{-1}, which may affect the calculation of μ_{max} of AOB and NOB. Thus, with a b of 0.065 d^{-1}, the μ_{max} of AOB and NOB in this study were 0.24 and 0.31 d^{-1}, respectively. The μ_{max} of AOB and NOB were lower than the median values of 0.47 and 0.62 d^{-1} from the literature studies (Table 5-1). It is evident from Figure 5-5 that, despite the wide variability in the projected literature growth rates based on the broad range of temperature coefficients, the growth rates measured in this study are well below most of the literature. The kinetics of this study are directly measured with sludge cultivated at 14 °C, whereas all the literature kinetics are measured with sludge cultivated at 20 °C to 35 °C (as shown in Table 5-1), and converted to 14 °C by temperature coefficients, determined mostly within the 20 °C to 35 °C, which may not be applicable to other temperature ranges.

5.4 Discussion

5.4.1 Analyzing the Factors Affecting Nitrification Performance.

Generally, it is believed that low dissolved oxygen is more favorable to AOB than NOB, which is confirmed in this study, as the determined *K*o for AOB is lower than that for NOB. To date, all of the studies adopting low dissolved oxygen as the selection factor are conducted at temperatures equal to, or higher than, 20 °C, whereas the optimal conditions for partial nitrification at high temperatures and low temperatures may be different.

It is suggested that at high temperatures (>20 °C), AOB grow faster than NOB, and slower at low temperatures [31]. In this study, it was found that NOB had a higher maximum growth rate than AOB at 14 °C. However, despite temperature, the actual growth rates of AOB and NOB are also affected by other factors, like dissolved oxygen concentration. Wiesmann [50] suggested that, at dissolved oxygen concentrations below 1.8 mg/L, the specific growth rate of AOB is superior to NOB, which was observed in this study as well. It has been reported that dissolved oxygen concentrations below 1.0 mg/L favor the dominance of ammonium oxidizers [51,52]. Stable partial nitrification has been reported at 0.5 mg dissolved oxygen/L [40] and 0.2 mg/L [53,54]. In this study, at an SRT of 10d, low dissolved oxygen favored AOB over NOB. However, as the dissolved oxygen decreased towards 0.8 to 1.0 mg/L, washout of both AOB and NOB was observed, because of low growth rates in the presence of low temperature and low dissolved oxygen concentration.

It must be stressed that, despite dissolved oxygen concentration, SRT is another selection factor for AOB cultivation and NOB washout. Usually, SRTs shorter than the doubling time of NOB, and longer than the doubling time of AOB, are required. As mentioned above, at temperatures higher than 20 °C, it is relatively easy to adopt the proper SRT, as AOB grow faster than NOB. Bock et al. [55] reported the minimum doubling times of AOB and NOB at 35 °C to be 7 to 8 h and 10 to 13 h, respectively. An SRT of 1 to 2.5 days was suggested at 35 °C by Van Kempen et al. [56]. However, the results of this work suggested that a long SRT is needed when operating at low dissolved oxygen, because of the low growth rates of nitrifiers. For example, based on the AOB and NOB kinetics determined in this study, at a dissolved oxygen of 0.8 mg/L, an SRT of between 25 d to 50 d may be required to allow AOB growth and NOB washout. The recommended SRT for full nitrification at DOs of 1, 1.5, 2, 3, and 5 mg/L at 14^{o}C based on the kinetics of this study (excuding the b value of 0.1 d^{-1}) and the median literature b value of 0.065 d^{-1} from Table

5-1 is depicted in Table 5-4. In Table 5-4, NA means not applicable as at this condition the SRT_{min} of NOB is lower than that of AOB. At DO higher than 3 mg O_2/L, partial nitrification could not be achieved. Hafez et al. [57] reported successful full nitrification at a temperature of 12ºC, SRT of 7.1 d, and DO 3-5 mg/L, which agrees with the recommended SRT ranges in Table 5-4. While practically full nitrification has been reported at low temperature and SRTs below the 25-50 d determined above, these plants typically operate at DO>1.5-2.0 mg/L in winter. Furthermore, the uncertainty in estimating Ko at 14ºC in this study may have contributed to the atypical high estimated SRT.

Table 5-4. Recommend SRT range for partial and full nitrification at DOs of 1-5 mgO_2/L at 14ºC

DO (mg/L)	SRT range for partial nitrification (d)	SRT range for full nitrification (d)
1	18-27	>27
1.5	12-14	>14
2	9.8-10.5	>10.5
3	NA	>7.8
4	NA	>6.9
5	NA	>6.4

5.4.2 Feasibility of Achieving Nitritation by Low Dissolved Oxygen and LowTemperature.

The analysis of the actual growth rates for AOB and NOB, summarized in Table 5-5, based on the kinetics determined in this study, also confirmed that nitrification could be sustained in phases I and II but not III. As AOB had a lower *K*o than NOB, as shown in Table 5-5, it is possible to realize nitritation by decreasing the dissolved oxygen concentration. In fact, the NAR value

increased as dissolved oxygen decreased, as shown in Table 5-2. However, based on the performance, low dissolved oxygen led to AOB washout as well.

Table 5-5. Calculated growth rates for AOB and NOB during different phases.

Phases	I	II	III
$\mu_{maxAOB}^{DO-limitation}$	0.24	0.18	0.11
$\mu_{maxNOB}^{DO-limitation}$	0.25	0.18	0.09
μ for AOB	0.01 to 0.1	-0.05 to 0.04	-0.12 to -0.03
μ for NOB	0.02 to 0.11	-0.05 to 0.04	-0.14 to -0.05

As evident from the actual growth rates (μ), the factors affecting actual growth rate (μ) are dissolved oxygen concentration and SRT. Using the kinetic values in this study, the relationship between dissolved oxygen and minimum SRT is depicted in Figure 5-6. For example, to achieve complete nitrification at 14 °C and 10 d SRT, a minimal dissolved oxygen of 2.3 mg/L should be maintained. At dissolved oxygen higher than 2 mg/L, the minimum SRT of AOB and NOB are quite close, making it difficult to washout NOB by dissolved oxygen control. In addition, at dissolved oxygen concentrations over 4 mg/L, the minimum SRT for NOB is slightly lower than that for AOB (8 d vs 9 d), as NOB have higher growth rates than AOB at 14 °C. However, at dissolved oxygen levels lower than 2 mg/L, the minimum SRT of AOB and NOB start to separate from each other. Therefore, it seems that controlling the dissolved oxygen at a low level, that is, 1 mg/L, while maintaining a long SRT, that is, 40 d, can achieve stable nitritation.

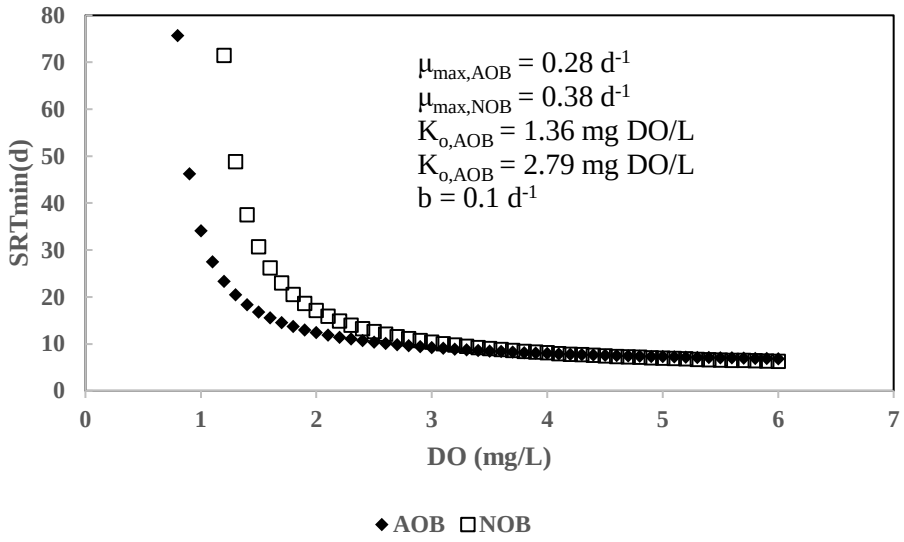

Figure 5-6. Relationship between dissolved oxygen and minimum SRT, for AOB and NOB at 14 °C.

5.4.3 Kinetic Rationalization of SBR Performance.

As shown above, each time, the dissolved oxygen concentration was reduced, either from 5 to 6 mg/L towards 2 to 3 mg/L, or further towards 0.8 to 1.0 mg/L, ammonia accumulation occurred, which may be explained by kinetics. The effects of dissolved oxygen limitation on μ_{max} are shown in eqs 5.13-5.14.

$$\mu_{maxAOB}^{DO-limitation} = \mu_{max} \times \frac{DO}{DO+K_{O,AOB}} \quad \text{(Eq.5.13)}$$

$$\mu_{maxNOB}^{DO-limitation} = \mu_{max} \times \frac{DO}{DO+K_{O,NOB}} \quad \text{(Eq.5.14)}$$

The calculated $\mu_{maxAOB}^{DO-limitation}$ and $\mu_{maxNOB}^{DO-limitation}$ during the three phases are shown in Table 4. The kinetics during phase III, at a dissolved oxygen of 0.8 to 1.0 mg/L, were not measured directly because of the low biomass, and were assumed not to have changed from phase II. Besides, actual

growth rates (μ) as $\mu_{max}^{DO-limitation} - b - \frac{1}{SRT}$ were also calculated [2]. Average dissolved oxygen values of 5.5, 2.4, and 0.9 mg/L during the 3 phases, as well as a b value of 0.1 d^{-1}, were used for calculations.

The actual growth rates of AOB and NOB were positive during phase I, slightly negative to positive during phase II, and very negative during phase III. Taking into consideration that the decay coefficient (b) varies from 0.04 to 0.13 d^{-1}, as shown in Table 4, the actual growth rates of AOB and NOB were almost zero during phase II and always negative during phase III. The performance of the SBR can be explained well, based on kinetics. In addition, the kinetic analysis explained why the AOR_{max} and NOR_{max} decreased with dissolved oxygen.

5.5 Conclusions

An SBR was operated for over 4 months treating low-ammonia (40 mg N/L) synthetic wastewater at a low temperature (14 °C) and an SRT of 10 days. The dissolved oxygen effect was investigated at dissolved oxygen levels of 5 to 6 mg/L, 2 to 3 mg/L, and 0.8 to 1.0 mg/L. The decrease in ambient dissolved oxygen concentration resulted in ammonia accumulation, as well as an increase in the nitrite accumulation ratio. Various kinetic parameters were determined or estimated. The performance of the SBR was explained by kinetics. The low growth rates of AOB and NOB, caused by low temperature, were the reason for biomass loss. Low dissolved oxygen, combined with a long SRT, appears to be a viable strategy for stable nitritation at low temperatures (14 °C).

5.6 Acknowledgments

This work was financially supported by the Natural Sciences and Engineering Research Council of Canada, under grant number CRDPJ 458990-13.

5.7 Reference

[1] Metcalf and Eddy, Wastewater Engineering: Treatment, Disposal, Reuse, Metcalf & Eddy, Inc McGraw-Hill N. Y. (2003).

[2] X. Liu, M. Kim, G. Nakhla, Operational conditions for successful partial nitrification in a sequencing batch reactor SBR based on process kinetics, Environ. Technol. 38 (2017) 694–704.

[3] P.L. McCarty, J. Bae, J. Kim, Domestic wastewater treatment as a net energy producer–can this be achieved?, Env. Sci Technol. 45 (2011) 7100–7106.

[4] B. Abbassi, S. Dullstein, N. Räbiger, Minimization of excess sludge production by increase of oxygen concentration in activated sludge flocs; experimental and theoretical approach, Water Res. 34 (2000) 139–146.

[5] R. Blackburne, Z. Yuan, J. Keller, Demonstration of nitrogen removal via nitrite in a sequencing batch reactor treating domestic wastewater, Water Res. 42 (2008) 2166–2176.

[6] H.J. Laanbroek, S. Gerards, Competition for limiting amounts of oxygen between Nitrosomonas europaea and Nitrobacter winogradskyi grown in mixed continuous cultures, Arch. Microbiol. 159 (1993) 453–459.

[7] S. Park, W. Bae, B.E. Rittmann, Operational boundaries for nitrite accumulation in nitrification based on minimum/maximum substrate concentrations that include effects of oxygen limitation, pH, and free ammonia and free nitrous acid inhibition, Environ. Sci. Technol. 44 (2009) 335–342.

[8] A.O. Sliekers, S.C.M. Haaijer, M.H. Stafsnes, J.G. Kuenen, M.S.M. Jetten, Competition and coexistence of aerobic ammonium-and nitrite-oxidizing bacteria at low oxygen concentrations, Appl. Microbiol. Biotechnol. 68 (2005) 808–817.

[9] J. Wang, N. Yang, Partial nitrification under limited dissolved oxygen conditions, Process Biochem. 39 (2004) 1223–1229.

[10] H. Daebel, R. Manser, W. Gujer, Exploring temporal variations of oxygen saturation constants of nitrifying bacteria, Water Res. 41 (2007) 1094–1102.

[11] R. Manser, W. Gujer, H. Siegrist, Consequences of mass transfer effects on the kinetics of nitrifiers, Water Res. 39 (2005) 4633–4642.

[12] P. Regmi, M.W. Miller, B. Holgate, R. Bunce, H. Park, K. Chandran, B. Wett, S. Murthy, C.B. Bott, Control of aeration, aerobic SRT and COD input for mainstream nitritation/denitritation, Water Res. 57 (2014) 162–171.

[13] M. Arnaldos, Y. Amerlinck, U. Rehman, T. Maere, S. Van Hoey, W. Naessens, I. Nopens, From the affinity constant to the half-saturation index: Understanding conventional modeling concepts in novel wastewater treatment processes, Water Res. 70 (2015) 458–470.

[14] S. Ge, S. Wang, X. Yang, S. Qiu, B. Li, Y. Peng, Detection of nitrifiers and evaluation of partial nitrification for wastewater treatment: a review, Chemosphere. 140 (2015) 85–98.

[15] Z. Hu, T. Lotti, M. de Kreuk, R. Kleerebezem, M. van Loosdrecht, J. Kruit, M.S.M. Jetten, B. Kartal, Nitrogen removal by a nitritation-anammox bioreactor at low temperature, Appl. Environ. Microbiol. 79 (2013) 2807–2812.

[16] E.M. Gilbert, S. Agrawal, S.M. Karst, H. Horn, P.H. Nielsen, S. Lackner, Low temperature partial nitritation/anammox in a moving bed biofilm reactor treating low strength wastewater, Environ. Sci. Technol. 48 (2014) 8784–8792.

[17] F. Persson, R. Sultana, M. Suarez, M. Hermansson, E. Plaza, B.-M. Wilén, Structure and composition of biofilm communities in a moving bed biofilm reactor for nitritation–anammox at low temperatures, Bioresour. Technol. 154 (2014) 267–273.

[18] H. De Clippeleir, S.E. Vlaeminck, F. De Wilde, K. Daeninck, M. Mosquera, P. Boeckx, W. Verstraete, N. Boon, One-stage partial nitritation/anammox at 15 C on pretreated sewage: feasibility demonstration at lab-scale, Appl. Microbiol. Biotechnol. 97 (2013) 10199–10210.

[19] E. Isanta, C. Reino, J. Carrera, J. Pérez, Stable partial nitritation for low-strength wastewater at low temperature in an aerobic granular reactor, Water Res. 80 (2015) 149–158.

[20] T. Lotti, R. Kleerebezem, Z. Hu, B. Kartal, M.S.M. Jetten, M.C.M. Van Loosdrecht, Simultaneous partial nitritation and anammox at low temperature with granular sludge, Water Res. 66 (2014) 111–121.

[21] N.K. Shammas, Interactions of temperature, pH, and biomass on the nitrification process, J. Water Pollut. Control Fed. (1986) 52–59.

[22] R. Salvetti, A. Azzellino, R. Canziani, L. Bonomo, Effects of temperature on tertiary nitrification in moving-bed biofilm reactors, Water Res. 40 (2006) 2981–2993.

[23] B.E. Rittmann, P.L. McCarty, Model of steady-state-biofilm kinetics, Biotechnol. Bioeng. 22 (1980) 2343–2357.

[24] A. Guisasola, I. Jubany, J.A. Baeza, J. Carrera, J. Lafuente, Respirometric estimation of the oxygen affinity constants for biological ammonium and nitrite oxidation, J. Chem. Technol. Biotechnol. 80 (2005) 388–396.

[25] J. Pérez, E. Costa, J.-U. Kreft, Conditions for partial nitrification in biofilm reactors and a kinetic explanation, Biotechnol. Bioeng. 103 (2009) 282–295.

[26] M.S. Moussa, C.M. Hooijmans, H.J. Lubberding, H.J. Gijzen, M.C.M. Van Loosdrecht, Modelling nitrification, heterotrophic growth and predation in activated sludge, Water Res. 39 (2005) 5080–5098.

[27] A. Schramm, D. de Beer, J.C. van den Heuvel, S. Ottengraf, R. Amann, Microscale Distribution of Populations and Activities ofNitrosospira and Nitrospira spp. along a Macroscale Gradient in a Nitrifying Bioreactor: Quantification by In Situ Hybridization and the Use of Microsensors, Appl. Environ. Microbiol. 65 (1999) 3690–3696.

[28] B. Wett, A. Omari, S.M. Podmirseg, M. Han, O. Akintayo, M.G. Brandón, S. Murthy, C. Bott, M. Hell, I. Takács, Going for mainstream deammonification from bench to full scale for maximized resource efficiency, Water Sci. Technol. 68 (2013) 283–289.

[29] S.W. Van Hulle, E.I. Volcke, J.L. Teruel, B. Donckels, M. van Loosdrecht, P.A. Vanrolleghem, Influence of temperature and pH on the kinetics of the Sharon nitritation process, J. Chem. Technol. Biotechnol. 82 (2007) 471–480.

[30] A. Galí, J. Dosta, M.C.M. Van Loosdrecht, J. Mata-Alvarez, Two ways to achieve an anammox influent from real reject water treatment at lab-scale: Partial SBR nitrification and SHARON process, Process Biochem. 42 (2007) 715–720.

[31] C. Hellinga, A. Schellen, J.W. Mulder, M.C.M. Van Loosdrecht, J.J. Heijnen, The SHARON process: an innovative method for nitrogen removal from ammonium-rich waste water, Water Sci. Technol. 37 (1998) 135–142.

[32] G. Liu, J. Wang, Role of solids retention time on complete nitrification: mechanistic understanding and modeling, J. Environ. Eng. 140 (2013) 48–56.

[33] J.H. Hunik, C.G. Bos, M.P. van den Hoogen, C.D. De Gooijer, J. Tramper, Co ‐ immobilized Nitrosomonas europaea and Nitrobacter agilis cells: validation of a dynamic model for simultaneous substrate conversion and growth in κ ‐ carrageenan gel beads, Biotechnol. Bioeng. 43 (1994) 1153–1163.

[34] H.-D. Park, D.R. Noguera, Characterization of two ammonia ‐ oxidizing bacteria isolated from reactors operated with low dissolved oxygen concentrations, J. Appl. Microbiol. 102 (2007) 1401–1417.

[35] D. Kaelin, R. Manser, L. Rieger, J. Eugster, K. Rottermann, H. Siegrist, Extension of ASM3 for two-step nitrification and denitrification and its calibration and validation with batch tests and pilot scale data, Water Res. 43 (2009) 1680–1692.

[36] M.J. Kampschreur, C. Picioreanu, N. Tan, R. Kleerebezem, M.S.M. Jetten, M. van Loosdrecht, Unraveling the source of nitric oxide emission during nitrification, Proc. Water Environ. Fed. 2007 (2007) 843–860.

[37] B. Wett, W. Rauch, The role of inorganic carbon limitation in biological nitrogen removal of extremely ammonia concentrated wastewater, Water Res. 37 (2003) 1100–1110.

[38] S.Y. Weon, S.I. Lee, B. Koopman, Effect of temperature and dissolved oxygen on biological nitrification at high ammonia concentrations, Environ. Technol. 25 (2004) 1211–1219.

[39] A. Apha, Wef, Stand. Methods Exam. Water Wastewater 20th Ed Wash. DC Am. Public Health Assoc. Am. Water Work Assoc. Water Environ. Fed. 252 (1998).

[40] K. Hanaki, C. Wantawin, S. Ohgaki, Nitrification at low levels of dissolved oxygen with and without organic loading in a suspended-growth reactor, Water Res. 24 (1990) 297–302.

[41] F. Cui, Cold CANON: Anammox at low temperatures, Delft University of Technology, 2012.

[42] M. Henze, W. Gujer, T. Mino, M. Van Loosedrecht, Activated sludge models ASM1, ASM2, ASM2d and ASM3, (2006).

[43] C.P.L. Grady, H.C. Lim, Biological Wastewater Treatment, 2nd ed., Marcel Dekker, NY, 1980.

[44] C.L. Grady Jr, G.T. Daigger, N.G. Love, C.D. Filipe, Biological wastewater treatment, CRC press, 2011.

[45] J. Guo, Y. Peng, H. Huang, S. Wang, S. Ge, J. Zhang, Z. Wang, Short-and long-term effects of temperature on partial nitrification in a sequencing batch reactor treating domestic wastewater, J. Hazard. Mater. 179 (2010) 471–479.

[46] S. Sözen, D. Orhon, H.A. San, A new approach for the evaluation of the maximum specific growth rate in nitrification, Water Res. 30 (1996) 1661–1669.

[47] E. Görgün, G. Insel, N. Artan, D. Orhon, Model evaluation of temperature dependency for carbon and nitrogen removal in a full-scale activated sludge plant treating leather-tanning wastewater, J. Environ. Sci. Health Part A. 42 (2007) 747–756.

[48] S. Zhang, Y. Wang, W. He, M. Wu, M. Xing, J. Yang, N. Gao, M. Pan, Impacts of temperature and nitrifying community on nitrification kinetics in a moving-bed biofilm reactor treating polluted raw water, Chem. Eng. J. 236 (2014) 242–250.

[49] G. Munz, C. Lubello, J.A. Oleszkiewicz, Factors affecting the growth rates of ammonium and nitrite oxidizing bacteria, Chemosphere. 83 (2011) 720–725.

[50] U. Wiesmann, Biological nitrogen removal from wastewater, in: Biotechnics/Wastewater, Springer, 1994: pp. 113–154.

[51] H.-D. Park, D.R. Noguera, Evaluating the effect of dissolved oxygen on ammonia-oxidizing bacterial communities in activated sludge, Water Res. 38 (2004) 3275–3286.

[52] T. Tokutomi, Operation of a nitrite-type airlift reactor at low DO concentration, Water Sci. Technol. 49 (2004) 81–88.

[53] H.-P. Chuang, A. Ohashi, H. Imachi, M. Tandukar, H. Harada, Effective partial nitrification to nitrite by down-flow hanging sponge reactor under limited oxygen condition, Water Res. 41 (2007) 295–302.

[54] S. Wyffels, S.W.H. Van Hulle, P. Boeckx, E.I.P. Volcke, O.V. Cleemput, P.A. Vanrolleghem, W. Verstraete, Modeling and simulation of oxygen‐limited partial nitritation in a membrane‐assisted bioreactor (MBR), Biotechnol. Bioeng. 86 (2004) 531–542.

[55] E. Bock, H.-P. Koops, H. Harms, Cell biology of nitrifying bacteria, (1986).

[56] R. Van Kempen, J.W. Mulder, C.A. Uijterlinde, M.C.M. Loosdrecht, Overview: full scale experience of the SHARON® process for treatment of rejection water of digested sludge dewatering, Water Sci. Technol. 44 (2001) 145–152.

[57] H. Hafez, E. Elbeshbishy, N. Chowdhury, G. Nakhla, J. Fitzgerald, A. Van Rossum, & G. Gauld, Pushing the hydraulic retention time envelope in Modified Ludzack Ettinger systems. Chemical Engineering Journal, 163(3) (2010) 202-211.

Chapter 6

6 Acute and chronic toxicity of nickel to nitrifiers at low temperature

Chronic toxicity of nickel to nitrification of low ammonia synthetic wastewater was investigated at 10°C in two SBRs with 1 mg/L nickel dosing either from the beginning or after biomass concentration decreased to 300 mg/L. Significant nickel inhibition occurred at Ni/MLSS ratio of 2.7 mg Ni/ g MLSS. At a Ni/MLSS ratio of 4-7 mg Ni/g MLSS, the final ammonia oxidizing bacteria (AOB) activity was inhibited by 47%-58% after acclimatization. After long-term acclimatization to nickel at 10°C, high DO(~7mg/L) and SRT of 63-70 days, the μ_{max}, b and Ko of AOB and NOB were determined as 0.16 d^{-1}, 0.098 d^{-1} and 2.08 mg O_2/L, and 0.16 d^{-1}, 0.098 d^{-1} and 2.12 mg O_2/L, respectively. Acute toxicity of nickel to nitrification at 10°C, 23°C, and 35°C was evaluated by short-term batch tests. The nickel inhibition half-velocity constants based on a modified non-competitive model for nitrification at 10°C, 23°C, and 35°C were determined. Long-term SBRs operation and short-term batch tests results were consistent. Short-term nickel inhibition of nitrifying bacteria was completely reversible, as evidenced by same ammonia oxidization rate (AOR) and nitrite oxidization rate (NOR) using returned activated sludge without nickel, and with nickel inhibition for 2 hours.

6.1 Introduction

Nitrification, carried out by ammonia oxidizing bacteria (AOB) and nitrite oxidizing bacteria (NOB), is the rate-limiting process in biological nitrogen removal (BNR) process. Both AOB and NOB are autotrophs [1]. Nitrifiers grow slowly and are very sensitive to environmental conditions such as pH, dissolved oxygen (DO) concentrations, temperature, and toxic chemicals [2–4].

A variety of organic and inorganic chemical species can affect the specific growth rate of the nitrifiers [5]. The influence of heavy metals on the conventional activated sludge system has been thoroughly studied [6–10]. However, most research studied the effect of metal on organic carbon removal [11].

Nickel (Ni) is a common metal which exists at various ranges in the influents of different wastewater treatment plants. Although the typical influent nickel concentration in municipal wastewater treatment plant (MWWTP) is low (<50μg/L), still some plants receiving industrial wastes may suffer from high influent nickel concentrations, as shown by the following cases. Busetti et al. [12] reported a nickel concentration of 1-39 μg/L in the influent of Fusina (Venice, Italy) MWWTP. Carletti et al. [13] reported an influent nickel concentration of 3.5-61.7 μg/L from 5 MWWTPs in Italy. A higher influent nickel concentration range of 20.2-107.6 μg/L from the Depurbaix (Barcelona, Spain) MWWTP was reported by Teijon et al. [14]. The report of European Communities:*Pollutants in urban wastewater and sewage sludge* reported that nickel concentration in municipal wastewater ranged from 40-170 μg/L in Austria[15]. A high influent nickel concentration of up to 970 μg/L in Thessaloniki (Greece) MWWTP was reported by Karvelas et al. [16].

The three most important factors of nickel inhibition on nitrification are: 1. the sludge type i.e., either activated sludge or nitrifying culture; 2. the exposure mode, either long-term dose or short-term; and 3. the temperature [17]. Studies on nickel inhibition of nitrification are summarized in Table 6-1. The literature results are not always consistent. For example, Hu et al. [18] conducted short-term batch tests at 25^{o}C and found that AOB were more sensitive to nickel than NOB while Aslan & Sozudogru [4] conducted short-term batch tests at 35^{o}C, and observed that NOB were more affected than AOB, as evidenced by the increase in ratio of NO_2-N/NO_x-N from 0.002 to 0.3

upon addition of 4.0 mg/L of Ni^{2+}. Randall & Buth [19] operated an activated sludge system at 14, 17, and 30^{o}C and reported that nickel is more toxic to nitrifiers at low temperature. In the study of Randall & Buth [19], nickel was more toxic to NOB at 14^{o}C, and equally toxic for both AOB and NOBs at 17^{o}C and 30^{o}C. The reported nickel inhibition thresholds for nitrification are limited. You et al. [11] conducted short-term batch tests on activated sludge (1678-2133 mg MLSS/L) at room temperature and reported that the 50% inhibition concentration (IC50) for AOB is 1.2-3.0 mg Ni/ g MLSS, respectively. To date, the long-term effect of nickel on nitrification performance of nitrifying cultures at low temperature (10^{o}C) has not been studied.

Table 6-1. Summary of previous studies on nickel inhibition on nitrification

Reference	Biomass type	Biomass concentration (mg MLSS/L)	Exposure mode	Temperature	Conclusion	IC50 based on Ni concentration (mg Ni/L)	IC50 based on Ni/MLSS ratio (mg Ni/g MLSS)
[18]	Nitrifying culture	NA	Short term batch test	25°C	Nickel inhibited AOB but not NOB up to total concentrations of approximately 58.5 mg/L		
[11]	Activated sludge	1678-2133	Short term batch test	Room		AOB: 2.5-5	1.2-3.0
[20]	Activated sludge	2150	Short term batch test	Room	No inhibition occurred at 1 mg Ni/L of added; Little inhibition occurred at 5 and 10 mg Ni/L. Significant inhibition occurred at 50 mg/L.		
[19]	Activated sludge	900-3300	Long term dose	14, 17 and 30°C	Nickel is more toxic to NOB than to AOB at 14°C and equal for AOB and NOB at 17 and 30°C; Nickel is more toxic at low temperature; The toxic effects of nickel on activated sludge was a function of nickel-to-MLVSS ratio.		
[4]	Nitrifying culture	NA	Short term batch test	35 °C	No inhibition of AOB and NOB activity were observed up 0.5 mg Ni/L; NH_4-N removal efficiency decreased from 98.6% to 64.3% by increasing the inlet Ni^{2+} concentrations from 0.5 to 4.0 mg/L; NOB was more affected than AOB as evidenced by the ratio of NO_2-N/NO_x-N elevated from 0.002 to 0.3 by adding 4.0 mg/L of Ni^{2+}.		
This study	Nitrifying culture	100-350 mg/L	Long term dose	10°C	Significant acute nickel inhibition of 33% activity loss occurred at Ni/MLSS ratio of 2.7 mg Ni/g MLSS and the SBRs lost 47%-58% activity of AOB & NOB		

				at Ni/MLSS ratio of 4-7 mg Ni/g MLSS after re-acclimatization.	
Activated sludge	340-2720 mg/L	Short term batch test	10,23, and 35^{o}C	Short-term nickel inhibition was much more serious for NOB than AOB at 35^{o}C and slightly more serious for NOB than AOB at 23^{o}C. With temperature decreasing further to 10^{o}C, the inhibition was equal or less for NOB than AOB.	AOB: 5.4, 4.6, and 9.1 mg Ni/g MLSS at 10,23, and 35^{o}C NOB: 5.6, 3.5, and 2.7 mg Ni/g MLSS at 10,23, and 35^{o}C

The objectives of this study are: 1) comparison of the long-term nickel impact on the nitrification performance of nitrifying culture with or without long-term acclimatization at low temperature(10^{o}C); 2) determination of the nitrification kinetics at low temperature after long-term nickel dosing; 3) study of the acute toxicity effects of nickel to nitrification at different temperatures and; 4) assessment of the reversibility of acute nickel toxicity to nitrification.

6.2 Methodology

6.2.1 Nitrification reactors

Two SBRs with a working volume of 10 L were used in this study. The reactor height and the diameter are 30 cm and 24cm, respectively. Two pumps (Masterflex L/S, Cole-Parmer, Montreal, Canada) were used, one feeding the wastewater to the SBR and the other withdrawing the treated wastewater. Aeration was provided with an air pump (Rena Air 400, Rena Aquatic Supply, Charlotte, U.S.) through an air diffuser. The SBRs were operated at 10 ^{o}C with a water bath (PolySciences Heated Circulating Bath, 1 SD07R-20-A11B). DO was maintained high (~7 mg/L). Each cycle consisted of 20 min feed, 10 hrs 50 min mixing and aerobic reaction, 30 min settling and 20 min effluent discharge. The exchange ratio was 50%. pH was not controlled, and during each cycle pH decreased with time.

SBR1 was operated initially without nickel until the biomass concentration decreased to 300 mg MLSS/L after which nickel was dosed at 1 mg/L while SBR2 was operated with a nickel does of 1 mg/L from the beginning.

6.2.2 Synthetic Wastewater and Activated Sludge Characteristics.

The synthetic wastewater was composed of NH_4Cl (40-60 mg N/L), NaHCO3 (480-720 mg/L), KH_2PO_4 (8-12 mg P/L), $MgSO_4 \cdot 7H_2O$ (100 mg/L), $CaCl_2$ (100 mg/L), 1 ml/L water of trace elements solution I (composition in g/L as follows: EDTA 15, $ZnSO_4$ 0.43, $CoCl_2$ 0.24, $MnCl_2$ 0.63, $CuSO_4$ 0.25, Na_2MoO_4 0.22, $NiCl_2$ 0.19, Na_2SeO_4 0.21, H_3BO_3 0.01, and $NaWO_4$ 0.05), and 1 ml/L water of trace elements solution II containing $FeSO_4$ and EDTA at 5 g/L each[21]. The alkalinity to ammonia-nitrogen ratio was 7.17:1[1]. The seed sludge was return activated sludge (RAS) taken from the Greenway water pollution control plant in London, Ontario.

6.2.3 Analytical Methods.

Effluent ammonia, nitrite, and nitrate were measured using HACH methods every two days. Mixed liquid suspended solids (MLSS) concentrations in the SBR and effluent were measured in triplicates using Whatman GF/A filters (VWR International, Mississauga, Canada), in accordance with Standard Methods [22] once a week. Nickel concentrations in the influent, SBR, and effluent were measured by inductively coupled plasma optical emission spectrometry (ICP-OES) (Vista-Pro, VARIAN) with a flame temperature in a range from 6000 to 10000 K according to Standard Methods (3120) [22] after acid digestion with HNO_3 and filtration through a 0.45 μm filter paper. The pH of the filtrate was adjusted to below 2, using concentrated nitric acid (67-70 %) prior to measurement. The detection limit of Ni is 0.01 mg/L.

Dissolved oxygen and pH were measured using a dissolved oxygen meter (HACH HQ 40d) and a pH meter (VWR B10P), respectively.

6.2.4 Online batch tests

Online batch tests were conducted in SBR 2 during the last stage of the experiment at different DOs to determine the biomass ammonia oxidation rate (AOR) and nitrite oxidization rate (NOR), as suggested by [21,23]. At the end of the study, the reactor was fed with deionized water and 1mg/L of nickel, after which the SBR was mixed and aerated for several days to determine the decay coefficient (b) [21].

Kinetic modelling was carried out based on the important pertinent equations summarized below [24]:

$$Y \cdot Q \cdot (S_0 - S) - b \cdot V \cdot X - \frac{VX}{SRT} = 0 \quad \text{(Eq.6.1)}$$

$$X_{AOB} = \frac{Y_{AOB} \cdot Q \cdot (S_{0,NH} - S_{NH})}{V \cdot (b + \frac{1}{SRT})} = \frac{SRT}{HRT} \cdot \frac{Y_{AOB} \cdot (S_{0,NH} - S_{NH})}{1 + b \cdot SRT} \quad \text{(Eq.6.2)}$$

$$X_{NOB} = \frac{Y_{NOB} \cdot Q \cdot (S_{NO3} - S_{0,NO3})}{V \cdot (b + \frac{1}{SRT})} = \frac{SRT}{HRT} \cdot \frac{Y_{NOB} \cdot (S_{NO3} - S_{0,NO3})}{1 + b \cdot SRT} \quad \text{(Eq.6.3)}$$

$$q = \frac{\mu}{Y} \quad \text{(Eq.6.4)}$$

$$AOR = X_{AOB}\, q_{AOB} = q_{AOB} \cdot \frac{SRT}{HRT} \cdot \frac{Y_{AOB} \cdot (S_{0,NH} - S_{NH})}{1 + b \cdot SRT} \quad \text{(Eq.6.5)}$$

$$NOR = X_{NOB}\, q_{NOB} = q_{NOB} \cdot \frac{SRT}{HRT} \cdot \frac{Y_{NOB} \cdot (S_{NO3} - S_{0,NO3})}{1 + b \cdot SRT} \quad \text{(Eq.6.6)}$$

$$\mu_{AOB} = \frac{AOR \cdot HRT \cdot (b_{AOB} + \frac{1}{SRT})}{S_{0,NH} - S_{NH}} \quad \text{(Eq.6.7)}$$

$$\mu_{NOB} = \frac{NOR \cdot HRT \cdot (b_{AOB} + \frac{1}{SRT})}{S_{NO3} - S_{0,NO3}} \quad \text{(Eq.6.8)}$$

where b_{AOB} and b_{NOB} are endogenous decay coefficients for AOB and NOB, respectively; Y_{AOB} and Y_{NOB} are biomass yield coefficients for AOB and NOB, respectively; q_{AOB} and q_{NOB} are the maximum specific substrate utilization rates for AOB and NOB, respectively; X_{AOB} and X_{NOB} are the active AOB and NOB biomass concentrations, respectively; AOR and NOR are the ammonia oxidation rate and nitrite oxidation rate, respectively; $S_{NH}$and S_{NO2} are effluent ammonia and nitrite concentrations, respectively; $(S_{0,NH} - S_{NH})$ and $(S_{NO3} - S_{0,NO3})$ are ammonia and nitrite oxidized, respectively; and HRT is the hydraulic retention time.

In addition, the Monod model was used in this study to calculate AOR_{max} and NOR_{max} as well as the DO-half saturation concentration (*K*o), as shown below:

$$\text{AOR} = AOR_{max} \cdot \frac{DO}{DO + K_{O,AOB}} \quad \text{(Eq.6.9)}$$

$$\text{AOR} = NOR_{max} \cdot \frac{DO}{DO + K_{O,NOB}} \quad \text{(Eq.6.10)}$$

The ammonia conversion ratio (ACR) and nitrite accumulation ratio (NAR) were calculated based on influent and effluent quality as shown below in eqs 10 and 11.

$$\text{ACR} = \frac{S_{0,NH} - S_{NH}}{S_{0,NH}} \quad \text{(Eq.6.11)}$$

$$\text{NAR} = \frac{S_{NO2}}{S_{NO2} + S_{NO3}} \quad \text{(Eq.6.12)}$$

in which, $S_{0,NH}$ is influent ammonia, and S_{NH}, S_{NO2} and S_{NO3} are effluent ammonia, nitrite, and nitrate, respectively.

6.2.5 Offline batch tests

Acute nickel toxicity to nitrification was determined using offline batch tests in small beakers (500 ml) using RAS from the Greenway water pollution control plant. The design of the offline batch tests is depicted in Table 6-2. The initial ammonia concentration in the batch tests was 25-30 mgN/L with an alkalinity-to-nitrogen ratio of 7.14 mg $CaCO_3$/mg N and a constant DO of 7 mg/L. The batch tests were conducted at 10^{o}C, 23^{o}C and 35^{o}C. The objective of batches A-E was to evaluate the effect of different nickel concentrations on nitrification with the same MLSS concentration and thus batch tests A-E have the same biomass concentration (340 mg MLSS/L) while the nickel dose increased from 0 to 2.0 mg/L. The objective of batches C & F-I was to evaluate the effect of same nickel concentration on nitrification at different MLSS concentrations and therefore batch tests C & F-I have the same nickel dose (1.0 mg/L) while the biomass concentration increased from 340 to 2720 mg MLSS /L. Samples were taken with time regularly and ammonia, nitrite, and nitrate were determined by the aforementioned HACH methods.

Table 6-2. Offline batch tests design

	A	B	C	D	E	F	G	H	I
Ni concentration (mg/L)	0	0.5	1.0	1.5	2.0	1.0	1.0	1.0	1.0
MLSS concentration (mg/L)	340	340	340	340	340	680	1020	1360	2720
MLVSS concentration (mg)	260	260	260	260	260	520	780	1040	2080

6.2.6 Short-term nickel inhibition modelling

As nickel is not a substrate for nitrifying bacteria, the inhibition of nickel may potentially be modelled by non-competitive inhibition model, as shown below in Eqs.6.13-6.16[25].

$$SAOR = SAOR_{max} \cdot \frac{K_{I,Ni}}{K_{I,Ni}+Ni} \quad \text{(Eq.6.13)}$$

$$SNOR = SNOR_{max} \cdot \frac{K_{I,Ni}}{K_{I,Ni}+Ni} \quad \text{(Eq.6.14)}$$

$$\frac{1}{SAOR} = \frac{I}{SAOR_{max} \cdot K_{I,Ni}} + \frac{1}{SAOR_{max}} \quad \text{(Eq.6.15)}$$

$$\frac{1}{SNOR} = \frac{I}{SNOR_{max} \cdot K_{I,Ni}} + \frac{1}{SNOR_{max}} \quad \text{(Eq.6.16)}$$

In this study, as the toxicity of nickel is a function of Ni/MLSS ratio[19,26], a modified non-competitive inhibition model based on Ni/MLSS ratio (Eqs.6.17-6.20), was used.

$$SAOR = SAOR_{max} \cdot \frac{K_{I,Ni/MLSS}}{K_{I,Ni/MLSS}+Ni/MLSS} \quad \text{(Eq.6.17)}$$

$$SNOR = SNOR_{max} \cdot \frac{K_{I,Ni/MLSS}}{K_{I,Ni/MLSS}+Ni/MLSS} \quad \text{(Eq.6.18)}$$

$$\frac{1}{SAOR} = \frac{I}{SAOR_{max} \cdot K_{I,Ni/MLSS}} + \frac{1}{SAOR_{max}} \quad \text{(Eq.6.19)}$$

$$\frac{1}{SNOR} = \frac{I}{SNOR_{max} \cdot K_{I,Ni/MLSS}} + \frac{1}{SNOR_{max}} \quad \text{(Eq.6.20)}$$

SAOR and SNOR are specific ammonia oxidation rate and specific nitrite oxidation rate (mg N/g MLSS-hr), $K_{I,Ni}$ is the half-velocity inhibition nickel concentration (mg Ni/L), and $K_{I,Ni/MLSS}$ is the half-velocity inhibition constant based on Ni/MLSS ratio (mg Ni/g MLSS).

6.2.7 Toxicity Reversibility tests

The reversibility of the acute nickel toxicity was investigated through offline batch tests in 500 ml beakers. The batch tests were conducted at 23ºC. RAS was taken from the Greenway water pollution control plant in London, Ontario. Batch tests A, B and C had the same biomass concentration (340 mg MLSS/L). The initial ammonia concentration was around 26 mg N/L with an alkalinity-to-nitrogen ratio of 7.14 mg $CaCO_3$/mg N. In batch test A, nitrification was conducted without nickel. In batch test B, the RAS was first inhibited by nickel dose of 1 mg/L for 2hrs, after which the RAS was washed, resuspended in distilled water, and tested for nitrification activity. In batch test C, nitrification was conducted with 1 mg/L of nickel. Samples were taken every two hours and ammonia, nitrite, and nitrate were determined by aforementioned HACH methods.

6.3 Results and Discussion

6.3.1 SBR performance

Table 6-3 summarizes the performance of the two SBRs. Figure 1A shows the nitrification performance for the SBR 6-1. The operation of SBR 1 can be divided into two phases, that is, phase 1 from day 0 to day 94 with no nickel addition, and phase 2 from day 95 to day 137 with 1.0 mg/L of nickel addition. After a quick acclimatization period (<10d), relatively stable effluent quality was observed during phase 1. The average effluent ammonia, nitrite, and nitrate concentrations from day 66 to day 96 were 8.3±3.0 mg N/L, 1.4±0.6 mg N/L and 30.2±2.9 mg N/L, respectively. The stable biomass concentration of 280±14 mg MLSS/L and the aforementioned stable effluent quality indicated good nitrifying culture. AOBs were not able to convert all the ammonia, due to the low activity

of AOB at low temperature (10^{o}C). The average ACR and NAR were 79.1±7.5% and 4.5±1.8%, respectively. Due to the low temperature (10^{o}C) and high DO (~7.0 mg/L), NOB dominated the system and full nitrification was achieved. A significant drop of AOB and NOB activity was observed with effluent of 28.7 mg NH_4-N/L, 0.6 mg NO_2-N/L and 10.7 mg NO_3-N/L after adding nickel on day 95. In the following week, the performance deteriorated even further with effluent NH_4-N, NO_2-N and NO_3-N concentrations of 33.6, 0.3 and 6.1 mg N/L on day 104, respectively. After day 104, acclimatization of nitrifiers was observed and the effluent stabilized at 26.6±3.3 mg NH_4-N/L, 0.4±0.4 mg NO_2-N/L, and 13.0±3.1 mg NO_3-N/L. Compared with phase 1, the final average activity of AOB dropped by 58% due to nickel addition.

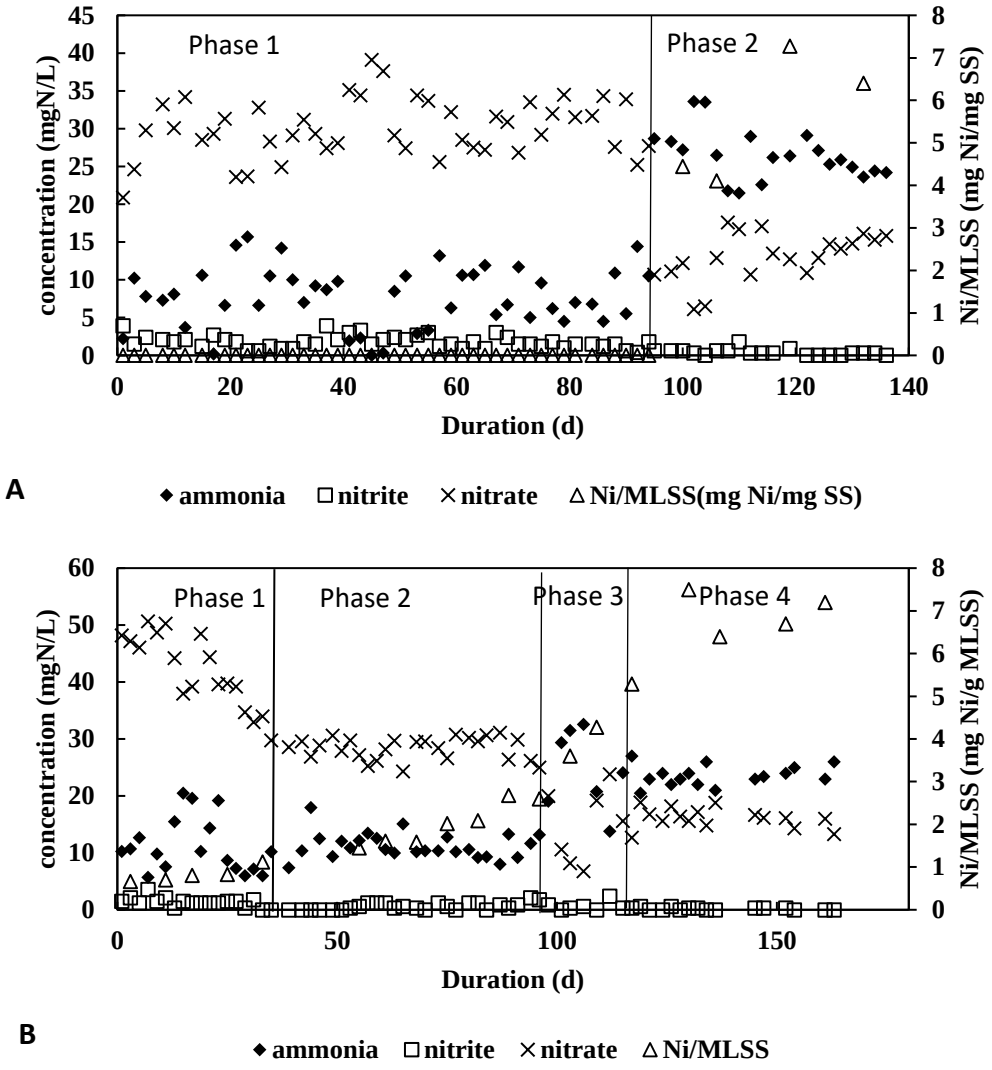

Figure 6-1. Effluent ammonia, nitrite, and nitrate concentrations and Ni/MLSS ratio of SBR 1 (A) and SBR 2 (B).

Table 6-3. Performance of the SBRs

SBR No.	Phase	Ammonia (mg N/L)	Nitrite (mg N/L)	Nitrate (mg N/L)	AOB activity loss (%) vs SBR1 phase 1
1	1	8.3±3.0	1.4±0.6	30.2±2.9	0
	2	26.6±3.3	0.4±0.4	13.0±3.1	58
2	2	11.2±2.2	0.6±0.6	28.4±1.9	8
	4	23.0±2.8	0.3±0.5	16.5±2.4	47

Figure 6-1B shows the nitrification performance for the SBR 2 with 1.0 mg/L of nickel addition from the start. The operation of SBR 2 can be divided into four phases, that is, phase 1 from day 0 to day 34 as start-up period, phase 2 from day 35 to day 95 as steady-state period, phase 3 from day 96 to day 112 as unstable period, and phase 4 from day 113 to day 164 as acclimatization period. The initial biomass could convert 40-50 mg N/L of ammonia, which is higher than that of 30-40 mg N/L in SBR1, due to higher initial RAS concentration (1.4g/L versus 1.0 g/L). After around 1 month, relatively stable effluent with constant ammonia, nitrite, and nitrate was observed for a long time (phase 2). The average effluent ammonia, nitrite, and nitrate concentrations from day 35 to day 96 were 11.2±2.2 mg N/L, 0.6±0.6 mg N/L and 28.4±1.9 mg N/L. The average ACR and NAR were 72.1±4.9% and 2.1±2.1%, respectively.

Ni/MLSS ratio is one of the major parameters for nickel inhibition. During Phases 1 and 2, the Ni/MLSS ratio was below 2.6 mg Ni/g MLSS, and no obvious nickel inhibition was observed. On day 98, when Ni/MLSS reached 2.7 mg Ni/g MLSS, significant drop of nitrifiers' activity was observed with effluent of 19.1 mg NH_4-N/L, 0.9 mg NO_2-N/L and 20 mg NO_3-N/L. Thus, AOB and NOB activity dropped by 34% relative to SBR1 phase 1.

In the following week, the performance deteriorated with effluent NH_4-N, NO_2-N and NO_3-N concentrations of 32.6, 0.6 and 6.8 mgN/L on day 106, respectively. After day 112, the biomass acclimatized, and the effluent stabilized at 23.0±2.8 mg NH_4-N/L, 0.3±0.5 mg NO_2-N/L, and 16.5±2.4 mg NO_3-N/L. Compared with SBR1 phase 1, the final average activity of AOB dropped by 47%.

One-way ANOVA analysis suggested that the effluent quality data are significantly different at the 95% confidence limit for SBR 1 phase 1 and SBR 2 phase 2, and SBR 1 phase 2 and SBR 2 phase 4.

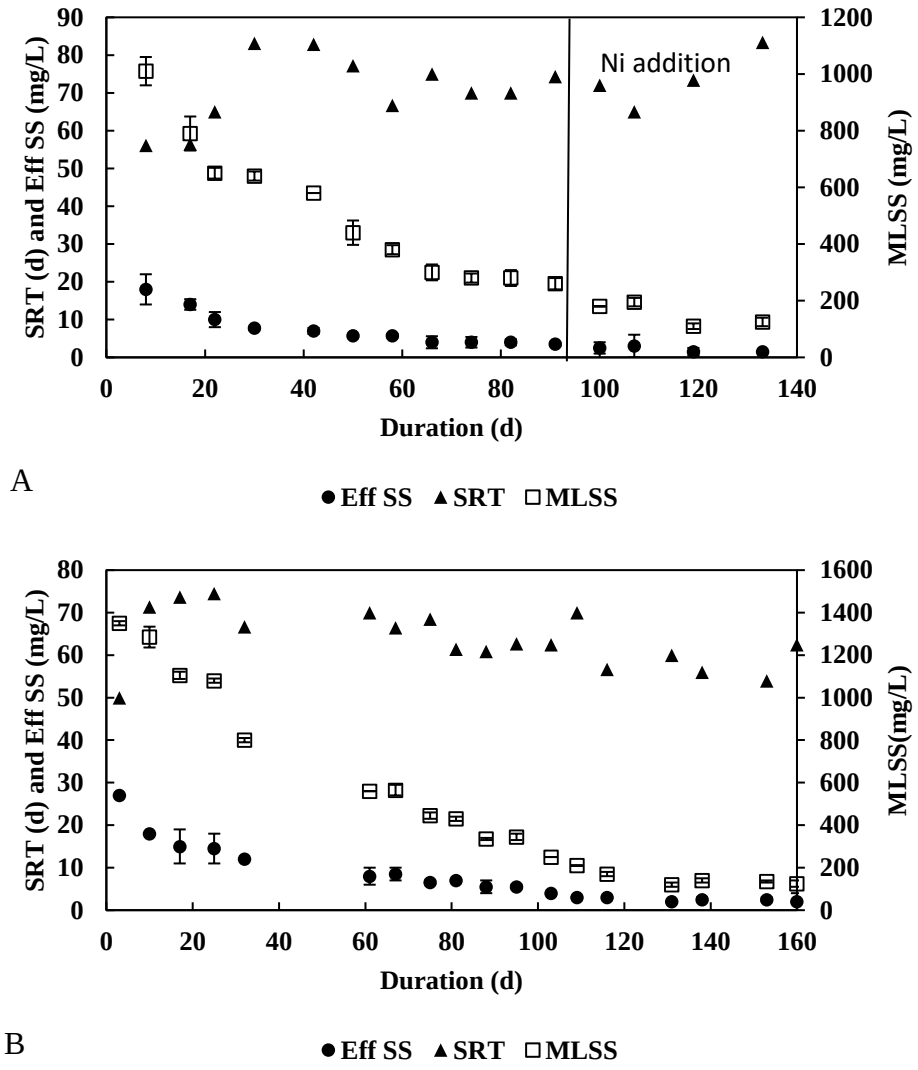

Figure 6-2. MLSS, effluent SS, and SRTs of SBR 1 (A) and SBR 2 (B).

Figures 6-2A and 6-2B show the mixed liquor suspended solids (MLSS), effluent suspended solids (SS), and SRTs for SBRs 1 and 2, respectively. No sludge wastage was carried out and the SRTs were estimated based on reactor and effluent biomass. In this study, both SBRs were operated at long SRTs. The average, maximum, and minimum SRTs of SBR 1 were 71d, 83 d, and 56 d, respectively. The average, maximum and minimum SRTs of SBR 2 were 64d, 75 d, and 50 d, respectively.

The initial inoculum concentrations were around 1.0 g SS/L and 1.4g SS/L for SBR 1 and SBR 2, respectively, with a volatile fraction of 77%. MLSS decreased with time for both SBRs due to decay of heterotrophic bacteria as there was no COD in the influent, which is similar to our previous observations [21,24]. The MLSS concentration in SBR 1 between days 66, and day 91 was 260-300 mg/L. After nickel dosing at 1 mg/L on day 95 and acclimatization, the MLSS in SBR 1 dropped to 100-120 mg/L between days 120 and 140. The MLSS concentration in SBR 2 was 125-140 mg/L between days 130 and 160. The effluent TSS concentration in SBR1 decreased from an initial value of 18 mg/L to stabilize at 3.9±0.2 mg/L on days 66-91 before nickel addition, and decreased further after nickel addition to 2.1±0.6 mg/L on days 100-133. Similarly, the effluent TSS concentration in SBR2 decreased from an initial value of 27 mg/L to 2.5±0.4 mg/L on days 109-160.

6.3.2 Online Batch Tests.

Online batch tests were conducted in SBR 2 at three different DO levels (3.0, 5.0 and 7.4 mg/L, respectively) between days 120, and 140 with nickel dosing, and the results are shown in Figure 6-3. The Ni/MLSS ratio (Figures 1A & 1B) in SBR 2 between days 120 and 140 ranged from 5.2-7.5 mg Ni/g MLSS. At the ambient ammonia concentrations of 17-26 mgN/L, nitrite concentration of 0.2-0.6 mg N/L, and the pH of 7.0-7.5, the free ammonia (FA) concentration was 0.04-0.3 mg/L while free nitrous acid (FNA) was almost 0 mg/L. Thus, free ammonia and FNA inhibition did not occur since free ammonia and FNA concentrations of 1.0 and 0.1 mg N/L did not inhibit AOB and NOB in previous studies [21]. Alkalinity was sufficient as the influent alkalinity-to-ammonia ratio was 7.14 mg $CaCO_3$/mg NH_4-N while around 13-16 mg NO_3-N/L accumulated in the effluent.

Influent alkalinity was about 330 mg $CaCO_3$/L, and effluent alkalinity was around 130 to 170 mg$CaCO_3$/L, with around 160 to 200 mg $CaCO_3$/L consumed.

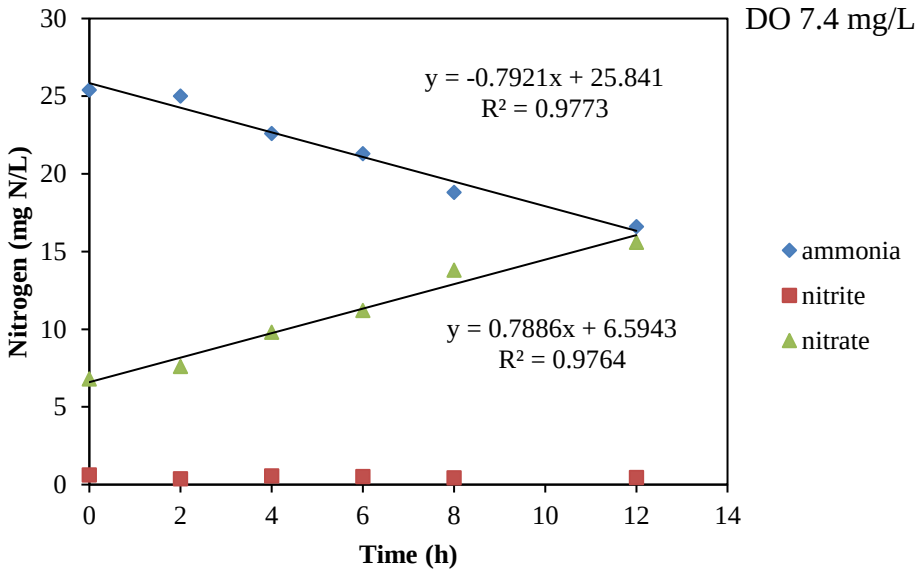

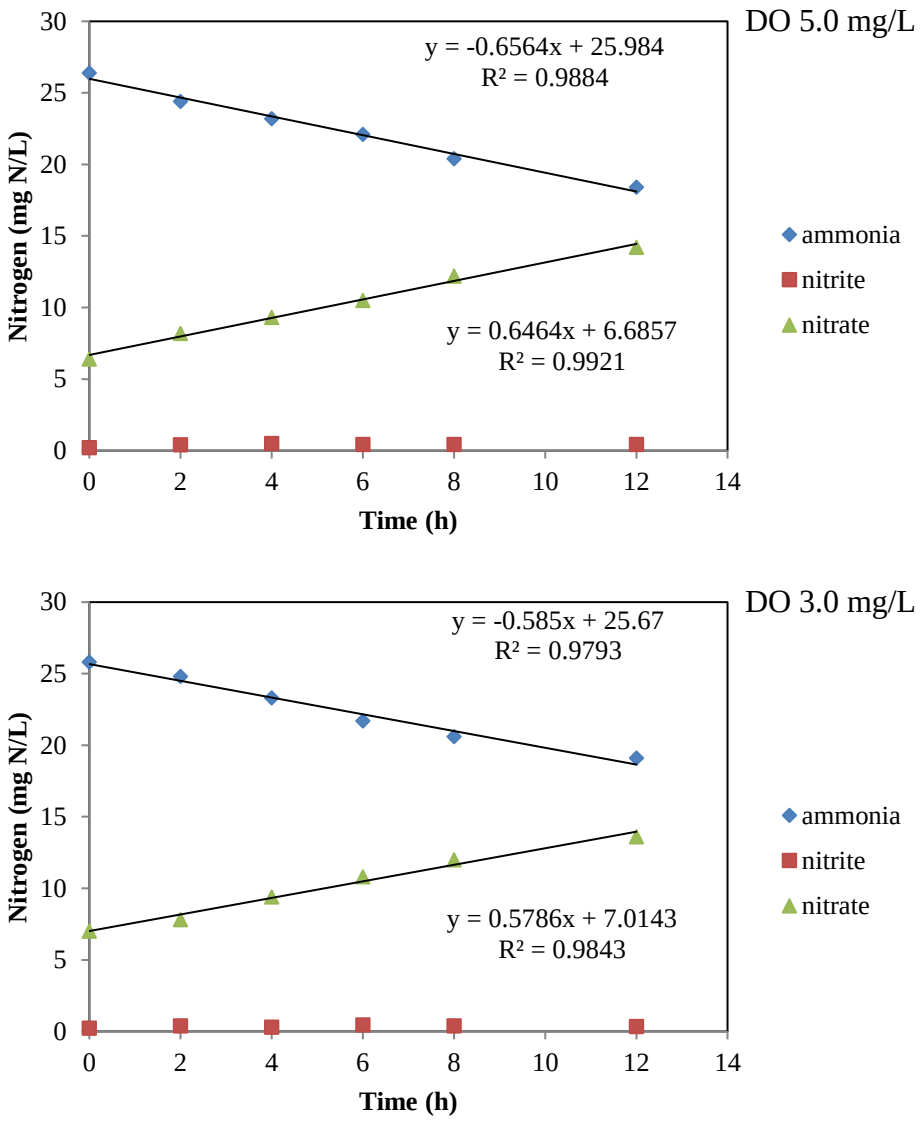

Figure 6-3. Online batch tests at different DOs in SBR 2

The AOR at DOs of 7.4, 5.0, and 3.0 mg/L were 0.79, 0.66, and 0.59 mgN/L-hr, respectively. The AOR at a DO of 5.2 mg/L was 1.7 mgN/L-hr at 14^{o}C without nickel inhibition [24]. Considering a temperature coefficient of 1.072 for AOB [1], the estimated AOR without nickel inhibition at DO of 5.2 mg/L at 10^{o}C is 1.3 mgN/L-hr. Thus, the AOR value of 0.7 mgN/L-hr at DO of 5.0 mg/L observed here with nickel inhibition suggests

about 50% inhibition. Based on the AORs at different DOs, the estimated AOR_{max} and $K_{O,AOB}$, using equation 9, were 0.98 mgN/L-hr and 2.08 mg O_2/L, respectively. The NOR at DOs of 7.4, 5.0, and 3.0 mg/L were 0.79, 0.65, and 0.58 mgN/L-hr, respectively. Based on the NORs at different DOs, the estimated NOR_{max} and $K_{O,NOB}$, using equation 9, were 0.98 mgN/L-hr and 2.12 mg O_2/L, respectively.

In order to determine the decay coefficient, the sludge was starved for 12 d after day 160 with aeration and biomass concentration was measured every two to three days, as shown in Figure 6-4. Based on the data, the decay coefficient (b) of nitrifiers was calculated as 0.098 d^{-1} at 10ºC. The reported b value at 14ºC was in the range of 0.035-0.13 d^{-1} with a temperature coefficient of 1.029[1,24]. Thus, the b value at 10ºC is estimated to be in the range of 0.031-0.115 d^{-1}, i.e. the b value of 0.098 d^{-1} reported here is well within the range.

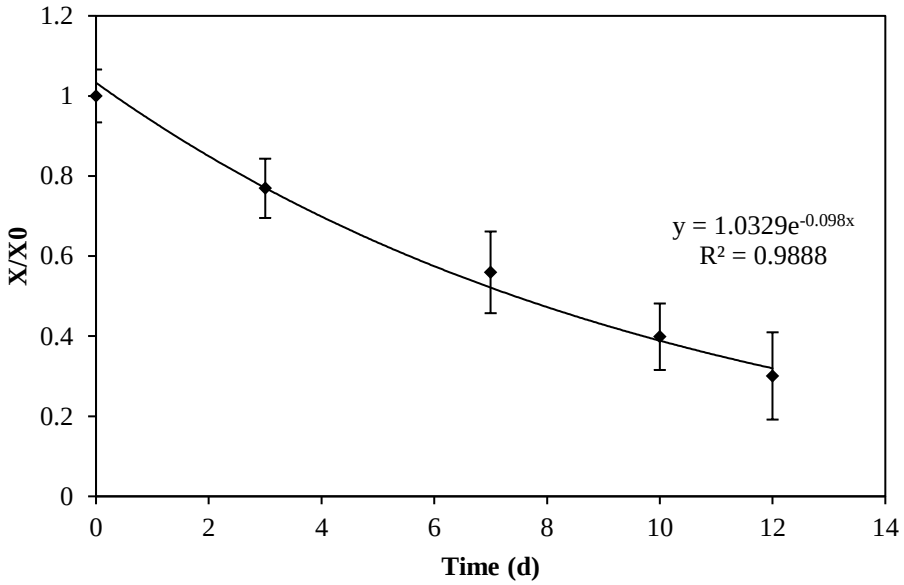

Figure 6-4. Evolution of biomass concentration during starvation test.

Thus, based on eq7, using the average effluent concentrations of 23.0 mg NH_4-N/L, 0.3 mg NO_2-N/L, and 16.5 mg NO_3-N/L in SBR 2 between day 112-140 (Table 3), and AOR_{max} of 0.98 mgN/L-hr, the maximum growth rate of AOB ($\mu_{max,AOB}$) at 10°C was 0.16 d^{-1} with nickel inhibition. The reported $\mu_{max,AOB}$ at 14°C ranges from 0.13-0.99 d^{-1} with a median value of 0.47 d^{-1} [24]. The typical temperature coefficient for $\mu_{max,AOB}$ is 1.072 [1]. Thus, the estimated $\mu_{max,AOB}$ at 10°C range from 0.10 to 0.75 d^{-1}. The $\mu_{max,AOB}$ value of 0.16 d^{-1} falls within the aforementioned range, albeit much lower than the 0.35 d^{-1} based on the median without inhibition. Based on Eq.6.8, using the average effluent concentrations of 23.0 mg NH_4-N/L, 0.3 mg NO_2-N/L, and 16.5 mg NO_3-N/L in SBR 2 between day 112-140 (Table 3), and and AOR_{max} of 0.98 mgN/L-hr, the maximum growth rate of NOB ($\mu_{max,NOB}$) at 10°C was 0.16 d^{-1} with nickel inhibition.

6.3.3 Offline Batch Acute Toxicity Tests.

The offline batch test results at 10°C, 23°C, and 35°C are summarized below in Figure 6-5, with the detailed results shown in Appendix B Figures B6-(1-3). The maximum SAOR at 10°C, 23°C, and 35°C were 1.03, 4.97, and 9.63 mg N/g MLSS-hr, respectively. The maximum SNOR at 10°C, 23°C, and 35°C were 0.96, 4.32 and 6.46 mg N/g MLSS-hr. The temperature coefficients (θ) for AOBs between 10°C and 23°C and between 23°C and 35°C were 1.13 and 1.056, while those for NOB between 10 °C and 23°C and between 23°C and 35°C were 1.123 and 1.034. The reported θ value for AOB ranged between 1.023 to 1.172 [1,27–30]. The θ value of 1.13 between 10°C and 23°C and 1.056 between 23 and 35°C are well within the aforementioned range. In the study of Guo et al. [28], the θ value was 1.172 at 5-20°C with activation energy (E_a) of 111.5 kJ mol^{-1}, and 1.062 at 20-35°C with E_a of 42.0 kJ mol^{-1}, respectively. Thus, the θ value was lower at higher temperature ranges,

which is in agreement with this study. Compared with AOBs, there are fewer studies on the temperature dependency of kinetic coefficients for NOBs. However, the general consensus is that the θ values for NOB are lower than those for AOB [27], consistent with the findings of this study.

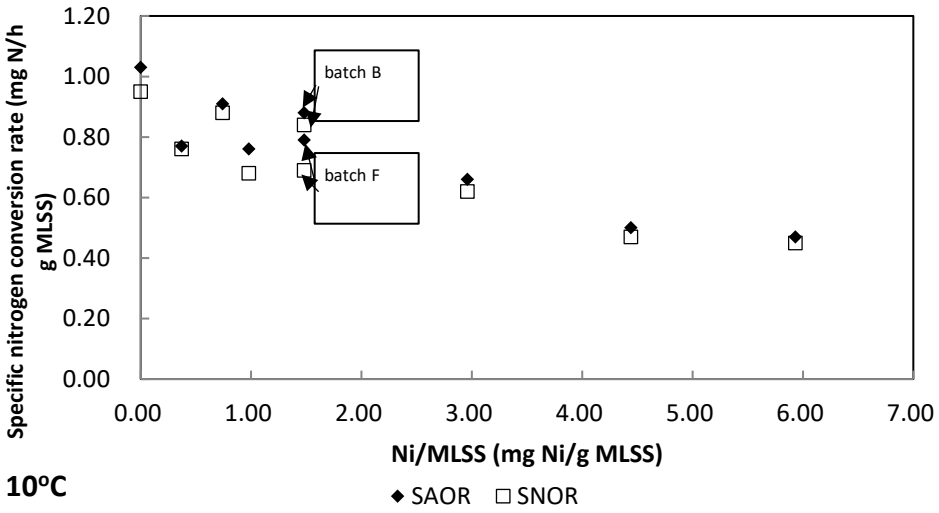

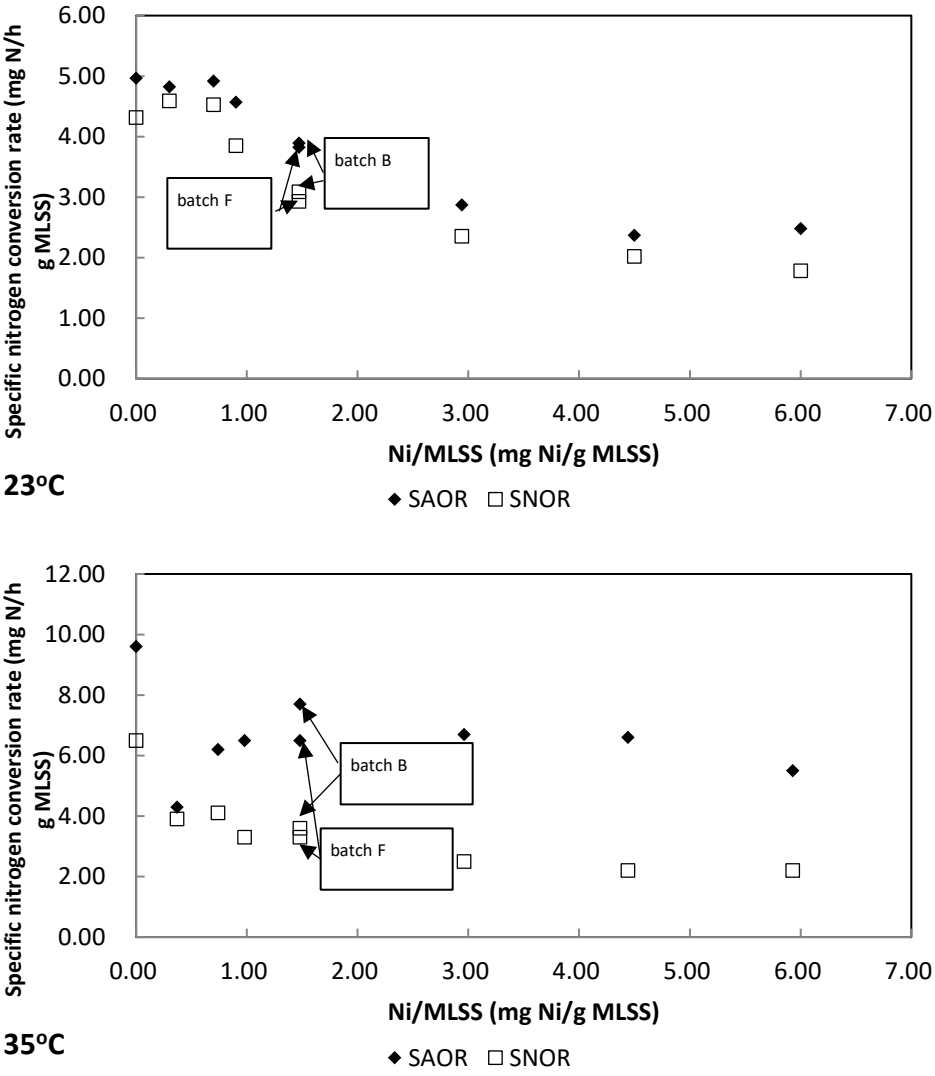

Figure 6-5. Specific ammonia oxidation rate (SAOR) and specific nitrite oxidation rate (SNOR) versus Ni/MLSS at 10°C, 23°C and 35°C

At 10°C, nickel inhibition was observed at low Ni/MLSS ratio. However, up to a Ni/MLSS ratio of 1.5 mg Ni/g MLSS, slight inhibition (<22%) for AOB and NOB was observed. With Ni/MLSS ratio increasing to 3.0 mg Ni/g MLSS, both AOB and NOB activities were inhibited by 36%. A Ni/MLSS ratio of 4.4 mg Ni/g MLSS resulted in 51% inhibition of both AOB and NOB activities. At 10°C the SNOR was almost the same as SAOR. In

conclusion, at 10°C, the acute nickel toxicity is predominantly to AOB, with equal or less inhibition for NOB. At 23°C, no nickel inhibition was observed at Ni/MLSS ratio lower than 0.7 mg Ni/g MLSS. 24% of AOB activity inhibition and 33% of NOB activity were observed at Ni/MLSS ratio of 1.5 mg Ni/g MLSS. With Ni/MLSS ratio increasing to 3.0 mg Ni/g MLSS, AOB and NOB activity were inhibited by 42% and 47%, respectively. A Ni/MLSS ratio of 4.4 mg Ni/g MLSS resulted in over 52% inhibition of AOB activity and 56% inhibition of NOB activity. In conclusion, at 23°C, the acute nickel toxicity was more serious for NOB rather than AOB. At 35°C, unlike at 10°C and 23°C, the SNOR is much lower than SAOR. Additionally, the nitrifying bacteria may have experienced difficulties acclimatizing to the short-term temperature shocks. 20%-32% AOB inhibition and 45%-49% NOB inhibition were observed at a Ni/MLSS ratio of 1.5 mg Ni/g MLSS. With Ni/MLSS ratio increasing to 3.0 mg Ni/g MLSS, AOB and NOB activity were inhibited by 30% and 61%, respectively. A Ni/MLSS ratio of 4.4 mg Ni/g MLSS resulted in over 32% inhibition of AOB activity and 66% inhibition of NOB activity. In conclusion, at 35°C, the acute nickel toxicity was much more serious for NOB rather than AOB.

To summarize, the acute nickel toxicity was much more serious for NOB than AOB at 35°C and slightly more serious for NOB than AOB at 23°C. With temperature decreasing further to 10°C, the inhibition was equal or less for NOB than AOB. The results of this study are in agreement with Aslan & Sozudogru [4] who also observed that NOB were more affected than AOB at 35°C in short-term batch tests.

To further describe the short-term nickel inhibition on AOB and NOB activity, non-competitive inhibition model and modified non-competitive inhibition model were assessed. The half-velocity inhibition constant, which is equal to the IC50, was determined

through linearization of equations 6.13-6.16, as illustrated in Figures 6-6 and 6-7 for non-competitive inhibition model and modified non-competitive inhibition model, respectively. Generally, the curve based on Ni/MLSS ratio (Figure 6-7) fitted the experimental data better as evidenced by the higher R^2 values compared to Figure 6, suggesting that the modified non-competitive inhibition model is better than non-competitive inhibition model in terms of accuracy.

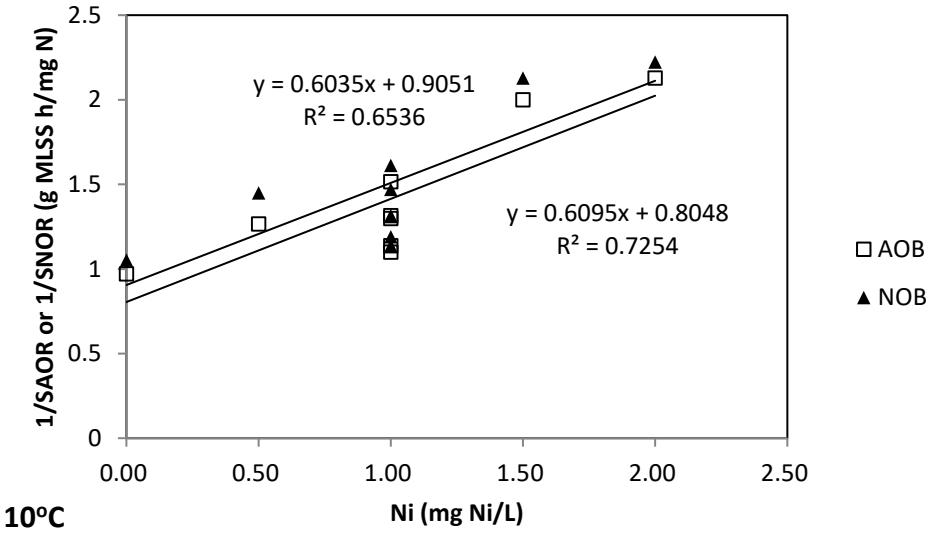

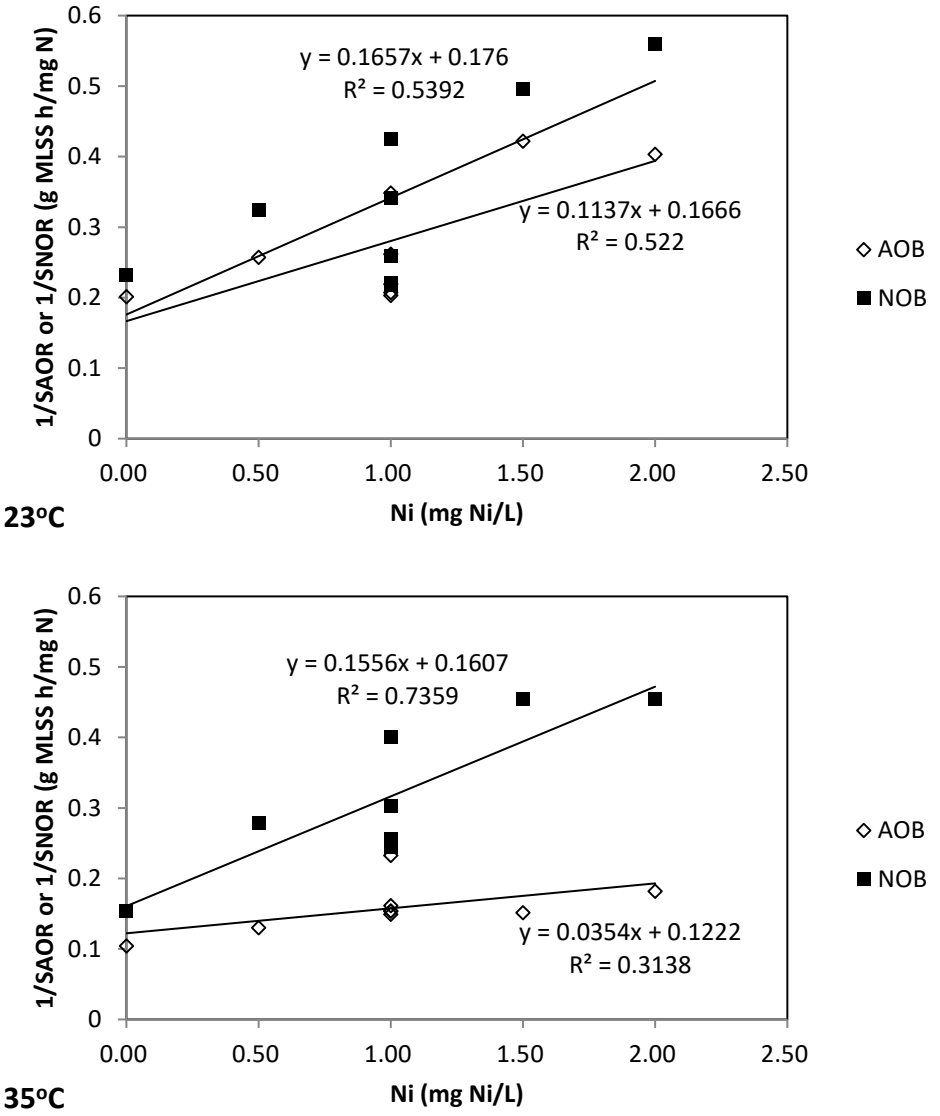

Figure 6-6. 1/SAOR and 1/SNOR versus Ni at 10ºC, 23ºC and 35ºC

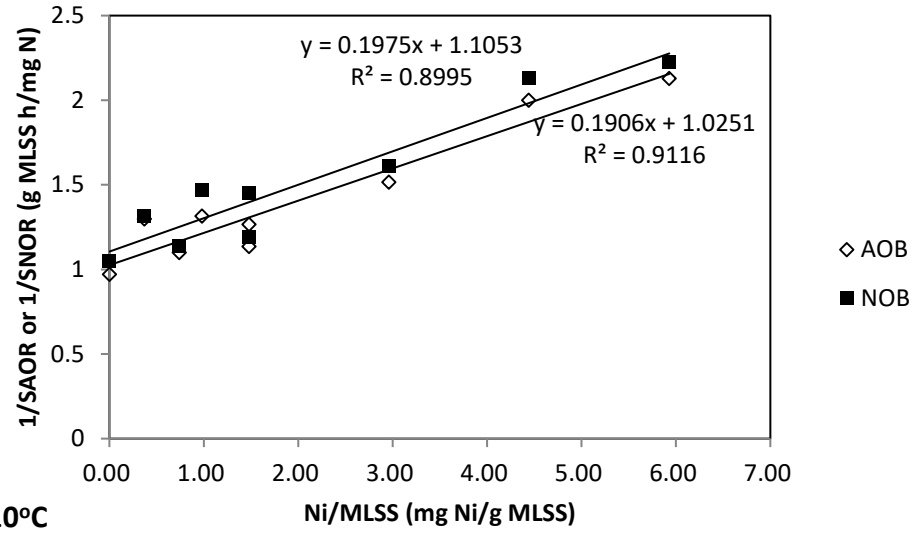
y = 0.1975x + 1.1053
R² = 0.8995
y = 0.1906x + 1.0251
R² = 0.9116
1/SAOR or 1/SNOR (g MLSS h/mg N)
Ni/MLSS (mg Ni/g MLSS)
AOB
NOB

10°C

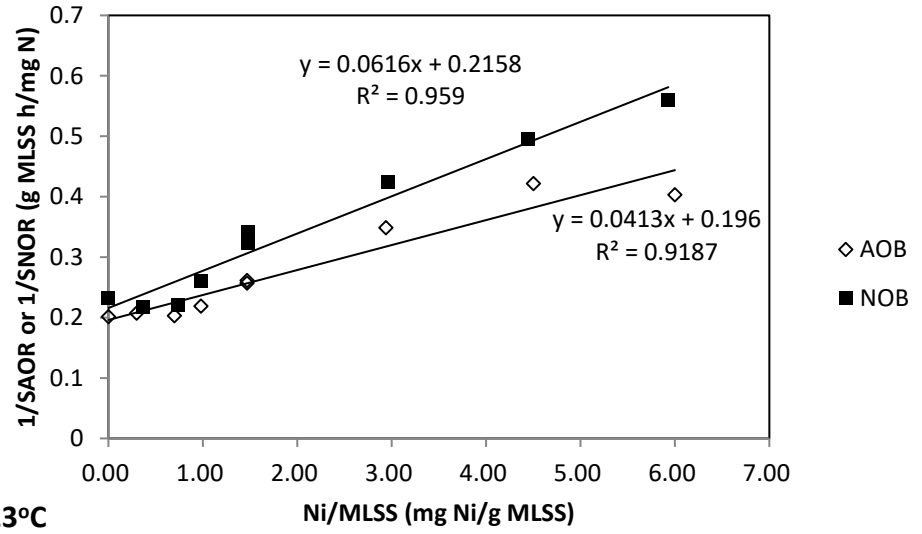
y = 0.0616x + 0.2158
R² = 0.959
y = 0.0413x + 0.196
R² = 0.9187
1/SAOR or 1/SNOR (g MLSS h/mg N)
Ni/MLSS (mg Ni/g MLSS)
AOB
NOB

23°C

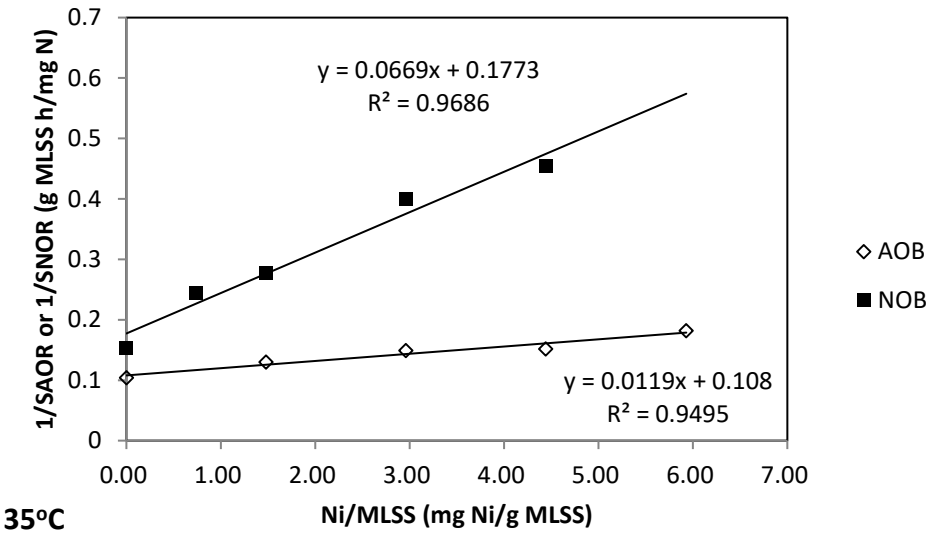

Figure 6-7. 1/SAOR and 1/SNOR versus Ni/MLSS at 10ºC, 23ºC and 35ºC

Table 6-4. Nickel inhibition constant for AOB and NOB at 10 ºC, 23 ºC and 35ºC

Bacteria species	Temperature (ºC)	Maximum SAOR or SNOR (mg N/g MLSS-hr)	$K_{I,Ni}$ (mg Ni/g MLSS)
AOB	10	1.0	5.4
	23	5.2	4.6
	35	9.3	9.1
NOB	10	0.9	5.6
	23	4.6	3.5
	35	5.7	2.7

Based on Figure 6-7, the half-velocity inhibition constants based on Ni/MLSS ratio were calculated by equations 19 and 20, and are presented in Table 6-4. The Ni/MLSS-ratio-based nickel half-velocity inhibition constant ($K_{I,Ni/MLSS}$) for AOB at 10ºC, 23ºC and 35ºC were 5.4, 4.6, and 9.1 mg Ni/g MLSS, respectively. The Ni/MLSS-ratio-based nickel half-

velocity inhibition constant ($K_{I,Ni/MLSS}$) for NOB at 10°C, 23°C and 35°C were 5.6, 3.5 and 2.7 mg Ni/g MLSS, respectively. Thus, nickel inhibition seems more serious for AOB at 10°C and 23°C than at 35°C, while the nickel inhibition for NOB increased with temperature. By far, there are very limited studies on temperature effect on nitrification. Randall & Buth [19] operated an activated sludge system at 14 °C, 17 °C, and 30°C and reported that both AOBs and NOBs are more tolerate to nickel inhibition at higher temperatures after acclimatization. Both the IC50 for AOB and NOB based on Ni/MLSS ratio at 14 °C, 17 °C and 30°C were >0.47, 1.6-5.0, and 1.9-5.6 mg Ni/g MLSS [19]. You et al. [11] reported an IC50 for AOB of 1.2-3.0 mg Ni/ g MLSS at room temperature, which is lower than the IC50 for AOB of 4.6 mg Ni/g MLSS in this study.

6.3.4 Reversibility of acute nickel toxicity

The reversibility of acute nickel toxicity was evaluated by offline batch tests as mentioned above. The results of offline batch tests are illustrated in Table 6-5. Based on Table 6-5, acute nickel toxicity to nitrifying bacteria is reversible.

Table 6-5. Offline reversibility batch tests results

Test No.	AOR (mg N/L-hr)	NOR (mg N/L-hr)
A	1.7	1.5
B	1.6	1.4
C	1.0	0.8

6.3.5 Comparison of chronic and acute toxicity

In short-term batch tests, the Greenway biomass (6.5 g/L) was diluted to 340 mg SS/L to 2720 mg SS/L, as can be seen from Figure 5, at 10°C, the nickel inhibition of AOB was 9%-12% at Ni/MLSS ratio below 1.5 mg Ni/g MLSS. In SBR 2, during phase 2, the

Ni/MLSS ratio was mostly between 1.0-2.0 mg Ni/g MLSS with an activity drop of 8.3% compared with SBR 1 phase 1, which agrees with the short-term batch tests. In addition, a significant drop of AOB activity (33%) was observed in short-term batch tests at Ni/MLSS ratio of 2.7 mg Ni/g MLSS. In SBR 2, on day 98, when Ni/MLSS reached 2.7 mg Ni/g MLSS, significant drop of AOB and NOB activity was observed with effluent of 19.1 mg NH_4-N/L, 0.9 mg NO_2-N/L and 20 mg NO_3-N/L. Compared with SBR 1 phase 1, nitrifying bacteria dropped by 34%, which corroborates the short-term batch test results. Besides, based on Figure 5, AOB activity dropped by 43%-57% in the acute toxicity test at 10°C at Ni/MLSS ratio of 4-7 mg Ni/g MLSS, which is in agreement with the activity loss of 47% in SBR 2, during phase 4 and 58% in SBR 1 during phase 2(Table 3). In summary, the results of the long-term SBRs operation and short-term batch tests were consistent.

6.4 Conclusion

1) Upon comparing the performances of SBR 1(late Ni addition) and SBR 2(Ni addition during start-up), it appears that after acclimatization, AOB activity dropped by 47% in SBR 2 and 58% in SBR1 at Ni/MLSS ratio of 4-7 mg Ni/g MLSS, indicating that after long-term acclimatization since the start, nitrifiers are more tolerant to nickel inhibition at 10°C.

2) After long-term acclimatization to nickel dose at 10°C and high DO and SRT, the $\mu_{max,AOB}$, b and Ko of AOB in SBR 2 were determined as 0.16 d^{-1}, 0.098 d^{-1} and 2.08 mg O_2/L, respectively.

3) A modified non-competitive nickel inhibition model using Ni/MLSS was established for AOB and NOB at 10°C, 23°C and 35°C based on short-term offline batch tests results.

4) The nickel inhibition constant ($K_{I,Ni}$) for AOB and NOB based on Ni/MLSS ratio at 10°C, 23°C and 35°C are 5.4 and 5.6 mg Ni/g MLSS, 4.6 and 3.5 mg Ni/g MLSS, and 9.1 and

2.7 mg Ni/g MLSS, respectively.

5) Long-term SBRs operation and short-term batch tests inhibition results with respect to extent of inhibition and corresponding Ni/MLSS ratio were consistent.

6) Short-term nickel inhibition of nitrifying bacteria was reversible.

6.5 Acknowledgments

This work was supported by the Natural Sciences and Engineering Research Council of Canada (CRDPJ 458990-13).

6.6 Reference

[1] E. Metcalf, M. Eddy, Wastewater engineering: treatment and Resource recovery, Mic Graw-Hill USA. (2014).

[2] S. Ge, S. Wang, X. Yang, S. Qiu, B. Li, Y. Peng, Detection of nitrifiers and evaluation of partial nitrification for wastewater treatment: a review, Chemosphere. 140 (2015) 85–98.

[3] M. Soliman, A. Eldyasti, Ammonia-Oxidizing Bacteria (AOB): opportunities and applications—a review, Rev. Environ. Sci. Biotechnol. (2018) 1–37.

[4] S. Aslan, O. Sozudogru, Individual and combined effects of nickel and copper on nitrification organisms, Ecol. Eng. 99 (2017) 126–133.

[5] D.J. Blum, R. Speece, A database of chemical toxicity to environmental bacteria and its use in interspecies comparisons and correlations, Res. J. Water Pollut. Control Fed. (1991) 198–207.

[6] F.B. Dilek, C.F. Gökçay, Microbiology of activated sludge treating wastewater containing Ni (II) and Cr (VI), Water Sci. Technol. 34 (1996) 183–191.

[7] A.S. Stasinakis, D. Mamais, N.S. Thomaidis, T.D. Lekkas, Effect of chromium (VI) on bacterial kinetics of heterotrophic biomass of activated sludge, Water Res. 36 (2002) 3341–3349.

[8] L. Cheng, X. Li, R. Jiang, C. Wang, H. Yin, Effects of Cr (VI) on the performance and kinetics of the activated sludge process, Bioresour. Technol. 102 (2011) 797–804.

[9] G.R. Hernandez-Martinez, D. Ortiz-Alvarez, M. Perez-Roa, N.A. Urbina-Suarez, F. Thalasso, Multiparameter analysis of activated sludge inhibition by nickel, cadmium, and cobalt, J. Hazard. Mater. 351 (2018) 63–70.

[10] L. Yuan, W. Zhi, Y. Liu, S. Karyala, P.J. Vikesland, X. Chen, H. Zhang, Lead toxicity to the performance, viability, and community composition of activated sludge microorganisms, Environ. Sci. Technol. 49 (2015) 824–830.

[11] S.-J. You, Y.-P. Tsai, R.-Y. Huang, Effect of heavy metals on nitrification performance in different activated sludge processes, J. Hazard. Mater. 165 (2009) 987–994.

[12] F. Busetti, S. Badoer, M. Cuomo, B. Rubino, P. Traverso, Occurrence and removal of potentially toxic metals and heavy metals in the wastewater treatment plant of Fusina (Venice, Italy), Ind. Eng. Chem. Res. 44 (2005) 9264–9272.

[13] G. Carletti, F. Fatone, D. Bolzonella, F. Cecchi, Occurrence and fate of heavy metals in large wastewater treatment plants treating municipal and industrial wastewaters, Water Sci. Technol. 57 (2008) 1329–1336.

[14] G. Teijon, L. Candela, K. Tamoh, A. Molina-Díaz, A. Fernández-Alba, Occurrence of emerging contaminants, priority substances (2008/105/CE) and heavy metals in treated wastewater and groundwater at Depurbaix facility (Barcelona, Spain), Sci. Total Environ. 408 (2010) 3584–3595.

[15] European Communities. Pollutants in urban wastewater and sewage sludge;, Office for Official Publications of the European Communities, Luxembourg, 2001.

[16] M. Karvelas, A. Katsoyiannis, C. Samara, Occurrence and fate of heavy metals in the wastewater treatment process, Chemosphere. 53 (2003) 1201–1210.

[17] X. Li, V. Kapoor, C. Impelliteri, K. Chandran, J.W.S. Domingo, Measuring nitrification inhibition by metals in wastewater treatment systems: current state of science and fundamental research needs, Crit. Rev. Environ. Sci. Technol. 46 (2016) 249–289.

[18] Z. Hu, K. Chandran, D. Grasso, B.F. Smets, Comparison of nitrification inhibition by metals in batch and continuous flow reactors, Water Res. 38 (2004) 3949–3959.

[19] C. Randall, D. Buth, Nitrite build-up in activated sludge resulting from combined temperature and toxicity effects, J. Water Pollut. Control Fed. (1984) 1045–1049.

[20] C.-H. Yeung, C.A. Francis, C.S. Criddle, Adaptation of nitrifying microbial biomass to nickel in batch incubations, Appl. Microbiol. Biotechnol. 97 (2013) 847–857.

[21] X. Liu, M. Kim, G. Nakhla, Operational conditions for successful partial nitrification in a sequencing batch reactor SBR based on process kinetics, Environ. Technol. 38 (2017) 694–704.

[22] A. Apha, WEF, 2005, Stand. Methods Exam. Water Wastewater. 21 (2005) 258–259.

[23] G. Liu, J. Wang, Role of solids retention time on complete nitrification: mechanistic understanding and modeling, J. Environ. Eng. 140 (2013) 48–56.

[24] X. Liu, M. Kim, G. Nakhla, Performance and kinetics of nitrification of low ammonia wastewater at low temperature, Water Environ. Res. 90 (2018) 498–509.

[25] Z. Lewandowski, Behaviour of biological reactors in the presence of toxic compounds, Water Res. 21 (1987) 147–153.

[26] S. Sujarittanonta, J.H. Sherrard, Activated sludge nickel toxicity studies, J. Water Pollut. Control Fed. (1981) 1314–1322.

[27] C.L. Grady Jr, G.T. Daigger, N.G. Love, C.D. Filipe, Biological wastewater treatment, CRC press, 2011.

[28] J. Guo, Y. Peng, H. Huang, S. Wang, S. Ge, J. Zhang, Z. Wang, Short-and long-term effects of temperature on partial nitrification in a sequencing batch reactor treating domestic wastewater, J. Hazard. Mater. 179 (2010) 471–479.

[29] S. Zhu, S. Chen, The impact of temperature on nitrification rate in fixed film biofilters, Aquac. Eng. 26 (2002) 221–237.

[30] R. Salvetti, A. Azzellino, R. Canziani, L. Bonomo, Effects of temperature on tertiary nitrification in moving-bed biofilm reactors, Water Res. 40 (2006) 2981–2993.

Chapter 7

7 Conclusions and recommendations

7.1 Conclusions

A mathematical model for successful shortcut nitrification conditions determination based on MSC values was established. At any given operational condition, the model was able to predict if shortcut nitrification can be achieved and provide the operational DO range which is higher than the DO_{min} of AOB and lower than that of NOB. This is the first model that involves all the operational factors like pH, DO, TAN, TNN, temperature, and SRT, which makes it a quite effective method to predict operational conditions for partial nitrification. In addition, the model not only suggests a DO range for partial nitrification, but also provide information for partial nitrification systems design and operation.

At 35ºC, stable nitrite accumulation was observed at two conditions: a-influent ammonia concentration of 190 mg N/L and continuous aeration and a DO of 0.6–3.0 mg/L with average FA of 4.4 mg N/L, and b-influent ammonia concentration of 100 mg N/L, intermittent aeration and a DO of 0.15–2.0 mg/L with average FA of 2.2 mg N/L. Combinition of FA inhibition and DO limitation could be a good way to achieve partial nitrification at 35ºC. This is the first time that an SBR was used to treat relatively low ammonium wastewater (100-200 mg N/L) at 35ºC with the support of kinetic analysis. In addition, this is the first attempt to mathematically identify the contributions of factors to partial nitrification based on kinetics.

At 14ºC with an influent of 40 mg N/L to a SBR operated at a SRT of 10 d, the decrease in ambient dissolved oxygen concentration from 5.5 mg/L to 2.5 mg/L, and further to 0.8

mg/L, resulted in ammonia accumulation, as well as an increase in the nitrite accumulation ratio. Low dissolved oxygen (<1 mg/L), combined with a long SRT (>30 d), appears to be a strategy for stable nitritation at low temperatures (14 ^{o}C). This is the first study in which partial nitrification performance at different DO concentrations, based on long-term operation at low temperature (14^{o}C), were compared. In addition, this study is the first attempt to directly determine the kinetc parameters of nitrifiers with sludge cultivated at 14^{o}C.

At 10^{o}C, after acclimatization, AOB activity dropped by 47%-58% at Ni/MLSS ratio of 4-7 mg Ni/g MLSS. Short-term nickel inhibition was much more serious for NOB than AOB at 35^{o}C and slightly more serious for NOB than AOB at 23^{o}C. With temperature decreasing further to 10^{o}C, the inhibition was equal or less for NOB than AOB. Short-term nickel inhibition on nitrifying bacteria was reversible. This is the first study to evaluate and compare the acute and chronic nickel toxicity to nitrification systematically at low temperature.

7.2 Recommendations for future work

Based on the findings of this research, future research should address the following areas:

1. Study the feasibility of achieving partial nitrification at low temperature by adopting low DO and long SRT, as suggested by the findings of this work.
2. Investigate the effect of COD on the feasibility of achieving partial nitrification at low temperature.
3. Inverstigate the effect of other heavy metals or chemical inhibitors on nitrification at low temperature.

Appendices

Appendix A. Supplementary information for Chapter 3

Table A3-1. DO concentrations causing nitrite accumulation

Reference	DO(mg/L)	NO_2/NO_x(%)	System
Chung et al. (2007)	<2	93%	activated sludge with biofilm carriers
Galí et al. (2007)	>3	99%	sequential batch reactor
Yamamoto et al. (2008)	5	93%	up-flow reactor with biomass carrier
Fux et al. (2004)	2-4	94%	moving bed biofilm reactor
Yan andHu (2009)	2	100%	Sequencing batch reactor
	2	>90%	continuous stirred-tank reactor
Chen et al. (2010)	>1.5	95.7%	continuous stirred-tank reactor
	>1	85.3%	continuous stirred-tank reactor
Sinha andAnnachhatre (2007)	0.3-0.5	81%	continuous stirred-tank reactor
Chuang et al. (2007)	0.16-0.2	>90%	closed down-flow hanging sponge (DHS) reactor
Ruiz et al. (2006)	0.7	67%	activated sludge reactor
Ciudad et al. (2005)	1.4	80%	activated sludge reactor
van Dongen et al. (2001)	NA	100%	SHARON reactor
Kong et al. (2013)	0.05-1.33	90%	sequencing batch biofilm reactor (SBBR)
Hanaki et al. (1990)	0.5	NA	Suspended growth
Blackburne et al. (2008)	0.4	15-95%	Continuous-flow reactor
Kim et al. (2003)	1.0	100%	Biofilm airlift reactor
Garrido et al. (1997)	1.5	100%	Biofilm airlift suspension reactor
Joo et al. (2000)	2.0-5.0	100%	Biological aeraated reactor
Bernet et al. (2001)	0.5	90%	Completely stirred biofilm reactor
Wang andYang (2004)	1.5	NA	

Park et al. (2010)	1.3±0.3	98%	suspended-growth

Text A3-1. Derivation of the equation of minimum substrate concentration curve

The derivation of the general MSC equation follows the steps of the traditional S_{min} derivation based on a CSTR system. The steady-state mass balance for biomass at steady state in a nitrification CSTR is shown in eq.1.

$$0 = Q \cdot X_0 - Q \cdot \mathrm{X} + \mu_{max} \cdot \frac{DO}{K_O+DO} \cdot \frac{S}{S+K_S} \cdot X \cdot V - b \cdot X \cdot V \quad (1)$$

Dividing by active biomass concentration, X and flow rate, Q, converts eq 1 to eq 2.

$$0 = \frac{X_0}{X} - 1 + \mu_{max} \cdot \frac{DO}{K_O+DO} \cdot \frac{S}{S+K_S} \cdot \frac{V}{Q} - b \cdot \frac{V}{Q} \quad (2)$$

Since V/Q can be defined as the hydraulic retention time (HRT) and influent biomass, X_0=0, eq.2 is simplified to eq.3.

$$\mu_{max} \cdot \frac{DO}{K_O+DO} \cdot \frac{S}{S+K_S} - b - \frac{1}{HRT} = 0 \quad (3)$$

As HRT go to infinity eq 3 becomes eq 4.

$$\frac{\mu_{max} \cdot DO}{DO+K_O} \cdot \frac{S}{K_S+S} - \mathrm{b} = 0 \quad (4)$$

then we get,

$$\frac{\mu_{max} \cdot DOmin}{DOmin+K_O} \cdot \frac{S}{K_S+S} - \mathrm{b} = 0 \quad (5)$$

$$\frac{\mu_{max} \cdot DO}{DO+K_O} \cdot \frac{Smin}{K_S+Smin} - \mathrm{b} = 0 \quad (6)$$

Reference

Bernet N, Dangcong P, Delgenes JP, Moletta R (2001) Nitrification at low oxygen

concentration in biofilm reactor. Journal of Environmental Engineering-Asce 127: 266-271

Blackburne R, Yuan ZG, Keller J (2008) Partial nitrification to nitrite using low dissolved oxygen concentration as the main selection factor. Biodegradation 19: 303-312

Chen JW, Zheng P, Yu Y, Mahmood Q, Tang CJ (2010) Enrichment of high activity nitrifers to enhance partial nitrification process. Bioresource Technology 101: 7293-7298

Chuang HP, Ohashi A, Imachi H, Tandukar M, Harada H (2007) Effective partial nitrification to nitrite by down-flow hanging sponge reactor under limited oxygen condition. Water Research 41: 295-302

Chung J, Bae W, Lee YW, Rittmann BE (2007) Shortcut biological nitrogen removal in hybrid biofilm/suspended growth reactors. Process Biochemistry 42: 320-328

Ciudad G, Rubilar O, Munoz P, Ruiz G, Chamy R, Vergara C, Jeison D (2005) Partial nitrification of high ammonia concentration wastewater as a part of a shortcut biological nitrogen removal process. Process Biochemistry 40: 1715-1719

Fux C, Huang D, Monti A, Siegrist H (2004) Difficulties in maintaining long-term partial nitritation of ammonium-rich sludge digester liquids in a moving-bed biofilm reactor (MBBR). Water Science and Technology 49: 53-60

Galí A, Dosta J, van Loosdrecht MCM, Mata-Alvarez J (2007) Two ways to achieve an anammox influent from real reject water treatment at lab-scale: Partial SBR nitrification and SHARON process. Process Biochemistry 42: 715-720

Garrido JM, vanBenthum WAJ, vanLoosdrecht MCM, Heijnen JJ (1997) Influence of dissolved oxygen concentration on nitrite accumulation in a biofilm airlift suspension reactor. Biotechnology and Bioengineering 53: 168-178

Hanaki K, Wantawin C, Ohgaki S (1990) NITRIFICATION AT LOW-LEVELS OF DISSOLVED-OXYGEN WITH AND WITHOUT ORGANIC LOADING IN A SUSPENDED-GROWTH REACTOR. Water Research 24: 297-302

Joo SH, Kim DJ, Yoo IK, Park K, Cha GC (2000) Partial nitrification in an upflow biological aerated filter by O-2 limitation. Biotechnology Letters 22: 937-940

Kim DJ, Chang JS, Lee DI, Han DW, Yoo IK, Cha GC (2003) Nitrification of high strength ammonia wastewater and nitrite accumulation characteristics. Water Science and Technology 47: 45-51

Kong Q, Zhang J, Miao MS, Tian L, Guo N, Liang S (2013) Partial nitrification and nitrous oxide emission in an intermittently aerated sequencing batch biofilm reactor. Chemical Engineering Journal 217: 435-441

Park S, Bae W, Rittmann BE, Kim S, Chung J (2010) Operation of suspended-growth shortcut biological nitrogen removal (SSBNR) based on the minimum/maximum substrate concentration. Water Research 44: 1419-1428

Ruiz G, Jeison D, Rubilar O, Ciudad G, Chamy R (2006) Nitrification-denitrification via nitrite accumulation for nitrogen removal from wastewaters. Bioresource Technology 97: 330-335

Sinha B, Annachhatre AP (2007) Assessment of partial nitrification reactor performance through microbial population shift using quinone profile, FISH and SEM. Bioresource Technology 98: 3602-3610

van Dongen U, Jetten MSM, van Loosdrecht MCM (2001) The SHARON((R))-Anammox((R)) process for treatment of ammonium rich wastewater. Water Science and Technology 44: 153-160

Wang JL, Yang N (2004) Partial nitrification under limited dissolved oxygen conditions. Process Biochemistry 39: 1223-1229

Yamamoto T, Takaki K, Koyama T, Furukawa K (2008) Long-term stability of partial nitritation of swine wastewater digester liquor and its subsequent treatment by Anammox. Bioresource Technology 99: 6419-6425

Yan J, Hu YY (2009) Comparison of partial nitrification to nitrite for ammonium-rich organic wastewater in sequencing batch reactors and continuous stirred-tank reactor at laboratory-scale. Water Science and Technology 60: 2861-2868

Appendix B. Supplementary information for Chapter 6

Table B6-1. Offline batch tests design

	A	B	C	D	E	F	G	H	I
Ni concentration (mg/L)	0	0.5	1.0	1.5	2.0	1.0	1.0	1.0	1.0
MLSS concentration (mg/L)	340	340	340	340	340	680	1020	1360	2720
MLVSS concentration (mg)	260	260	260	260	260	520	780	1040	2080

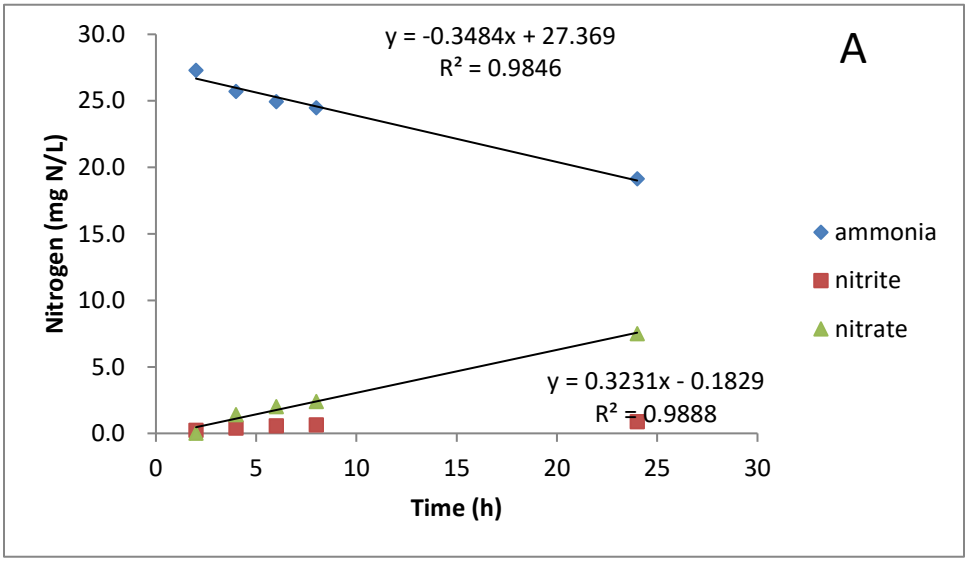

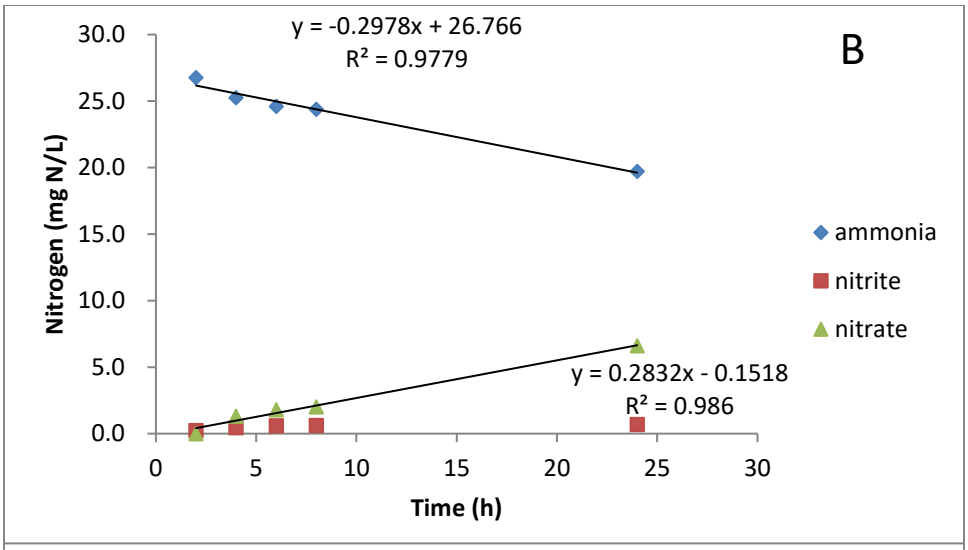
B
y = -0.2978x + 26.766
R² = 0.9779
y = 0.2832x - 0.1518
R² = 0.986
Nitrogen (mg N/L)
Time (h)
ammonia
nitrite
nitrate

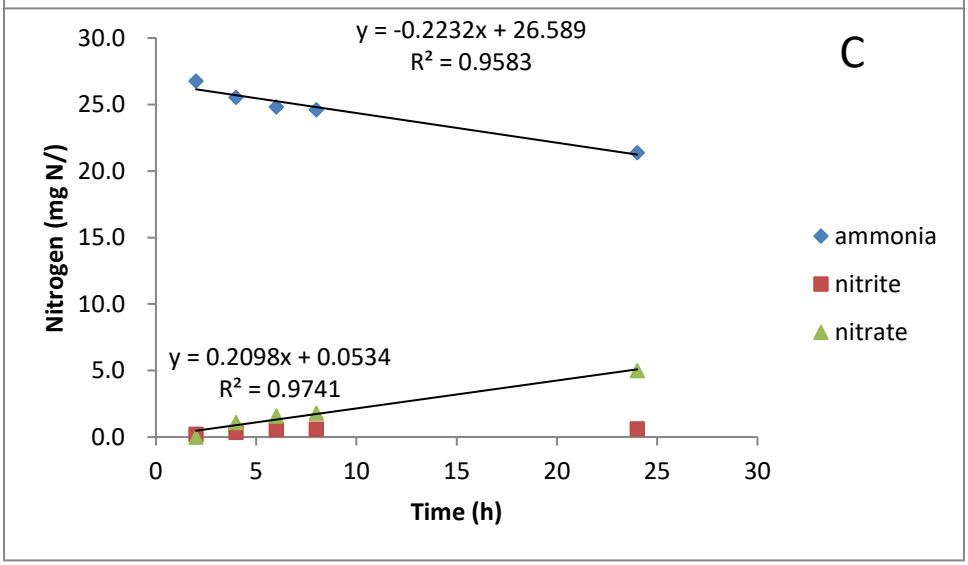
C
y = -0.2232x + 26.589
R² = 0.9583
y = 0.2098x + 0.0534
R² = 0.9741
Nitrogen (mg N/)
Time (h)
ammonia
nitrite
nitrate

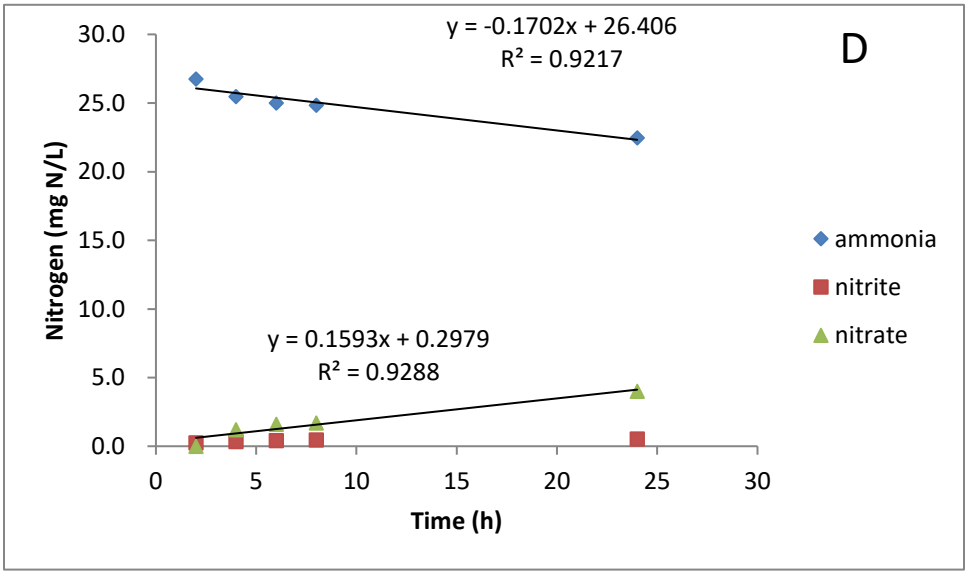
D
y = -0.1702x + 26.406
R² = 0.9217
y = 0.1593x + 0.2979
R² = 0.9288
Nitrogen (mg N/L)
Time (h)
ammonia
nitrite
nitrate

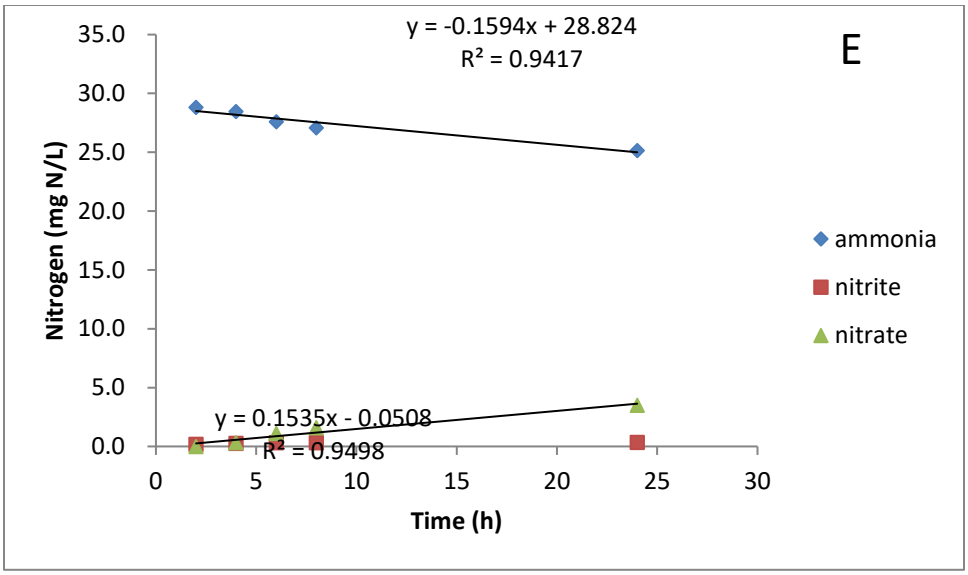
E
y = -0.1594x + 28.824
R² = 0.9417
y = 0.1535x - 0.0508
R² = 0.9498
Nitrogen (mg N/L)
Time (h)
ammonia
nitrite
nitrate

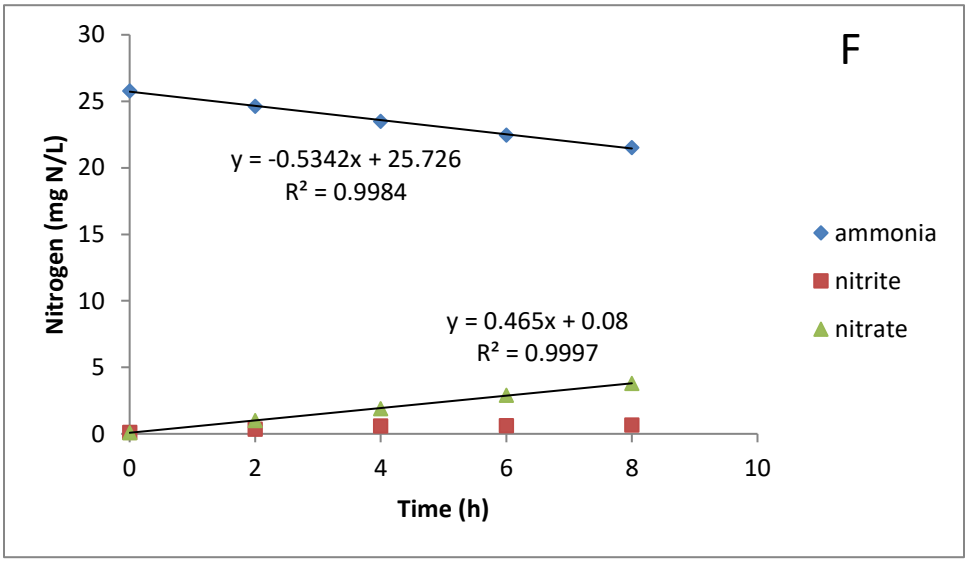
F
y = -0.5342x + 25.726
R² = 0.9984
y = 0.465x + 0.08
R² = 0.9997
Nitrogen (mg N/L)
Time (h)
ammonia
nitrite
nitrate

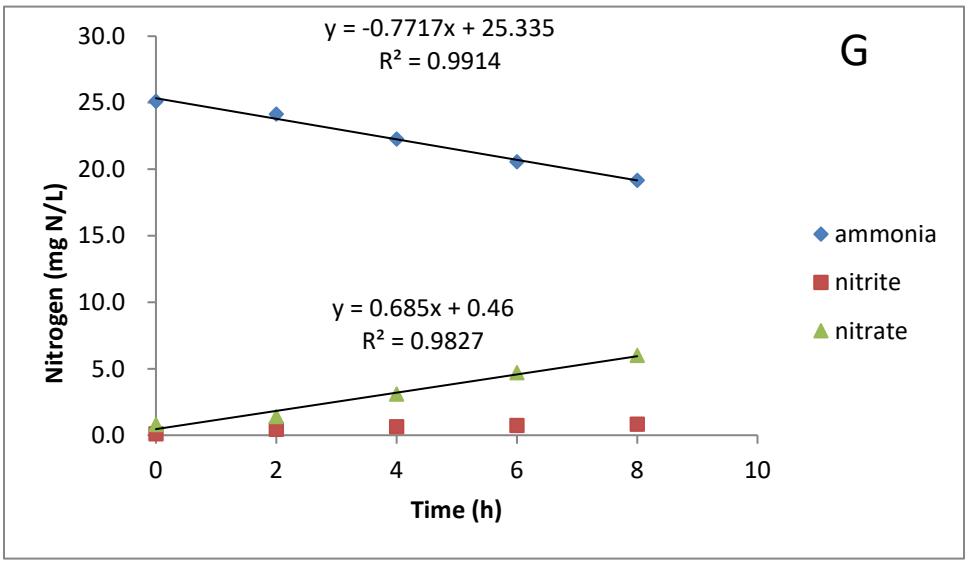
G
y = -0.7717x + 25.335
R² = 0.9914
y = 0.685x + 0.46
R² = 0.9827
Nitrogen (mg N/L)
Time (h)
ammonia
nitrite
nitrate

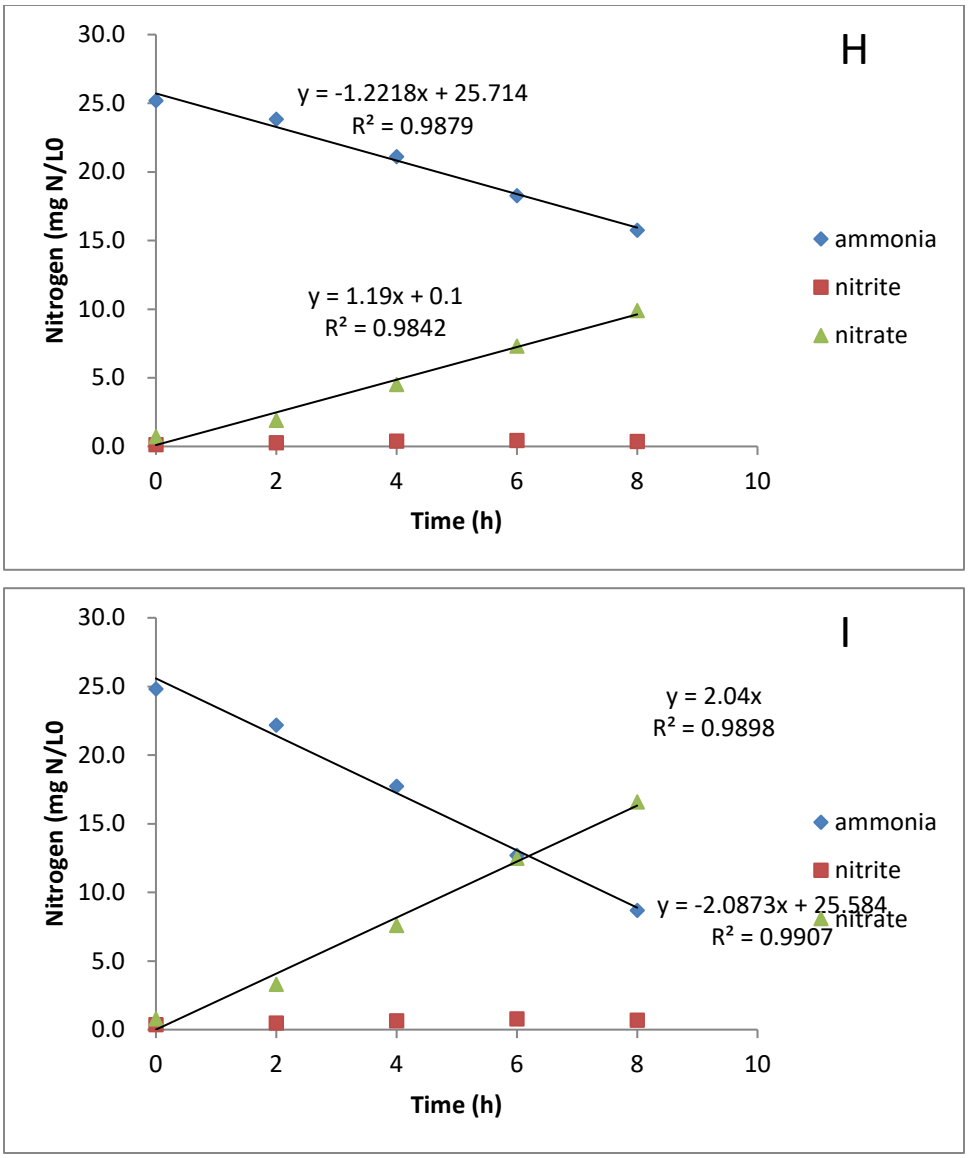

Figure B6-1. Short-term batch tests results at 10°C

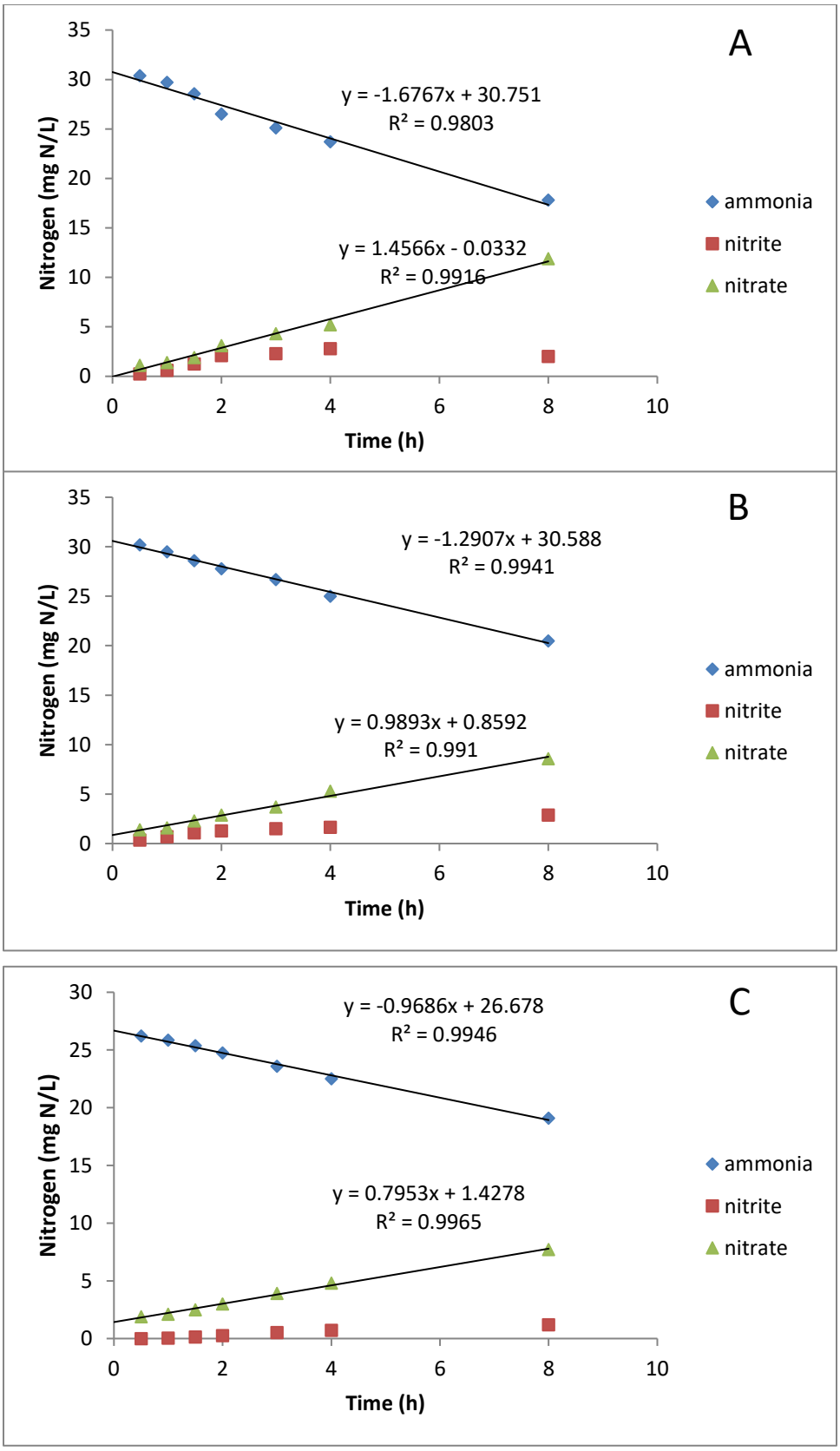
A
y = -1.6767x + 30.751
R² = 0.9803
y = 1.4566x - 0.0332
R² = 0.9916
Nitrogen (mg N/L)
Time (h)
ammonia
nitrite
nitrate
B
y = -1.2907x + 30.588
R² = 0.9941
y = 0.9893x + 0.8592
R² = 0.991
Nitrogen (mg N/L)
Time (h)
ammonia
nitrite
nitrate
C
y = -0.9686x + 26.678
R² = 0.9946
y = 0.7953x + 1.4278
R² = 0.9965
Nitrogen (mg N/L)
Time (h)
ammonia
nitrite
nitrate

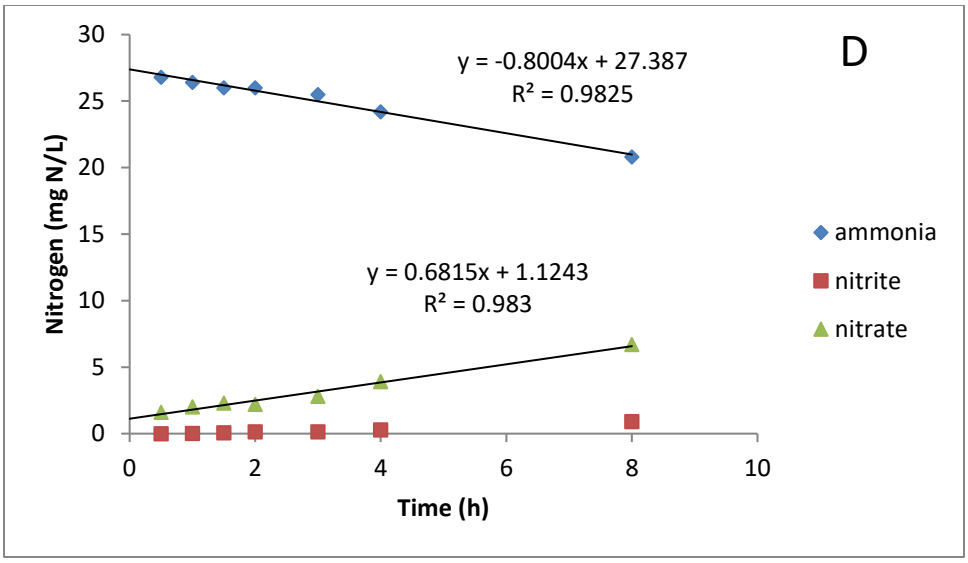
D
y = -0.8004x + 27.387
R² = 0.9825
y = 0.6815x + 1.1243
R² = 0.983
Nitrogen (mg N/L)
Time (h)
ammonia
nitrite
nitrate

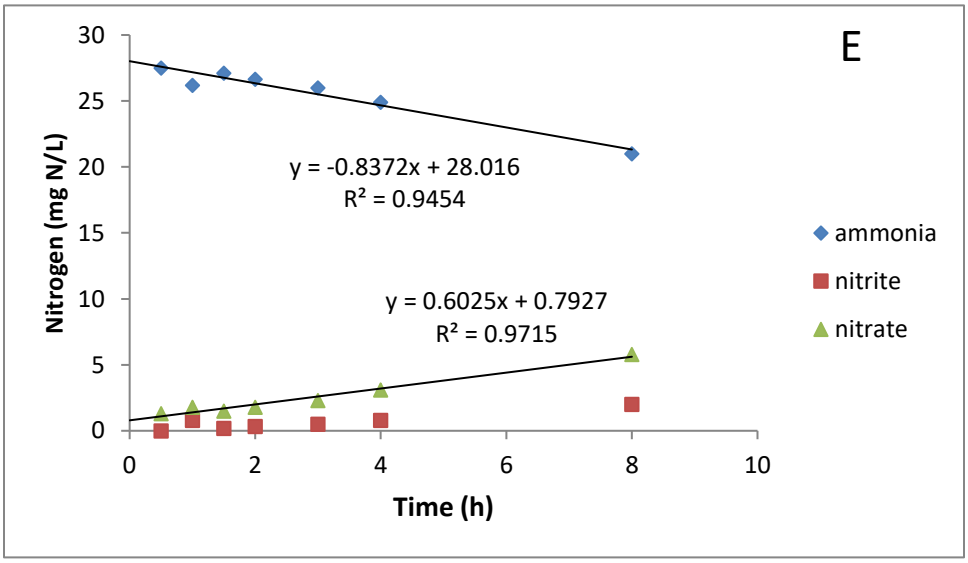
E
y = -0.8372x + 28.016
R² = 0.9454
y = 0.6025x + 0.7927
R² = 0.9715
Nitrogen (mg N/L)
Time (h)
ammonia
nitrite
nitrate

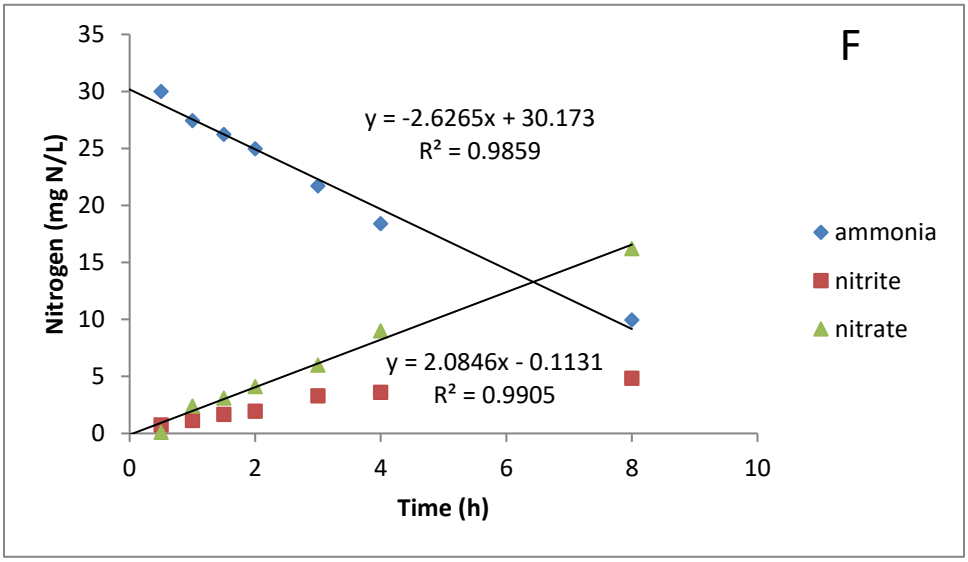
F
y = -2.6265x + 30.173
R² = 0.9859
y = 2.0846x - 0.1131
R² = 0.9905
Nitrogen (mg N/L)
Time (h)
ammonia
nitrite
nitrate

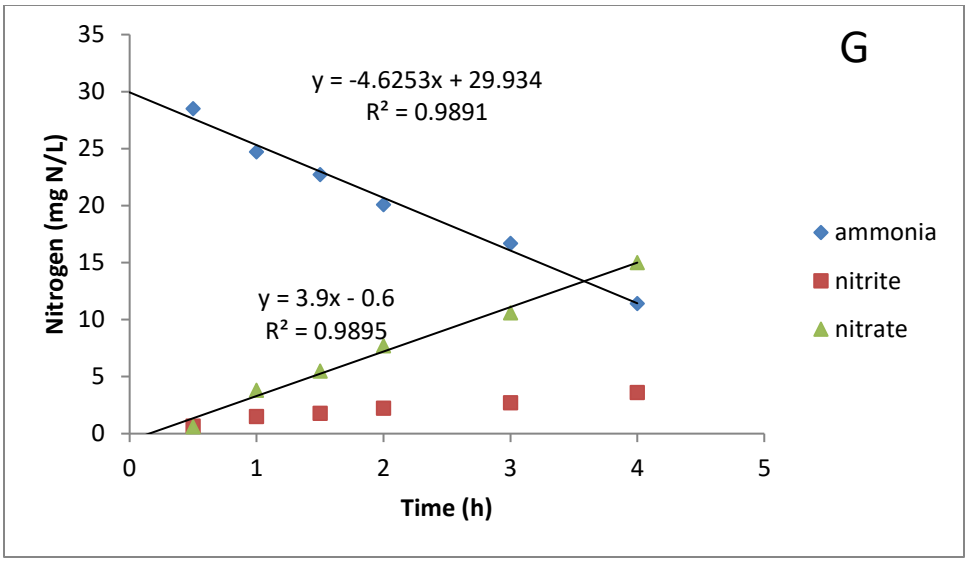
G
y = -4.6253x + 29.934
R² = 0.9891
y = 3.9x - 0.6
R² = 0.9895
Nitrogen (mg N/L)
Time (h)
ammonia
nitrite
nitrate

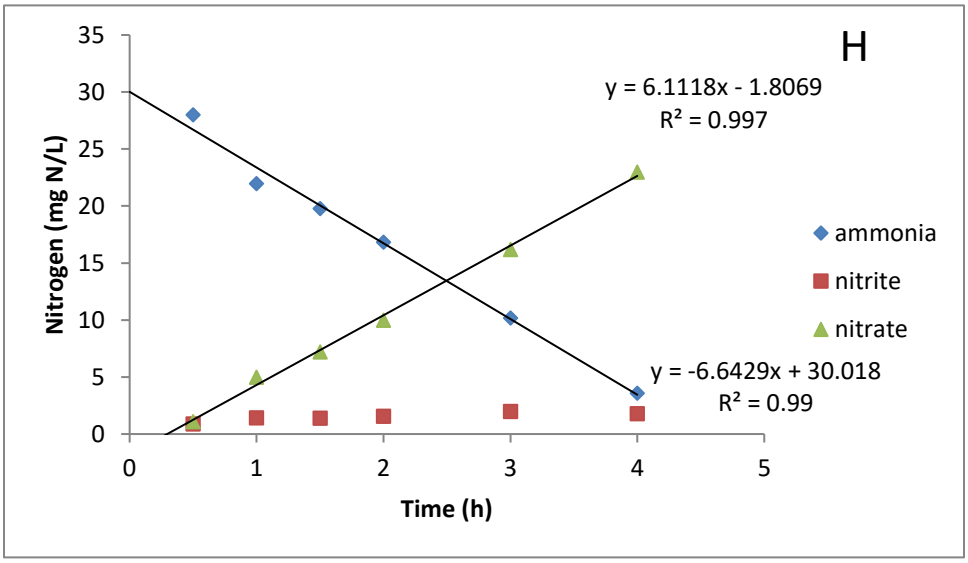
H
y = 6.1118x - 1.8069
R² = 0.997
y = -6.6429x + 30.018
R² = 0.99
Nitrogen (mg N/L)
Time (h)
ammonia
nitrite
nitrate

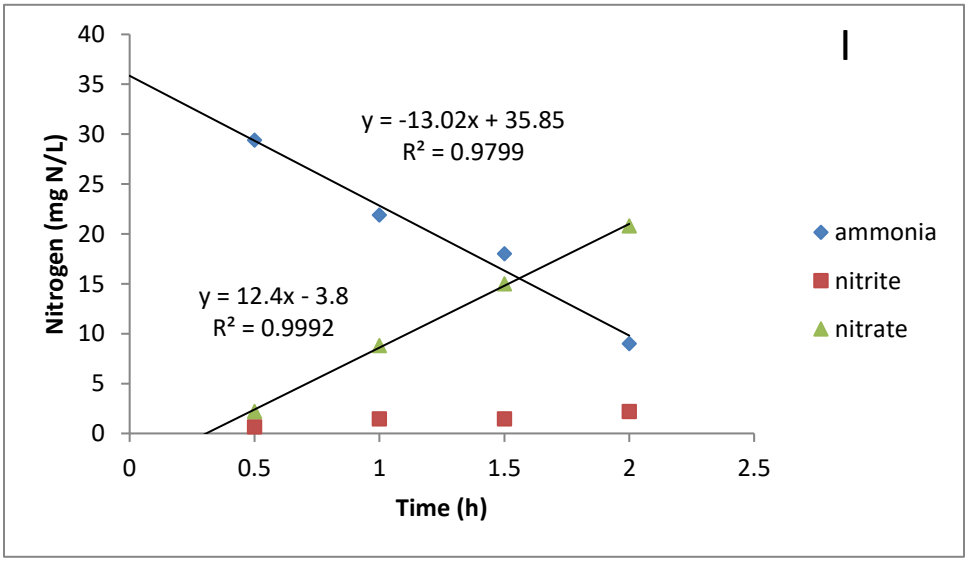
I
y = -13.02x + 35.85
R² = 0.9799
y = 12.4x - 3.8
R² = 0.9992
Nitrogen (mg N/L)
Time (h)
ammonia
nitrite
nitrate

Figure B6-2. Short-term batch tests results at 23ºC

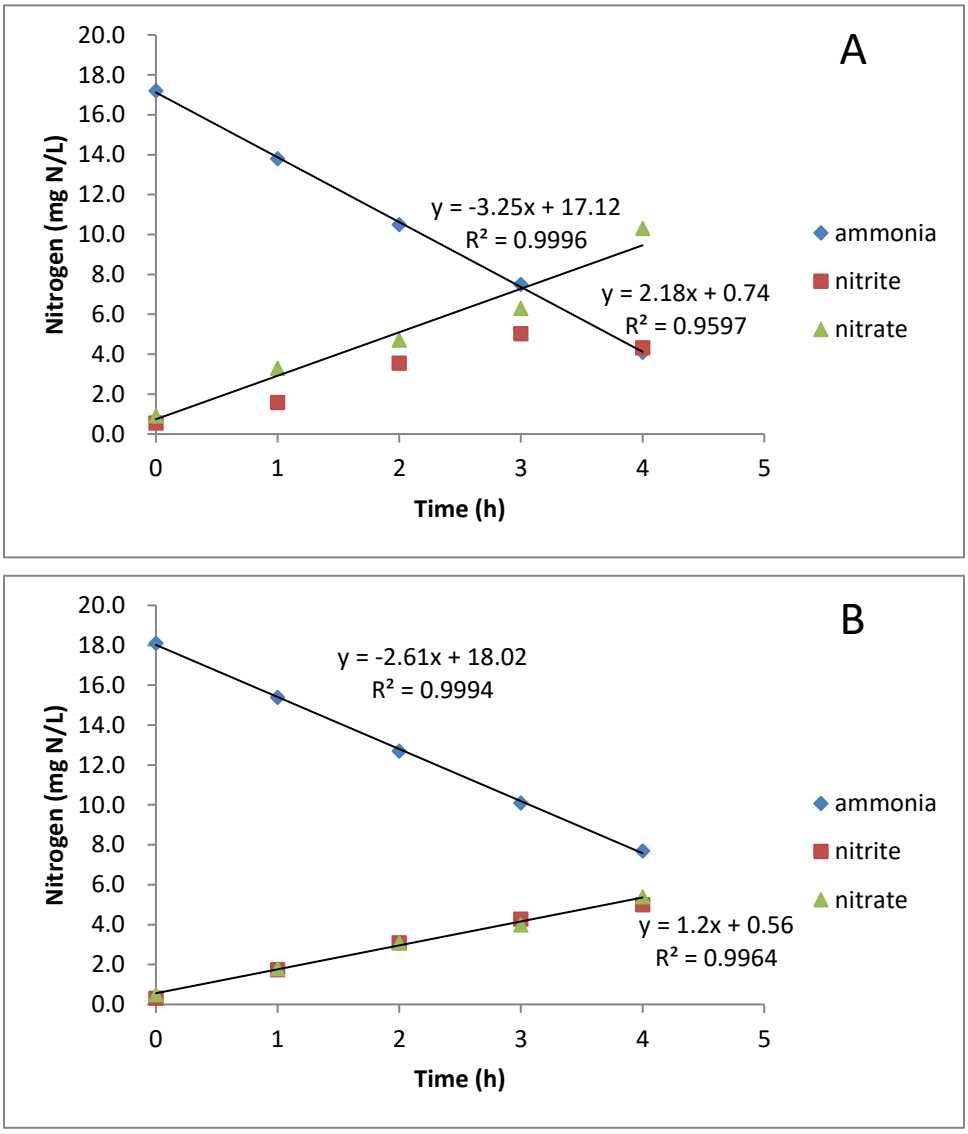

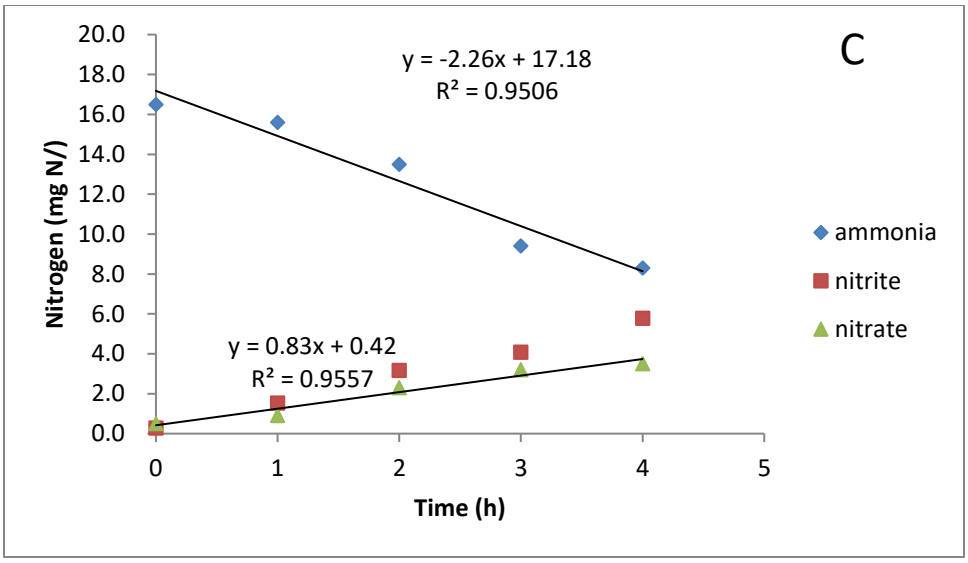
C
y = -2.26x + 17.18
R² = 0.9506
y = 0.83x + 0.42
R² = 0.9557
Nitrogen (mg N/)
Time (h)
ammonia
nitrite
nitrate

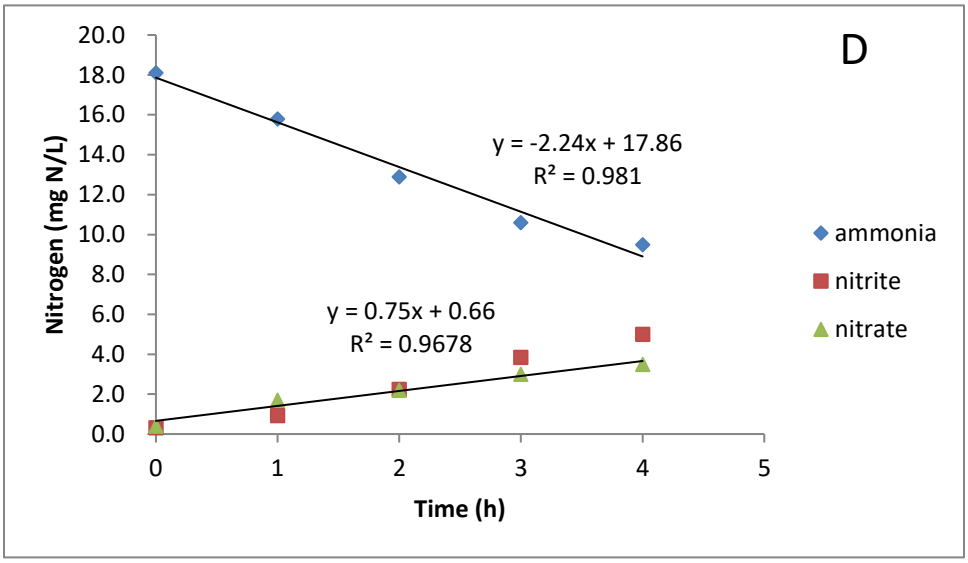
D
y = -2.24x + 17.86
R² = 0.981
y = 0.75x + 0.66
R² = 0.9678
Nitrogen (mg N/L)
Time (h)
ammonia
nitrite
nitrate

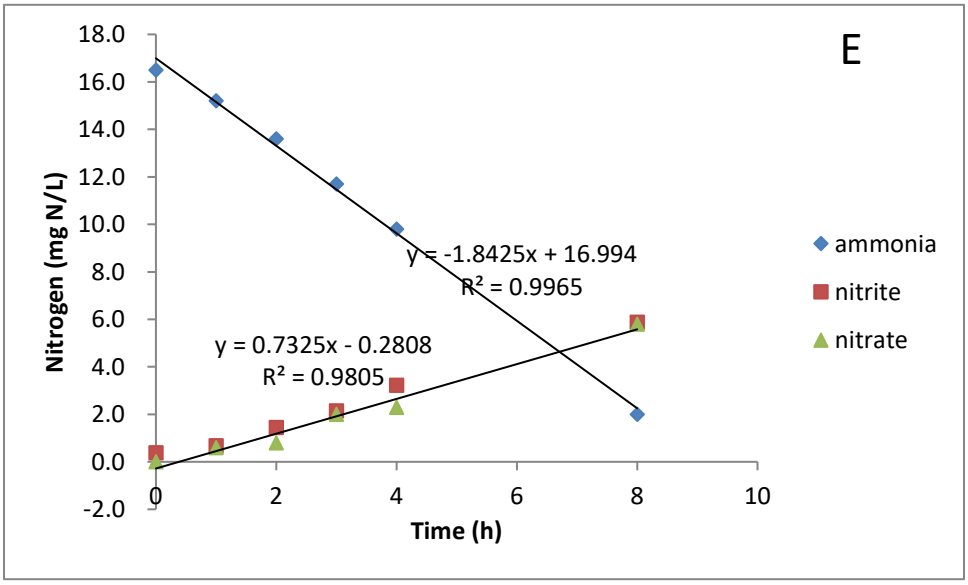
E
y = -1.8425x + 16.994
R² = 0.9965
y = 0.7325x - 0.2808
R² = 0.9805
Nitrogen (mg N/L)
Time (h)
ammonia
nitrite
nitrate

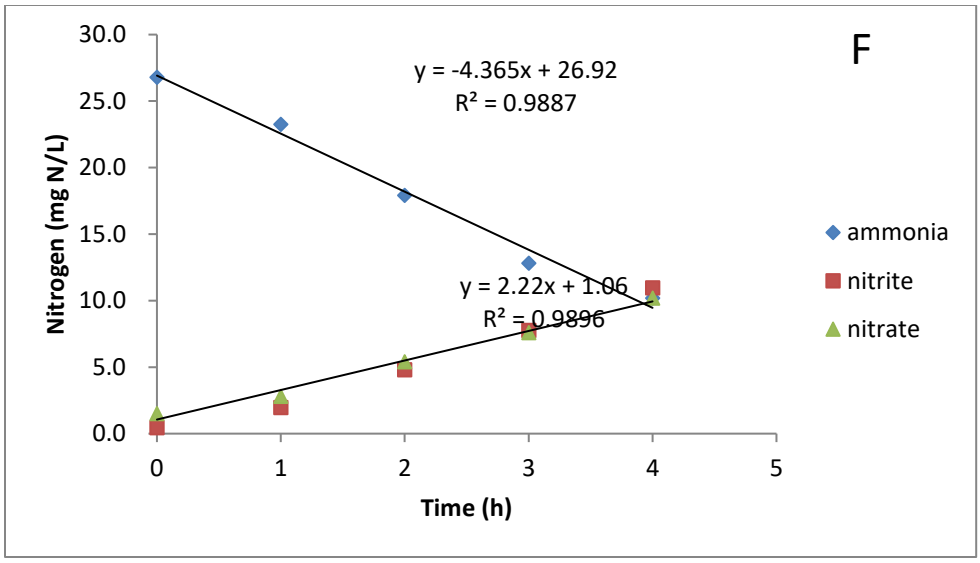
F
y = -4.365x + 26.92
R² = 0.9887
y = 2.22x + 1.06
R² = 0.9896
Nitrogen (mg N/L)
Time (h)
ammonia
nitrite
nitrate

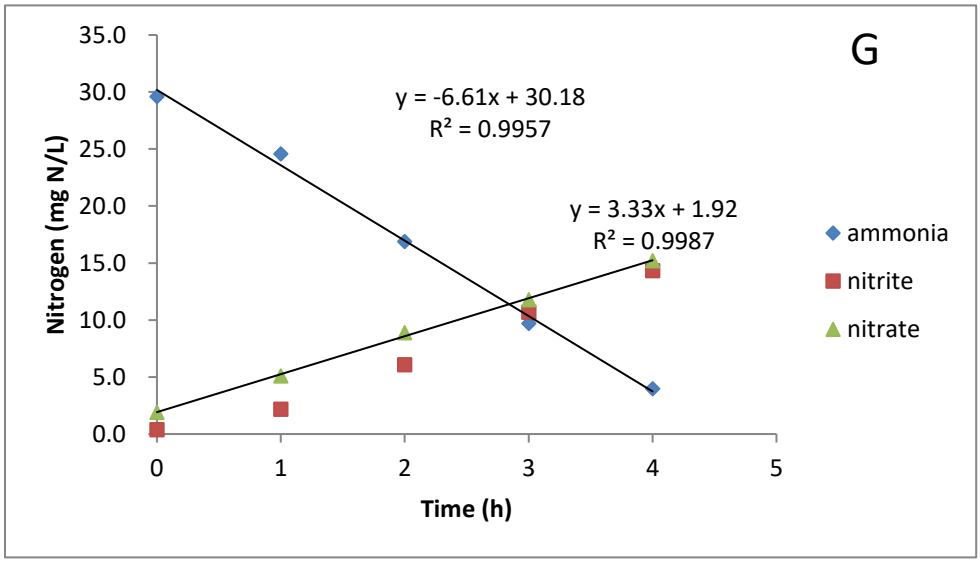
G
y = -6.61x + 30.18
R² = 0.9957
y = 3.33x + 1.92
R² = 0.9987
Nitrogen (mg N/L)
Time (h)
ammonia
nitrite
nitrate

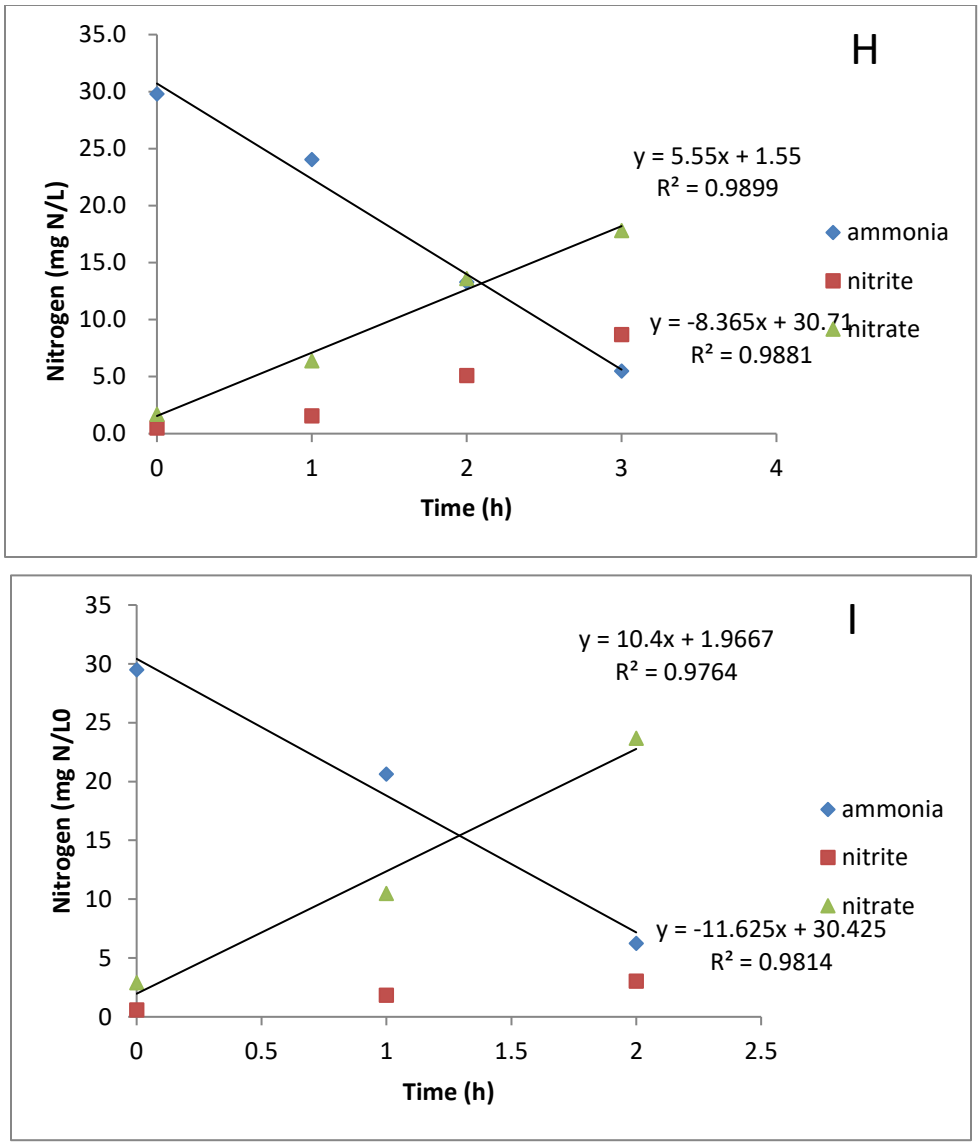

Figure B6-3. Short-term batch tests results at 35°C

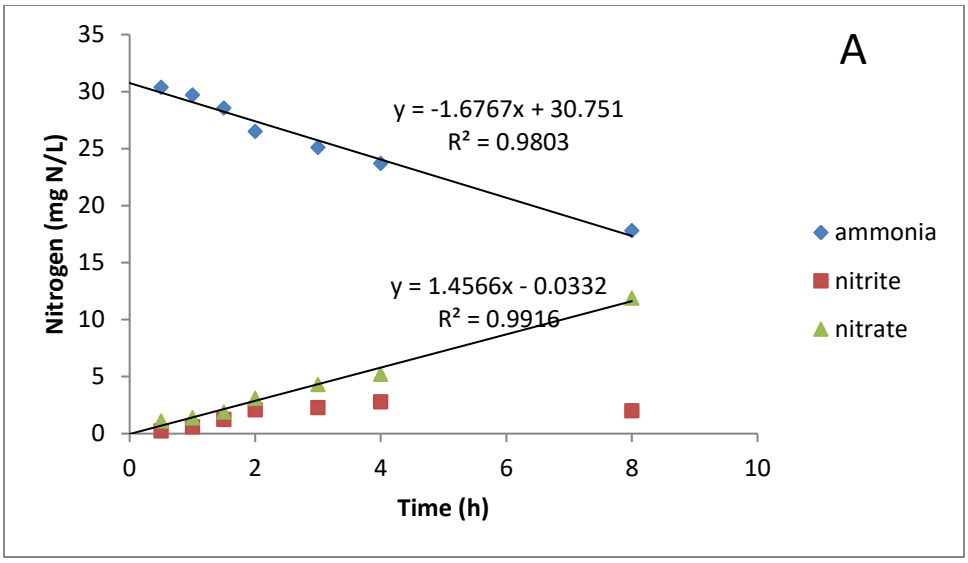
A
y = -1.6767x + 30.751
R² = 0.9803
y = 1.4566x - 0.0332
R² = 0.9916
Nitrogen (mg N/L)
Time (h)
ammonia
nitrite
nitrate

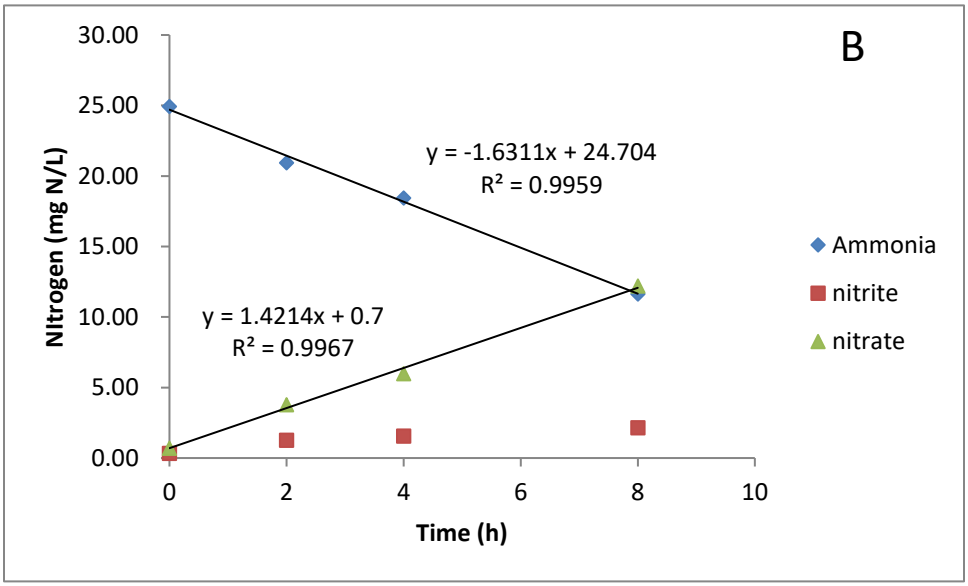
B
y = -1.6311x + 24.704
R² = 0.9959
y = 1.4214x + 0.7
R² = 0.9967
Nitrogen (mg N/L)
Time (h)
Ammonia
nitrite
nitrate

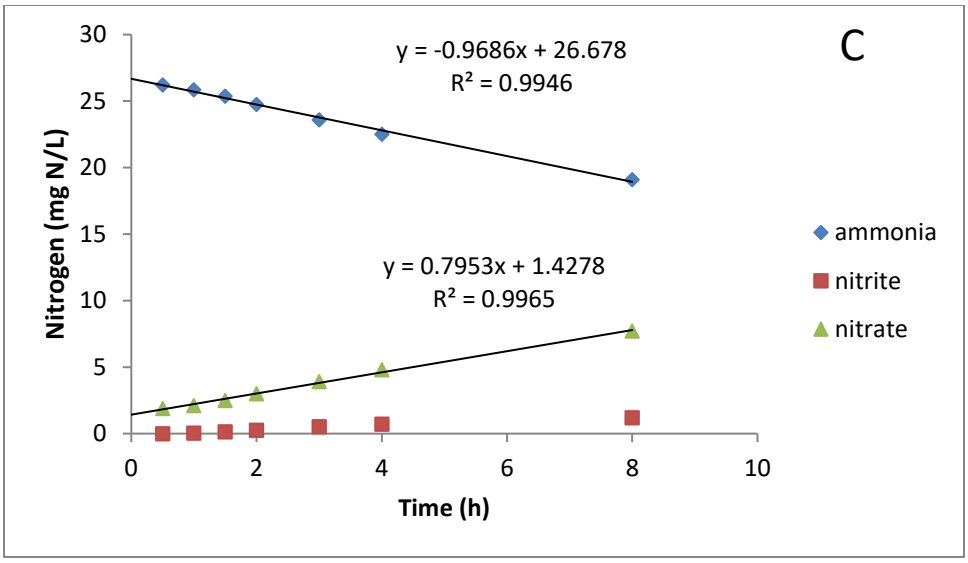

Figure B6-4. Reversibility of nickel inhibition

Curriculum Vitae

Name:	Xiaoguang Liu
Post-secondary Education and Degrees:	Tongji University Shanghai, China 2007-2011 B.A. Tongji University Shanghai, China 2011-2014 M.A. The University of Western Ontario London, Ontario, Canada 2014-2018 Ph.D.
Honours and Awards:	The University of Western Ontario Graduate Research Scholarship 2014-2018
Related Work Experience:	Graduate Teaching Assistant The University of Western Ontario 2014-2018 Graduate Research Assistant The University of Western Ontario 2014-2018 Visiting researcher City of Toronto September 2016 - December 2016

Conferences: 52nd CENTRAL Canadian Symposium on Water Quality Research

Toronto, ON, Canada

Oral presentation

Feb, 2017

53rd CENTRAL Canadian Symposium on Water Quality Research

Toronto, ON, Canada

Oral presentation

Feb, 2018

2018 WEAO Technical Symposium and OPCEA Exhibition

London, ON, Canada

Oral presentation

April, 2018

4th IWA Specialized International Conference on ecoSTP

London, ON, Canada

Poster presentation

June, 2018

Publications:

Liu, X., Kim, M., & Nakhla, G. (2017). Operational conditions for successful partial nitrification in a sequencing batch reactor (SBR) based on process kinetics. Environmental technology, 38(6), 694-704.

Liu, X., Kim, M., & Nakhla, G. (2017). A model for determination of operational conditions for successful shortcut nitrification. Environmental Science and Pollution Research, 24(4), 3539-3549.

Liu, X., Kim, M., & Nakhla, G. (2018). Performance and kinetics of nitrification of low ammonia wastewater at low temperature. Water Environment Research.